UNIVERSITÀ DEGLI STUDI DI MILANO

SCUOLA DI DOTTORATO
Scienze della Nutrizione

DIPARTIMENTO
Scienze della Salute (DISS)

CORSO DI DOTTORATO
Scienze della Nutrizione-29°ciclo-codice R27

TESI DI DOTTORATO DI RICERCA

"The microbiota: a complex interplay between host, bacterial communities and diet in health and disease"

sigla del settore/i scientifico disciplinare/i
MED/07 (Microbiologia e Microbiologia Clinica)

NOME DEL DOTTORANDO
Alessandra Riva
Matr: R10538

NOME E COGNOME DEL TUTOR
Prof.ssa Giulia Morace

NOME E COGNOME DEL COORDINATORE DEL DOTTORATO
Prof. Gianvincenzo Zuccotti

A.A.
(ANNO ACCADEMICO 2015-2016)

INDEX

List of manuscripts……...4

Summary……...5

CHAPTER 1: The gut microbiota……..8
1.1 Definition of microbiota and microbiome…….9
1.2 The evolution of the gut microbiota……10
1.2.1 Mother-child symbiosis……...10
1.2.2 From birth into adulthood……11
1.3 The gut microbiota composition……..13
1.3.1 Paneth cells……. …...17
1.3.2 Goblet cells and mucus layer: structure and composition……..18
1.3.3 MUC2…….20
1.3.4 Mucusa-associated microbiota has distinct composition……....23
1.3.5 Mucin-degrading specialists…….....24
1.4 The role of the gut microbiota…….26
1.4.1 Short chain fatty acids (SCFAs)……..26
1.4.2 Microbial production of SCFAs……26-27
1.5 Techniques to study the gut microbiota……..30
1.5.1 Fingerprinting tecniques…….30
1.5.2 Fluorescence *in situ* hybridization……..31
1.5.3 Sequencing of SSU rRNA clone libraries…….32
1.5.4 Metagenomic, metatrascriptomic, metaproteomic and metabolomics…..33
CHAPTER 2:**The gut microbiota and childhood obesity**……....35
2.1 Gut microbiota and childhood obesity…….36
2.2 Mechanism linking altered gut microbiota to obesity……..40
2.2.1 Fasting-induced adipose factor (FIAF) and AMP-activated protein kinase (AMPK)……...40
2.2.2 Activity of short chain fatty acids and monosaccharides……40-41
2.2.3 Increased permeability of the gut barrier……42
2.2.4 Control of food intake and appetite…….42
2.3 Interventional strategies in childhood obesity…….43
2.4 Aim of the project:"The gut microbiota in obese and normal-weight children"44
2.4.2 Experimental design……45
2.5 Manuscript 1:"Relative abundance in bacterial and fungal gut microbes in obese children: A case control study"…….46
2.6 Manuscript 2: "Pediatric obesity is associated with an altered gut microbiota and discordant shifts in *Firmicutes* populations"……...54
2.7 Conclusion……...80
CHAPTER 3:**The influence of diet on gut microbiota by using murine models**……...82
3.1 Diet and its impact on gut microbiota composition……....83
3.1.1 Plasticity of the gut microbiota……..85
3.2 Murine models to study the gut microbiota……87
3.2.1 The anatomy of the mouse and human intestinal tract……..87
3.2.2 Dietary impact……... 90
3.2.3 Methods to manipulate the gut microbiota: gnotobiotic definied microbiota…….91

3.3 Aim of the project: “Fine-scale spatial architecture of intestinal microbiota in a mouse model of diet”……....93
3.4 Preliminary data……..94
3.4.1 Experimenatl design……...94
3.4.2 Material and methods…….95
3.4.3 Results……..105
3.4.4 Discussion……137
CHAPTER 4: **The oral microbiota**……..144
4.1 The oral microbiota……...145
4.1.1 Composition of the oral microbiota……..145
4.1.2 Metabolic pathways of oral bacteria…….150
4.1.3 The oral microbiota is modulated by dietary habits and environmental factors……151
4.1.4 Cross-talk between oral microbiota and immunity……...152
4.1.5 Future research into functions of the oral microbiota……...154
4.2 Aim of the project: “An altered oral microbiota is associated with IL-8 production status of gingival epithelial cells in healthy individuals”…….155
4.3 Preliminary data……156
4.3.1 Experimental design…….156
4.3.2 Material and methods……...157
4.3.3 Results……..171
4.3.4 Discussion……172
CHAPTER 5: **Conclusions and perspectives**……..178
Bibliography……..182

LIST OF MANUSCRIPTS

Manuscript 1
Borgo, F., Verduci, E., **Riva, A**., Lassandro, C., Riva, E., Morace, G., and Borghi, E.
Relative abundance in bacterial and fungal gut microbes in obese children: a case control study. *Childhood Obesity* 2016 [Epub ahead of print].

Manuscript 2
Riva, **A**., Borgo, F., Lassandro, C., Verduci, E., Morace, G., Borghi, E., Berry, D.
Pediatric obesity is associated with an altered gut microbiota and discordant shifts in *Firmicutes* populations**.** *Environ Microbiol*. 2016 [Epub ahead of print]

Manuscript 3
Fine-scale spatial architecture of intestinal microbiota in a mouse model of diet.
Manuscript in preparation.

Manuscript 4
Schueller, K., **Riva**, **A**., Pfeiffer, S., Berry, D., and Somoza, V.
An altered oral microbiota is associated with IL-8 production status of gingival epithelial cells in healthy individuals.
Manuscript in preparation.

Manuscript not included in the thesis:
Riva, **A**., Borghi, E., Cirasola, D., Colmegna, S., Borgo, F., Amato, E., Pontello, M.M., and Morace, G.
Methicillin-resistant *Staphylococcus aureus* in raw milk: prevalence, scc*mec* typing, enterotoxin characterization, and antimicrobial resistance patterns. *Journal of Food Protection* 2015 78:1142–1146.

SUMMARY

The microbiota of the gastro-intestinal tract plays an important role in human health. In addition to their metabolic interactions with dietary constituents, gut bacteria may also be involved in more complex host interactions, such as modulation of the immune system. Changes in the microbiota during an individual's lifespan are accompanied by modifications in multiple health parameters, and such observations have prompted intense scientific efforts aiming to understand the complex interactions between the microbiota and its human host, as well as how this may be influenced by diet (Milani *et al*., 2016). To investigate the role of diet of the microbiota we performed three studies. In the first study we investigated the human gut microbiota composition in obese and normal-weight children; in the second project we studied the role of polysaccharide and fiber privation in wild type mice to gain more insight into the role of diet on gut microbiota. In the third study we analyzed the role of another important microbiota communities: the oral microbiota, in association with diet and release of the inflammatory marker IL-8 from gingival epithelial cells (GEC).

An altered gut microbiota has been linked to obesity in adulthood, though little is known about childhood obesity. In this study we characterized the composition of the gut microbiota in a large cohort of obese (n=42) and normal-weight school-aged children (n=36). The obese group was characterized by a more elevated intake of kcal/die and macronutrients (g/die) respect to normal-weight. Body mass index (BMI) z-score was significantly associated with gut microbiota composition, as determined with 16S rRNA gene amplicon sequencing, as well as levels of bacterial fermentation products (short chain fatty acids [SCFAs]). Obesity was associated with an altered gut microbiota characterized by elevated levels of *Firmicutes* and depleted levels of *Bacteroidetes*. Members of the *Bacteroidetes* were generally better predictors of BMI z-score and obesity than *Firmicutes*, which was likely due to discordant responses of *Firmicutes* OTUs.

Correlation network analysis revealed that the gut microbiota of obese children also had increased correlation density and clustering of operational taxonomic units (OTUs). Moreover, we identified several bacterial taxa significantly associated with BMI z-score as well as SCFA levels. This suggests that alterations in the microbiota are linked to increased fermentation, which may play a role in promoting childhood obesity.

To gain more insight into the role of diet on gut microbiota composition we studied the intestinal microbiota by using immunofluorescence images of fixed colon cross-sections for quantification and spatial organization of bacteria and laser capture microdissections (LCM) of specific areas from proximal to distal colon in wild-type mice. Subsequently, we sequenced LCM and stool samples by using 16S rRNA gene amplicon sequencing. We applied this protocol to three groups of mice with control diet (CON), fiber free (FF) and polysaccharide free (PF) demonstrating that elimination of microbiota-accessible carbohydrates from the diet, resulted in a decrease of diversity, changes in microbial composition along colon compartments and in stool samples, in a thinner mucus layer and in a reduced biovolume fraction of goblet cells. This high-resolution system to capture and examine spatial organization of intestinal microbes demonstrated the strong impact of diet on gut microbiota community but even on mucus layer structure and goblet cells.

In the third study we examined the oral microbiota community in healthy humans and its association with nutrition, oral hygiene habits, and the release of the inflammatory marker IL-8 from GEC with and without stimulation with bacterial endotoxins to identify possible indicator operational taxonomic units (OTUs) for the initiation of oral diseases. GECs from 21 healthy participants were incubated with/without addition of bacterial lipopolysaccharides (LPS), and the oral microbiota was profiled using 16S rRNA gene-targeted sequencing. Members of the oral microbiota were associated with basal IL-8 levels, the intake of meat, tea, white wine, sweets and the use of chewing gum, as well as flossing habits, allergies, gender and BMI. Interestingly, the stimulation with bacterial endotoxin revealed 11 indicator bacterial

OTUs, 9 of which were associated with high basal levels of IL-8 and an increase in IL-8 release after challenge with LPS and the other two with low level and high basal level of IL8 irrespective of response to LPS challenge. The identification of indicator bacteria in healthy subjects with high levels of IL-8 release may be promising early-warning indicators for the possible onset of oral inflammations.

In conclusion, in these three studies we demonstrated the importance of diet in the modulation of gut and oral microbiota in humans and wild-type mice and in health and disease, improving our understanding of host-microbes interactions.

CHAPTER 1:

THE GUT

MICROBIOTA

1. The gut microbiota

1.1 Definition of microbiota and microbiome

The term microbiota was coined for the first time by Joshua Lederberg in 2001 to signify “the ecological community of commensal, symbiotic, and pathogenic microorganisms that literally share our body space and can be determinants of health and disease”. Specifically, the term “microbiota” represents the microbial taxa associated with human body and the term “microbiome” is the catalog of these microbes and their genes. The Human Microbiome Project and Metagenomics of the Human Intestinal Tract (MetaHIT) (www.metahit.eu/) project clearly demonstrated that gut microorganisms are not just passive residents, carrying out a range of biological functions that are important in nutrition and well-being of the individual (Dewhirst et al., 2010; The Human Microbiome Project Consortium, 2012).

1.2 The evolution of the gut microbiota

The first colonisation of the intestine is one of the most profound immunological exposures faced by the newborn and it is influenced by external and internal factors. The early composition of human microbiota could have long-lasting metabolic effects and the initial composition of human intestinal bacteria is also known to affect postnatal immune system development. Mode of delivery and feeding as an infant have a major role on the composition of intestinal microbiota in early infancy (Biasucci *et al*., 2010).

1.2.1 Mother–child symbiosis

The mother–child symbiosis, tend to prepare a dynamic baseline on the newborn gut microbiota. An incorrect maternal behavior (smoking, weight gain in pregnancy), poor social condition and diseases during pregnancy can negatively influence the newborn gut microbiota composition (Figure 1.1 and 1.2A) (Putignani *et al*., 2014).

Theoretically, during its uterine life, the fetus develops in a sterile environment (Putignani *et al*., 2014). Recent studies in animals have demonstrated that the association between the microbiome and fat deposition and resultant development of metabolic syndrome may begin as early as the prenatal period. Bacteria from pregnant mice gut have been demonstrated in mesenteric lymph nodes and are thought to possibly be transferred through the placenta into the fetus. Bacteria have been demonstrated even in meconium, which is the first stool passed by the fetus and thought to be sterile (Jiménez *et al*., 2008).

The composition of the gut microbiota ecosystem is a complex but continuous process, affected by endogenous and exogenous determinants of variability, with an immediate effect at the time of birth that continue for several years during childhood through subsequent stages (Figure 1.2B). One of the major causes of onset and modulation of the newborn gut microbiota is the mode of delivery. Children born by natural delivery develop a microbiota similar to their mothers' vaginal microbiota (*Lactobacillus* spp., *Prevotella* spp., *Sneathia* spp.), while children born by Caesarean section (CS) are characterized by microbiota similar to mother skin microbiota (*Staphylococcus* spp., *Corynebacterium* spp., *Propionibacterium* spp.). Babies born by CS, present a microbiota not necessarily mother induced, but often reflecting skin ecosystems of healthcare workers, surfaces, etc., which may come into contact with the baby during delivery. In addition, breastfeeding exposes infants predominantly to *Bifidobacteria* (90%), whereas formula-feeding is associated with a more diverse bacterial population, including *Bacteroidetes* and *Clostridia* species (Putignani *et al*., 2014).

This initial “bacterial imprinting” may later on differentially contribute to the onset of atopic diseases, allergies, asthma (Biasucci *et al*., 2010), and obesity described as more frequent in CS-born children rather than in those naturally delivered (Goldani *et al*., 2011; Mueller *et al*., 2015; Portela *et al*., 2015)

1.2.2 From birth into adulthood

In the pediatric age scale, 0–18 y (Figure 1.2B), feeding, environmental, social, biological, and genetic factors progressively influence the entire individual psychosomatic development, intimately connected to the gut microbiota onset and modulation. From 0 to 1 year infant gut interacts with mother and from 2 to 19 years child gut microbiota plays a crucial role in energy storage and metabolism, immune function, barrier integrity, epithelial cell proliferation, and intestinal motility. During toddlerhood, the intake of solid food and the maturation of immune system profoundly modify the gut microbiota profiles toward adult gut microbiota setting. During childhood and in teens, the maturation of hormonal and sexual development, social behavior, and adult-like diet and lifestyle changes continue to affect the gut microbiota shaping (Putignani *et al*.,2014).

Information regarding the structure and function of the gut microbiota during childhood is limited. Although it has been suggested that the microbiota reaches a relatively stable adult-like state in the first three years of life, other evidence indicates that it continues to develop through adolescence. As such, childhood may provide unique opportunities for microbiota interventions to promote health or prevent disease. It is therefore vital to establish a baseline understanding of pediatric gut microbiota structure and function, as during this period the gastro-intestinal tract undergoes a transition from an immature to a mature state (Hollister *et al*., 2015).

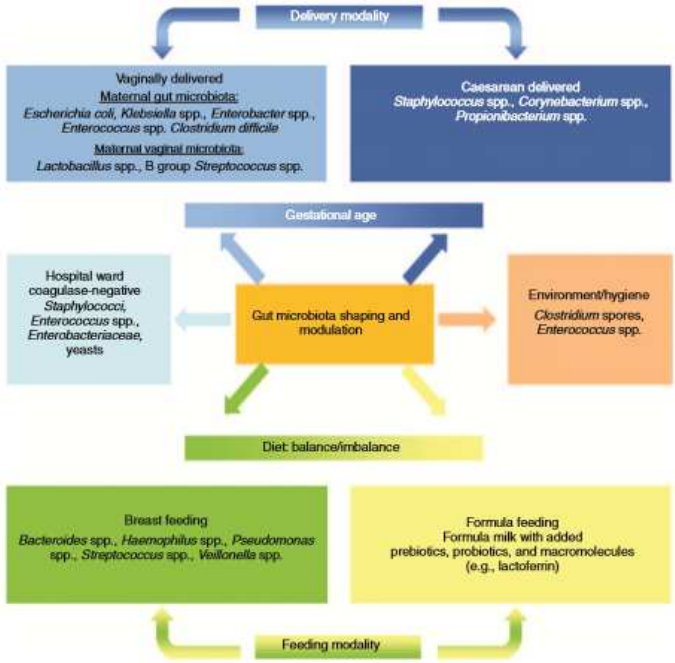

Figure 1.1 Illustration of the main determinants of variability affecting the gut microbiota ecosystem. During early life, several external factors, such as delivery mode, feeding modality, environmental influences, antibiotic exposure, and functional food intake, can affect microbiota shaping and composition. Vaginally born babies acquire bacterial communities that resemble their mother's vaginal microbiota, while Caesarean delivered babies harbor bacterial communities that are similar to the skin surface communities of the mothers. Additionally, breast-fed newborns show a more uniform and stable bacteria population compared with formula-fed newborns. Moreover, the environment during delivery, antibiotic treatment, and hygiene measures can influence the composition of the gut microbiota in neonates. Finally, the intake of functional foods, containing probiotic, prebiotic, or bioactive proteins (e.g., lactoferrin), modify the gut microbiota, reducing pathogen growth (Putignani *et al*., 2014).

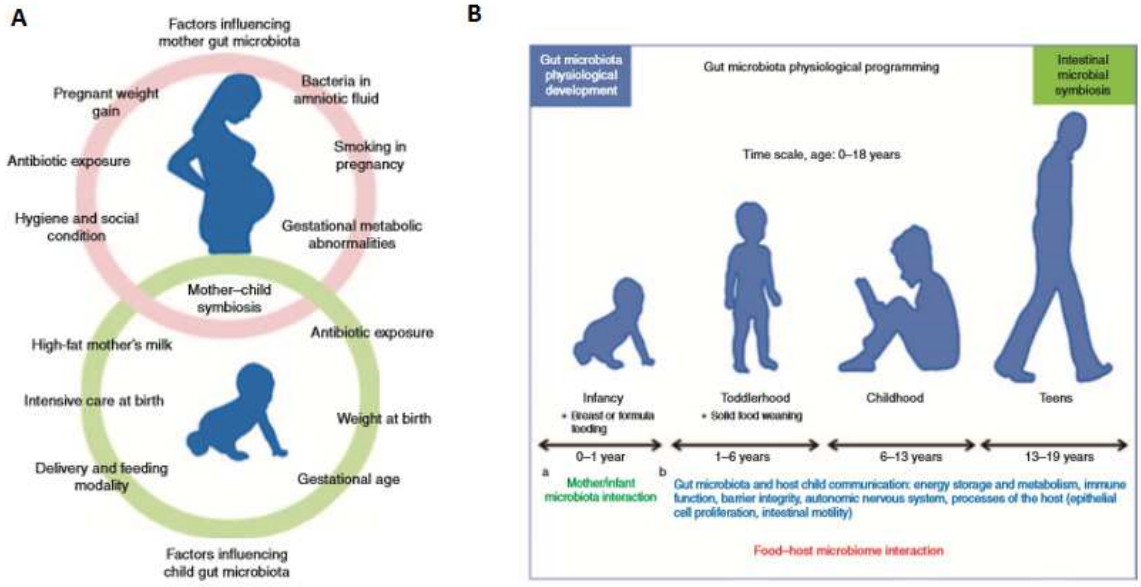

Figure 1.2 (A) Mother–child symbiosis elements affecting the onset and modulation of the newborn gut microbiota. **(B)** Physiological conditions of the gut microbiota during age of development from birth to adulthood (Putignani *et al*., 2014).

1.3 The gut microbiota composition

The microorganisms that inhabit the human gastro-intestinal tract comprise a complex ecosystem with functions that significantly contribute to our systemic metabolism and have an impact on health and disease. The gastro-intestinal ecosystem constituting the microbiota can be represented as a “microbial organ” (named superorgan), located in the host organism (superorganism) and characterized by a dynamic interaction with food and host cells (Putignani *et al.*,2014). In line with its importance, the human gastro-intestinal microbiota has been extensively studied. Despite the fact that a significant part of the intestinal microorganisms has not yet been cultured, presently over 1000 different microbial species that can reside in the human gastro-intestinal tract are composed by all three domains of life: Bacteria, Archaea, and Eukarya (Figure 1.3) (Rajilic´-Stojanovic´ *et al.*, 2014).

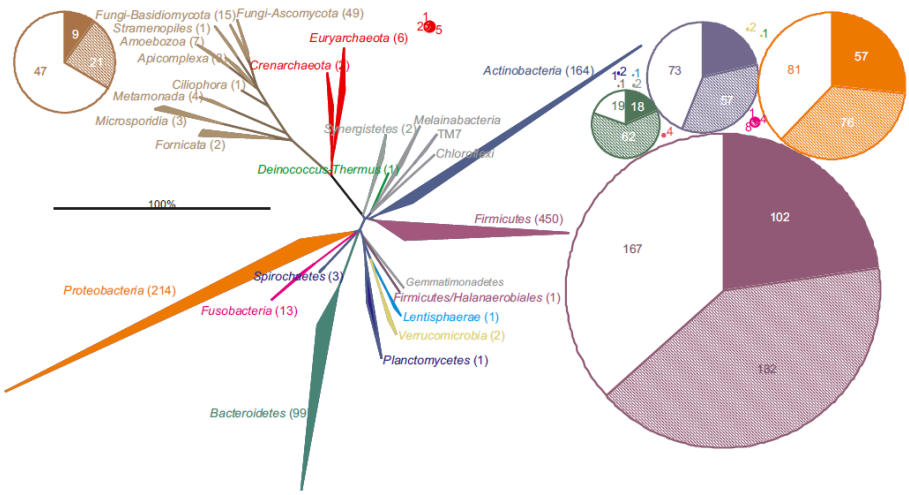

Figure 1.3. Phylogenetic tree of the human gastro-intestinal microbiota. The numbers in parentheses indicate thenumber of cultured species given per phylum. The pie charts illustrate distribution between the number of species with full genome sequence genome (full sectors), the number of species with partial genomesequence (semi full sectors) and number of species without any genome sequence (empty sectors) given for Archaea, Eukarya and per phylum for Bacteria. The color code of pies corresponds to the color code of the phylogenetic tree (Rajilic´-Stojanovi *et a*l.,2014).

It is estimated that the human microbiota contains 10^{14} bacterial cells, a number that is 10 times greater than the number of human cells present in our bodies. The microbiota colonizes virtually every surface of the human body that is exposed to the external environment. Microbes are present on our skin and in the genitourinary, gastro-intestinal, and respiratory tracts. By far the most heavily colonized organ is the gastro-intestinal tract; the colon alone is estimated to contain over 70% of all the microbes in the human body. Additionally, the gastro-intestinal tract is rich in molecules that can be used as nutrients by microbes, making it a preferred site for colonization (Sekirov *et al*., 2010).

The intestinal microbiota is not homogeneous. The number of bacterial cells present in the mammalian gut shows a continuum that goes from 10^1 to 10^3 bacteria per gram of contents in the stomach and duodenum, progressing to 10^4 to 10^7 bacteria per gram in the jejunum and ileum and culminating in 10^{11} to 10^{12} cells per gram in the colon (Figure 1.4). Although there have been over 50 bacterial phyla described to date, the human gut microbiota is dominated by only 2 of them: the *Bacteroidetes* and the *Firmicutes*, whereas *Proteobacteria*, *Verrucomicrobia*, *Actinobacteria*, *Fusobacteria*, and *Cyanobacteria* are present in minor proportions (Sekirov *et al*., 2010). The *Firmicutes* phylum comprises gram positive organisms from greater than 200 different genera including *Catenibacterium*, *Clostridium*, *Eubacterium*, *Dorea*, *Faecalibacterium*, *Lactobacillus*, *Roseburia*, *Ruminococcus*, and *Veillonella* while the *Bacteroidetes* phylum consists of gram negative bacteria from approximately 20 genera including *Bacteroides*, *Odoribacter*, *Prevotella*, and *Tannerella* (John and Mullin, 2016).

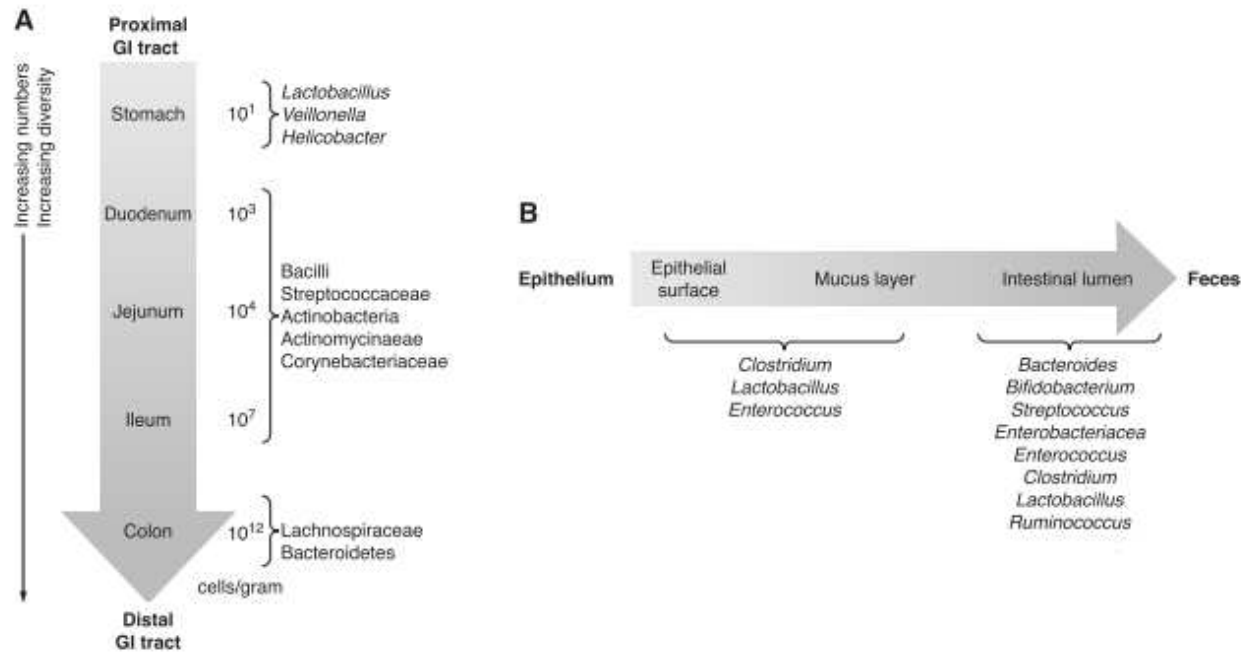

Figure 1.4. Spatial and temporal aspects of intestinal microbiota composition. **(A)** variations in microbial numbers and composition across the length of the gastro-intestinal tract. **(B)** longitudinal variations in microbial composition in the intestine (Sekirov *et al*., 2010).

The mammalian lower gastro-intestinal tract contains a variety of distinct microbial habitats along the small intestine, caecum and large intestine (colon). Physiological variations along the lengths of the small intestine and colon include chemical and nutrient gradients, as well as compartimentalized host immune activity, all of which are known to influence bacterial community composition. The small intestine is more acidic, has a lower pH, lower transit time of complex polysaccharides, higher levels of oxygen and antimicrobials than the colon (Figure 1.5) (Donaldson *et al*., 2015; Swidsinski *et al*., 2007). Therefore, the microbial community of the small intestine is dominated by fast-growing facultative anaerobes that tolerate the combined effects of bile acids and antimicrobials while still effectively competing with both the host and other bacteria for the simple carbohydrates that are available in this region of the gastro-intestinal tract. Bile acids, secreted through the bile duct at the proximal end of the small intestine, are bactericidal to certain species owing to their surfactant properties and are known to broadly shape the composition of the microbiota, especially in the small intestine (Donaldson *et al*., 2015).

The bacteria in the small intestine are potentially competing with the host for nutrients, host-derived bile acids and antimicrobial peptides limit bacterial growth to low densities in proximal regions. Only at the distal end of the small intestine, in the terminal ileum, bacterial densities reach saturating levels similar to those found in the large intestine (Figure 1.5). The caecum and colon cultivate the most dense and diverse communities of all body habitats. In the caecum and colon, microorganisms are responsible for the breakdown of otherwise 'resistant' polysaccharides that are not metabolized during transit through the small intestine. Lower concentrations of antimicrobials, slower transit time and a lack of available simple carbon sources facilitate the growth of fermentative polysaccharide-degrading anaerobes, notably the *Bacteroidaceae* and *Clostridia* (Donaldson *et al*., 2015).

In the mouse, the caecum is enriched in species of the families *Ruminococcaceae* and *Lachnospiraceae*, whereas the colon is enriched in members of the families *Bacteroidaceae* and *Prevotellaceae* (Gu *et al*., 2013). Species from the family *Rikenellaceae* are prominent in both the caecum and the colon (Gu *et al*., 2013). As well as the variation in microbial community composition longitudinally within the gut, various host factors drive community differences over the cross-sectional axis of the gut. The entire wall of the colon folds over itself, creating compartments between folds (inter-fold regions) that are distinct from the central lumenal compartment (Figure 1.5). In mouse studies that used laser capture microdissection to profile the composition of the microbial communities in discrete regions, significant differences were observed between the central lumenal compartment and the inter-fold regions (Nava *et al*., 2011; Pédron *et al*., 2012). Specifically, the *Firmicutes* families *Lachnospiraceae* and *Ruminococcaceae* were enriched between folds, whereas the *Bacteroidetes* families *Prevotellaceae*, *Bacteroidaceae* and *Rikenellaceae* were enriched in the digesta (Nava *et al*., 2011). Relative to the digesta, the inter-fold regions are likely to contain greater amounts of mucus, which can serve as a nutrient source for certain bacteria (Donaldson *et al*., 2015).

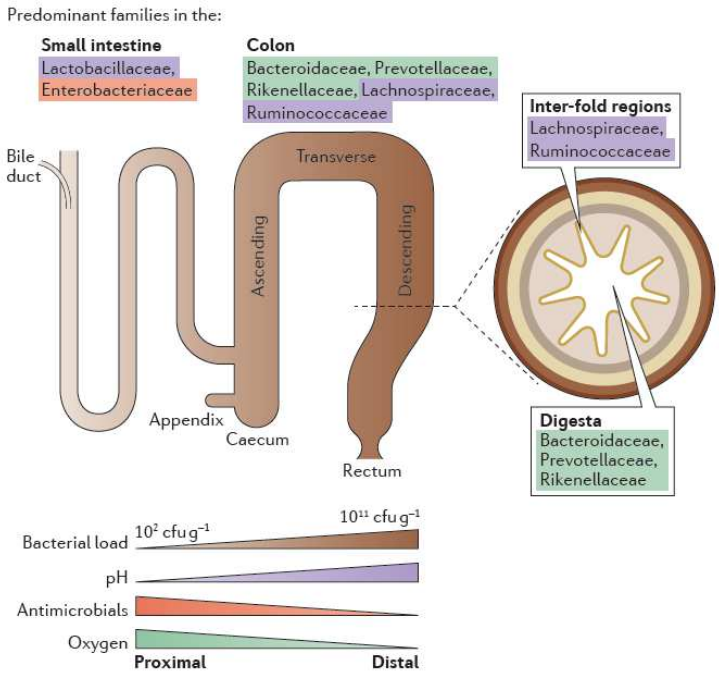

Figure 1.5. Microbial habitats in the human lower gastro-intestinal tract. The dominant bacterial phyla in the gut are *Bacteroidetes*, *Firmicutes*, *Actinobacteria*, *Proteobacteria* and *Verrucomicrobia*. The dominant bacterial families of the small intestine and colon reflect physiological differences along the length of the gut. For example, a gradient of oxygen, antimicrobial peptides (including bile acids, secreted by the bile duct) and pH limits the bacterial density in the small intestinal community, whereas the colon carries high bacterial loads. In the small intestine, the families *Lactobacillaceae* and *Enterobacteriaceae* dominate, whereas the colon is characterized by the presence of species from the families *Bacteroidaceae*, *Prevotellaceae*, *Rikenellaceae*, *Lachnospiraceae* and *Ruminococcaceae* (colours correspond with the relevant phyla). A cross-section of the colon shows the digesta, which is dominated by *Bacteroidaceae*, *Prevotellaceae* and *Rikenellaceae*, and the inter-fold regions of the lumen, which are dominated by *Lachnospiraceae* and *Ruminococcaceae*. cfu, colony-forming units (Donaldson *et al*., 2015).

1.3.1 Paneth cells

The large and small intestine are lined with a single layer of columnar epithelial cells that are linked *via* complexes of junctional proteins and desmosomes creating a sealed yet dynamic barrier. Enterocytes and enteroendocrine cells are found throughout the gastro-intestinal tract and are involved in nutrient and water absorption and hormone production (Bowcutt *et al*., 2014). The base of the crypts in the gastro-intestinal tract contain undifferentiated stem cells from which progenitor cells are derived and develop into any of one of four major differentiated epithelial cell types; enterocytes, Paneth cells, goblet cells, enteroendocrine cells (Bowcutt *et al*., 2014; Kim and Ho, 2010).

Paneth cells, a specialized lineage of cells unique to the small intestine, are a major source of antimicrobial peptides (AMPs) including α-defensins, lysozyme, ribonucleases [such as angiogenin 4 (ANG4)], secretory phospholipase A2 and C-type lectins [such as the regenerating islet derived protein (REG3) family]. AMPs are thought to act as mediators in host defence against pathogens and in shaping the microbiome composition for the maintenance of homeostasis. AMPs such as REG3γ and REG3β promote spatial segregation of microbial populations from the epithelial surface of the small intestine. AMPs also help shape microbial diversity and thus may contribute to the relatively low bacterial burden in the duodenum compared with the large intestine. In addition to the production of AMPs, Paneth cells may directly recognise pathogens *via* pattern recognition receptors enabling them to initiate innate immune responses (Bowcutt *et al*., 2014; Nakamura *et al*., 2016).

1.3.2 Goblet cells and mucus layer: structure and composition

Goblet cells exhibit a non-homogenous distribution along the intestinal epithelium. The proportion of goblet cells among epithelial cell types increases caudally from duodenum (4%) to distal colon (16%), similar to the increasing number of microbial organisms present in the proximal intestine to colon (Kim and Ho, 2010). They release a panel of bioactive compounds including mucins, AMPs such as resistin-like molecule β (Relmβ), ANG4, REG3γ, regenerating REG3β and trefoil peptides that further contribute to innate immune defence (Bowcutt et al., 2014).

Another important role perfomed by goblet cells is mucus secretion forming a mucus layer of varying thickness that partially or fully covers the epithelium, creating a boundary between the gut lumen and the host tissue (Figure 1.6) (Donaldson *et al*., 2015; Kim and Ho, 2010).

The small intestine harbours a single, tightly attached mucus layer (Figure 1.6A). In the colon, mucus is organized into two distinct layers: an inner, stratified mucus layer that is firmly adherent to the epithelial cells and approximately 50 μm thick in the mouse; and an outer, non attached layer that is usually approximately 100 μm thick as measured in mouse layers (Figure 1.6B) (Li *et al*., 2015;

Johansson *et al*, 2011). The inner mucus layer is dense and theoretically does not allow bacteria to penetrate, thus keeping the epithelial cell surface free from bacteria. Interestingly other evidence suggest that tightly adhering inner mucus layer and the crypts could be penetrated at low density by a more restricted community that includes *Bacteroides fragilis* and *Acinetobacter* spp. (Donaldson *et al*, 2015, Nava et al., 2011; Pédron *et al*., 2012). The mucus is continuously secreted and the inner mucus layer is converted into the outer layer, which is the habitat of the commensal microbiota. The outer mucus layer has an expanded volume due to proteolytic activities provided by the host but probably also caused by commensal bacterial proteases and glycosidases. In mice, a viscosity gradient of the gel-forming mucus increases from the proximal colon (which includes the caecum and the ascending and transverse colon) to distal colonic sites (which include the descending colon and the sigmoid colon connecting to the rectum). In addition to mucus density, itself serving as a physical obstacle for microorganisms, antimicrobial molecules and oxygen secreted from the epithelium accumulate at high local concentrations within the mucosa, especially in the small intestine, greatly restricting potential microbial inhabitants (Figure 1.6A). Therefore, the mucus layers of the gastro-intestinal tract creates distinct environments for specific bacterial ecosystems that thrive in proximity to host tissue (Donaldson *et al*, 2015).

Many diseases of the gastro-intestinal tract and extra-intestinal conditions are associated with intestinal barrier alterations. This includes both functionality (permeability) and immune or structural parameters of the barrier such as secretion of antimicrobial peptides and mucins, in which the microbiota can play a central role. Alterations in barrier function by bacteria has been associated in animal studies with increases in translocation of bacteria, uptake of microbial products and dietary antigens, and it has been proposed that this could promote a proinflammatory state. Clinically, small intestinal bacterial overgrowth is associated with changes in barrier function in humans, however mechanisms and bacterial culprits or constituents are unknown (McCarville *et al*., 2016).

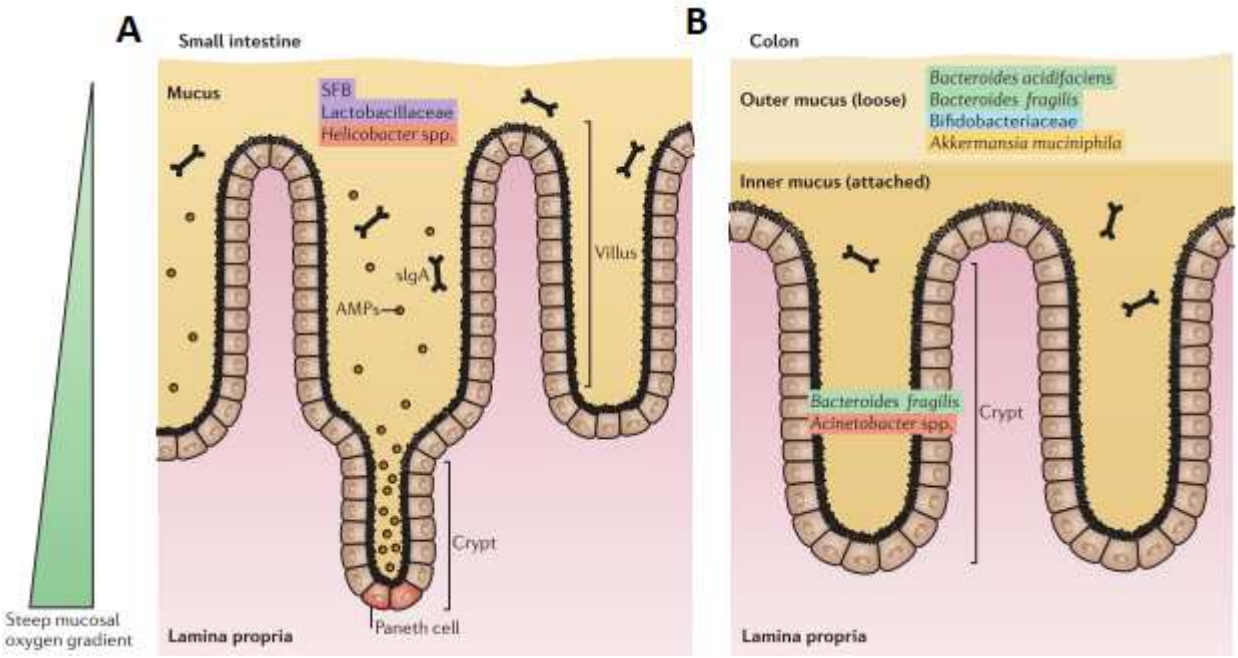

Figure 1.6. The mucus layers of the small intestine and colon. Several factors limit the ability of gut bacteria to access host cells, such as the mucus layers in the small intestine and the colon; antimicrobial peptides (AMPs) in the small intestine, including those produced by Paneth cells at the base of the crypts; secreted immunoglobulin A (sIgA) in both the small intestine and colon; and a steep oxygen gradient that influences which bacteria are capable of surviving close to the epithelial surface. (**A)** The surface of the small intestine is shaped into villi and crypts and is colonized by certain adherent species, including segmented filamentous bacteria (SFB), *Lactobacillaceae* and *Helicobacter* spp. (**B)** The colon has two distinct mucus structures: the loose outer layer is colonized by mucin-degrading bacteria and is characterized by the presence of *Bacteroides acidifaciens*, *Bacteroides fragilis*, *Bifidobacteriaceae* and *Akkermansia muciniphila*; the tightly adhering inner mucus layer and the crypts are penetrated at low density by a more restricted community that includes *Bacteroides fragilis* and *Acinetobacter* spp. (Donaldson *et al*., 2015).

1.3.3 MUC2

Up to 20 different mucin genes have been identified, from MUC1 to MUC20 according to order of their discovery. Mucin genes are expressed in tissue and cell type-specific manner and are broadly classified into two types, secretory and membrane-associated. Gel-forming secretory mucins such as MUC2, MUC5AC, MUC5B, and MUC6 are localized on chromosome 11.5.5 as a cluster. In small and large intestine, MUC2 is the major secretory mucin synthesized and secreted by goblet cells, whereas goblet and absorptive cells express membrane-bound mucins, MUC1, MUC3, MUC4, MUC13, and/or MUC17, in the apical membrane. Secretory and membrane mucins have distinct structural features and biosynthetic pathways. MUC2 is the first human secretory mucin to be

identified and characterized (Kim and Ho, 2010) and typically the mucus is structurally built around the MUC2 mucin that after secretion from the goblet cell expands dramatically and forms sheets of MUC2 networks that stack and form the stratified mucus layer (Jakobsson *et al*, 2015). The MUC2 mucin encodes a protein of approximately 5200 amino acids. Its central part contains two so-called PTS domains which are rich in the amino acids proline (P), threonine (T) and serine (S). PTS domains are often highly repetitive (as in the second MUC2 domain) but lack sequence conservation between species. The abundant hydroxy amino acids act as attachment sites for the O-glycans. Once the mucin apoprotein reaches the Golgi apparatus, it is densely decorated by consecutive additions of monosaccharides. These highly glycosylated domains are called mucin domains and characterize all mucins. The O-glycans make the mucin domains highly protease resistant and give mucins their high waterbinding capacity (Swidsinski *et al*., 2007) (Figure 1.7).

Commensal bacteria use these glycans as an important energy source. That commensal bacteria have the opportunity to degrade indigestible glycans has been crucial for the coevolution of host and its microbiota, because this increases the energy extraction from food significantly. The bacteria use its high number of glycan hydrolytic enzymes to degrade polysaccharides and other glycoconjugates that come to the colon from food via the small intestine. However, it is not only the extra energy that comes from the nondigestible food important, the bacterial degradation of the mucins and glycans also provide significant energy. This will allow the host to recover some of the energy spent to produce the protective mucus (Johansson *et al*, 2011). The numerous O-glycans on the MUC2 mucin not only serve as nutrients for the bacteria but also as attachment sites and, as such, probably contribute to the selection of the species-specific colonic microbiota (Johansson *et al*, 2011).

The removal of microbiota accessible carbohydrates, which are typically abundant in dietary fiber and serve as primary metabolic input for the gut microbiota, shift the balance of the microbiota towards mucus-consuming bacteria (Earle *et al*, 2015). The mucosa-associated microbial composition differs from the luminal content and can be particularly important for nutrient exchange,

communication with the host, development of the immune system, and resistance against invading pathogens (Ouwerkerk *et al*, 2013). It has been demonstrated in mice that the mucosa-associated microbiota has adapted to the glycan rich environment by the production of mucus-degrading enzymes and mucus-binding extracellular proteins, and include mucus degrading specialists such as *Akkermansia muciniphila*, *Bacteroides thetaiotaomicron* (Ouwerkerk *et al*, 2013) and *Bacteroides acidifaciens* (Donaldson *et al*, 2015).

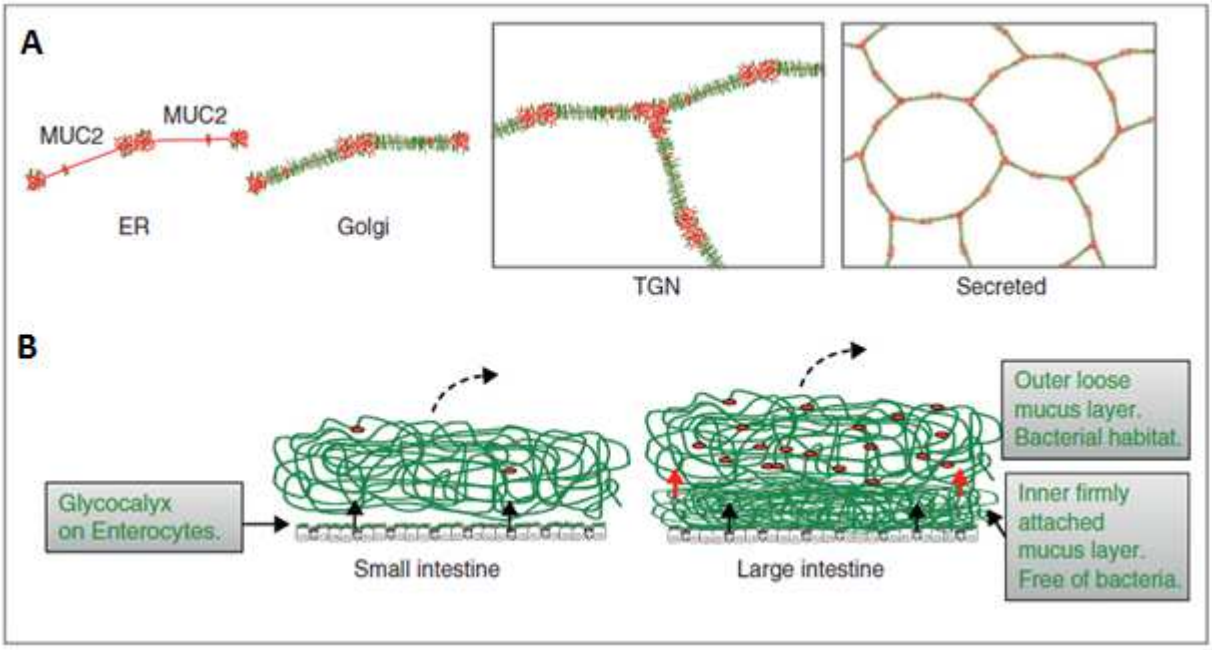

Figure 1.7. Schematic outline of the MUC2 mucin and its formation of mucus in the small and large intestine. **(A)** Assembly of the MUC2 mucin (protein core red) into dimeric forms in the endoplasmic reticulum (ER), O-glycosylation (green) in the Golgi apparatus, formation of trimeric forms in the trans Golgi network (TGN) and a schematic picture of the secreted MUC2 polymer. **(B)** The MUC2 mucin is secreted from the goblet cells (black arrows) to form the mucus. Colon has a two layered mucus where the inner layer is converted (red arrows) to the outer mucus layer. The stomach has a mucus essentially as that of colon (not shown). Red dots symbolize bacteria (Swidsinski *et al*., 2007).

1.3.4 Mucosa-associated microbiota has distinct composition

Within the mucus layer the *Firmicutes* are generally higher in abundance compared to the *Bacteroidetes* both in humans and rodents. The mucosa-associated microbiota in the ascending, transverse, and descending colon is highly similar within individuals (Ouwerkerk *et al*., 2013). Studies based on 16S RNA gene sequences in mice show an increased abundance of the following genera and species in the mucosa: *Lachnospiraceae, Ruminococcaceae* (Nava *et al*., 2011) and both *Bifidobacterium bifidum* and *Bifidobacterium longum* (Van den Abbeele *et al*., 2011). Bacteria belonging to *Clostridium* cluster XIVa have been associated in vitro with the colonization of a mucin rich environment, and include butyrate producers *Retortamonas intestinalis* and *Eubacterium rectale* (Van den Abbeele *et al*., 2012). The *Verrucomicrobia* were found to be enriched in the mucus layer compared to the luminal content, implicating colonization of the only known *Verrucomicrobia* in the gut: the mucus degrading *Akkermansia muciniphila* (Derrien *et al*., 2004). Additional evidence comes from fluorescence *in situ* hybridization (FISH) based studies showing that mucosa-associated bacteria include the following family, genera and species in human: *Lachnospiraceae*, *Enterobacteriaceae*, *Bacteroides*, *Eubacterium rectale*, *Faecalibacterium prausnitzii*, *Eubacterium cylindroides*, *Clostridium histolyticum*, *Clostridium lituseburense* (Swidsinski *et al*., 2008). Not found but predicted to colonize close to the mucus layer are sulphate-reducing bacteria, methanogenic archaea and acetogenic bacteria, all hydrogenotrophic microbes that are associated with the colonic mucosa of healthy subjects (Nava *et al*., 2012; Ouwerkerk *et al*., 2013).

1.3.5 Mucin-degrading specialists

Mucus-degrading bacteria have an advantage in the mucosal niche that is rich in endogenous glycoproteins both from excreted mucin proteins and shed epithelial cells. However, these bacteria need several linkage specific enzymes to degrade the highly diverse glycans present in the mucus layer, such as glycosidases, sulphatases, and sialidases. After degradation there are several microbial

strategies to harvest the glycans, including the starch utilization system (Sus)-like system of the Gram negative *Bacteroidetes* and ABC transporters for carbohydrate uptake in Gram-positive bacteria (Koropatkin *et al*., 2012). Mucus-degrading specialists possess a variety of enzymes to degrade the mucus glycans, subsequently harvest the oligosaccharides for their own metabolism, and therefore have a colonization advantage competing for this niche. A second advantage is that their energy source is permanently present, because the production of endogenous mucins is not depending on the diet that may fluctuate. Mucin-degrading specialists are scattered among the microbiota-associated phyla and include the following species: *Akkermansia muciniphila*, *Bacteroides thetaiotaomicron*, *Bifidobacterium bifidum*, *Bacteroides fragilis*, *Ruminococcus gnavus*, and *Ruminococcus torques*. These specialists degrade the mucin protein, which possibly leads to the availability of oligosaccharides for other bacteria that do not harbour the correct enzymes for this process (Ouwerkerk *et al*., 2013).

1.4 The role of the gut microbiota

The gut microbiota is involved in the regulation of multiple host pathways and participates in metabolic and immune-inflammatory axes connecting the gut with the liver, muscle, and brain. (Nicholson *et al*., 2012). Compositional alterations that disturb the normal balance of the gut microbiota, a phenomenon referred as gut dysbiosis, may promote or cause the development of metabolic disorders such as obesity, as well as gut diseases such as inflammatory bowel disease and colon cancer (Figure 1.8).

Gut microbes exert a wide variety of physiological functions that have an influential role in intestinal and extra-intestinal homeostasis (Fernandez *et al*., 2014). The gut microbiota has critical roles in the protection against pathogenic bacteria producing bacteriocins, blocking adhesion of pathogens and in the fermentation of indigestible plant polysaccharides (see paragraph below) and host-produced

glycans (e.g.mucin) (Milani *et al*., 2016). In particular, the microbiota is involved in the production of vitamin K, multiple B vitamins, H_2, CO_2, methane gas, lysine, and the conversion of urea to ammonia. It also metabolizes ingested foreign compounds (xenobiotics) and modulates the enter-hepatic circulation of compounds detoxified by the liver and excreted in the bile.

Commensal microorganisms have important roles in the development and in the modulation of the immune system and in the production of secretory IgA (Tsai *et al*., 2009). There is evidence that the gut microbiota exerts a key role in inducing immunoglobulin A production, as well as maintaining the homeostasis of several T cell populations in the gut, including regulatory T cells (Treg), T helper 1 (Th1) and T helper 17 (Th17) cells and also mucosal-associated T cells (Milani *et al*.,2016). Certain microbiota components have been shown to promote Treg development (*Bacteroides fragilis*, *Clostridium* strains, *Lactobacillus* spp and *Bifidobacterium* spp), whereas others induce Th17 development (*Candidatus arthromitus*). A balanced autochthonous microbiota is required to drive the normal development of both mucosa-associated lymphoid tissue and mucosally-induced tolerance mechanisms involving the generation of Treg cells (Milani *et al*., 2016) (Figure 1.8).

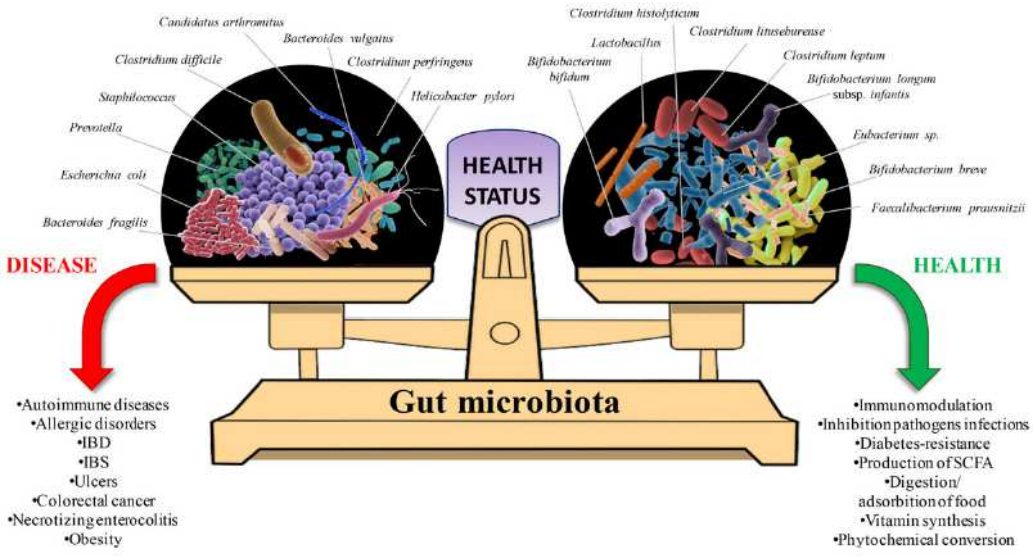

Figure 1.8. Schematic representation of the functional roles of key members of the human gut microbiota in health and disease. IBD, inflammatory bowel disease; IBS, irritable bowel syndrome; SCFA, short-chain fatty acid.(Milani *et al*., 2016).

1.4.1. Short chain fatty acids (SCFAs)

One of the main activities of the gut microbiota is to breakdown substrates such as resistant starch and dietary fiber, which are incompletely hydrolyzed by host enzymes in the small intestine. The main fermentation products resulting from fiber degradation are the short chain fatty acids (SCFAs) acetate, propionate, and butyrate (Schwiertz *et al*., 2009). SCFAs concentration are highest in the large intestine, mainly because of greater carbohydrate availability. Studies using intestinal material obtained from human sudden death victims found that acetate:propionate:butyrate values were similar in different regions of the large intestine (about 57:22:21) (Macfarlane S and Macfarlane G, 2003). SCFAs play different roles in energy salvage: normal colonic epithelia derive 60–70% of their energy supply from SCFAs, particularly butyrate. Propionate is largely taken up by the liver and is a good precursor for gluconeogenesis, liponeogenesis and protein synthesis and acetate enters the peripheral circulation to be metabolized by peripheral tissues and is a substrate for lipid and cholesterol synthesis (Martins dos Santos *et al*., 2010). Moreover, intracellular butyrate and propionate (but not acetate) inhibit the activity of histone deacetylases (HDACs) in colonocytes and immune cells, which promotes the hyperacetylation of histones, in addition to some transcription factors and proteins that are involved in signal transduction. This has multiple consequences for gene expression and cellular differentiation, including the downregulation of pro-inflammatory cytokines, such as interleukin-6 (IL-6) and IL-12 in colonic macrophages (Louis *et al*., 2014).

1.4.2 Microbial production of SCFAs

The production of microbial SCFAs is influenced by diet. Between 10% and 20% of ingested dietary carbohydrates are resistant to small intestinal digestion, increasing colonic fermentation, gut transit and stool output and decreasing the pH of the intestinal lumen. These non-digestible dietary carbohydrates include certain forms of starch that are resistant to amylase digestion (resistant starch: cereals, raw banana, potato) as well as non-starch polysaccharides (pectin, cellulose). Non-digestible

dietary carbohydrates enter the colon and are fermented by colonic bacteria to SCFA, lactate, and gases such as CO2, H2, and methane (Ramakrishna *et al*., 2013).

The relative synthesis of the different fermentation products varies according to the composition of the microbiota and environmental conditions, including pH, hydrogen partial pressure and available substrates (Louis *et al*., 2014).

Acetate, which is the most abundant SCFA, is produced by most enteric bacteria as a fermentation product, but it is also formed by acetogenic bacteria, such as *Blautia hydrogenotrophica*, from H_2 and CO_2 or from formate via the Wood–Ljungdahl pathway (Figure 1.9). Acetogenic bacteria can produce three molecules of acetate from one molecule of glucose, but non-acetogenic anaerobes which comprise most of the microbiota, these produce other SCFAs in addition to or instead of acetate, including succinate, propionate, butyrate, formate, d-lactate, l-lactate (Figure 1.9) (Louis *et al*., 2014). Propionate is mostly formed via the succinate pathway by *Bacteroidetes* and by some *Firmicutes* that belong to the *Negativicutes* class (such as *Phascolarctobacterium succinatutens*, *Dialister* spp. and *Veillonella* spp.). Succinate is a metabolic end-product for some bacteria under some environmental conditions. Two other pathways also contribute to the formation of propionate: the acrylate pathway and the propanediol pathway (Figure 1.9). The acrylate pathway, in which lactate is a substrate, shows a limited distribution, whereas the propanediol pathway, in which deoxyhexose sugars (such as fucose and rhamnose) are substrates, is present in some *Firmicutes* (including *Roseburia inulinivorans* and *Ruminococcus obeum*) and in *Proteobacteria*. The proportion of propionate that is present in total faecal SCFA correlates with the relative abundance of *Bacteroidetes*, which confirms that the succinate pathway is the dominant source of propionate (Louis *et al*., 2014).

Analysis of the genetic potential of gut microbiota indicates that *Bacteroides* species possess genes for a large number of enzymes involved in carbohydrate utilization including glycoside hydrolases, glycosyl transferases, polysaccharide lyases, and carbohydrate esterases. *Bacteroides* are able to degrade non-digestible dietary carbohydrates as well as host carbohydrates including mucus proteins,

and may switch to the latter when dietary non-digestible dietary carbohydrates are less abundant (Ramakrishna *et al*., 2013) producing high levels of acetate and propionate (Martins dos Santos *et al*., 2010).

Butyrate is produced by some *Firmicutes* using either the butyryl-CoA:acetate CoA-transferase enzyme or, less commonly, phosphotransbutyrylase and butyrate kinase to catalyse the final steps of the pathway (Figure 1.9). Species that use the butyryl-CoA:acetate CoA-transferase route include several of the most abundant species in the healthy gut microbiota (including *Faecalibacterium prausnitzii*, *Roseburia* spp., *Eubacterium rectale*, *Eubacterium hallii* and *Anaerostipes* spp.) which are generally net users of acetate such that the concentration of acetate in the gut lumen is determined by the balance of production, use and mucosal uptake. A subset of *Lachnospiraceae*, including *Eubacterium hallii* and *Anaerostipes* spp., can use lactate and acetate to produce butyrate. Thus, these organisms may have an important role in stabilizing the microbial ecosystem by preventing the accumulation of lactate (Louis *et al*., 2014).

Bacteria belonging to *Clostridium* clusters IV (*Clostridium leptum*, *Ruminococcus bromii*, and *Faecalibacterium prausnitzii*) and XIV (*Clostridium coccoides*, *Eubacterium rectale*, *Roseburia* species, and *Butyrivibrio fibrisolvens*) are considered to be very important carbohydrate-fermenting bacteria that are particularly effective in fermenting starch with the production of butyrate (Martins dos Santos *et al*., 2010; Ramakrishna *et al*., 2013). Moreover, members of *Clostridium* cluster XIVa convert lactate produced by several microbial species from carbohydrate to butyrate while members of *Clostridium* cluster IX convert lactate to propionate (Ramakrishna *et al*., 2013).

Bifidobacterium strains have been reported to be very good at hydrolyzing high amylose starch (resistant starch), because they have a metabolic pathway that utilize human milk oligosaccharides and host glycoproteins. *Bifidobacterium longum* and *Bifidobacterium adolescentis* produce acetate from glucose while the former has an ATP-binding cassette-type carbohydrate transporter that also allows it to use fructose to produce acetate (Ramakrishna *et al*., 2013) (Figure 1.9).

Only a few anaerobes are known to produce both propionate and butyrate, and they do so from different substrates: *Roseburia inulinivorans* produces butyrate from glucose and produces propionate from fucose, whereas *Coprococcus catus* produces butyrate from fructose and produces propionate from lactate (via the acrylate pathway) (Louis *et al*., 2014).

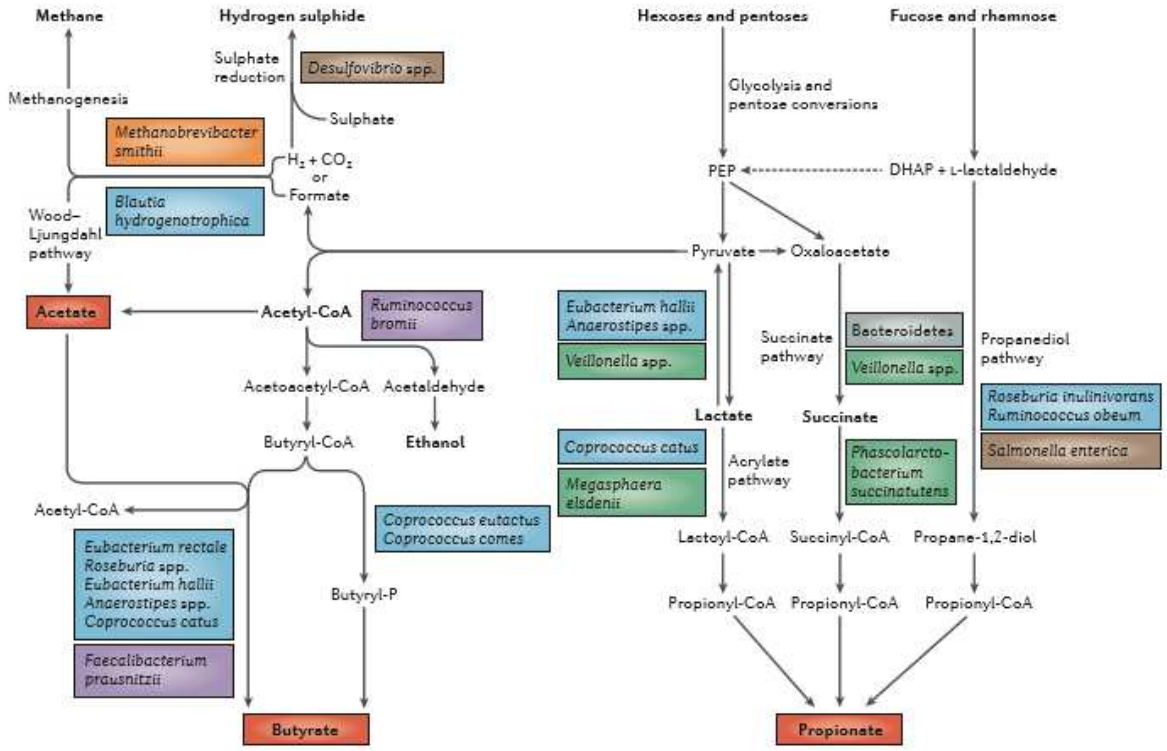

Figure 1.9. Pathways that are responsible for the biosynthesis of the major microbial metabolites that result from carbohydrate fermentation and bacterial cross-feeding. Of the three main short-chain fatty acids (SCFAs; shown in red), acetate can be produced by many enteric bacteria from pyruvate via acetyl-CoA and also via the Wood–Ljungdahl pathway by acetogens, such as *Blautia hydrogenotrophica*. Butyrate is formed from two molecules of acetyl-CoA by several *Firmicutes*, and the butyryl-CoA:acetate CoA-transferase is usually used to catalyze the last enzymatic step41. The main propionate production pathway is the succinate pathway, which is used by *Bacteroidetes* to generate propionate from carbohydrates and by some *Firmicutes* to produce propionate from lactate or succinate. Two other propionate formation pathways are found in some gut bacteria: the acrylate pathway, which uses lactate, and the propanediol pathway, which uses deoxyhexose sugars (such as fucose and rhamnose). Pathways that are involved in hydrogen metabolism and ethanol production are also shown. The bacterial species that are shown are based on studies of cultured isolates of dominant species and metagenomic analyses and are thus not exhaustive. Archaea are shown in orange, *Bacteroidetes* are shown in grey, *Lachnospiraceae* (*Firmicutes*) are shown in blue, *Ruminococcaceae* (*Firmicutes*) are shown in purple, *Negativicutes* (*Firmicutes*) are shown in green and *Proteobacteria* are shown in brown. DHAP, dihydroxyacetonephospate; PEP, phosphoenolpyruvate (Louis *et al*., 2014).

1.5 Techniques to study the gut microbiota

Traditionally, gastro-intestinal bacteria have been studied via cultivation-based techniques, recently, findings from culture-based methods have been supplemented with molecular ecology techniques that are based on the 16S rRNA gene. These techniques enable characterization and quantification of the microbiota, while also providing a classification scheme to predict phylogenetic relationships (Zoetendal *et al*., 2004). In recent years, several next-generation sequencing technologies have been developed, which further facilitate the analysis of a large number of microorganisms in different environments and human body sites, including the human gut. 16S rRNA sequence analysis and metagenomics are two effective sequencing approaches, and both have been used to study uncultivated gut microbial communities. The research based on 16S rRNA sequence attempts to reveal "who's there?" in a given microbial community, while shotgun metagenomic sequencing can be used to answer the complementary question of "what can they do?" (Wang *et al*., 2015).

The choice of a particular molecular-based approach depends on the questions being addressed. Microbial community structure can be analyzed via fingerprinting techniques, fluorescence *in situ* hybridization to measure abundance of particular taxa. Others approaches, such as those based on functional genes and their expression and the combined use of stable isotopes and biomarkers, are being developed and optimized to study metabolic activities of groups or individual organisms *in situ* (Zoetendal *et al*., 2004) (Figure 1.10).

1.5.1 Fingerprinting techniques

Several so-called fingerprinting techniques have been used to study bacterial communities and appear to be ideal for monitoring community shifts and comparing communities between gastro-intestinal sites and among animals. Denaturing gradient gel electrophoresis (DGGE) was first applied in microbial ecology to study bacterial diversity in a marine ecosystem. Since this pioneering study, a

variety of microbial ecosystems have been analysed using DGGE or similar techniques, including temperature gradient gel electrophoresis (TGGE), and only occasionally temporal temperature gradient gel electrophoresis (TTGE). Two additional microbial community fingerprinting techniques are single strand conformation polymorphism (SSCP) and terminal-restriction fragment length polymorphism (TRFLP) analyses. Although the principles and technical procedures vary, all microbial community fingerprinting techniques are PCR-based and generate profiles representing the sequence diversity within the selected ecosystem. DGGE, TGGE, and TTGE are based on sequence-specific melting behaviour of amplicons, SSCP on the secondary structure of single stranded DNA, and T-RFLP on specific target sites for restriction enzymes. Interestingly, with the exception of T-RFLP, all other techniques have been used successfully in mutation detection in clinical research before being applied to microbial ecology, which demonstrates their discriminative power (Zoetendal *et al*., 2004).

1.5.2 Fluorescence *in situ* hybridization

A frequently applied culture-independent approach to quantify bacterial cells in environmental samples is FISH using SSU rRNA-targeted oligonucleotide probes. This method combines the power of SSU rRNA probe hybridization with epiflourescent light microscopy, confocal laser microscopy, or flow cytometry for direct quantification of individual bacteria. This approach can be used to determine the relative importance of specific groups or genera of bacteria. FISH is being increasingly used to study the bacterial composition of the gastro-intestinal tract (Zoetendal *et al*., 2004) and it has been automated and combined with computerized image analysis (Daims, 2009). FISH enables five ecological issues to be addressed simultaneously: 1) to identify subpopulations in natural ecosystems and to locate their habitat; 2) to obtain information on community structure by using nested sets of probes; 3) to circumvent cultivation problems; 4) to determine in situ cellular rRNA content; and 5) to accurately enumerate defined cell populations (Zoetendal *et al*., 2004).

1.5.3 Sequencing of SSU rRNA clone libraries

The construction of small subunit (SSU) rRNA libraries is required to inventory bacteria and archaea present in a given environment. In fact, sequencing of SSU rRNA genes has became a standard procedure in the identification of isolates, and it is now impossible to adequately describe microbial communities without SSU rRNA sequence data (Zoetendal *et al*., 2004).

As the 16S rRNA gene is universally present across bacteria, is highly conserved, and can be easily amplified using universal primers, environmental microbial analyses are often performed using 16S rRNA amplicon sequencing. Although the 16S rRNA gene is highly conserved, there are nine hypervariable regions that can be used to distinguish between different organisms. The typical pipeline for 16S amplicon analyses starts with using primers designed to amplify the hypervariable regions of the 16S rRNA gene (typically the V1–V3 region or the V3–V5 region). Sequences are clustered into bins called 'Operational Taxonomic Units' (OTUs) based upon similarity. A common similarity threshold used is 97%, which was derived from an empirical study that showed most strains had 97% 16S rRNA sequence similarity (Nguyen *et al*., 2016).

After library construction, the sequences of the cloned amplicons are determined and compared to sequences deposited databases (http://www. ncbi. nlm.nih.gov/BLAST/ and http://rdp.cme.msu.edu/html), and followed by phylogenetic analysis. Sequencing of SSU rRNA clone libraries from human feces, colonic and ileal samples and the oral cavity have confirmed that a significant fraction of resident bacteria have not been described previously (Zoetendal *et al*., 2004).

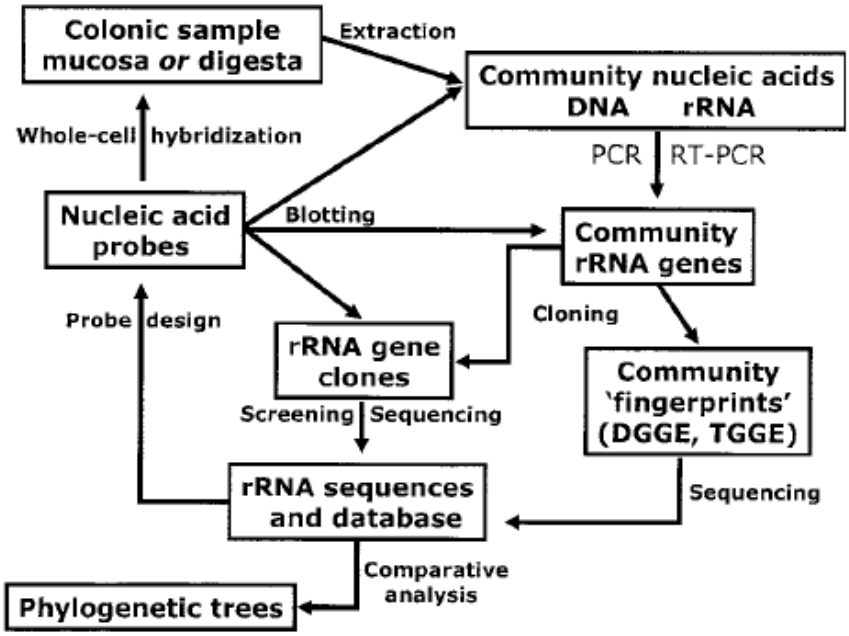

Figure 1.10. Molecular methods used singularly or in combination to analyse complex microbial ecosystems (Zoetendal *et al*., 2004).

1.5.4 Metagenomics, metatrascriptomics, metaproteomics and metabolomics

Metagenomics is an extremely powerful tool that can be used to describe the genetic potential of the microorganisms present in a given environment. Metagenomics can be used to study intestinal microbiome diversity and dysbiosis, as well as its relationship to health and disease. Moreover, functional metagenomics can identify novel functional genes, microbial pathways, antibiotic resistance genes, functional dysbiosis of the intestinal microbiome, and determine interactions and co-evolution between microbiota and host. However, it has a very limited function in revealing their activity or gene expression. With the rapid development of metatranscriptomics, metaproteomics and metabolomics, the functional activity of a microbial community can be identified. Metatranscriptomic sequencing can be used to determine the activity of genes in a defined environment and metabolomics can disentangle the complex array of proteins produced by the intestinal microbiota. Some human intestinal disorders, such as colorectal cancer, inflammatory bowel disease and irritable bowel syndrome (IBS), have been studied using metabolomics. On the one hand, the metabolomics databases, as well as metatrascriptomic and metaproteomic databases, are incomplete and

insufficient, and there are many metabolites that are not included in the databases. Although there are some limitations with these approaches, they have significant potential clinical applications and the combination of the meta-omics may be sufficiently powerful to elucidate the ecologic roles of the human gut microbiome (Wang *et al*., 2015) (Figure 1.11).

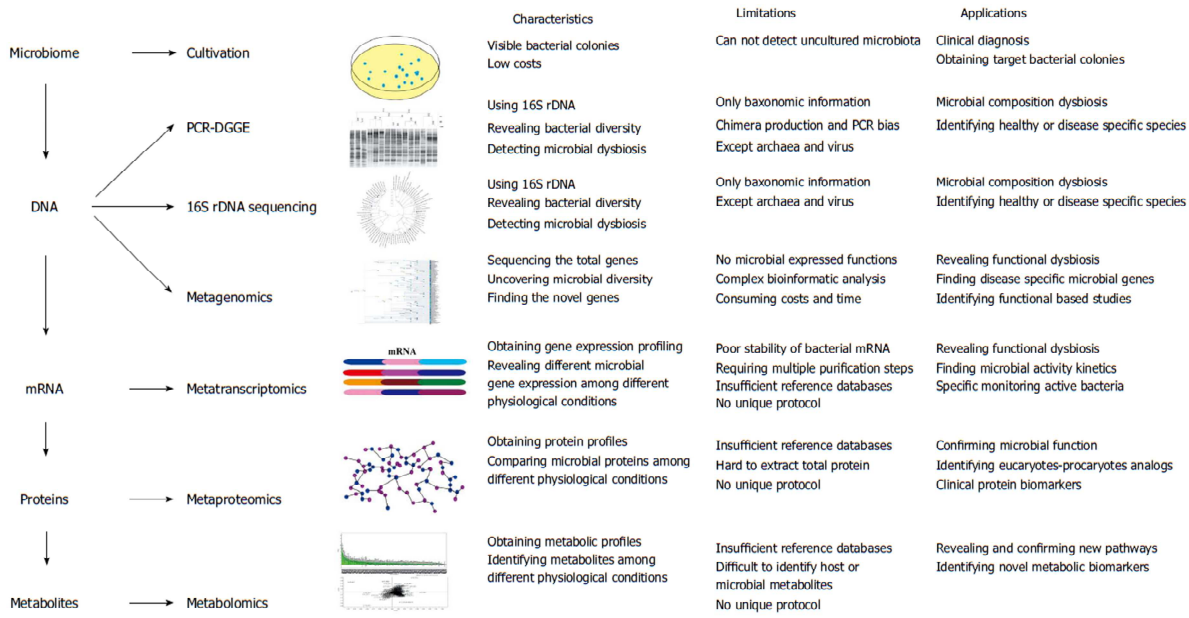

Figure 1.11. Comparison of different gut microbiome study approaches. The characteristics, limitations, and applications of different gut microbiome approaches from cultivation to metabolomics are presented.
DGGE: Denaturing gradient gel electrophoresis (Wang *et al*., 2015).

CHAPTER 2:

THE GUT MICROBIOTA AND CHILDHOOD OBESITY

Introduction

2.1 Gut microbiota and childhood obesity

The adult human gut microbiota has been extensively studied in relation to its role in gut homeostasis and various diseases (Schwiertz *et al*., 2009). Notably, alterations in the gut microbiota and metabolome have been associated with the development of metabolic disorders such as obesity (Choquet *et al*., 2010; Vinolo *et al*., 2011). Obesity is a serious public health issue affecting both children and adults and it is defined as a condition in which excess body fat negatively affects the human's health and wellbeing (Aguilera *et al*., 2013; Choquet *et al*., 2010). Prevention of obesity is proposed to begin in childhood because the comorbidities related to obesity can impact the adulthood exerting a long-term effect (Sanchez *et al*.,2015).

Current data estimates that approximately 600 million people around the world are obese, with an additional 1.9 billion people being overweight (John and Mullin, 2016). In recent years, the prevalence of childhood obesity has increased substantially worldwide. Since 1980, the prevalence of overweight and obesity has increased remarkably in developed countries; 23.8% of boys and 22.6% of girls were overweight or obese in 2013, compared with 16.9% of boys and 16.2% of girls in 1980. The prevalence of overweight and obesity is also rising in children and adolescents in developing countries, increasing from 8.1% in 1980, to 12.9% in 2013 for boys and 8.4% to 13.4% in girls. In both developed and developing countries, sex differences in the levels and trends of overweight and obesity are small (Ng *et al*., 2014) (Figure 2.1A and B). In Italy, 20.9% of children are overweight, 9.8% obese, and 2.2 severe obese, with highter prevalence in centre and Southern Italy, according to Istituto Superiore di Sanità report (http://www.epicentro.iss.it/okkioallasalute/default.asp) (Fig 2.2). Obesity has been associated with several comorbidities, such as cardiovascular events, hypertension (Aguilera *et al*., 2013), insulin resistance (Aguilera *et al*., 2013; Choquet *et al*., 2010), dyslipidaemia,

metabolic syndrome, liver steatosis, orthopaedic problems, and sleep apnoea, which can occur in either the short or long term. Of all the complications of obesity, a cluster of anthropometric, clinical, and metabolic alterations, as low levels of high-density lipoprotein-cholesterol (HDL-c), high triacylglycerols, high blood pressure and impaired glucose metabolism, predisposes the affected individuals to the development of obesity, type 2 diabetes mellitus and cardiovascular diseases. The mechanisms linking obesity to its metabolic complications are extremely complex and remain hotly debated (Aguilera *et al*., 2013). Multiple factors drive the obesity epidemic including genetic and environmental contributions such as increased food availability, high fat diet, physical inactivity (Tsai *et al*., 2009; Dibaise *et al*., 2008; Martin *et al*., 2010) and early feeding environment during pre and post-natal period (Bervoets *et al*., 2013). Epidemiological evidence (Bervoets *et al*., 2013; Karlsson *et al*., 2012; Ismail *et al*., 2011; Kalliomaki *et al*., 2008) suggests that the constant increase in obesity can't be fully accounted for by genetic, food availability and behavioral change alone. There is increasing evidence that our gut microbiota plays a critical role in energy balance and metabolism, suggesting that it can be considered a major factor in the development of obesity (Tsai *et al*., 2009; Dibaise *et al*., 2008).

One of the most cited microbiota related factors differentiating obese and healthy individuals has been the shift in the proportion of gut bacterial communities belonging to the *Firmicutes* and *Bacteroidetes* phyla, which together comprise about 90 % of the microbiota of the adult gut. However, subsequent studies have shown discrepancies in the proportion of *Bacteroidetes*/*Firmicutes* and its relation to obesity and it is likely that the influence of the gut microbiota on obesity is much more complex than simply an imbalance in the proportion and or interaction of these phyla (John and Mullin, 2016; Riva *et al*., 2016).

Analysis of >5000 16S rRNA sequences revealed that genetically obese mice (ob/ob, characterized by a mutation in the leptin gene) had a 50% reduction in the abundance of *Bacteroidetes*, and a correspondent increase in the proportion of *Firmicutes*, compared with lean (ob/+ and Ob+/Ob+)

mice. Moreover, the obesity-associated microbiome harbored a substantial increase in genes encoding enzymes involved in the breakdown of dietary polysaccharides and SCFAs metabolism. Accordingly, these mice had a significantly higher cecal concentrations of SCFAs and a lower fecal energy losses than conventional animals, highlighting the increased capacity of the obese microbiome for energy extraction from the diet (Ramakrishna *et al*., 2013; Zoetendal *et al*., 2004). Furthemore, Bäckhed et al found that the germ free mice (GF) had about 40% less total body fat than mice with a normal gut microbiota, even though the latter ate 30% less diet than did the GF mice. To get more insight into these findings, the authors conventionalized GF mice with a normal gut microbiota harvested from the cecum of a "normal" mouse, and found that this conventionalization produced a 60% increase in body fat content and insulin resistance within 2 weeks, despite a significant lower food intake. The mechanisms of the apparent weight gain implied an increase in the intestinal glucose absorption energy extraction from non-digestible food component, and concomitant higher glycemia and insulinemia, two key metabolic factors regulating lipogenesis (Bäckhed *et al*., 2004).

Human association studies in different parts of the world confirm that there are alterations in the gut microbiota in obese compared with lean individuals. *Faecalibacterium prausnitzii* was increased in the fecal microbiota of obese children in southern India that used real-time polymerase chain reaction to quantitate specific bacterial groups (Balamurugan *et al*., 2010). Increases in *Lactobacillus* spp. associated with reduction in *Bacteroidetes* spp. were reported in obese adults in France (Armougom *et al*., 2009). On the other hand, obese preschool children in Sweden had increased *Enterobacteriaceae*, and reduced *Desulfovibrio* spp. and *Akkermansia* spp. compared with their healthy counterparts (Karlsson *et al*., 2012). Interestingly, it is also reported that gut of obese people is greatly inhabited with H_2-oxidizing methanogenic Archaea. It is supposed that these microorganisms oxidize H_2 produced by H_2-producing bacteria from *Prevotellaceae* family. Rapid H_2-utilization accelerates fermentation of polysaccharides by *Prevotellaceae* and consequently results in the more considerable energy uptake by obese individuals (Zhang *et al*., 2008).

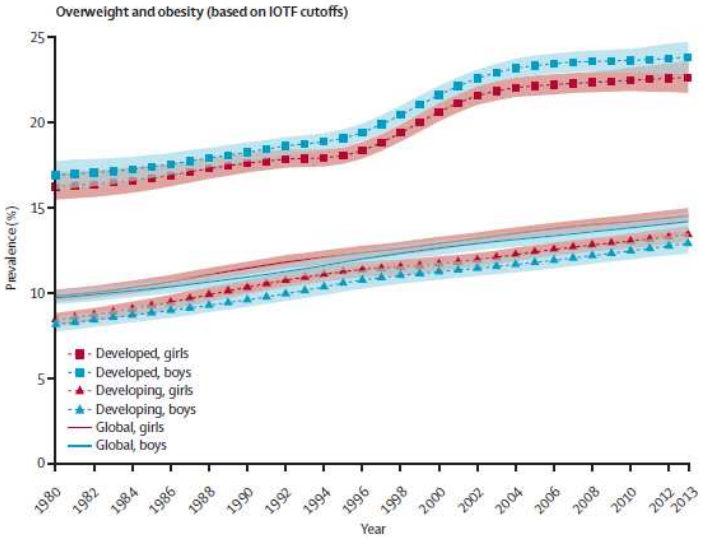

Figure 2.1. Age-standardised prevalence of overweight and obesity based on the International Obesity Task Force (IOTF) cutoffs. Data are shown based on age (2−19 years), sex, years (1980−2013) and countries (developing and developed countries) (Ng *et al*., 2014).

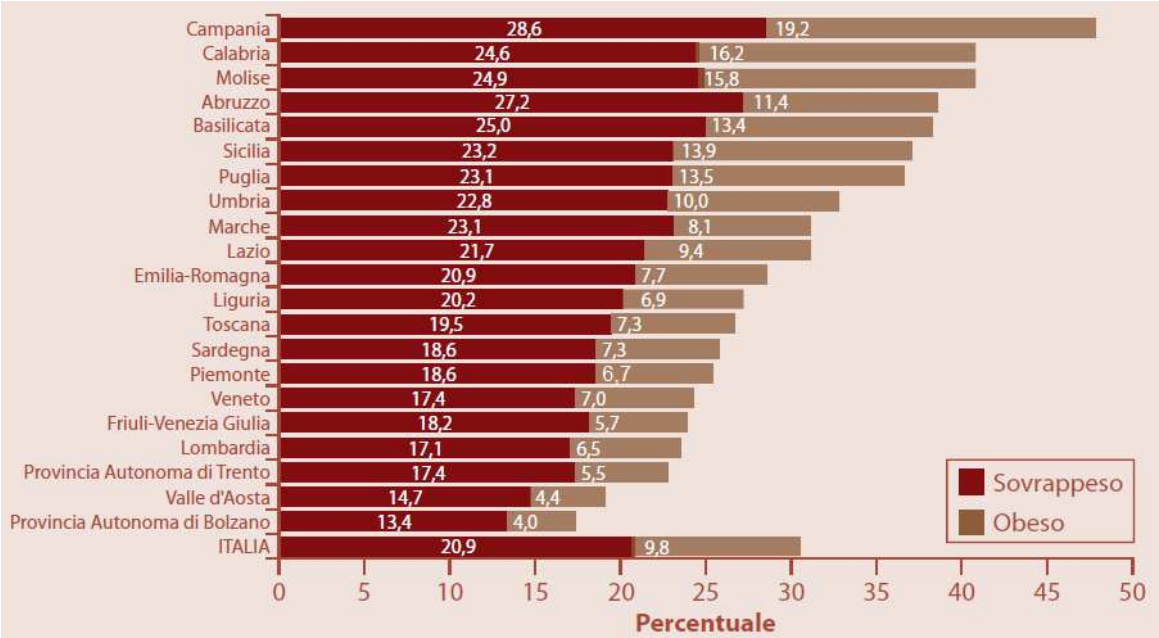

Figure 2.2. Overweight and obese (%) children from 8 to 9 years old divided by Italian regions. Report 2014 Istituto Superiore di Sanità http://www.epicentro.iss.it/okkioallasalute/default.asp.

2.2 Mechanism linking altered gut microbiota to obesity

2.2.1 Fasting-induced adipose factor (FIAF) and AMP-activated protein kinase (AMPK)

One of the key mechanisms by which GF animals are protected from diet-induced obesity is elevated levels of fasting-induced adipose factor (FIAF). FIAF is a circulating lipoprotein lipase (Lpl) inhibitor produced by the intestine, liver and adipose tissue. Conventionalization of GF mice suppresses expression of Fiaf in the gut epithelial cells. This leads to a higher adipocyte Lpl activity and results in increased cellular uptake of fatty acids, adipocyte triglyceride accumulation and greater fat storage (Kobyliak *et al*., 2015). GF Fiaf–/– mice fed a high-fat high-carbohydrate diet were not protected from diet induced obesity, suggesting that FIAF is a mediator of microbial regulation of energy storage (Bäckhed *et al*., 2007). Backhed and colleagues have also demonstrated that GF mice exhibit increased levels of phosphorylated AMPK in muscle and liver. AMPK is a key enzyme that controls cellular energy status, which in turn activates key enzymes of mitochondrial fatty acid oxidation, including acetyl-CoA carboxylase and carnitine-palmitoyltransferase I. This enzyme activation is indicative of increased energy expenditure. The exact pathway through which the microbiota signals to liver and skeletal muscle AMPK is unclear, but appears to be independent from FIAF (Bäckhed *et al*., 2007) (Figure 2.3).

2.2.2 Activity of short chain fatty acids and monosaccharides

The gut microbiota that digests complex dietary carbohydrates produces many monosaccharides and short chain fatty acids (SCFAs), important energy source and nutrition of the intestinal epithelium (Kobyliak *et al*., 2015). Conventionalization of GF mice doubles the density of small intestinal villi capillaries (Stappenbeck *et al*., 2002), and enhances an uptake of SCFAs from the gut into the portal blood and eventually participates in hepatic de novo lipogenesis promoting fat accumulation in the

liver and adipose tissue. This reaction is controlled by carbohydrate responsive element binding protein (ChREBP) and sterol responsive element binding protein (SREBP-1). Furthermore, monosaccharides that are produced by microbial fermentation and absorbed and transferred to the liver via portal vein, activate ChREBP, which increases the transcription of several proteins involved in hepatic de novo lipogenesis (Kobyliak *et al*., 2015).

SCFAs act in the gut as signaling molecules and are specific ligands for at least two G protein-coupled receptors, GPR41 and GPR43, mainly expressed in intestinal epithelial cells (Kobyliak *et al*., 2015). Samuel et al. have demonstrated that conventionally raised Gpr41–/– mice and GF Gpr41–/– mice colonized with only *Bacteroides thetaiotaomicron* and *Methanobrevibacter smithii* are significantly leaner than wild-type littermates. Gpr41-deficiency is associated with reduced expression of peptide YY (PYY), an enteroen-docrine cell-derived hormone that normally inhibits gut motility, increased intestinal transit rate, and reduced harvest of energy (short-chain fatty acids) from the diet. These results reveal that Gpr41 is a regulator of host energy balance through effects that are dependent upon the gut microbiota (Samuel *et al*., 2008) (Figure 2.3).

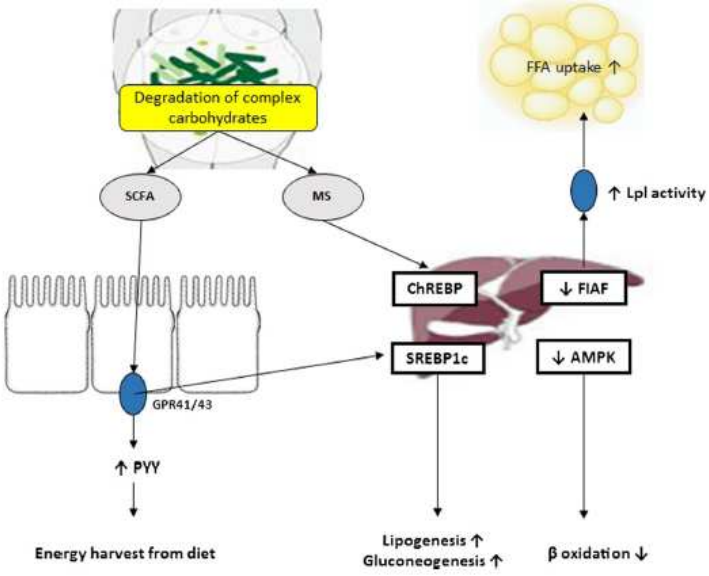

Figure 2.3. Mechanism linking altered gut microbiota to obesity (Kobyliak *et al*., 2015).

2.2.3 Increased permeability of the gut barrier

Another mechanism may include the permeability of the intestinal wall. A high-fat diet can alter the composition of the intestinal microbiota and this modification may lead to an increased permeability of the gut barrier by an altered distribution of some tight junction proteins (ZO-1 and occludin). This modification of the wall permeability may also lead to an increase in certain molecules in plasma such as lipopolysaccharide (LPS), resulting in metabolic endotoxemia. The LPS can bind to TLR4/CD14 (toll-like receptor-4/cluster of differentiation-14) receptors that are responsible for signaling cascades. These signaling cascades lead to the production of proinflammatory cytokines, particularly tumor necrosis factor alpha (TNF-α) and interleukin-6 (IL-6), which are involved in the development of atherosclerosis, obesity and insulin resistance (Sanchez *et al*., 2015).

2.2.4 Control of food intake and appetite

It has been suggested that gut microbiota may also affect food intake and satiety via gut peptide signalling. Gastro-intestinal hormones such as glucagon-like peptide-1 (GLP-1), PYY, cholecystokinin (CCK) and ghrelin play a critical role in relaying signals of nutritional and energy status from the gut to the central nervous system in order to control food intake and glycemic regulation (Sanchez *et al*., 2015).

Experimental studies have shown that GLP-1 is upregulated by prebiotics in obese mice suggesting that alterations in intestinal microbiota may stimulate or suppress the secretion of gastro-intestinal hormones (Cani *et al*., 2004; Cani *et al*., 2009).

2.3 Interventional strategies in childhood obesity

At the moment, the most important strategies to manage childhood obesity are therapeutic lifestyle changes, such as changing dietary habits and the physical activity level (Bervoets *et al*., 2013). Dietary factors are based on limited consumption of sugar-sweetened beverages and meals with servings of vegetable and fruits, avoiding fast foods, and encouraging limited portions of food. Physical activity is based on levels of activity from moderate to vigorous for one or more hours/day. Sedentary activity should be limited to less than 2 h/day after age two (Magrone and Jirillo, 2015).

When lifestyle modifications continue to fail, pharmacological interventions and possibly bariatric surgery could be considered (Bervoets *et al*., 2013). Future treatments for obesity may be possible through the modulation of gut microbiota using antibiotics, probiotics, prebiotics, and possibly even microbiota transplants (Tsai *et al*., 2009).

2.4 Aim of the project

"The gut microbiota in obese and normal-weight children"

Childhood obesity is one of the mayor public health problem. Prevention and management of obesity is proposed to begin in childhood when environmental factors exert a long-term effect on the risk for obesity in adulthood (Sanchez *et al*., 2015). It is generally believed that the gut microbiota is established during the first 3 years of life but data are scarce regarding its development during childhood. Although it has been suggested that the microbiota reaches a relatively stable adult-like state in the first three years of life, other evidence indicates that it continues to develop through adolescence (Hollister *et al*., 2015). As such, childhood may provide unique opportunities for microbiota interventions to promote health or prevent disease. It is therefore vital to establish a baseline understanding of pediatric gut microbiota structure and function, as during this period the gastro-intestinal tract undergoes a transition from an immature to a mature state (Hollister *et al*., 2015).

The goal of the present study was to characterize the composition of the gut microbiota in obese and normal-weight children. We firstly performed a preliminary analysis on 61 patients from the same geographic area to reduce variation unrelated to obesity using DGGE (*denaturing gradient gel electrophoresis*) and Real-time PCR in order to quantify specific target bacteria. We evaluated the gut microbiota biodiversity, both bacterial and fungal, in obese and normal-weight school-aged children. We choose a wide pediatric age from 6 to 16 years old as most of the studies on gut microbiota in children were performed in the first 3 years of life. After a first evaluation that a microbial differences existed between obese and normal-weight, we enlarged the cohort and we studied the gut microbiota composition by using 16S rRNA gene-targeted sequencing. We further

compared the gut microbiota profiles with BMI z-scores and short chain fatty acids (SCFAs) the main fermentative metabolites produced by bacteria, to gain insights into the structure and activity of the microbiota in pediatric obesity.

We present a detailed analysis of the alterations of the gut microbiota and changes in correlation network structure linked to childhood obesity.

2.4.1 EXPERIMETAL DESIGN:

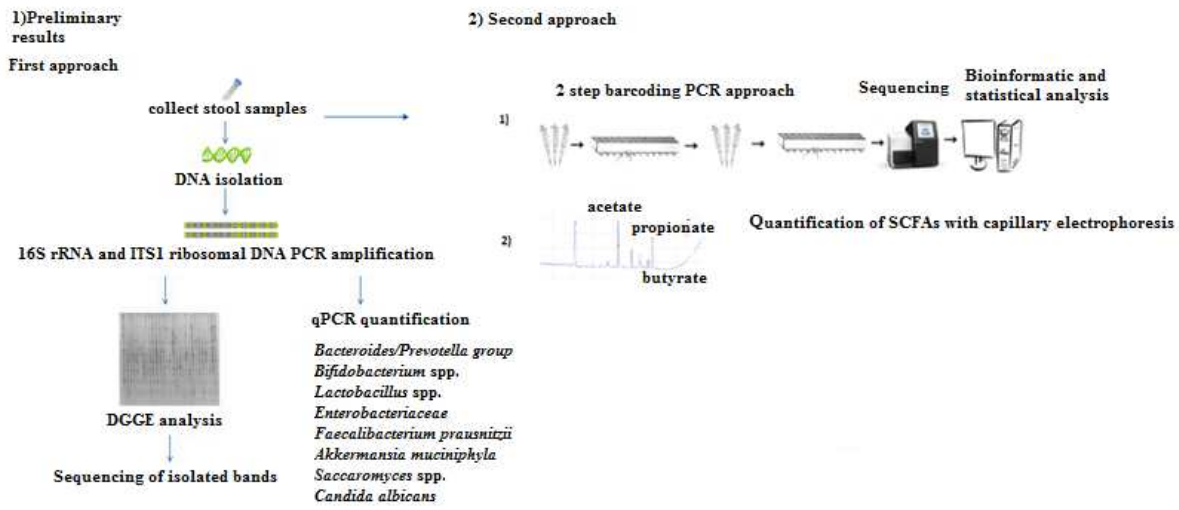

Figure 2.4. Experimental and project design. First experimental approach by using DGGE and qPCR tecniques. In the second part of the project the numbers of participants were increased and 16S gene target-sequencing and SCFAs quantification were performed to analyze the gut microbiota composition and the microbial fermentation activity.

2.5 Manuscript 1:

”Relative abundance in bacterial and fungal gut microbes in obese children: A case control study”

Published in:
Childhood Obesity, 2016

(Page numbers are relative to paper)

CHILDHOOD OBESITY
Month 2016 | Volume 12, Number X

DOI: 10.1089/chi.2015.0194

Relative Abundance in Bacterial and Fungal Gut Microbes in Obese Children: A Case Control Study

Francesca Borgo, PhD,[1] Elvira Verduci, MD,[2] Alessandra Riva, MSc,[1] Carlotta Lassandro, MSc,[1] Enrica Riva, MD,[2] Giulia Morace, PhD,[1] and Elisa Borghi, PhD[1]

Abstract

Background: Differences in relative proportions of gut microbial communities in adults have been correlated with intestinal diseases and obesity. In this study we evaluated the gut microbiota biodiversity, both bacterial and fungal, in obese and normal-weight school-aged children.

Methods: We studied 28 obese (mean age 10.03 ± 0.68) and 33 age- and sex-matched normal-weight children. BMI z-scores were calculated, and the obesity condition was defined according to the WHO criteria. Fecal samples were analyzed by 16S rRNA amplification followed by denaturing gradient gel electrophoresis (DGGE) analysis and sequencing. Real-time polymerase chain reaction (PCR) was performed to quantify the most representative microbial species and genera.

Results: DGGE profiles showed high bacterial biodiversity without significant correlations with BMI z-score groups. Compared to bacterial profiles, we observed lower richness in yeast species. Sequence of the most representative bands gave back *Eubacterium rectale*, *Saccharomyces cerevisiae*, *Candida albicans,* and *C. glabrata* as present in all samples. *Debaryomyces hansenii* was present only in two obese children. Obese children revealed a significantly lower abundance in *Akkermansia muciniphyla, Faecalibacterium prausnitzii*, *Bacteroides*/*Prevotella* group, *Candida* spp., and *Saccharomyces* spp. ($P = 0.031$, $P = 0.044$, $P = 0.003$, $P = 0.047$, and $P = 0.034$, respectively).

Conclusion: Taking into account the complexity of obesity, our data suggest that differences in relative abundance of some core microbial species, preexisting or diet driven, could actively be part of its etiology. This study improved our knowledge about the fungal population in the pediatric school-age population and highlighted the need to consider the influence of cross-kingdom relationships.

Introduction

Over the last decade, the microbial composition of the gut has been widely investigated, and recognized as having an impact in various physiological and pathological conditions.[1] The Human Microbiome Project[2] and Metagenomics of the Human Intestinal Tract (MetaHIT) (www.metahit.eu/) project clearly demonstrated that gut microorganisms are not just passive residents, carrying out a range of biological functions that are important in nutrition and well-being of the individual.

Molecular analyses revealed the presence of more than 1000 microbial species and highlighted the deep diversity within human gastrointestinal (GI) tracts.[3] However, these species belong to only 8 of the 55 known bacterial phyla, with the *Firmicutes* (low-GCC gram-positives), *Bacteroidetes,* and *Actinobacteria* (high-GCC gram-positives) being the most widely represented.[4]

Moreover, the human microbiota is more complex than a bacterial community. It also involves Archeabacteria and fungi.[5] Very few studies encompass the fungal gut population, and even fewer in the pediatric population. Thus, the exact role of colonizing fungi has not been fully explored. Coexistence of cross-kingdom communities within the human gut could affect the final relationship with the host. The most representative genera are *Candida* and *Saccharomyces.*[6]

The composition and activity of the gut microbiota co-develop with the host from birth and is subjected to a complex interplay that depends on the host genome,

[1]Department of Health Sciences, Università degli Studi di Milano, Milan, Italy.
[2]Department of Pediatrics, San Paolo Hospital, Milan, Italy.

nutrition, and lifestyle. The gut microbiota in relation to pediatric metabolic disorders has been poorly studied, although in recent years has emerged as a significant factor involved in obesity, even if no causal relationship has been established.[7]

Turnbaugh et al.[8] reported that adult obesity is associated with microbial compositional changes at the phylum level. They found that individuals with high BMIs had a lower proportion of *Bacteroidetes* and a higher proportion of *Actinobacteria* when compared to leaner individuals. However, a number of studies have failed to confirm this association or reported the opposite association.[9,10] Karlsson et al.[11] investigated the gut microbial biodiversity in preschool children with normal and excessive body weight; they found in the overweight group a significant reduction of *Akkermansia muciniphyla* and *Desulfovibrio* spp., together with an increase of *Enterobacteriaceae*.

In our study we aimed at evaluating, both qualitatively and quantitatively, gut microbiota biodiversity in obese and normal-weight children aged 8–12 years. Prevention and treatment of childhood obesity involve mainly school-aged children, and additional research needs to be done on such a cohort in order to understand the critical window of a child's life in which environmental factors such as diet and microbiota can be shaped to promote health.

Methods

Subjects and Sample Collection

This observational case control study included 28 obese children (15 females and 13 males), mean age 10.03 (standard deviation [SD] 0.68), among patients consecutively admitted to the pediatric department of the San Paolo Hospital, Milan, Italy, between December 2013 and September 2014 in order to evaluate obesity-related metabolic profile, and 33 sex- and age-matched normal-weight children. Inclusion criteria were children living in north Italy born from Caucasian parents with birthweight ≥2500 grams, gestational age 37–42 weeks, singleton birth, no neonatal disease or congenital malformation. Exclusion criteria were having chronic or acute intestinal diseases and treatments with antibiotic and probiotic/prebiotic in the previous month, obesity-related comorbidity conditions (*e.g.,* insulin resistance, nonalcoholic fatty liver disease).

Data were collected for all subjects concerning mode of delivery and exclusively breastfeeding or formula feeding. Weight (kg), height (cm), and BMI (kg/m^2) were transformed to age- (in days) and sex-specific z scores according to WHO growth standards.[12,13] Obesity was defined by using WHO criteria.[14] Fasting blood samples were analyzed for insulin and glucose. Insulin resistance was estimated by homeostatic model assessment (HOMA) and defined as HOMA >3.16 according to the most recent cut-off for the pediatric population.[15] Abdominal ultrasonography (US) was performed according to a randomized sequence to evaluate liver echogenicity.

A fresh fecal sample was self-collected at home by each enrolled subject and stored immediately at −20°C. The collection took place in the same week as the dietary record. Subsequently, the fecal samples were transported to the laboratory and stored at −20°C until further analysis. The dietary habits of the children were assessed at recruitment by means of an age-adjusted food frequency questionnaire made up of 116 items.[16]

DNA Extraction and 16S Ribosomal (rRNA Bacteria) and ITS Ribosomal (Fungi) DNA Amplification

Total microbial DNA extraction was performed with the Spin Stool DNA Plus Kit (Stratec Molecular, Berlin, Germany) according to manufacturer instruction, using 200 mg aliquot of wet feces. The V2-V3 region of the gene that encodes for 16S rRNA was amplified using the following primers: HDA1-GC (5′-CGC CCG GGG CGC GCC CCG GGC GGG GCG GGG GCACGG GGG G-ACT CCT ACG GGA GGC AGCAGT-′3) and HDA2 (5′-GTA TTA CCG CGG CTG CTG GCA C-′3). Primers were used in a reaction mix (Thermo Scientific Dream Taq Master Mix) at a final concentration of 0.5 μM. The amplification cycles were as follow: initial denaturation at 94°C for 5 minutes, followed by 35 cycles at 94°C for 1 minute, 56°C for 1 minute, 68°C for 1 minute, and a final extension at 68°C for 7 minutes.[17] Polymerase chain reaction (PCR) products (220 bp) were visualized on a 1.5% agarose gel and subsequently subjected to denaturing gradient gel electrophoresis (DGGE) analysis. For fungi, the 5.8S ITS rDNA region was amplified by means of a nested-PCR approach using the primers ITS1 (5′-TCC GTA GGT GAA CCT GCG G-3′), ITS4 (5′-TCC TCC GCT TAT TGA TAT GC-3′), NL1 with a GC clamp (5′-CGC CCG CCG CGC GCG GCG GGC GGG GCG GGG GCA TAT CAA TAA GCG GAG GAA AAG-3′), and LS2 (5′-ATT CCC AAA CAA CTC GAC TC-3′). Amplification cycles were as follows: initial denaturation at 94°C for 3 minutes and 35 cycles of 94°C for 30 seconds, 52°C for 30 seconds, and 74°C for 2 minutes followed by 74°C for 10 minutes.[18] PCR products were separated by gel electrophoresis on a 1.0% (wt/vol) agarose gel, detected by ethidium bromide staining, and subsequently subjected to DGGE analysis.

Denaturing Gradient Gel Electrophoresis Analysis

DGGE was performed using a PhorU system (Ingeny International, Goes, The Netherlands) in 1X tris-acetate-EDTA (TAE) buffer at 60°C. PCR products were loaded onto 8% polyacrylamide gels in 1X TAE. The electrophoretic conditions were the following: 18 hours at 90 V in a 40%–60% denaturating agent gradient. The gels were stained in 1X TAE buffer with SYBR Green I nucleic acid stain (Roche Products Ltd., Welwyn Garden City, UK) for 30 minutes and visualized by UV radiation. Banding patterns of DGGE profiles were analyzed with Fingerprinting II software (Bio-Rad Laboratories, Hercules, CA), using the Pearson product moment correlation coefficient and the unweighted-pair group method with averages (UPGMA) for

the generation of dendrograms. Pearson coefficient is a measure of the degree of similarity. Two identical profiles create a similarity value of 100%, whereas completely different profiles result in a similarity value of 0%.[8]

Excision and Sequence Analysis of Products

Individual bands were cut out from the gel, placed in 50 μl sterile distilled water, and incubated overnight at 4°C. Two microliters of the eluate were amplified with the original primer pairs and amplification products checked by agarose gel electrophoresis. PCR products were purified using the NucleoSpin Extract II kit (Macherey-Nagel GmbH, Düren, Germany) and subjected to Sanger sequencing (Eurofins Biolab S.r.l., Milan, Italy). The sequences were compared with those available in the National Center for Biotechnology Information (NCBI) GenBank (www.ncbi.nlm.nih.gov/) and those in the Ribosomal Database Project (RDP) using the Sequence Map tool (rdp.cme.msu.edu/).

Quantification by Real-Time Polymerase Chain Reaction

Absolute quantification by real-time PCR was performed using the following control strains: *Escherichia coli* American Type Culture Collection (ATCC) 25922^T, *Akkermansia muciniphyla* DSM 22959^T, *Candida albicans* ATCC 90028^T, Deutsche Sammlung von Mikroorganismen und Zellkulturen; *Bacteroides uniformis*, *Lactobacillus reuteri*, *Bifidobacterium animalis*, *Faecalibacterium prausnitzii,* and *Saccharomyces cerevisiae* (from the Clinical Microbiology Laboratory collection, Health Sciences Department, Università degli Studi di Milano). Firstly, the microbial DNA was extracted for each control strain using Prepman Ultra (Applied Biosystems, Foster City, CA). Real-time PCR was carried out using the StepOne instrument (Applied Biosystems) and SYBR® Green chemistry (Thermo Scientific, Waltham, MA). The analysis was performed in a total volume of 15 μl and each sample analyzed in triplicate. Standard curve was carried out for each qPCR run using five serial dilutions of control DNA. The specific 16S rRNA primers and qPCR conditions used for *Bacteroides*/*Prevotella* group, *Bifidobacterium* spp., *Enterobacteriaceae* group, and *F. prausnitzii* are reported by Bartosch et al.;[16] for *Lactobacillus* spp. and *A. muciniphyla* we used the conditions designed by Delroisse et al.[17] and Collado et al.[20] The specific yeast quantification was carried out for *Candida* spp. and *Saccharomyces* spp. as described by Hierro et al.[21] and Zott et al.,[22] respectively.

Data Analysis

Statistical analysis has been performed using Graph Pad Prism (Graph Pad Software, La Jolla, CA) statistical software. Variables have been expressed as mean and standard deviation. Mean values were compared among subjects using the Whitney U test, and ANOVA was used to compare variables between all groups. A probability value (P value) less than 0.05 was considered statistically significant.

Results

Cohort Composition

Twenty-eight children were included in the obese (O) group and 33 in the control normal-weight (N) group. BMI z-scores were 2.9 (SD 0.66) and 0.29 (SD 0.79), respectively ($P < 0.001$). Eighty percent of normal-weight and 54% of obese children were born by vaginal delivery; furthermore, 50% of N and 53% of O were exclusively breastfed. Compared to normal-weight children, obese children showed higher dietary intakes of energy—1906 (SD 474) Kcal vs. 2593 (SD 989) Kcal, $P = 0.0007$; proteins, 64 (SD 13) grams vs. 97 (SD 31) grams, $P < 0.0001$; carbohydrates 271 (SD 55) grams vs. 368 (SD 137) grams, $P = 0.0004$; total fats 58 (SD 15) grams vs. 92 (SD 37) grams, $P < 0.0001$; saturated fats 19 (SD 6) grams vs. 31.5 (SD 11) grams, $P < 0.0001$; monounsaturated fats 20 (SD 6) grams vs. 31 (SD 11) grams, $P < 0.0001$; and polyunsaturated fats 7 (SD 3.5) grams vs. 13 (SD 7) grams, $P < 0.0001$.

Gut Microbial Ecosystem

The DGGE analysis of the gut bacterial population indicated a high degree of individual variation in the intestinal microbial community profiles obtained by using universal 16S rRNA primers (Figure 1a), while the DGGE patterns obtained for the yeast population contained a relatively low number of bands and had low interindividual variability (Figure 1b).

Figure 1a shows an example of the unweighted pair group method with arithmetic mean (UPGMA) dendrogram obtained for the children's microbiota. Two main clusters (50% similarity) are reported; one is represented by a sole severely obese child and the other group included four subclusters without significant differences among BMI z-score groups. The most representative bands—13 individual bands, identified from A to P (Figure 1a)—were excised from DGGE gel and subjected to sequencing. The respective bacterial species are indicated in Table 1. A similarity rate ≥90% was considered significant. In particular, sequencing of excised bands revealed that band F/G (*Eubacterium rectale*) was present in all children, while band H (*F. prausnitzii)* were absent in two severely obese children. The UPGMA dendrogram obtained for the fungal gut population revealed two main clusters (37% similarity), one represented by the sole severely obese child and the second composed by two subclusters without significant differences among BMI z-score groups (Figure 1b). The sequencing of fungal gut population DGGE excised bands, reported in Table 1, revealed that the bands relative to *Saccharomyces cerevisiae*, *Candida albicans*, and *Candida glabrata* were present in all samples, whereas bands 7 and 11 (*Debaryomyces hansenii*) were present only in two obese children.

Microbial Genome Quantification by Real-Time Polymerase Chain Reaction

Quantification of the bacterial and yeast groups using real-time PCR was performed on N and O distinct populations

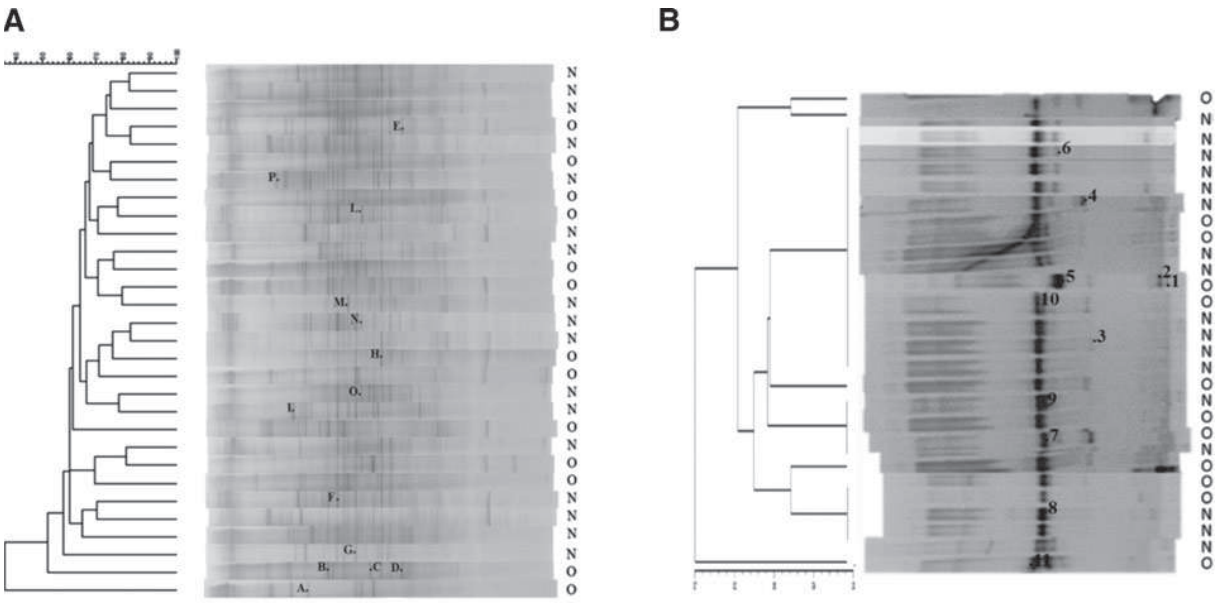

Figure 1. Representative cluster analysis of DGGE profiles in obese and normal-weight children (panels A and B). Panel A: bacterial population; panel B: fungal population. O = obese; N = normal weight.

(Figure 2). We did not observe differences in the *Bifidobacterium* spp. ($P = 0.606$), *Lactobacillus* spp. ($P = 0.420$), and *Enterobacteriaceae* ($P = 0.168$), whereas *A. muciniphyla*, *F. prausnitzii*, and *Bacteroides*/*Prevotella* group were significantly less abundant in obese children ($P = 0.031$, $P = 0.044$, and $P = 0.003$, respectively). The average copy number of the yeasts was higher in the normal-weight population compared to the obese population, with a significant P value for *Candida* spp. ($P = 0.047$) and for *Saccharomyces* spp. ($P = 0.034$). No significant differences in microbiota

Table 1. Sequenced DGGE bands and relative species identification

	Band letters	Nearest species	Similarity	Accession number
Bacterial species	A	*Parabacteroides distasonis*	92%	NR 074376
	B	*Alistipes putredinis.*	98%	NR 113152
	C	*Clostridium parabutiricum*	98%	NR 11903
	D	*Paraprevotella clara*	96%	NR 113073
	E	*Flavonifractor plautii*	94%	NR 452852
	F/G	*Eubacterium rectale*	100%	NR 074634
	H	*Faecalibacterium prausnitzii*	97%	NR 043680
	L	*Clostridium aldenense*	100%	NR 043680
	M	*Clostridium* spp.	97%	NR 029355
	N/O	*Gemmiger formicilis*	93%	NR 104846
	P	*Flavobacterium* spp.	96%	NR 108535
Fungal species	1/2/4/5/6/13	*Saccharomyces cerevisiae*	100%	KM103045
	10	*Candida albicans*	99%	AM998790
	3	*Candida parapsilosis*	99%	EF568035
	7/11	*Debaryomyces hansenii*	98%	KF214434.1
	8/9/11	*Candida glabrata*	99%	AF336837

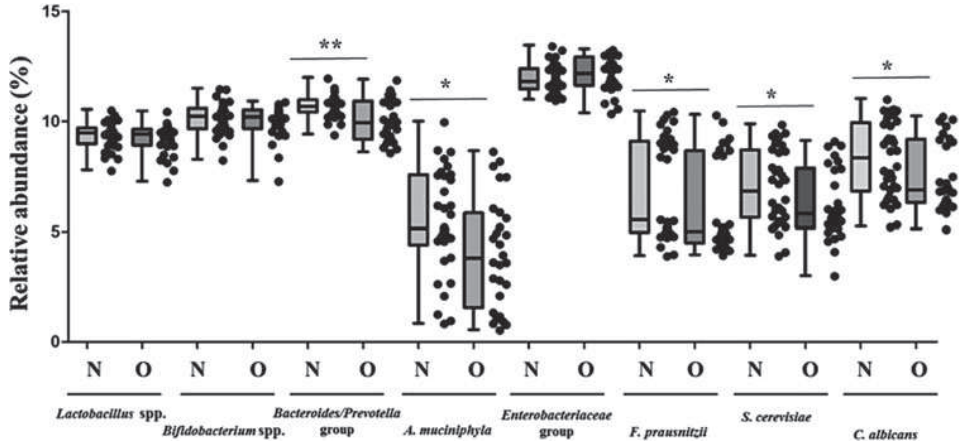

Figure 2. Box and whisker plots to compare relative abundance of microbial species in obese and normal-weight children. The box plot representation shows the median (designated by a line) and the 25th and 75th percentiles. Significant values (*P*-values) between the two groups are displayed on the plots. *$P < 0.05$; **$P < 0.01$. O = obese; N = normal weight.

composition were observed comparing different types of delivery: *Bifidobacterium* spp. ($P = 0.868$), *Lactobacillus* spp. ($P = 0.908$), *Enterobacteriaceae* ($P = 0.959$), *A. muciniphyla* ($P = 0.800$), *F. prausnitzii,* ($P = 0.389$), *Bacteroides/Prevotella* group ($P = 0.070$), *Candida* spp. ($P = 1$), and *Saccharomyces* spp. ($P = 0.959$).

The lack of significant differences was also observed comparing breast and formula feeding: *Bifidobacterium* spp. ($P = 0.228$), *Lactobacillus* spp. ($P = 0.354$) and *Enterobacteriaceae* ($P = 0.102$), *A. muciniphyla* ($P = 0.384$), *F. prausnitzii* ($P = 0.612$), *Bacteroides/Prevotella* group ($P = 0.236$), *Candida* spp. ($P = 0.658$), and *Saccharomyces* spp. ($P = 0.684$).

Discussion

Key activities of the gut microbiota are the efficient extraction of calories from ingested food and the regulation of fat storage by modulation of lipoprotein lipase activity and subsequent triglyceride storage. The diet could induce strong modifications of the gut microbiota composition, and indeed, obese people have been reported to have lower bacterial diversity in the gastrointestinal tract compared to lean subjects.[23] Modifications in the proportions of microorganisms in the gut and, consequently, in the concentrations of metabolites produced and released by them in the lumen, have been suggested to play a role in the development of several pathological conditions[24] such as metabolic disorders.

In this study we evaluated, both qualitatively and quantitatively, the gut microbiota biodiversity in obese and normal-weight children. The combined use of two methods—DGGE (qualitative) and real-time (quantitative)—allows for a good evaluation of microbial ecology profile in the two studied populations. The DGGE profiles of total bacterial population demonstrated high interindividual heterogeneity in the microbial species. We failed to find common pattern strongly associated to high BMI z-score, even though a lower microbial biodiversity was highlighted in subjects with severe obesity.

The presence of interindividual differences is well reported in the literature, although the presence has been demonstrated of a core of microbiota, relatively stable and resilient,[25] that depends on the age, health, diet, and even geographical location of the individuals. To rule out differences related to the above conditions, our cohort was selected to minimize differences related to age and geographical location. Both groups of children had a ''Western-style'' diet, high in fat and refined sugars. The quantification of the common genera that are part of the core microbiota showed no significant differences in the number of genomes of *Lactobacillus* spp., *Bifidobacterium* spp., and *Enterobacteriaceae*.

It is well known from the literature that the significant less abundance of *A. muciniphyla* is related with an excessive weight in adult and preschool children.[11,26] In this study we corroborate this finding in school-aged children. *A. muciniphyla* is a mucin-degrading bacterium (phylum *Verrucomicrobia*) and the dominant colonizer of the intestinal mucus layer.[27] In the mouse, a high-fat diet induced increased body mass, endotoxemia, adiposity, fasting hyperglycemia, and insulin resistance, while all of the above were reversed with the administration of *A. muciniphyla.*[26] In addition, *A. muciniphyla* increases the expression of acylglycerols, important compounds in gut barrier integrity, and reverses the thinning of the mucus layer caused by a high-fat diet.

In addition, we found in obese children a reduction of *F. prausnitzii.* Different authors suggested that a lower presence of *F. prausnitzii* could result from a long-standing inflammation.[28] *F. prausnitzii* appears to have significant anti-inflammatory activity with decreased production of proinflammatory cytokines (IL-8, IL-12, and IFN-γ) and increased production of anti-inflammatory IL-10 in cell cultures.[29] Studies in germ-free mice suggest that *F. prausnitzii* in conjunction with another common commensal, *Bacteroides thetaiotaomicron*, plays a role in goblet

cells differentiation and in the production of the mucus layer.[30] An intact mucus layer is an important component of the intestinal barrier that limits exposure of the epithelial monolayer to proinflammatory bacteria in the gut lumen. Concerning the *Bacteroides*/*Prevotella* group, we found a lower abundance of this microbial group in obese subjects. This data is in agreement with other authors reporting in the obese adult population a variation of the *Firmicutes/Bacteroides* ratio, with an increase in *Firmicutes*.[7–8,31]

In order to obtain a complete picture of the studied cohort, the fungal microbiota has been investigated. DGGE profiles of fungal population showed a lower biodiversity, expressed by a lower bands number, compared with bacteria profiles, without significant differences between normal-weight and obese children. However, we have to consider that the overall fungal population is underrepresented compared to the bacterial one, and the DGGE technique may in turn underestimate some species that are quantitatively poorly present. At this time, our knowledge on commensal fungi inhabiting the gut of children is incomplete. Nonetheless, the few literature data on adult population are in agreement with our results on Ascomycota as the most detected phylum. Indeed, *C. albicans*, *C. glabrata,* and *S. cerevisiae* were the most representative species in both groups. *Debaryomyces hansenii,* sequenced from two excised bands, was found only in two obese children; this species in closely related to food, in particular to cheeses and dry-cured meat products. Future studies are needed to better understand if the presence of *D. hansenii* is due to the ingestion of yeast-containing foods or if this species might contribute to obesity pathology.

However, we found significant differences in the two groups in terms of abundance. Normal-weight group was characterized by a higher number of genomes of *Candida* spp. and of *Saccharomyces* spp. Hoffmann and coworkers[32] analyzed the influence of diet on fungal and bacterial levels in the gastrointestinal tract. *Candida* spp. was positively correlated with carbohydrate consumption and negatively correlated with total saturated fatty acids, but no correlation was observed for *Saccharomyces* spp. with both diets. Moreover, *Candida* species are well-known human commensals, whereas for the *Saccharomyces* species we cannot rule out if they are transiently present because of diet (bread, pizza) or true commensals.

The influence of trans-kingdom relationships and diet on the coexistence of the microbial communities within the human gut has not yet been defined. One possible scenario could be the role of *Candida* spp. in breaking down starch in carbohydrate foods, leading to the release of simple sugars, which are in turn fermented by bacteria (for example, *Prevotella* and *Ruminococcus*).

One limitation of the present study is that Archaebacteria are not included in the analysis of the gut microbial ecology, although their contribution to obesity is still debated. Animal studies suggested a potential role for methanogens Archaea, mainly *Methanobrevibacter smithii*, in promoting obesity.[33,34] Literature data on humans, however, are inconsistent, with some authors reporting a negative association with BMI[35,36] and others reporting a positive association.[37,38] Further studies, especially on obese children, would be useful in elucidating their role.

In conclusion, taking into account the complexity of obesity, our data suggest that changes of some core microbial species, preexisting or diet induced, could actively be part of the syndrome's etiology. Obese children are highly prone to become obese adults, and in order to fight obesity-related complications, prevention and prompt treatment are crucial. The most important strategies to manage childhood obesity are therapeutic lifestyle changes, but the failure rate of such interventions is still high. The microbiota analysis of obese children could provide new elements of the puzzle to pave the way for designing customized diets and improve the current strategies.

Ethical Considerations

The medical ethical committee of our institution approved this study (protocol number 2015/ST/135). Written informed consent was signed by a parent of all the enrolled subjects.

Author Disclosure Statement

The authors declare that no competing financial interests exist.

References

1. Khan I, Yasir M, Azhar EI, et al. Implication of gut microbiota in human health. *CNS Neurol Disord Drug Targets* 2014;13:1325–1333.
2. Human Microbiome Project Consortium. Structure, function and diversity of the healthy human microbiome. *Nature* 2012;486: 207–214.
3. O'Hara AM, Shanahan F. The gut flora as a forgotten organ. *EMBO Reports* 2006;7:688–693.
4. Turnbaugh PJ, Ley RE, Hamady M, et al. The human microbiome project. N*ature* 2007;449:804–810.
5. Wang ZK, Yang YS, Stefka AT, et al. Review article: Fungal microbiota and digestive diseases. *Aliment Pharmacol Ther* 2014; 39:751–766.
6. Huffnagle GB, Noverr MC. The emerging world of the fungal microbiome. *Trends Microbiol* 2013;21:334–341.
7. Ley RE, Turnbaugh PJ, Klein S, et al. Microbial ecology: Human gut microbes associated with obesity. *Nature* 2006;444:1022–1023.
8. Turnbaugh PJ, Hamady M, Yatsunenko T, et al. A core gut microbiome in obese and lean twins. *Nature* 2009;457:480–484.
9. Mueller S, Saunier K, Hanisch, C, et al. Differences in fecal microbiota in different European study populations in relation to age, gender, and country: A cross-sectional study. *Appl Environ Microbiol* 2006;72:1027–1033.
10. Schwiertz A, Taras D, Schäfer K, et al. Microbiota and SCFA in lean and overweight healthy subjects. *Obesity* 2010;18:190–195.
11. Karlsson CLJ, Önnerfält J, Xu J, et al. The microbiota of the gut in preschool children with normal and excessive body weight. *Obesity* 2012; 20:2257–2261.
12. World Health Organization (WHO). www.who.int/childgrowth/software/en/ (Last accessed March 16, 2016.)

13. World Health Organization (WHO). www.who.int/growthref/tools/en/ (Last accessed March 16, 2016.)
14. World Health Organization (WHO). www.who.int/growthref/who2007_bmi_for_age/en/ (Last accessed March 16, 2016.)
15. Keskin M, Kurtoglu S, Kendirci M, et al. Homeostasis model assessment is more reliable than the fasting glucose/insulin ratio and quantitative insulin sensitivity check index for assessing insulin resistance among obese children and adolescents. *Pediatrics* 2005;115:e500–e503.
16. Verduci E, Radaelli G, Stival G, et al. Dietary macronutrient intake during the first 10 years of life in a cohort of Italian children. *J Pediatr Gastroenterol Nutr* 2007;45:90–95.
17. Delroisse JM, Bolvin AL, Parmentier I, et al. Quantification of *Bifidobacterium* spp. and *Lactobacillus* spp. in rat fecal samples by real-time PCR. *Microbiol Res* 2008;163:663–670.
18. Nisiotou AA, Spiropoulos AE, Nychas GJ. Yeast community structures and dynamics in healthy and Botrytis-affected grape must fermentations. *Appl Environ Microbiol* 2007;73:6705–6713.
19. Bartosch S, Fite A, Macfarlane GT, et al. Characterization of bacterial communities in feces from healthy elderly volunteers and hospitalized elderly patients by using Real-Time PCR and effects of antibiotic treatment on the fecal microbiota. *Appl Environ Microbiol* 2004;6:3575–3581.
20. Collado MC, Derrien M, Isolauri E, et al. Intestinal integrity and *Akkermansia muciniphila*, a mucin-degrading member of the intestinal microbiota present in infants, adults, and the elderly. *Appl Environ Microbiol* 2007;73:7767–7770.
21. Hierro N, Esteve-Zarzoso B, González A, et al. Real-time quantitative PCR (QPCR) and reverse transcription-QPCR for detection and enumeration of total yeasts in wine. *Appl Environ Microbiol* 2006;72:7148–7155.
22. Zott K, Claisse O, Lucas P, et al. Characterization of the yeast ecosystem in grape must and wine using real-time PCR. *Food Microbiol* 2010;27:559–567.
23. Mujico JR, Baccan GC, Gheorghe A, et al. Changes in gut microbiota due to supplemented fatty acids in diet-induced obese mice. *Br J Nutr* 2013;110:711–720.
24. Tabbaa M, Golubic M, Roizen MF, et al. Docosahexaenoic acid, inflammation, and bacterial dysbiosis in relation to periodontal disease, inflammatory bowel disease, and the metabolic syndrome. *Nutrients* 2013;5:3299–3331.
25. Schloss PD, Iverson KD, Petrosino JF, et al. The dynamics of a family's gut microbiota reveal variations on a theme. *Microbiome* 2014;2:25–38.
26. Everard A, Belzer C, Geurts L, et al. Cross-talk between *Akkermansia muciniphila* and intestinal epithelium controls diet-induced obesity. *Proc Natl Acad Sci USA* 2013;110:9066–9071.
27. Derrien M, van Passel MW, van de Bovenkamp JH et al. Mucin-bacterial interactions in the human oral cavity and digestive tract. *Gut Microbes* 2010;1:254–268.
28. Fujimoto T, Imaeda H, Takahashi K, et al. Decreased abundance of *Faecalibacterium prausnitzii* in the gut microbiota of Crohn's disease. *J Gastroen Hepatol* 2013;28:613–619.
29. Sokol H, Pigneur B, Watterlot L, et al. *Faecalibacterium prausnitzii* is an anti-inflammatory commensal bacterium identified by gut microbiota analysis of Crohn disease patients. *Proc Natl Acad Sci USA* 2008;105:16731–16736.
30. Wrzosek L, Miquel S, Noordine ML, et al. *Bacteroides thetaiotaomicron* and *Faecalibacterium prausnitzii* influence the production of mucus glycans and the development of goblet cells in the colonic epithelium of a gnotobiotic model rodent. *BMC Biol* 2013;11:61–74.
31. Xu P, Li M, Zhang J, et al. Correlation of intestinal microbiota with overweight and obesity in Kazakh school children. *BMC Microbiol* 2012;12:283–289.
32. Hoffmann C, Dollive S, Grunberg S, et al. Archea and fungi of the human gut microbiome: Correlations with diet and bacterial resident. *Plos One* 2013;8:e66019.
33. Mathur R, Kim G, Morales W, et al. Intestinal Methanobrevibacter smithii but not total bacteria is related to diet-induced weight gain in rats. Obesity 2013;21:748–754.
34. Samuel BS, Gordon JI. A humanized gnotobiotic mouse model of host-archaeal- bacterial mutualism. *Proc Natl Acad Sci USA* 2006;103:10011–10016.
35. Schwiertz A, Taras D, Schafer K, et al. Microbiota and SCFA in lean and overweight healthy subjects. Obesity 2010;18:190–195.
36. Million M, Angelakis E, Maraninchi M, et al. Correlation between body mass index and gut concentrations of Lactobacillus reuteri, Bifidobacterium animalis, Methanobrevibacter smithii and Escherichia coli. Int J Obes 2013;37:1460–1466.
37. Zhang H, DiBaise JK, Zuccolo A, et al. Human gut microbiota in obesity and after gastric bypass. *Proc Natl Acad Sci USA* 2009;106:2365–2370.
38. Mbakwa CA, Penders J, Savelkoul PH, et al. Gut colonization with methanobrevibacter smithii is associated with childhood weight development. *Obesity* 2015;23:2508–2516.

Address correspondence to:
Elisa Borghi, PhD
Department of Health Sciences
Università degli Studi di Milano
via di Rudinì, 8
Milan, Italy

E-mail: elisa.borghi@unimi.it

2.6 Manuscript 2:

” Pediatric obesity is associated with an altered gut microbiota and discordant shifts in *Firmicutes* populations”

Published in:
Environmental Microbiology, 2016

(Page numbers are relative to paper)

environmental microbiology

Environmental Microbiology (2016) **00**(00), 00–00 doi:10.1111/1462-2920.13463

Pediatric obesity is associated with an altered gut microbiota and discordant shifts in *Firmicutes* populations

Alessandra Riva,[1,2] Francesca Borgo,[2] Carlotta Lassandro,[3] Elvira Verduci,[3] Giulia Morace,[2] Elisa Borghi[2] and David Berry[1]*

[1]*Department of Microbiology and Ecosystem Science, Division of Microbial Ecology, Research Network Chemistry Meets Microbiology, University of Vienna, Althanstrasse 14, Vienna, Austria.*

[2]*Department of Health Sciences, Università degli Studi di Milano, via di Rudinì, 8, Milan, Italy.*

[3]*Department of Pediatrics, San Paolo Hospital, via di Rudinì, 8, Milan, Italy.*

Summary

An altered gut microbiota has been linked to obesity in adulthood, although little is known about childhood obesity. The aim of this study was to characterize the composition of the gut microbiota in obese ($n = 42$) and normal-weight ($n = 36$) children aged 6 to 16. Using 16S rRNA gene-targeted sequencing, we evaluated taxa with differential abundance according to age- and sex-normalized body mass index (BMI *z*-score). Obesity was associated with an altered gut microbiota characterized by elevated levels of *Firmicutes* and depleted levels of *Bacteroidetes*. Correlation network analysis revealed that the gut microbiota of obese children also had increased correlation density and clustering of operational taxonomic units (OTUs). Members of the *Bacteroidetes* were generally better predictors of BMI *z*-score and obesity than *Firmicutes*, which was likely due to discordant responses of *Firmicutes* OTUs. In accordance with these observations, the main metabolites produced by gut bacteria, short chain fatty acids (SCFAs), were higher in obese children, suggesting elevated substrate utilisation. Multiple taxa were correlated with SCFA levels, reinforcing the tight link between the microbiota, SCFAs and obesity. Our results suggest that gut microbiota dysbiosis and elevated fermentation activity may be involved in the etiology of childhood obesity.

Received 13 May, 2016; revised 27 June, 2016; accepted 19 July, 2016. *For corresponding. E-mail: berry@microbial-ecology.net; Tel. +43 1 4277 76612; Fax +43 1 4277 876612.

Introduction

The gut microbiota is involved in the regulation of multiple host pathways and participates in metabolic and immune-inflammatory axes connecting the gut with the liver, muscle and brain. The gut microbiota co-develops with its host from birth and is subjected to a complex interplay that is influenced by host genome, nutrition and lifestyle (Nicholson *et al.*, 2012). Diet can have a particularly marked impact on the gut environment, affecting factors such as gut transit time and pH. In particular, alterations in the intake of carbohydrates, proteins and fats can significantly affect the composition of the microbiota (Scott *et al.*, 2013). One of the main activities of the gut microbiota is to break down substrates such as resistant starch and dietary fiber, which are incompletely hydrolysed by host enzymes in the small intestine. The main fermentation products resulting from fiber breakdown are the short chain fatty acids (SCFAs) acetate, propionate and butyrate, which play different roles in energy salvage (Schwiertz *et al.*, 2009). Microbially-derived SCFAs provide an additional source of energy for the body: propionate is taken up by the liver and used as a precursor for liponeogenesis, gluconeogenesis and protein synthesis; acetate is used as a substrate for cholesterol synthesis; and butyrate is the main energy supply for colonic epithelial cells (Kallus *et al.*, 2012).

The adult human gastrointestinal tract microbiota has been extensively studied in relation to its role in gut homeostasis and various diseases (Schwiertz *et al.*, 2009). Notably, alterations in the gut microbiome and metabolome have been associated with the development of obesity (Choquet *et al.*, 2010; Vinolo *et al.*, 2011). Obesity is a multifactorial disease that predisposes to several comorbidities (Ang *et al.*, 2013) and is considered to be a global epidemic by the World Health Organisation (Schwiertz *et al.*, 2009). In recent years, the prevalence of childhood obesity has increased substantially worldwide,

and currently 23% of children and adolescents in developed countries can be classified as overweight or obese (Ng *et al.*, 2014).

Information regarding the structure and function of the gut microbiota during childhood is limited. Although it has been suggested that the microbiota reaches a relatively stable adult-like state in the first three years of life, other evidence indicates that it continues to develop through adolescence (Hollister *et al.*, 2015). As such, childhood may provide unique opportunities for microbiota interventions to promote health or prevent disease. It is, therefore, vital to establish a baseline understanding of pediatric gut microbiota structure and function, as during this period the gastrointestinal tract undergoes a transition from an immature to a mature state (Hollister *et al.*, 2015).

The goal of the present study was to characterize the composition of the gut microbiota in obese and normal-weight children using 16S rRNA gene-targeted sequencing. We recruited a large cohort of children from the same geographic area to reduce variation unrelated to obesity. We compared gut microbiota profiles with SCFAs and BMI *z*-scores to gain insights into the structure and activity of the microbiota in pediatric obesity.

Results

Pediatric cohort characteristics

A total of 78 children were enrolled at the Pediatric Department of San Paolo Hospital, Milan, Italy. Fecal samples were collected from 36 normal-weight (N) and 42 obese (O) children (N, BMI *z*-score: -2.12 to 1.56; O, BMI *z*-score: 2.14–5; $p < 0.0001$). Cohort characteristics, including age, sex, BMI *z*-score, mode of delivery in childbirth and history of breastfeeding or formula feeding as an infant were considered (Supporting Information Table S1). There was no significant relationship between history of breastfeeding or formula feeding as an infant with obese and normal-weight classification (Chi-square test; $p = 0.610$). Children born by Caesarean section tended to be obese, although this trend did not reach statistical significance at the $p = 0.05$ level (Chi-square test; $p = 0.068$). Dietary habits were also collected and obese children showed higher dietary intakes of energy and macronutrients (proteins, carbohydrates, sugars and fats) compared to normal-weight subjects (Supporting Information Table S3).

SCFAs are increased in the stool of obese children

We observed significantly higher concentrations of acetate, propionate and butyrate, as well as total SCFAs, in the stool of obese compared to normal-weight subjects ($p < 0.05$ for all comparisons; Supporting Information Table S2). Moreover, we found that the concentration of total SCFAs was significantly associated with obesity ($p = 0.0317$) and was positively correlated with BMI *z*-score ($p = 0.001$).

The intestinal microbiota is altered in obese children

At the phylum level, the predominant bacterial taxa in feces of both obese and normal-weight subjects were *Bacteroidetes* and *Firmicutes*, followed by *Actinobacteria*, *Verrucomicrobia* and *Proteobacteria* (Fig. 1A, Supporting Information Table S4). The most abundant families were *Ruminococcaceae*, *Lachnospiraceae*, *Bacteroidaceae*, *Veillonellaceae*, *Bifidobacteriaceae*, *Prevotellaceae*, *Verrucomicrobiaceae*, *Rikenellaceae* and *Christensenellaceae* (Fig. 1B, Supporting Information Table S4). The most abundant genera were *Bacteroides*, *Subdoligranulum*, *Faecalibacterium*, *Dialister*, *Bifidobacterium*, *Pseudobutyrivibrio* and *Blautia* (Supporting Information Fig. S1, Supporting Information Table S4).

The overall composition of the intestinal microbiota, considered at OTU level as well as taxonomic levels ranging from genus to phylum, was significantly affected by obesity, as determined by non-parametric multivariate analysis of variance testing (perMANOVA; $p < 0.05$ for all levels). Ordination showed that samples from normal-weight and obese children were distinctly grouped (Fig. 1C). This grouping was confirmed for every taxonomic level by the analysis of similarity (ANOSIM) test, which evaluates significance of sample grouping ($p < 0.01$ for all levels). The intestinal microbiota of obese children was enriched in *Firmicutes* (N: 60.9 ± 14.1, O: 72.1 ± 12.1; mean $\pm$ sd) and depleted in *Bacteroidetes* (N: 30 ± 12.6, O: 16.6 ± 11.8) (Supporting Information Table S5). Accordingly, the *Firmicutes*/*Bacteroidetes* ratio was significantly elevated in obese children ($p < 0.0001$; N: 2.6 ± 1.83, O: 7.7 ± 7.1) (Fig. 1D). In agreement with previous observations, the *Firmicutes*/*Bacteroidetes* ratio for obese children displayed a much larger range than for normal-weight children, which may be partially attributable to the wide range of BMI *z*-score in the obese group. Consistent with the shifts observed at phylum level, at the family level *Ruminococcaceae* (N: 33.3 ± 11.5, O: 42.5 ± 12.7) was enriched and *Bacteroidaceae* (N: 21.4 ± 12.2, O: 10 ± 7.1) was depleted. At the genus and OTU levels, we observed significant depletion of *Bacteroides* (N: 21.4 ± 12.2, O: 10.5 ± 7.1) as well as *Bacteroides* OTU 7 (best BLAST hit: *Bacteroides vulgatus* with 100% sequence similarity of 422 bp). There were, however, no significant shifts in members of the *Ruminococcaceae* (Supporting Information Table S5).

Gut microbiota richness estimates were not significantly different between samples from obese and normal-weight children (Observed species: $p = 0.59$; Chao1 estimated richness: $p = 0.98$). Likewise, alpha diversity metrics, which take into account both community richness and evenness, were not significantly different between groups

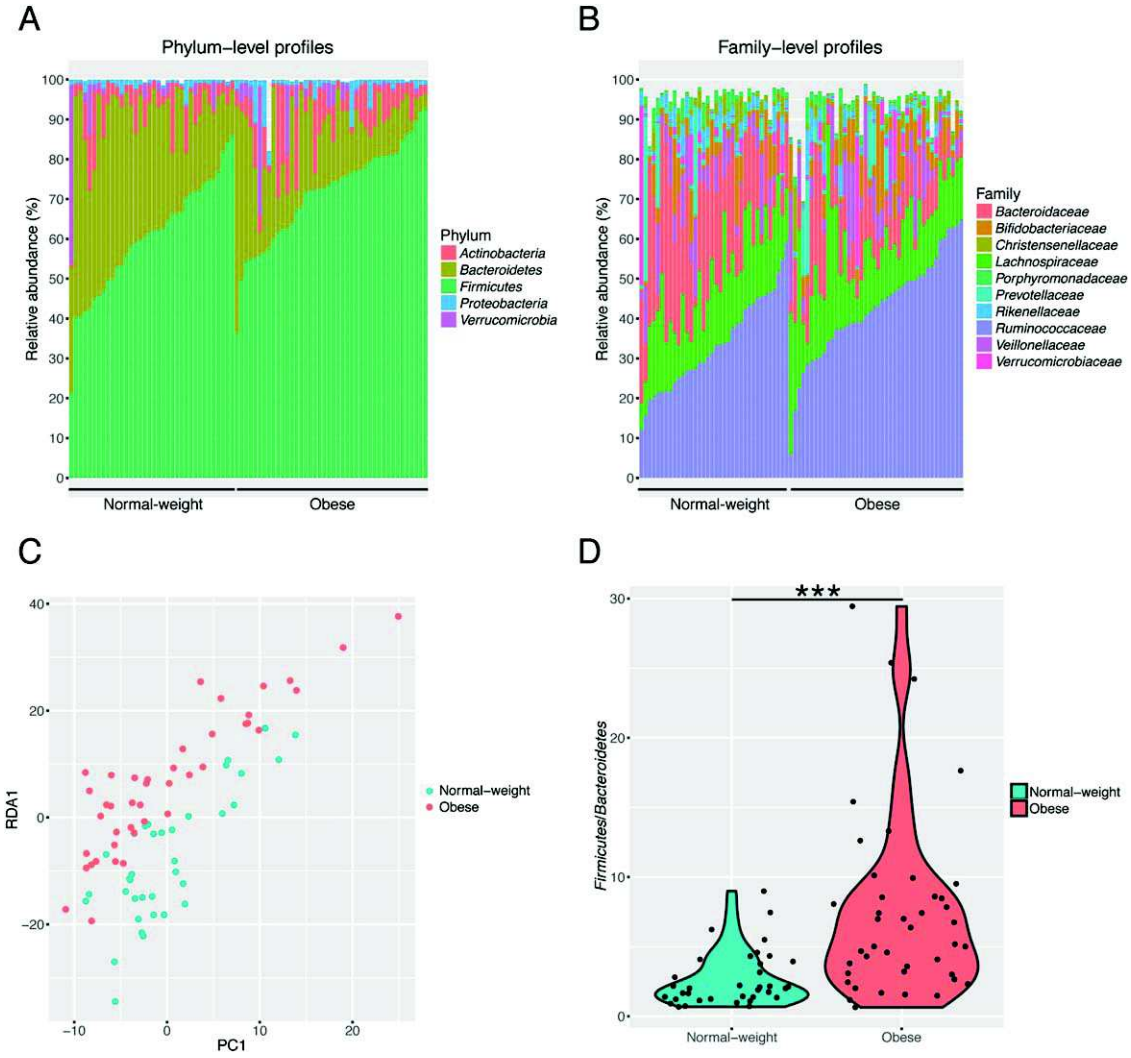

Fig. 1. Abundant bacterial taxa in stool samples of normal-weight ($n = 36$) and obese ($n = 42$) children.
Phylum-level (A) and family-level (B) taxon profiles are shown. Abundant taxa, defined as having a mean relative abundance of >1%, are shown.
C. Redundancy analysis ordination of the gut microbiota according to normal-weight (blue) and obese (red) groups.
D. *Firmicutes*/*Bacteroidetes* ratio for normal-weight (N) and obese (O) children. The ratio is significantly higher in obese compared to normal-weight children ($p < 0.0001$).

(Shannon: $p = 0.065$; inverse Simpson $p = 0.34$) (Supporting Information Fig. S2). We also found that mode of delivery and infant feeding were not significantly associated with microbiota composition at any taxonomic level (perMANOVA, $p > 0.05$ for all levels). In order to determine whether the higher proportion of Caesarean deliveries among the obese group could impact the difference in microbiota profiles, we grouped the samples according to delivery mode (vaginal or Caesarean section) and calculated if there was a difference in the abundance of taxonomic groups. No significant differences were found at any taxonomic level. Therefore, we conclude that delivery mode did not significantly influence the composition of the microbiota.

BMI z-score and SCFAs are associated with intestinal microbiota composition

Childhood obesity is typically defined using age and sex normalized BMI (BMI *z*-score), to classify subjects into normal-weight and obese. In order to gain a more fine-grained understanding of the relationship between the intestinal microbiota and obesity, we evaluated how BMI *z*-score was associated with microbiota composition. BMI *z*-score and the SCFAs acetate and propionate were significantly associated with microbiota composition at every taxonomic level (OTU to phylum; $p < 0.05$ at all levels). Additionally, alpha diversity metrics were largely negatively correlated with BMI *z*-score and SCFA levels (Supporting

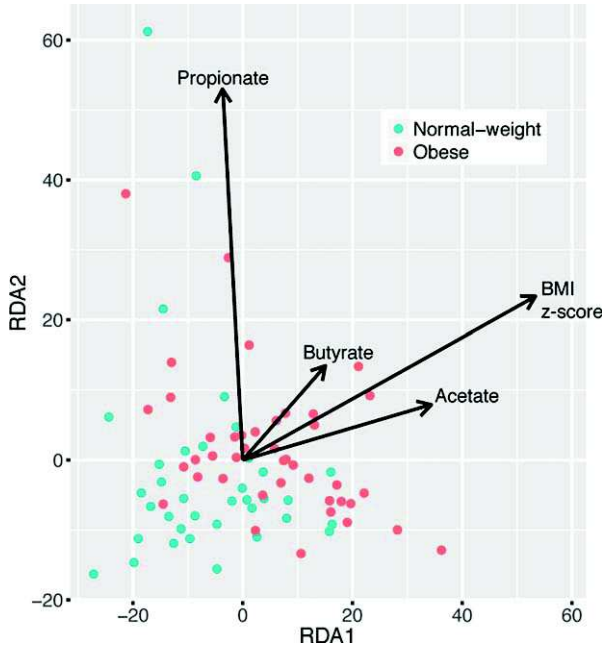

Fig. 2. Redundancy analysis of gut microbiota composition with respect to BMI *z*-score, acetate, propionate and butyrate. The direction of the arrows shows the correlation between variables. Normal-weight samples are represented by blue dots and obese with red dots.

Information Table S6). We performed redundancy analysis to visualize the relationship between microbiota composition, BMI *z*-score and SCFAs (Fig. 2). This analysis revealed a strong relationship between BMI *z*-score and acetate, and to a lesser extent, butyrate levels.

BMI *z*-score was positively correlated with the abundance of *Firmicutes* (as well as *Ruminococcaceae*) and negatively correlated with *Bacteroidetes* (as well as *Bacteroidaceae* and *Bacteroides*) (Table 1). At the OTU level, *Faecalibacterium* OTU 3 (Best BLAST hit: *Faecalibacterium prausnitzii* with 100% seq. similarity over 402 bp) was positively correlated with BMI *z*-score, and *Bacteroides* OTUs 7 and 49 (Best BLAST hit: *Bacteroides stercoris* spp. with 99% seq. similarity over 422 bp) were negatively correlated with BMI *z*-score.

The abundances of multiple taxa were also correlated with levels of major SCFAs. Several genera within the *Bacteroidetes* were negatively correlated with acetate levels, and multiple genera within the *Firmicutes* were either positively or negatively correlated with acetate (Supporting Information Table S7). At the OTU level, *Faecalibacterium* OTU 3 was positively correlated with acetate. Compared to acetate, the number of correlations was much more limited for propionate and butyrate. The family *Prevotellaceae*, the genus *Prevotella* as well as *Prevotella* OTU 26 (Best BLAST hit: *Prevotella copri* with 99% seq. similarity over 422 bp) were positively correlated with propionate levels. The genus *Faecalibacterium* as well as *Faecalibacterium* OTU 3 were positively correlated with butyrate levels.

Comparing models to predict BMI z-score based on microbiota composition

We next determined the best microbial predictors of BMI *z*-score by comparing generalized linear regression models at different taxonomic levels. This revealed that the total explanatory power of the models increased at more refined taxonomic levels (Supporting Information Fig. S3). *Bacteroides* was the main contributor to the genus-level model (relative importance: 0.172), followed by two genera of the *Ruminococcaceae*, *Faecalibacterium* and *Subdoligranulum* (rel. imp.: 0.08 and 0.03 respectively). At the OTU-level, the main contributors to the model were *Bacteroides* OTU 7 (rel. imp.: 0.12), *Faecalibacterium* OTU 3 (rel. imp.: 0.08) and *Bacteroides* OTU 49 (rel. imp.: 0.07) (Supporting Information Fig. S3).

The obese gut microbiota has an altered correlation network structure

We performed a correlation network analysis to evaluate if obesity was associated with changes in the correlation structure and putative interaction structure of the gut microbiota. We found that networks constructed from samples of normal-weight children had fewer edges, a lower mean degree and lower transitivity, indicating that there were fewer significant correlations and less clustering of OTUs compared to samples from obese children (Fig. 3A and B; Supporting Information Table S8). The betweenness centrality was higher in normal-weight sample networks, which indicates that only a few OTUs are highly connected in the network.

We next evaluated whether there were differences in intra-taxon correlations within the families *Bacteroidaceae* and *Ruminococcaceae*. Interestingly, in both networks *Bacteroidaceae* OTUs with intra-family correlations were positively correlated with one another, whereas *Ruminococcaceae* OTUs had both positive and negative intra-family correlations (Supporting Information Table S8). To further explore the difference in intra-taxon correlations between these groups we extracted clusters of correlating *Bacteroidaceae* and *Ruminococcaceae* OTUs (Supporting Information Table S9). We found that *Bacteroidaceae* OTUs form two communities based on co-abundance patterns, with the most abundant (*Bacteroidaceae* CB1: 8 OTUs, including OTUs 7 and 49) negatively correlated with BMI *z*-score and the less abundant not significantly correlated (*Bacteroidaceae* CB2: 2 OTUs). *Ruminococcaceae* was composed of three communities based on co-abundance patterns, and while the most abundant (*Ruminococcaceae* CR1: 11 OTUs, including OTU 3) was

Table 1. Bacterial taxa correlated with BMI *z*-score.

Taxonomic level	Taxon	*R*	*p*-value
Phylum	*Firmicutes*	0.4145	0.0001
	Bacteroidetes	−0.4538	<0.0001
Class	*Clostridia*	0.3688	0.0008
	Bacteroidia	−0.4538	<0.0001
Order	*Clostridiales*	0.3687	0.0008
	Bacteroidales	−0.4538	<0.0001
Family	*Ruminococcaceae*	0.3778	0.0006
	Bacteroidaceae	−0.4930	<0.0001
Genus	*Bacteroides*	−0.4930	<0.0001
OTU	OTU 7: *Bacteroides vulgatus*	−0.4321	<0.0001
	OTU 3: *Faecalibacterium prausnitzii*	0.3058	0.0064
	OTU 49: *Bacteroides stercoris*	−0.3252	0.003

Pearson correlation coefficient (*r*) and *p*-value are shown for significantly correlating taxa and operational taxonomic units (OTUs).

positively correlated with BMI *z*-score, the second was negatively correlated (*Ruminococcaceae* CR2: 8 OTUs), and the third (CR3: 20 OTUs) was not significantly correlated (Supporting Information Figs. S4 A, B).

Discussion

The gut microbiota is affected by many factors, such as diet, genetics, health status, environment and lifestyle (Rodríguez *et al.*, 2015). Childhood and adult obesity are accompanied by changes in the composition of the gut microbiota (Karlsson *et al.*, 2012; Bervoets *et al.*, 2013; Borgo *et al.*, 2016). In the present study we found alterations in gut microbiota composition and SCFA levels in a cohort of 42 obese and 36 normal-weight Italian children. We observed that children born by Caesarean section tended to be obese, although this result did not reach statistical significance. Past studies have found that Caesarean section delivery increases the risk of obesity (Goldani *et al.*, 2011; Mueller *et al.*, 2015; Portela *et al.*, 2015) and impacts the infant gut microbiota (Grönlund *et al.*, 1999). In our study, delivery mode and infant feeding history (breast-fed vs. formula-fed) were not significantly associated with obesity or the gut microbiota composition of children (mean age = 11). The impact of delivery mode and infant feeding history on the gut microbiota may, therefore, be lost after the first years of life, although it is still unclear exactly when (Penders *et al.*, 2006; Biasucci *et al.*, 2010). Gut microbiota composition has been reported to begin to converge toward an adult-like microbiota by the end of the first year of life and fully resemble the adult microbiota by 2.5 years of age (Clemente *et al.*, 2012), although other studies have shown that the microbiota of children up to 4 years of age differs from that of adults (Kulka *et al.*, 2013; Hollister *et al.*, 2015), suggesting that conversion to an 'adult-like' microbiota may be a long and gradual process.

Recent scientific advances implicate the gut microbiota as a contributor to over-nutrition. The gut microbiota enables hydrolysis of indigestible polysaccharides to easily-absorbable monosaccharides and activation of lipoprotein lipase by direct action of the villous epithelium. Consequently, glucose is rapidly adsorbed and fatty acids are stored in excess (Kalliomäki *et al.*, 2008), providing an additional source of energy for the body (Turnbaugh *et al.*, 2006). The significantly higher concentration of SCFAs in obese participants in our study may indicate that in obese children colonic fermentation is elevated, or alternatively that there is decreased SCFA absorption due to low-grade inflammation or more rapid gut transit. This has previously been observed in cohorts of both children (Payne *et al.*, 2011) and adults (Schwiertz *et al.*, 2009; Fernandes *et al.*, 2014). Elevated fecal concentrations of total or individual SCFAs might result from increased microbial production, shifts in microbial cross-feeding patterns or low mucosal absorption (Schwiertz *et al.*, 2009).

We observed a clear alteration in the gut microbiota in obese children at every taxonomic level. This was characterized at the phylum level by an increased abundance of *Firmicutes* and a decreased abundance of *Bacteroidetes* in obese children. It has been hypothesized that an increased ratio of *Firmicutes* to *Bacteroidetes* may contribute to the pathophysiology of obesity and is associated with increased production of SCFAs and energy harvest from colonic fermentation (Turnbaugh *et al.*, 2006; Fernandes *et al.*, 2014). Although an elevated *Firmicutes*/*Bacteroidetes* ratio in obese subjects has been reported in multiple studies (Turnbaugh *et al.*, 2009; Xu *et al.*, 2012; Bervoets *et al.*, 2013), a reduced *Firmicutes*/*Bacteroidetes* ratio in obese adults has also been found (Schwiertz *et al.*, 2009). A recent meta-analysis concluded that there were no statistically significant differences across multiple studies in the *Firmicutes*/*Bacteroidetes* ratio between obese and normal-weight adults (Walters *et al.*, 2014). In agreement with this meta-analysis, some pediatric studies have

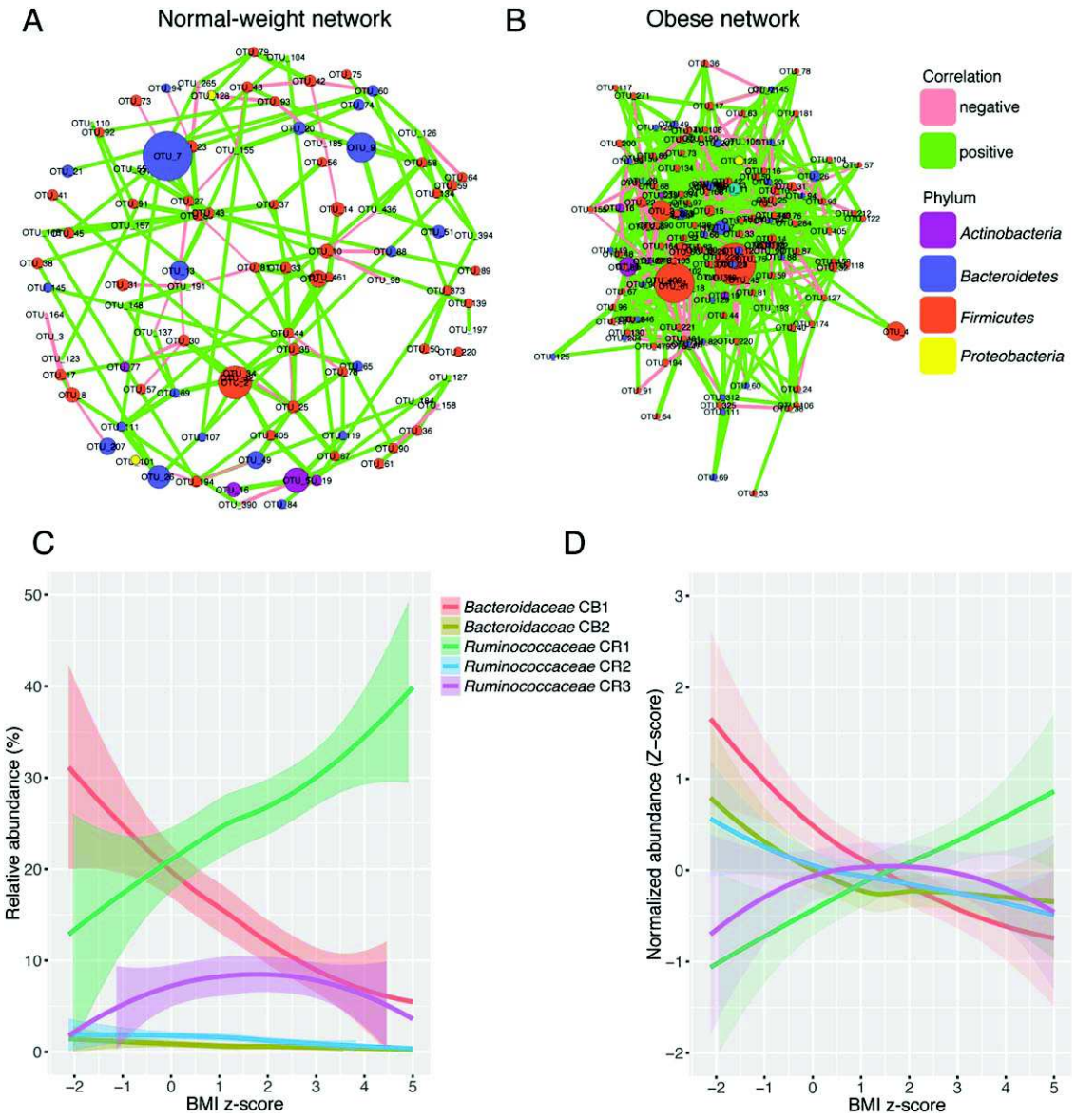

Fig. 3. Correlation networks of samples from normal-weight and obese children.
A, B. Networks show significant positive (green) and negative (pink) pairwise correlations between operational taxonomic units (OTUs). OTUs are coloured by phylum affiliation and sized by mean relative abundance.
C, D. Correlating communities of *Bacteroidaceae* (CB) and *Ruminococcaceae* (CR) and their abundances with respect to BMI *z*-score. Relative abundances (C) and *z*-score transformed abundances (D) are shown. Data points were processed using Lowess smoothing and 95% confidence intervals are shown.

found an increase in *Firmicutes* and a decrease in *Bacteroidetes* (Bervoets *et al.*, 2013; Ferrer *et al.*, 2013) while others have not (Abdallah Ismail *et al.*, 2011; Payne *et al.*, 2011). Although in our study the *Firmicutes*/*Bacteroidetes* ratio was significantly elevated in obese individuals, we observed large variation in the ratio, particularly within the obese group. This large variation, as well as the contradicting results from previous studies, suggests that the *Firmicutes*/*Bacteroidetes* ratio may not be a robust marker for obesity.

We reasoned that the classification of individuals into normal-weight and obese groups might be too coarse of a description for the physiological differences present at different BMI *z*-scores. We found that the alpha diversity of the gut microbiota was negatively correlated with BMI *z*-score and we recovered the same broad trends as we observed with obesity classification such as a positive correlation with the *Firmicutes*/*Bacteroidetes* ratio, but with additional insights such as positive correlation of *Faecalibacterium* OTU 3 (*F. prausnitzii*) with BMI *z*-score and a

negative correlation of *Bacteroides* OTU 7 and 49 (*B. vulgatus* and *B. stercoris* respectively) with BMI *z*-score. *Faecalibacterium*, a group of major butyrate producers in the colon (Louis *et al*., 2009), was also positively correlated with acetate and butyrate, reinforcing the tight link between SCFAs and obesity. Literature data are conflicting about the level of *F. prausnitzii* in obesity, with studies showing positive (Balamarugan *et al*., 2010), negative (Borgo *et al*., 2016) or no association (Feng *et al*., 2014). These contradictory results may be due to experimental factors such as small cohort sizes or the use of different primer sets, or may be explained by the existence of multiple *F. prausnitzii* phylotypes (Louis *et al*., 2009; Hippe *et al*., 2016). Indeed, Hippe and colleagues (2016) suggested that the two identified phylotypes display different physiological properties and seem to produce different amounts of butyrate in the gut. Propionate levels were positively correlated with members of the *Prevotellaceae*, which are known propionate producers (Schwiertz *et al*., 2009), although this was not related to BMI *z*-score. Interestingly, increase of colonic propionate has been shown to prevent weight gain in overweight adults by stimulating the release of PYY and GLP-1 from human colonic cells and thereby reducing energy intake (Chambers *et al*., 2014).

In order to determine if the structure of the gut microbiota is also altered in obesity, we performed a correlation network analysis and found that there were fewer correlations and less clustering of OTUs in normal-weight compared to obese children. The betweenness centrality was higher in the normal-weight network, which indicates that in the obese microbiota there are more OTUs that are highly connected to other OTUs. It is tempting to speculate that the altered network structure in obese children may be involved in the increased fermentation capacity of the gut microbiota.

Interestingly, intra-taxon correlations within the families *Bacteroidaceae* and *Ruminococcaceae* demonstrated that in both networks *Bacteroidaceae* OTUs were positively correlated with one another, whereas *Ruminococcaceae* OTUs had both positive and negative intra-family correlations. This indicates a lack of intra-family ecological cohesion for *Ruminococcaceae* across these samples and may explain why *Bacteroidetes* taxa were generally better predictors of BMI and obesity than *Firmicutes* taxa. To further investigate the difference between *Bacteroidaceae* and *Ruminococcaceae* responses, we extracted from the complete network the communities of co-abundant OTUs from these two groups. We identified five distinct correlating communities (2 *Bacteroidaceae* [CB1 and CB2] and 3 *Ruminococcaceae* [CR1-CR3]). Interestingly, while *Ruminococcaceae* CR1 was positively correlated with BMI *z*-score, *Ruminococcaceae* CR2 was negatively correlated. The divergent response of members of the *Ruminococcaceae* with respect to BMI *z*-score may indicate different niche preferences within this group and may also help to explain why the increased *Firmicutes*/*Bacteroidetes* ratio is not found in all studies, as it groups together *Firmicutes* populations with discordant shifts in obesity. Divergent responses of members of the clostridia have previously been observed in other conditions such as inflammation (Berry *et al*., 2012). It is likely that the extensive physiological and metabolic diversity in members of the clostridia is responsible for these contrasting responses, and additional studies are needed to better characterize and functionally categorize the members of this abundant group.

Although it is recognized that the gut microbiota has the potential to change along with the development of its host, information regarding the structure and function of the microbiome in children remains limited (Hollister *et al*., 2015). We hypothesized that an aberrant gut microbiota composition and activity might contribute to the development of childhood obesity. We found that members of the *Bacteroidetes* and certain populations of *Firmicutes* were associated with childhood obesity, although members of the *Firmicutes* exhibited contrasting shifts. Additional studies are needed to better characterize the members of *Firmicutes* and their roles in obesity. Obesity is often associated with altered dietary habits, and in the present study obese children had higher caloric intake. It is therefore not possible to determine if an altered microbiota is a causative factor in pediatric obesity or a consequence of diet, and this must be tested with future research that takes into account diet and physiology and which includes detailed functional analyses of the metabolic activity of the gut microbiota. Together, this will advance our understanding of the role of the gut microbiota in obesity and provide opportunities to improve health and prevent disease.

Experimental procedures

Subjects and sample collection

Seventy-eight children (36 males/42 females, 9–16 years) were enrolled in the study at the Pediatric Department of San Paolo Hospital in Milan from December 2013 to February 2015. The enrollment conditions were performed as previously described (Borgo *et al*., 2016). Briefly, children's BMI was calculated by reported weight/height^2 (kg m^{-2}), and classification of obese (O) and normal weight (N) was made according to Cole (Cole *et al*., 2000). Weight (kg), height (cm) and BMI (kg m^{-2}) were transformed to age and sex-specific *z*-scores (Cole *et al*., 1995). Inclusion criteria were: children living in Northern Italy born from Caucasian parents with birth weight $\geq$ 2500 g, gestational age 37–42 weeks and singleton birth. Children with neonatal disease, congenital malformation, antibiotic or probiotic/prebiotic usage in the previous six months, chronic or acute intestinal and obesity-related comorbidity conditions were excluded. Data concerning mode of delivery and type of feeding were collected for all subjects and the dietary habits were assessed at recruitment by means of an age-adjusted food frequency questionnaire made up of 116

items (Verduci *et al.*, 2007). Fecal samples were collected 24 h before medical examination and stored at −20°C until processing.

The study was conducted in accordance with the local medical ethical committee (protocol number 2015/ST/135). Written informed consent was given by a parent for all enrolled subjects.

DNA extraction and preparation of 16S rRNA gene amplicon libraries

The total bacterial DNA extraction was performed using the Spin stool DNA kit (Stratec Molecular, Berlin, Germany), according to the manufacturer's instructions and amplified by PCR. Amplification was performed with a two-step barcoding approach according to Herbold and colleagues, 2015. In the first-step PCR, 16S rRNA genes of all Bacteria were amplified with forward primer S-D-bact-0341-b-S-17 (5-CCTACGGGNGGCWGCAG-3′) and reverse primer S-D-bact-0785-a-A-21 (5-GACTACHVGGGTATCTAATCC-3′), which also contained head adaptors (5′-GCTATGCGCGAGCTGC-3′). In the second-step PCR, PCR products from the first step were amplified with primers consisting of the 16 bp head sequence and a sample-specific 8 bp barcode from a previously published list at the 5′ end (Hamady *et al.*, 2008). Each PCR reaction (20 μL in first step, 50 μL in second step) consisted of 10× Taq buffer (Fermentas, USA), 2 mM dNTPmix (Fermentas), 25 mM $MgCl_2$ (Fermentas), 5 U μl^{-1} Taq DNA polymerase (Fermentas), 20 mg ml^{-1} bovine serum albumin (Fermentas), 50 μM of each of the forward and reverse primers and 5 μl of sample. Thermal cycle conditions were: 95°C for 3 min; 95°C for 30 s, a primer-specific annealing temperature of 55°C for 30 s, 72°C for 1 min for 25 cycles and an elongation time of 72°C for 7 min (step1); 52°C for 30 s, 72°C for 1 min for 5 cycles (step 2) and an elongation step of 72°C for 7 min. The first PCR reaction was performed in triplicate, pooled for use as a template in the second step and evaluated qualitatively by gel electrophoresis. The barcoded amplicons were purified between the first step and the second step and after the second step with ZR-96 DNA Clean-up Kit (Zymo Research, USA) and quantified using the Quant-iT PicoGreen dsDNA Assay (Invitrogen, USA). An equimolar library was constructed by pooling samples, and the resulting library was sent sequenced on the Illumina MiSeq platform at Microsynth AG (Balgach, Switzerland). Sequence data have been deposited in the NCBI Short Read Archive under SRP073251.

Short chain fatty acids (SCFAs) measurement

Stool samples were analysed for acetic acid, propionic acid and butyric acid using capillary electrophoresis. For determination of SCFAs concentration one aliquot of frozen fecal sample (50 mg) was used and 200 μl of Milli-Q filtered water was added. The solution was mixed by vortexing for 10 min and then centrifuged 30 min at 21,000 × g. A standard mix composed of acetic acid, propionic acid, butyric acid, lactic acid, formic acid and succinic acid with consecutive concentration of 50 μM, 100 μM, 250 μm and 350 μM, were run as external standards and calibrated. Caproic acid (100 μM final concentration) was used as internal control. A buffer with 0.01M NaOH, 500 μM $CaCl_2$ and 100 μM caproic acid was prepared to run samples. Because we detected interference between phosphates and propionic acid peaks, a final concentration of 500 μM of $CaCl_2$ was added in order to precipitate phosphates usually present in human fecal matter. Ceofix Anions 5 kit (Beckman Coulter, USA) was utilized to prepare anion buffers for the machine. SCFAs concentration was determined in 100μl supernatant using P/ACE MDQ Molecular Characterisation System Beckam Coulter (USA) with a fused silica capillary of 75 μm internal diameter × 363 μm outer diameter (Polymicro Tecnologies, USA). Thirty-two karat software (Beckman Coulter, USA) was used for data processing. SCFAs concentration in fecal samples was expressed in micromoles per gram ($\mu mol\ g^{-1}$) of feces.

Sequence pre-processing and data analysis

Sequence data were sorted into libraries using the 8 nt sample-specific barcode and primer using a custom-made in-house script, quality-filtered according to the Earth Microbiome Project guidelines and paired end reads were concatenated (Bokulich *et al.*, 2013). Reads were then clustered into species-level operational taxonomic units (OTUs) of 97% sequence identity, checked for chimeras using USEARCH, and taxonomically classified using the Ribosomal Database Project näive Bayesian classifier (Wang *et al.*, 2007). Statistical analysis was performed using the statistical software R (https://www.r-project.org/). To avoid biases related to uneven library depth, sequencing libraries were subsampled to a number of reads smaller than the smallest library (2000 reads). The statistical significance of factors affecting microbiota composition was evaluated using non-parametric permutational multivariate analysis of variance (perMANOVA), significant clustering of groups was evaluated with analysis of similarities (ANOSIM), ordination was performed using redundancy analysis (RDA) in the vegan package (Oksanen *et al.*, 2010). Alpha and beta diversity metrics were also calculated with the vegan package. Indicator species analysis was performed using the indicspecies package (De Caceres *et al.*, 2009). Network analysis was performed for all OTUs present in at least 30% of samples as recommended in (Berry and Widder, 2014) using graphical lasso technique cclasso to mitigate biases associated with compositional data (Danaher *et al.*, 2014). Network topological and node-level properties were determined using the igraph package (Csardi, 2015) and networks were visualized using Cytoscape (Shannon *et al.*, 2003). Statistical analysis of cohort-related data was performed using Student's *t*-test, chi-square test, correlation analysis (Pearson correlation coefficient) and linear regression modeling. Variables were expressed as mean ± standard deviation (sd), and for multiple comparisons *p*-values were adjusted with the False Discovery Rate method. A *p*-value less than or equal to 0.05 was considered statistically significant.

Acknowledgement

This research was supported in part by the Austrian Science Fund (FWF; P26127-B20, P27831-B28) and the European Union Erasmus+ programme.

Conflict of interest

All authors declare no conflict of interest.

References

Abdallah Ismail, N., Ragab, S.H., Abd Elbaky, A., Shoeib, A.R., Alhosary, Y., and Fekry, D. (2011) Frequency of *Firmicutes* and *Bacteroidetes* in gut microbiota in obese and normal-weight Egyptian children and adults. *Arch Med Sci* **7:** 501–507.

Ang, Y.N., Wee, B.S., Poh, B.K., and Ismail, M.N. (2013) Multifactorial influences of childhood obesity. *Curr Obes Rep* **2:** 10–22.

Balamurugan, R., George, G., Kabeerdoss, J., Hepsiba, J., Chandragunasekaran, A.M., and Ramakrishna, B.S. (2010) Quantitative differences in intestinal *Faecalibacterium prausnitzii* in obese Indian children. *Br J Nutr* **103:** 335–338.

Berry, D., and Widder, S. (2014) Deciphering microbial interactions and detecting keystone species with co-occurrence networks. *Front Microbiol* **5:** 1–14.

Berry, D., Schwab, C., Milinovich, G., Reichert, J., Mahfoudh, K.B., Decker, T., *et al.* (2012) Phylotype-level 16S rRNA analysis reveals new bacterial indicators of health state in acute murine Colitis. *ISME J* **6:** 2091–2106.

Bervoets, L., Van Hoorenbeeck, K., Kortleven, I., Van Noten, C., Hens, N., Vael, C., *et al.* (2013) Differences in gut microbiota composition between obese and lean children: a cross-sectional study. *Gut Pathog* **5:** 10.

Biasucci, G., Rubini, M., Riboni, S., Morelli, L., Bessi, E., and Retetangos, C. (2010) Mode of delivery affects the bacterial community in the newborn gut. *Early Hum Dev* **86:** 13–15.

Bokulich, N.A., Subramanian, S., Faith, J.J., Gevers, D., Gordon, J.I., Knight, R., *et al.* (2013) Quality-filtering vastly improves diversity estimates from Illumina amplicon sequencing. *Nat Methods* **10:** 57–59.

Borgo, F., Verduci, E., Riva, A., Lassandro, C., Riva, E., Morace, G., and Borghi, E. (2016) Relative abundance in bacterial and fungal gut microbes in obese children: a case control study. *Child Obes*, Online early. doi:10.1089/chi.2015.0194.

Chambers, E.S., Viardot, A., Psichas, A., Morrison, D.J., Murphy, K.G., Zac-Varghese, S.E.K., *et al.* (2015) Effects of targeted delivery of propionate to the human colon on appetite regulation, body weight maintenance and adiposity in overweight adults. *Gut* **64:** 1744–1754.

Choquet, H., and Meyre, D. (2010) Genomic insights into early-onset obesity. *Genome Med* **2:** 1–12.

Clemente, J.C., Ursell, L.K., Parfrey, L.W., and Knight, R. (2012) The impact of the gut microbiota on human health: an integrative view. *Cell* **148:** 1258–1270.

Csardi, G. (2015) igraph: Network Analysis and Visualization. R package version 1.0.0 [WWW document]. URL http://igraph.org.

Cole, T.J., Freeman, J.V., and Preece, M.A. (1995) Body mass index reference curves for the UK, 1990. *Arch Dis Child* **73:** 25–29.

Cole, T.J., Bellizzi, M.C., Flegal, K.M., and Dietz, W.H. (2000) Establishing a standard definition for child overweight and obesity worldwide: international survey. *BMJ* **320:** 1240–1243.

Danaher, P., Wang, P., and Witten, D.M. (2014) The joint graphical lasso for inverse covariance estimation across multiple classes. *J R Stat Soc Series B Stat Methodol* **76:** 373–397.

De Caceres, M., and Legendre, P. (2009) Associations between species and groups of sites: indices and statistical inference. *Ecology* **90:** 3566–3574.

Feng, J., Tang, H., Li, M., Pang, X., Wang, L., Zhang, M., *et al.* (2014) The abundance of fecal *Faecalibacterium prausnitzii* in relation to obesity and gender in Chinese adults. *Arch Microbiol* **196:** 73–77.

Fernandes, J., Su, W., Rahat-Rozenbloom, S., Wolever, T.M.S., and Comelli, E.M. (2014) Adiposity, gut microbiota and faecal short chain fatty acids are linked in adult humans. *Nutr Diabetes* **4:** 1–7.

Ferrer, M., Ruiz, A., Lanza, F., Haange, S.B., Oberbach, A., Till, H., *et al.* (2013) Microbiota from the distal guts of lean and obese adolescents exhibit partial functional redundancy besides clear differences in community structure. *Environ Microbiol* **15:** 211–226.

Goldani, H.A.S., Bettiol, H., Barbieri, M.A., Silva, A.A.M., Agranonik, M., Morais, M.B., and Goldani, M.Z. (2011) Cesarean delivery is associated with an increased risk of obesity in adulthood in a Brazilian birth cohort study. *Am J Clin Nutr* **93:** 1344–1347.

Grönlund, M.M., Lehtonen, O.P., Eerola, E., and Kero, P. (1999) Fecal microflora in healthy infants born by different methods of delivery: permanent changes in intestinal flora after cesarean delivery. *JPGN* **28:** 19–25.

Hamady, M., Walker, J.J., Harris, J.K., Gold, N.J., and Knight, R. (2008) Error-correcting barcoded primers for pyrosequencing hundreds of samples in multiplex. *Nat Methods* **5:** 235–237.

Herbold, C.W., Pelikan, C., Kuzyk, O., Hausmann, B., Angel, R., Berry, D., and Loy, A. (2015) A flexible and economical barcoding approach for highly multiplexed amplicon sequencing of diverse target genes. *Front Microbiol* **6:** 1–8.

Hippe, B., Remely, M., Aumueller, E., Pointner, A., Magnet, U., and Haslberger, A.G. (2016) Faecalibacterium prausnitzii phylotypes in type two diabetic, obese, and lean control subjects. *Benef Microbes* [Epub ahead of print].

Hollister, E.B., Riehle, K., Luna, R.A., Weidler, E.M., Rubio-Gonzales, M., Mistretta, T.A., *et al.* (2015) Structure and function of the healthy pre-adolescent pediatric gut microbiome. *Microbiome* **3:** 1–13.

Kalliomäki, M., Collado, M.C., Salminen, S., and Isolauri, E. (2008) Early differences in fecal microbiota composition in children may predict overweight. *Am J Clin Nutr* **87:** 534–538.

Kallus, S.J., and Brandt, L.J. (2012) The Intestinal Microbiota and Obesity. *J Clin Gastroenterol* **46:** 16–24.

Karlsson, C.L.J., Önnerfält, J., Xu, J., Molin, G., Ahrné, S., and Thorngren-Jerneck, K. (2012) The microbiota of the gut in preschool children with normal and excessive body weight. *Obesity* **20:** 2257–2261.

Kulka, T.R., Cheng, J., Ringel, Y., Salojärvi, J., Carroll, I., Palva, A., de Vos, W.M., and Satokari, R. (2013) Intestinal microbiota in healthy U.S. young children and adults-a high throughput microarray analysis. *PLoS one* **8:** 1–10.

Louis, P., and Flint, H.J. (2009) Diversity, metabolism and microbial ecology of butyrate-producing bacteria from the human large intestine. *FEMS Microbiol Lett* **294:** 1–8.

Mueller, N.T., Whyatt, R., Hoepner, L., Oberfield, S., Dominguez-Bello, M.G., Widen, E.M., *et al.* (2015) Prenatal exposure to antibiotics, cesarean section and risk of childhood obesity. *Int J Obes (Lond)* **39:** 665–670.

Ng, M., Fleming, T., Robinson, M., Thomson, B., Graetz, N., Margono, C., *et al.* (2014) Global, regional, and national prevalence of overweight and obesity in children and adults during 1980–2013: a systematic analysis for the global burden of disease study 2013. *Lancet* **384:** 766–781.

Nicholson, J.K., Holmes, E., Kinross, J., Burcelin, R., Gibson, G., Jia, W., and Pettersson, S. (2012) Host-gut microbiota metabolic interactions. *Science* **336:** 1262–1267.

Oksanen, J., Blanchet, F.G., Kindt, R., Legendre, P., O'hara, R.B., Simpson, G.L., *et al.* (2010). Vegan: community ecology package, R package version 1.17-4. [WWW document] URL http://cran.r-project.org/.

Payne, A.N., Chassard, C., Zimmermann, M., Müller, P., Stinca, S., and Lacroix, C. (2011) The metabolic activity of gut microbiota in obese children is increased compared with normal-weight children and exhibits more exhaustive substrate utilization. *Nutr Diabetes* **1:** 1–8.

Penders, J., Thijs, C., Vink, C., Stelma, F.F., Snijder, B., Kummeling, I., Van den Brandt, P.A., and Stobberingh, E.E. (2006) Factors influencing the composition of the intestinal microbiota in early infancy. *Pediatrics* **118:** 511–521.

Portela, D.S., Vieira, T.O., Matos, S.M., de Oliveira, N.F., and Vieira, G.O. (2015) Maternal obesity, environmental factors, cesarean delivery and breastfeeding as determinants of overweight and obesity in children: results from a cohort. *BMC Pregnancy Childbirth* **15:** 1–10.

Rodríguez, J.M., Murphy, K., Stanton, C., Ross, R.P., Kober, O.I., Juge, N., *et al.* (2015) The composition of the gut microbiota throughout life, with an emphasis on early life. *Microb Ecol Health Dis* **26:** 1–17.

Scott, K.P., Gratz, S.W., Sheridan, P.O., Flint, H.J., and Duncan, S.H. (2013) The influence of diet on the gut microbiota. *Pharmacol Res* **69:** 52–60.

Shannon, P., Markiel, A., Ozier, O., Baliga, N.S., Wang, J.T., Ramage, D., *et al.* (2003) Cytoscape: A software environment for integrated models of biomolecular interaction networks. *Genome Res* **13:** 2498–2504.

Schwiertz, A., Taras, D., Schäfe, K., Beijer, S., Bos, A.N., Donus, C., and Hardt, D.F. (2009) Microbiota and SCFA in lean and overweight healthy subjects. *Obesity* **18:** 190–195.

Turnbaugh, P.J., Ley, R.E., Mahowald, M.A., Magrini, V., Mardis, E.R., and Gordon, J.I. (2006) An obesity associated gut microbiome with increased capacity for energy harvest. *Nature* **444:** 1027–1031.

Turnbaugh, P.J., Hamady, M., Yatsunenko, T., Cantarel, B.L., Duncan, A., Ley, R.E., *et al.* (2009) A core gut microbiome in obese and lean twins. *Nature* **457:** 480–484.

Verduci, E., Radaelli, G., Stival, G., Salvioni, M., Giovannini, M., and Scaglioni, S. (2007) Dietary macronutrient intake during the first 10 years of life in a cohort of Italian children. *J Pediatr Gastroenterol Nutr* **45:** 90–95.

Vinolo, M.A.R., Rodrigues, H.G., Nachbar, R.T., and Curi, R. (2011) Regulation of inflammation by short chain fatty acids. *Nutrients* **3:** 858–876.

Walters, W.A., Xu, Z., and Knight, R. (2014) Meta-analyses of human gut microbes associated with obesity and IBD. *FEBS Lett* **588:** 4223–4233.

Wang, Q., Garrity, G.M., Tiedje, J.M., and Cole, J.R. (2007) Naïve Bayesian Classifier for rapid assignment of rRNA sequences into the new bacterial taxonomy. *Appl Environ Microb* **73:** 5261–5267.

Xu, P., Li, M., Zhang, J., and Zhang, T. (2012) Correlation of intestinal microbiota with overweight and obesity in Kazakh school children. *BMC Microbiol* **12:** 1–6.

URL https://www.r-project.org/

Supporting information

Additional Supporting Information may be found in the online version of this article at the publisher's web-site.

Fig. S1. Abundant bacterial taxa in stool samples of normal-weight (n=36) and obese (n=42) children. Genus level taxon profiles are shown. Abundant taxa, defined as having a mean relative abundance of >1%, are shown.

Fig. S2. Intestinal microbiota richness and diversity in normal-weight and obese children. Observed species, Chao1 estimated richness, Shannon diversity, and inverse Simpson diversity estimators show no significant difference between the two groups (Observed species: p=0.59; Chao1: p=0.98; Shannon: p=0.065; Inverse Simpson p=0.34).

Fig. S3. Generalized linear regression models at different taxonomic levels. (A) The coefficient of determination (R^2), which indicates the proportion of the variance in the dependent variable that is predictable from the independent variable, increases at genus and OTU levels. (B) The Akaike information criterion (AIC), a measure of the relative quality of statistical models for a given set of data, is lowest at genus and OTU levels.

Fig. S4. Correlating communities of *Bacteroidaceae* (CB) and *Ruminococcaceae* (CR) and their abundances with respect to BMI z-score. Relative abundances (A) and z-score transformed abundances (B) are shown. Data points were processed using Lowess smoothing and 95% confidence intervals are shown.

Table S1. Characteristics of the study cohort. The cohort was composed of normal-weight (N) and obese (O) children. Body mass index (BMI) was calculated as weight/height^2 (kg/m^2), and was transformed to age- and sex-adjusted z-scores. Values are expressed as mean ± sd. [a]Information not available for two subjects. [b]Information not available for three subjects.

Table S2. Short chain fatty acid (SCFA) levels in the stool of normal-weight (N) and obese (O) subjects. Concentrations are calculated as μmol/g wet weight and are expressed as mean ± sd. Total SCFA is calculated as the sum of acetate, propionate, and butyrate concentrations.

Table S3. Daily caloric and dietary intake in obese and normal-weight children. Values are expressed as mean ± sd.

Table S4. The relative abundance of abundant bacteria taxa in the study. Abundant taxa are defined as having a mean abundance greater than 1%. *Taxa significantly increased or decreased in obese children (complete details are presented in Table S4).

Table S5. Taxa that were increased (+) or decreased (−) in abundance in obese children (O).

Table S6. Correlation of alpha diversity metrics with BMI z-score and SCFAs. Observed OTUs, Chao1 estimated richness, Shannon and inverse Simpson diversity indexes were correlated and the Pearson correlation coefficients (r) and respective p-values are shown. *indicates p<=0.05 and **indicates p <=0.01.

Table S7. Taxa correlated with acetate concentration. The Pearson correlation coefficients (r) and respective p-values are shown.

Table S8. Properties of correlation networks generated from samples from normal-weight (N) or obese children (O). Nodes are OTUs and edges are significant correlations between OTUs. Other parameters are metrics related to the topology of the network.

Table S9. Clusters of correlating *Bacteroidaceae* and *Ruminococcaceae* OTUs extracted from the correlation network. The closest cultured species and its similarity to each OTU (% sequence similarity) are shown.

SUPPLEMENTAL FIGURES AND TABLES

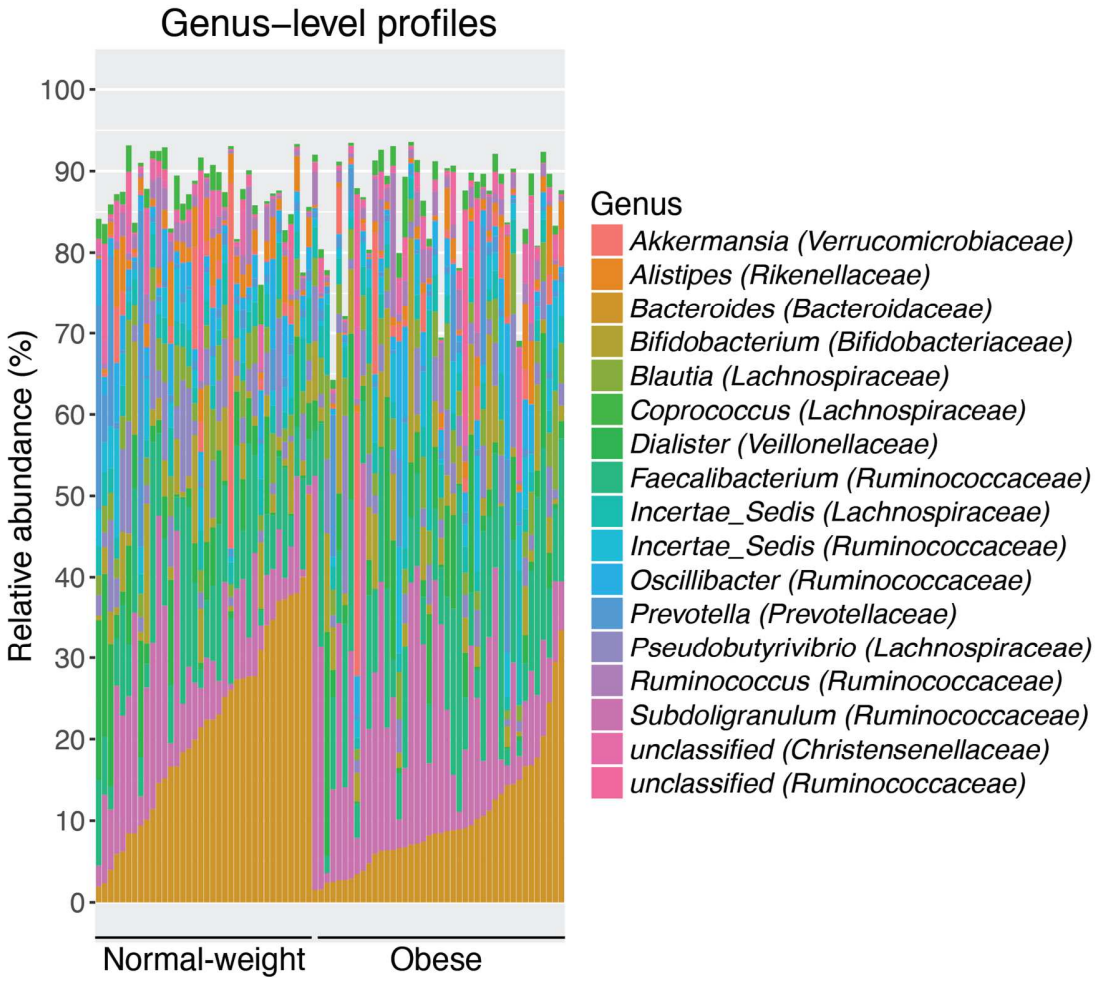

Figure S1. Abundant bacterial taxa in stool samples of normal-weight (n=36) and obese (n=42) children. Genus level taxon profiles are shown. Abundant taxa, defined as having a mean relative abundance of >1%, are shown.

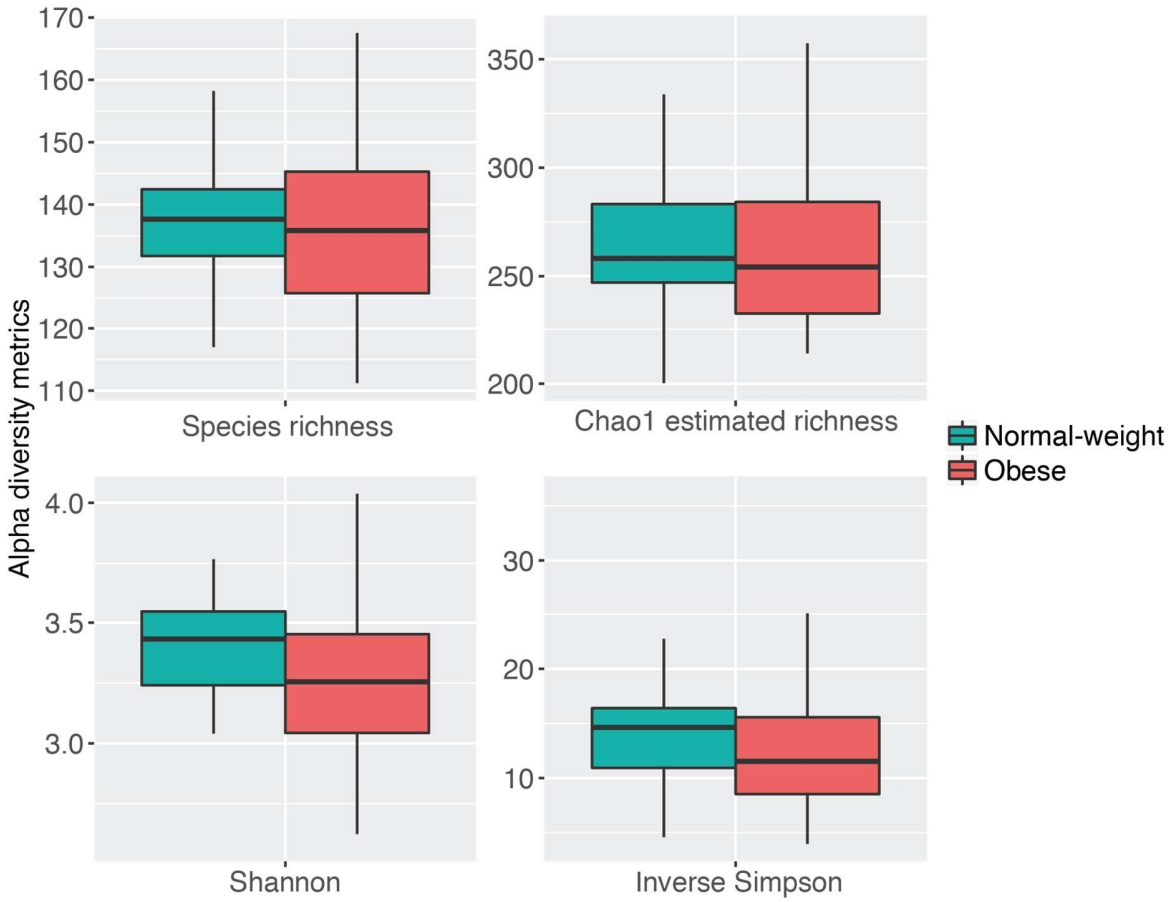

Figure S2. **Intestinal microbiota richness and diversity in normal-weight and obese children.** Observed species, Chao1 estimated richness, Shannon diversity, and inverse Simpson diversity estimators show no significant difference between the two groups (Observed species: p=0.59; Chao1: p=0.98; Shannon: p=0.065; Inverse Simpson p=0.34).

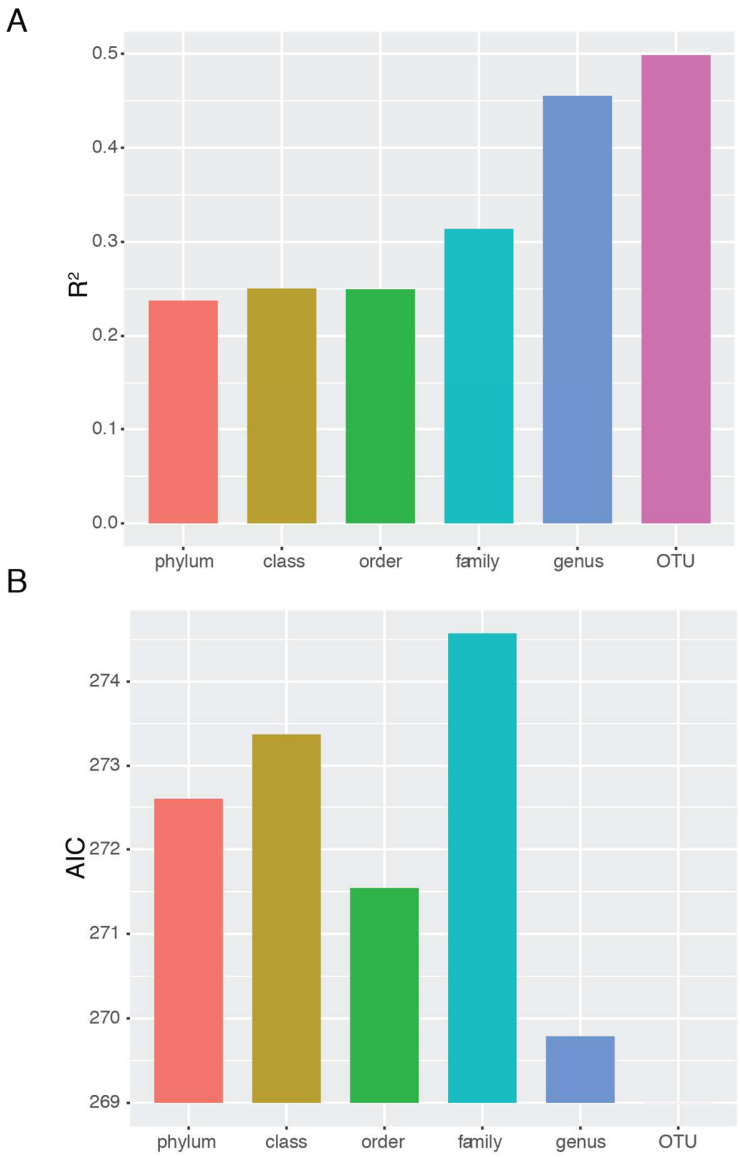

Figure S3. Generalized linear regression models at different taxonomic levels. (A) The coefficient of determination (R^2), which indicates the proportion of the variance in the dependent variable that is predictable from the independent variable, increases at genus and OTU levels. (B) The Akaike information criterion (AIC), a measure of the relative quality of statistical models for a given set of data, is lowest at genus and OTU levels.

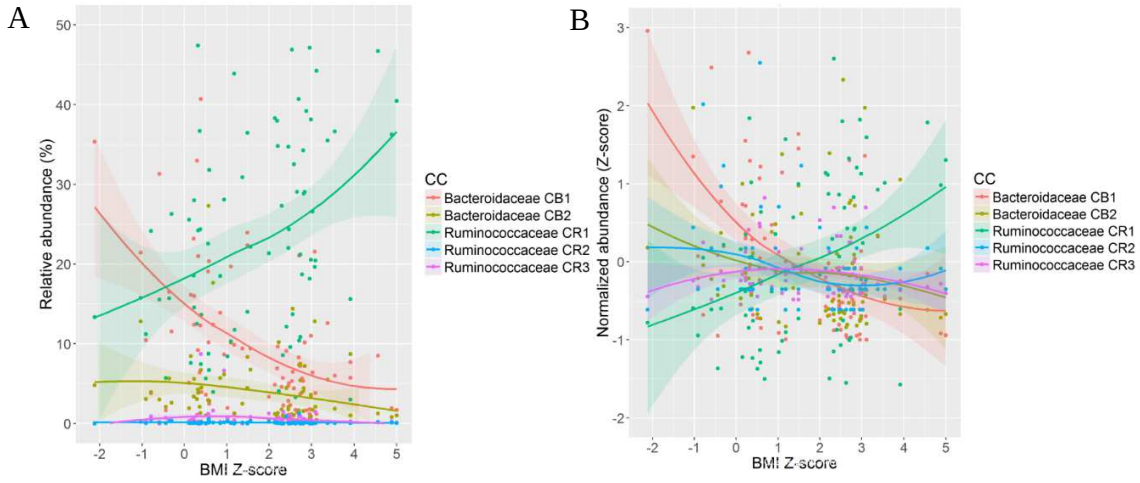

Figure S4: Correlating communities of *Bacteroidaceae* (CB) and *Ruminococcaceae* (CR) and their abundances with respect to BMI z-score. Relative abundances (A) and z-score transformed abundances (B) are shown. Data points were processed using Lowess smoothing and 95% confidence intervals are shown.

Table S1. Characteristics of the study cohort. The cohort was composed of normal-weight (N) and obese (O) children. Body mass index (BMI) was calculated as weight/height^2 (kg/m^2), and was transformed to age- and sex-adjusted z-scores. Values are expressed as mean ± sd. [a]Information not available for two subjects. [b]Information not available for three subjects.

	N (n=36)	O (n=42)
Age (years)	11±0.33	11±1.99
Sex (male:female)	17:19	21:21
BMI z-score	0.3±0.82	3.0±0.7
Delivery type (vaginal: caesarean)	28:8	22:18[a]
Infant diet (breast-fed: formula-fed)	14:22	18:21[b]

Table S2. **Short chain fatty acid (SCFA) levels in the stool of normal-weight (N) and obese (O) subjects.** Concentrations are calculated as μmol/g wet weight and are expressed as mean ± sd. Total SCFA is calculated as the sum of acetate, propionate, and butyrate concentrations.

	N (n=36)	O (n=42)	p-value
Acetate	30.3±13.0	40.4±18.9	0.0081
Propionate	8.8±5.8	12.5±7.7	0.0206
Butyrate	8.4±5.3	12.4±9.8	0.0272
Total SCFA	47.5±20.4	65.3±32.4	0.0049

Table S3. Daily caloric and dietary intake in obese and normal-weight children. Values are expressed as mean ± sd.

Variable	Obese children	Normal weight children	*P*-value	*P*-value†
kcal/day	2264.13 (746.31)	1722.01 (383.78)	0.001 *	0.001*
		Protein		
g/day	94.00 (32.76)	68.56 (19.47)	<0.001 *	0.001*
		Carbohydrates		
g/day	301.06 (120.66)	201.94 (47.66)	<0.001 *	0.001*
		Sugars		
g/day	110.16 (65.70)	75.12 (31.92)	0.005 *	0.012*
		Fats		
g/day	82.38 (30.80)	70.02 (18.36)	0.128	0.033*

† Adjusted for age and sex. *Statistically significant

Table S4. The relative abundance of abundant bacteria taxa in the study. Abundant taxa are defined as having a mean abundance greater than 1%. * Taxa significantly increased or decreased in obese children (complete details are presented in Table S4).

		Normal-weight		Obese	
Taxonomic level	Taxon	Mean	sd	Mean	sd
Phylum	*Bacteroidetes**	30	12.6	16.6	11.8
	*Firmicutes**	60.9	14.1	72.1	12.1
	Actinobacteria	5.6	6.1	6.3	4.9
	Verrucomicrobia	2.5	7.6	2.3	5.5
	Proteobacteria	1.2	1.1	2.0	2.9
Family	*Ruminococcaceae**	33.3	11.5	42.5	12.7
	Lachnospiraceae	16.4	6.5	17.9	9.7
	*Bacteroidaceae**	21.4	12.2	10	7.1
	Veillonellaceae	6.1	5.7	6.5	7.5
	Bifidobacteriaceae	5.1	6.0	5.3	4.5
	Prevotellaceae	3.6	8.5	2.8	5.2
	Verrucomicrobiaceae	2.5	7.6	2.3	5.5
	Rikenellaceae	2.8	2.0	2.0	2.6
	Christensenellaceae	2.0	2.3	2.3	3.7
Genus	*Bacteroides**	21.4	12.2	10.5	7.1
	Subdoligranulum	10.7	8.4	16.7	12.3
	Faecalibacterium	10.0	6.3	12.7	8.7
	Dialister	5.9	5.8	5.6	7.1
	Bifidobacterium	5.1	6.0	5.3	4.5
	Pseudobutyrivibrio	5.1	4.1	4.4	3.9
	Blautia	3.6	1.8	4.4	2.4

Table S5. Taxa that were increased (+) or decreased (-) in abundance in obese children (O).

Taxonomic level	Taxon	O	p-value
Phylum	*Firmicutes*	+	0.001
	Bacteroidetes	-	<0.0001
Class	*Clostridia*	+	0.004
	Bacteroidia	-	<0.0001
Order	*Clostridiales*	+	0.003
	Bacteroidales	-	<0.0001
Family	*Ruminococcaceae*	+	0.01
	Bacteroidaceae	-	<0.0001
Genus	*Bacteroides*	-	<0.0001
OTU	OTU 7: *Bacteroides vulgatus*	-	<0.0001

Table S6. **Correlation of alpha diversity metrics with BMI z-score and SCFAs.** Observed OTUs, Chao1 estimated richness, Shannon and inverse Simpson diversity indexes were correlated and the Pearson correlation coefficients (r) and respective p-values are shown. * indicates p<=0.05 and ** indicates p <=0.01.

	Observed OTUs		Chao1 richness		Shannon		Inverse Simpson	
	r	*p*-value	r	*p*-value	r	*p*-value	r	*p*-value
BMI z-score	-0.1562	0.1720	-0.0240	0.8345	-0.2657	0.0186*	-0.1946	0.0877
Acetate	-0.2956	0.0085**	-0.2826	0.0121*	-0.3513	0.0016**	-0.3581	0.0012 **
Propionate	-0.1876	0.1000	-0.2166	0.0567	-0.2584	0.0223*	-0.2575	0.0227*
Butyrate	-0.2387	0.0353*	-0.2701	0.0167*	-0.2639	0.0195*	-0.2354	0.0379*
Total SCFA	-0.2917	0.0095**	-0.3003	0.0075**	-0.3498	0.0016**	-0.3454	0.0019**

Table S7. **Taxa correlated with acetate concentration.** The Pearson correlation coefficients (r) and respective p-values are shown.

Taxonomic level	**Taxon**	**r**	**p-value**
Phylum	*Firmicutes*	0.3107	0.005
	Bacteroidetes	-0.3145	0.005
Class	*Clostridia*	0.2765	0.01
	Bacteroidia	-0.3145	0.005
Order	*Clostridiales*	0.2767	0.01
	Bacteroidales	-0.3145	0.005
Family	*Ruminococcaceae*	0.3120	0.005
	Bacteroidaceae	-0.2876	0.01
	Porphyromonadaceae	-0.2845	0.01
	Rikenellaceae	-0.3107	0.005
Genus	*Ruminococcaceae Incertae sedis (Firmicutes)*	-0.2683	0.01
	Bacteroides (Bacteroidetes)	-0.2876	0.01
	Parabacteroides (Bacteroidetes)	-0.2737	0.01
	Alistipes (Bacteroidetes)	-0.3117	0.005
	Oscillabacter (Firmicutes)	-0.3205	0.004
	Subdoligranulum (Firmicutes)	0.2737	0.01
	Faecalibacterium (Firmicutes)	0.4487	<0.0001
OTU	OTU 3: *Faecalibacterium prausnitzii*	0.4487	<0.0001

Table S8. **Properties of correlation networks generated from samples from normal-weight (N) or obese children (O).** Nodes are OTUs and edges are significant correlations between OTUs. Other parameters are metrics related to the topology of the network.

	N	**O**
Nodes	138	143
Edges	370	941
Mean Degree	5.36	13.16
Transitivity	0.047	0.131
Average Path Length	3.10	2.22
Assortativity	-0.0535	0.169
Fragmentation	0	0
Betweeness Centrality	0.0701	0.0226
Closeness Centrality	0.00123	0.00137
Percent Positive corr. in network	69.5	65.5
Bacteroidaceae (intra-family corr.; pos./neg.)	[2/0]	[13/0]
Ruminococcaceae (intra-family corr.; pos./neg.)	[31/5]	[50/18]

Table S9: Clusters of correlating *Bacteroidaceae* and *Ruminococcaceae* OTUs extracted from the complete correlation network. The closest related species and similary (%) are shown.

Bacteroidaceae			
Correlating community	**OTU_ID**	**Closest related species**	**Similarity (%)**
CB1	OTU_7	*Bacteroides vulgatus*	100
	OTU_60	*Bacteroides fragilis*	100
	OTU_13	*Bacteroides caccae*	100
	OTU_51	*Bacteroides thetaiotaomicron*	100
	OTU_49	*Bacteroides stercoris*	99
	OTU_119	*Bacteroides cellulosilyticus*	100
	OTU_9	*Bacteroides uniformis*	100
	OTU_207	*Bacteroides xylanisolvens*	99
CB2	OTU_312	*Bacteroides eggerthii*	99
	OTU_65	*Bacteroides finegoldii*	95
Ruminococcaceae			
Correlating community	**OTU_ID**	**Closest related species**	**Similarity (%)**
CR1	OTU_118	*Clostridium leptum*	92
	OTU_1	*Faecalibacterium prausnitzii*	100
	OTU_479	*Faecalibacterium prausnitzii*	97
	OTU_122	*Ruminococcus callidus*	99
	OTU_4	*Gemmiger formicilis*	100
	OTU_48	*Ruminococcus bicirculans*	100
	OTU_68	*Clostridium leptum*	95
	OTU_87	*Clostridium methylpentosum*	90
	OTU_127	*Ruminococcus flavefaciens*	95
	OTU_22	*Ruminococcus bromii*	98
	OTU_3	*Faecalibacterium prausnitzii*	100
CR2	OTU_58	*Clostridium papyrosolvens*	87
	OTU_38	*Gemmiger formicilis*	94
	OTU_96	*Ruminococcus bromii*	90
	OTU_63	*Clostridium thermocellum*	89
	OTU_78	*Ruminococcus bromii*	86
	OTU_53	*Ruminococcus champanellensis*	90
	OTU_164	*Clostridium methylpentosum*	94
	OTU_67	*Clostridium leptum*	100
CR3	OTU_37	*Ruminococcus lactaris*	95
	OTU_33	*Clostridium thermocellum*	90
	OTU_93	*Clostridium papyrosolvens*	88

	OTU_15	*Clostridium viride*	90
	OTU_23	*Ruminococcus bicirculans*	87
	OTU_17	*Ruminococcus bromii*	88
	OTU_44	*Clostridium viride*	90
	OTU_461	*Clostridium viride*	92
	OTU_168	*Ruminococcus flavefaciens*	91
	OTU_81	*Clostridium thermocellum*	88
	OTU_103	*Ruminococcus albus*	90
	OTU_29	*Clostridium viride*	92
	OTU_155	*Ruminococcus albus*	91
	OTU_110	*Clostridium thermocellum*	90
	OTU_83	*Ruminococcus albus*	90
	OTU_8	*Ruminococcus bicirculans*	91
	OTU_108	*Faecalibacterium prausnitzii*	93
	OTU_86	*Ruminococcus champanellensis*	85
	OTU_10	*Clostridium viride*	91
	OTU_181	*Clostridium viride*	89

2.7 Conclusion

In summary, according to the results of the papers presented above, a clear alteration in the gut microbiota composition and in SCFAs production is present in obese school-aged children. In our first results DGGE profiles showed high bacterial biodiversity without significant correlations with BMI z-score, but the use of specific primers in Real-Time PCR revealed a significantly lower abundance in some bacterial and fungal species in obese children.

The next use of a high-throughput technique as 16S gene targeting sequencing, allowed identifying significant differences in bacterial population, with a depletion in *Bacteroidetes* and an increasing in *Firmicutes* in obese children. Members of the *Bacteroidetes* resulted better predictors of BMI z-score and obesity than *Firmicutes*, which was likely due to discordant responses of *Firmicutes* OTUs, in particular within the members of *Ruminococcaceae.*

The correlation network analysis summarizes all the gut microbiota alterations found in both studies. The harmony and equilibrium between OTUs presented in normal-weight subjects seemed to be lost in obese children. The main hypothesis can be linked to an increased fermentation activity in the obese group creating preferential niches in the gut with subsequent formation of more correlation communities. In accordance with these observations, the main metabolites produced by gut bacteria, short chain fatty acids (SCFAs), were higher in obese children, suggesting elevated substrate utilization or more rapid transit time. The more elevated SCFAs production may be linked to the increased introduction of kcal and macronutrients by day in the obese children leading to an increased fermentation activity and SCFAs production, which are used as further source of energy for the body.

Another important evidence of gut microbiota implication with obesity, are the several correlations found between gut bacterial communities and SCFA levels and BMI z-score, reinforcing the tight link between the microbiota, SCFAs, and obesity.

In summary, our results suggest that gut microbiota dysbiosis and elevated fermentation activity may be involved in the etiology of childhood obesity. In particular, obesity was associated with an altered gut microbiota characterized by elevated levels of *Firmicutes* and a depletion of *Bacteroidetes*, with discordant responses in *Firmicutes* members. Therefore, future research should include a better characterization of *Firmicutes* members and a complete metabolites analysis in order to understand the complex interaction between gut microbiota, metabolites and diet.

CHAPTER 3:

THE INFLUENCE OF DIET ON GUT MICROBIOTA BY USING MURINE MODELS

Introduction

3.1 Diet and its impact on gut microbiota composition

Current evidence suggests that gut microbiota plays a role in metabolic regulation and food digestion and availability. Its potential to modulate energy regulation as well as systemic inflammation are pointed up in paragraph 2.2 (Sanchez *et al*., 2015).

In recent years, efforts to modify the intestinal microbiota composition by dietary interventions have substantially increased and the impact of different diets on the microbiota has been well demonstrated (Milani *et al*., 2016).

The effect of diet is clearly demonstrated by the changes seen over a period of 2.5 years in one infant gut microbiota with introduction of solid foods. In this study, using 16S rRNA gene sequencing the authors demonstrated increasing bacterial diversity over time, with ingestion of solid foods causing a sustained increase in *Bacteroidetes* spp., fecal short-chain fatty acid levels, enrichment of genes associated with carbohydrate utilization, vitamin biosynthesis, and xenobiotic degradation (Koenig *et al*., 2011).

The most significant data are available on the influence of specific diet components such as dietary fibers, fat and proteins on the human gut composition. In this context, it is very relevant to highlight the role of dietary fibers, defined as glycans consisting of tri or higher polymeric saccharides that are not adsorbed in the small intestine, nor digested by human enzymes. Humans consuming resistant starch undergo a gut microbiota change with a significant increase in *Ruminococcus bromii* and other starch-degrading bacteria such as *Oscillobacter* spp. and *Eubacterium rectale*. Dietary fibers are known to enhance growth and activity of butyrate-producing microorganisms such as *Roseburia* spp., *Eubacterium rectale* and *Faecalibacterium prausnitzii*. Moreover, *Bifidobacterium* spp. and lactobacilli populations are stimulated by the presence of dietary fibers directly or indirectly by cross-feeding (Milani *et al*., 2016).

Polysaccharides serve as primary modulators of the composition and function of the microbiota. Polysaccharides, which are widely consumed components of human food, are therefore functionally analogous to small-molecule drugs. Because of their relative safety (that is, their lack of acute toxicity), availability and low cost, it might be feasible systematically and empirically to determine which dietary polysaccharides, alone or in combinations, can improve human health in different situations (Sonnenburg and Bäckhed, 2016).

In a Western-based diet, which is characterised by a low presence of fibers and a high occurrence of fat, a paucity of fiber-degrading bacteria such as *Prevotella* spp., *Succinivibrio* spp., *Treponema* spp. and bifidobacteria has been observed (Milani *et al*., 2016). Furthemore, also the geographic area has an impact on gut microbiota composition as elegantly demonstrated by De Filippo and co-authors in which they compared the gut microbiota of children consuming a high fiber diet in Burkina Faso to a modern Western high-fat/high-sugar diet in Europe. They demonstrated that the gut microbiota in children from West Africa had a higher prevalence of *Bacteroidetes* and depletion in *Firmicutes* with some bacterial species being unique for fiber degradation such as *Prevotella* spp. and *Xylanibacter* spp. which were absent in the children from Europe (De Filippo *et al*., 2010).

A high-fat, high-sugar Western diet, instead of a low-fat, plant polysaccharide-rich diet, was shown to promote a shift in the gut microbiota composition toward high numbers of Clostridia and a significant decrease in *Bacteroidetes*. By contrast, a diet containing high levels of fibers promotes an increase of *Bacteroidetes* and a decrease of *Firmicutes* (Milani *et al*., 2016).

Very little is known about the influence of fat and protein intake on the gut microbiota composition. Recently, the comparison of the gut microbiota composition of two human cohorts, receiving either a plant or meat-based diet, highlighted distinct profiles. Notably, the meat-based diet was shown to increase the abundance of bile-tolerant bacteria such as genera of *Alistipes*, *Bilophila* and *Bacteroides*, with a concomitant decrease of *Firmicutes*, in a plant-based diet the most abundant members were associated with the metabolism of plant

polysaccharides such as *Roseburia* spp. *Eubacterium rectale* and *Ruminococcus bromii* (David *et al*., 2014).

Regarding meat consumption, recent investigations show that choline and carnitine, originating from fat and meat, are metabolized by specific components of the gut microbiota to trimethylamine, which in turn can be coverted to Trimethylamine- N-oxide (TMAO) in the liver. TMAO alters cholesterol metabolism in the intestines and in the liver. In the presence of TMAO, there is increased deposition of cholesterol in (and a decreased removal of cholesterol from) peripheral cells, such as those in the artery wall. In phosphatidylcholine-fed GF mice or mice treated with antibiotics, plasma levels of TMAO were increased, suggesting that the microbiota is involved in metabolic processing of dietary choline or carnitine. Specific microbiota profiles are associated with TMAO synthesis. In this context, individuals possessing an enterotype of *Prevotella* genus, displayed higher plasma TMAO concentrations compared to subjects with a different enterotype (Milani *et al*., 2016; Koeth *et al*., 2013).

Moreover, a protein-rich but carbohydrate-poor diet affects the gut microbiota and fatty acid profiles in obese individuals. Residual proteins and peptides are metabolized by the microbiota by proteolysis or through gut fermentation, leading to the production of gasses (e.g. H_2, CH_4, CO_2, H_2S and SCFAs) (Russell *et al*., 2011).

3.1.1 Plasticity of the gut microbiota

The human gut microbiota responds rapidly to large changes in diet. Evidences suggest the existence of these fast, diet-induced dynamics like the switch between plant and meat-based diets, as the addition of more than 30 grams per day of specific dietary fibers or a diet with high-fiber/low-fat or viceversa for 10 days. In all cases, the composition and function of the microbiota shifted over 1–2 days (Walker *et al*., 2011; Wu *et al*., 2011). Such marked shifts in response to nutrient availability are perhaps unsurprising given that populations of microbes can double within one hour and the gut extensively purges the community every 24–48 hours.

This responsiveness might represent an advantageous feature of enlisting microbes as part of the digestive structure, especially when considering the possible day-to-day variation in food that is available to foragers. It might also be an inescapable consequence of dealing with a complex and competitive microbial community that undergoes rapid turnover (Sonnenburg and Bäckhed, 2016).

Despite these rapid dynamics, long-term dietary habits are a dominant force in determining the composition of an individual's gut microbiota. Despite detectable responses of the microbiota within 24 hours of dietary intervention, a 10-day feeding study in 10 people failed to alter the major compositional features and the overall classification of each participant's microbiota (Wu *et al*., 2011). Some, but not all, cross-sectional studies reported that long-term dietary trends are linked to features of microbiota composition (Muegge *et al*., 2011; Wu *et al*., 2011; Koeth *et al*., 2013). A particular change in diet can have a highly variable effect on different people owing to the individualized nature of their gut microbiota. For example, *Ruminococcus bromii*-related taxa bloomed in response to resistant-starch intervention in most of the 14 obese men in one study; the lack of response in the other individuals might reflect an absence of such taxa in those people (Walker *et al*., 2011).

3.2 Murine models to study the gut microbiota

Murine models have been widely used in biomedical research. Extensive similarities in anatomy, physiology and genetics have allowed numerous information about biology. Experimental manipulations of murine models in gut microbiota research allow functional research on host-microbe interactions, thus helping to assess causality in disease-associated alterations in gut microbiota composition. Although results from such experiments have yielded important breakthroughs in understanding the dynamic and complex relationship between the gut microbiota and its host, the translation of such results from murine models to humans remains nontrivial due to the existence of some key differences between the two systems that need to be taken into account (Nguyen *et al*., 2015).

3.2.1 The anatomy of the mouse and human intestinal tract

Mice and humans are quite similar in physiology and anatomical structures, for this reason mouse models have been widely used in biomedical studies. However, the anatomy of the mouse and human intestinal tract have prominent differences (Table 3.1), which might be shaped by their diverging diets, feeding patterns, body sizes and metabolic requirements (Nguyen *et al*., 2015). For example, the gastro-intestinal tract is approximately 8.5 m long in humans and 30 cm long in mice (Bowcutt *et al*., 2014). The average small intestine/colon length ratio is 2.5 in mice versus 7 in humans and the surface ratio of small intestine/colon is only 18 in mice compared to 400 in humans (Nguyen *et al*., 2015). The mouse cecum is also large relative to its total gastro-intestinal tract and is an important site for the fermentation of plant materials as well as for the production of vitamin K and B, which mice reabsorb through coprophagy (Figure 3.1). By contrast, the human cecum is relatively small, with an anatomical structure similar to that of the colon and does not hold a clear function. These morphological differences reflect murine adaptation toward an expanded colon and cecum capacity, allowing

them to extract nutrients from the relatively larger proportion of indigestible food components in their diet, as compared with humans (Donaldson *et al*., 2013; Nguyen *et al*., 2015). Humans also have an appendix, which is absent in mice and mouse intestinal villi are taller than in humans. This morphological difference increases the surface area of the mouse small intestine like a compensation mechanism for the lack of mucosal folds in the mouse intestine. The mouse colon is rather smooth with no division, whereas the human large intestine is sub-compartmentalized into pouches (called haustra), which are absent in the mouse colon. These major anatomical differences in the gut compartmentalization between mice and humans, especially with regards to the greater fermentation capacity of mice (in the cecum), probably impact the diversity and composition of the gut microbial communities in the colon. These communities are not only responsible for the fermentation of indigestible food components, but also for the production of essential complements to the host such as vitamin K and B and short chain fatty acids (SCFAs) (Nguyen *et al*., 2015).

Table 3.1. Similarities and differences in the anatomy of the mouse and human gastro-intestinal tract (Nguyen *et al*., 2015).

Features	Mouse	Human
Overall anatomy: gastrointestinal tract is composed of mouth, esophagus, stomach, small intestine, large intestine and anus	Yes	Yes
Composition of sectional tissue of small intestine: mucosa, lamina propria, muscularis mucosae, submucosa, muscular tunics, nervous plexi, serosa	Yes	Yes
Presence of cells in small intestine: absorptive enterocytes, goblet cells, enteroendocrine cells, Paneth cells, microfold (M) cells, caveolated (chief) cells	Yes	Yes
Composition of sectional tissue of large intestine: mucosa, lamina propria, muscularis mucosae, submucosa, muscular tunics, serosa	Yes	Yes
Presence of cells in the colon: absorptive colonocytes, goblet cells, enteroendocrine cells, microfold (M) cells	Yes	Yes
Stomach	Divided into non-glandular/fore-stomach and glandular stomach, the two parts separated by limiting ridge	Lack fore-stomach, no limiting ridge
Small intestine	Taller vili with no mucosal folds	Shorter than mouse villi, presence of mucosal folds
Cecum	Large, fermentation happens here	Small, no fermentation
Appendix	No	Yes
Colon	Rather smooth and no division	Clearly divided into different sections: ascending, transverse and descending colon
Bowel of colon	Thin muscularis mucosae	Variable thickness
Presence of haustrum and taenia coli in the colon	No	Yes
Distribution of Paneth cells	Present only in the small intestine	In the cecum and proximal colon
Distribution of goblet cells	Abundant in proximal colon, number decrease at the base of the crypt in distal colon and rectum	Abundant from cecum to rectum
Distribution of transverse folds	Restricted to the cecum and proximal colon	Along the length of the colonic mucosa

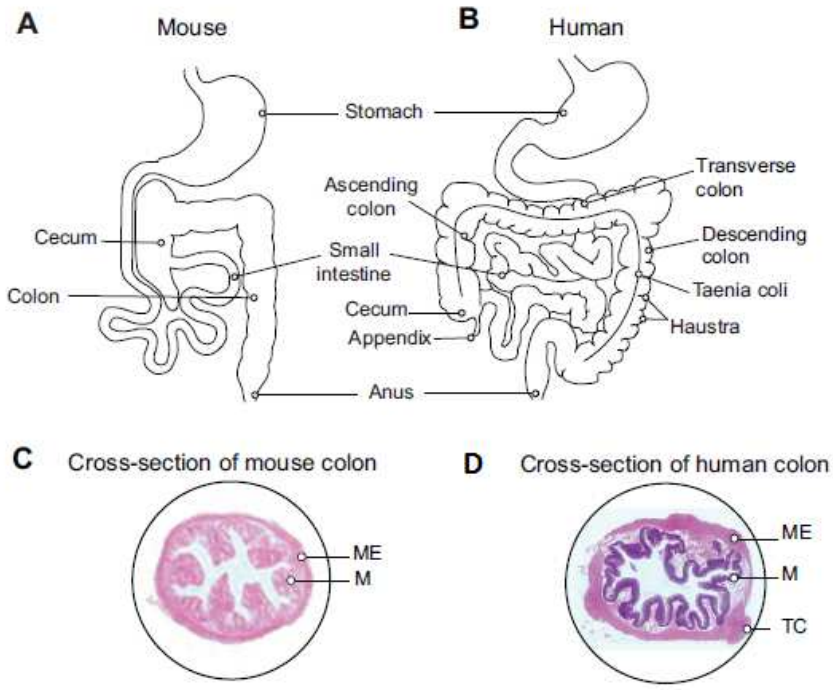

Figure 3.1. Gross anatomy of the human and the mouse gastro-intestinal tract. (A) The human colon is divided into different sections (i.e. ascending, transverse and descending colon) with the presence of taenia coli and compartmentalization in haustra, which are absent in the mouse colon **(B)**. **(C)** Cross-section of a human colon, which has a thicker muscular wall and mucosa compared with the mouse colon **(D)**. M, mucosa; ME, muscularis externa; TC, taenia coli.**Taenia coli:** three longitudinal smooth muscle ribbons along the outside of the colon. **Haptens:** small molecules that can elicit immune responses when attached to larger non-immunogenic carriers. **Haustra:** small pouches segmenting the large intestine, caused by tension of shorter exterior muscle ribbons (cf. taenia coli) (Nguyen *et al*., 2015).

3.2.2 Dietary impact

Usually, laboratory mice are fed a standardized chow diet, a closed formula diet in which the producer does not disclose the exact amount of each ingredient. In most experiments, mice are fed the same diet, obtained from the same supplier, throughout the experiment. The nutritional content of chow varies from batch to batch, depending on agronomical market fluctuations. Even with these variations, chow diet is composed mainly of plant materials and thus differs considerably to the composition of a daily human diet.

Some xenobiotics, such as antibiotics, can also strongly affect the gut microbiota composition and function. Humans, through diet or treatments, are often exposed to such compounds and their potential synergistic effects.The mouse models have the advantage of allowing researchers to control for the impact of such compounds on the gut microbiota, by either minimizing

exposure or recording levels of exposure. Furthermore, dietary variations between humans represent a large potential source of gut microbiota inter-individual variation, which would not be detected in lab mice under uniform chow diet. In summary, it is essential to keep in mind that the murine models' controlled diet might skew analyses by focusing only on a subset of the mouse gut microbiota inter-individual variance. On the other hand, controlling mouse diets provides a clearer experimental setup to disentangle the associations between the gut microbiota composition and function, and the perturbations studied, such as disease and host physiology (Nguyen *et al*., 2015).

3.2.3 Methods to manipulate the gut microbiota: gnotobiotic defined microbiota

The use of germ-free technology for investigating the interactions between the host and its associated microbiota has evolved substantially since the first conference on germ-free life in 1939. By controlling the microbial composition of the environment in which the animals are reared, scientists have been able to obtain information about how microorganisms affect the normal physiological functions of the host (Bibiloni, 2012).

Gnotobiotics or gnotobiology is the study of animals that are free of all microorganisms or colonized only by known species. The term arises from the Greek gnotos, meaning "known," and bios, meaning "life". Terms pertinent to any discussion of gnotobiology include:

- **Axenic or germ free (GF):** an animal free of all microorganisms including bacteria, viruses (with the exception of endogenous retroviruses), fungi, protozoa, and other parasites (Ericsson and Franklin, 2015).
- **Monoxenic or mono-associated animals:** animals colonized by only one microbial species. These animals are generated by reconstituting GF mice with a single agent.

  To create mono-associated mice, GF mice are inoculated with a pure bacterial culture, usually by gastric gavage. Monoassociated mice allow for the study of responses to a

single agent (most commonly bacterial) or identification of bacterial species responsible for specific bacterial products (Ericsson and Franklin, 2015).

- **Defined microbiota animals**: animals with a defined set of microorganisms. These are generated by reconstituting GF mice with "cocktails" or consortia of bacteria. GF mice may also be reconstituted with more complex microbiota that are not completely defined. Sources for reconstitution may include other mice or xenobiotic sources including humans and other animal species (Ericsson and Franklin, 2015).
- **Humanized gnotobiotic mice:** humanized gnotobiotic mice, which result from the inoculation of human gut microbiota samples in germ-free mice, provide a powerful tool for gut microbiota studies because these models can recapitulate a large part of the human gut microbiota phylogenetic composition (100% of phyla, 11/12 classes and ~ 88% of genus level taxa) (Nguyen *et al*., 2015). Humanizing the microbiota of mice usually involves gavage of either a fresh or a frozen fecal sample, resulting in the transfer of the entire complex microbiota. When transferring complex microbiota, much of the bacterial diversity is reproduced, and this humanized microbiota can be stably transferred to subsequent generations (Ericsson and Franklin, 2015).

In summary, mouse models are a powerful tool in gut microbiota research, and offer the possibility to perform experiments that would be too invasive for human subjects and with better control over confounding factors. These models provide unique possibilities to manipulate the human microbiota and assess causality in the role of the gut microbiota in health and disease and finally get closer the development of preventive and therapeutic treatments (Nguyen *et al*., 2015).

3.3 Aim of the project:

“Fine-scale spatial architecture of intestinal microbial communities in a mouse model of diet”

Extensive research has shown that diet modulates the composition and function of the gut microbiota in humans and other mammals.

We previously demonstrated the impact of diet linked to obesity and the possible role of gut microbiota in the pathophysiology of obesity. In order to obtain a more detailed idea of the role of the gut microbiota respect to diet, we performed a diet-shift experiment for one week in wild-type mice with different diets (polysaccharides free, fiber free and control diet) in order to evaluate the gut microbiota composition and its spatial organization in condition of fiber and polysaccharides privation. For this purpose, we collected faecal samples and samples from all colon’ compartments (proximal, middle and distal) and from lumen and ephitelium.We used genomic technologies to study the composition and diversity of host-associated microbial populations, we studied their spatial organization, and functional interactions by using fluorescence *in situ* hybridization (FISH) and laser capture microdissection (LCM) of fixed gut sections. First, highly penetrant organic fixatives were used to maintain the structure of the luminal contents throughout the entire sample preparation. Second, laser capture microdissection was used to specifically sample microbes that were either located from proximal to distal colon and near or distant to the mucosal surface. Third, we sequenced LCM samples and stool samples by using 16S gene target approach. To better determine the difference between lumen and epithelium contents, we focused on the distal colon using FISH analysis, to study target bacteria and investigate their spatial organization. Studying the

epithelium and lumen environments, we also addressed how mucus thickness and goblet cells were affected by increased microbial metabolization.

This high-resolution system to capture and examine spatial organization of intestinal microbes should facilitate microbial analysis, furthering our understanding of host–microbial interactions.

3.4 PRELIMINARY DATA

3.4.1 EXPERIMENTAL DESIGN:

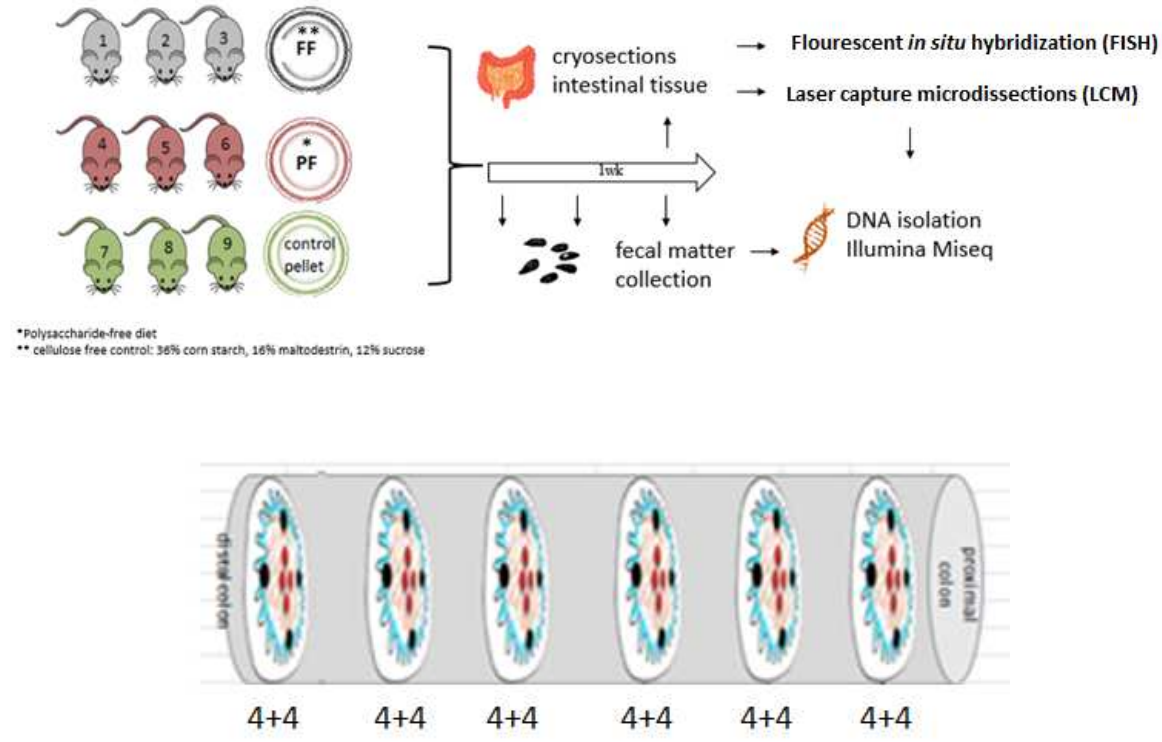

Figure 3.2. Experimental setup of mice experiments, sampling and analysis. Three groups of mice were fed with control diet, fiber free and polysaccharide free diet (Table 3.2). The entire colon was cryopreserved in OCT and then subsampled in 6 different blocks (1 cm each) corresponding to distal colon, middle colon and proximal colon. 4 areas from each secion-block were cut with the laser microdissection microscope, while faecal samples were collected at three different time points in one week. Bacterial DNA was extracted from laser microdissected samples and from fecal samples and the 16S rRNA region were amplified for sequencing analysis.

3.4.2 MATERIALS AND METHODS

Animal experiments and samples collection

9 Wild-type C57BL/6, 2 weeks old were fed with a standard diet (R/M-H Ssniff®, Germany). The mice were divided in 3 groups (n=3 per group): the first was submitted to a fiber free diet (FF) and the second to a polysaccharide free diet (PF) for 1 week. A control group (CON) was fed with the previous standard diet (Table 3.2). The mice were housed in a controlled environment (12h daylight cycle) with free access to food and water. Mice were weighed at day 1 and day 7 during the weekly dietary treatment and faecal pellet were collected three times during the week of diet shift (day 1, 4 and 7). At day 7, they were sacrificed by cervical dislocation, and the large intestine was collected, cryopreserved in OCT (Thermoscientific, USA) and stored at -80°C for further analysis.

Tissue fixation, fluorescence *in situ* hybridization (FISH)

The distal colon was fixed in 4% paraformaldehyde overnight and subsequently treated with 20% sucrose overnight. The tissues were immediately frozen with isopentane (VWR, USA) and then cut at the cryotome (Leica CM3050, Germany) (10 µm thickness) using superfrost ultra plus slides (Thermoscientific, USA). Cryosections were stored at -20°C or immediately use for FISH analysis. Briefly, cryosections were quickly washed in 1X PBS then submitted to a dehydration step in ethanol series (50-80-96%) for 3 minutes each. 20 µl of hybridization buffer were applied with subsequent adding of 5 µM of specific probes. After 2 hours of hybridization in a humidified chamber at 46°C, the slides were washed in specific wash buffers (Daims, 2009). The humidified chamber was made by folding a paper towel soaked up with hybridization buffer put into a 50 ml conical centrifuge tube. After hybridization, the slides were transferred into the preheated wash buffer and put into the water bath (48°C) for 10 minutes. Subsequenly, the slides was dipped into ice-cold MILLI-Q water (Millipore GmbH,

Vienna, Austria) for approximately three seconds and dried under an air-jet. Finally 1:1000 DNA stain, 4', 6 diamidino-2-phenylindole (DAPI) solution, (in PBS) were applied for 5 min and then washed in cold MILLI-Q water (Daims, 2009). All slides were stored in a box impermeable to light at -20 °C for analysis on the confocal laser scanning microscope (CLSM) and before visualization they were embedded with CitiFluor (Agar Scientific Ltd., Stansted, UK). The specific bacterial probes (Thermoscientific, USA) used for FISH analysis are listed in Table 3.3. Total bacteria were staining using the general bacterial probe mix (EUB338 I-III), and the NONEUB probe was used as a negative control. Hybridized samples were displayed on a confocal scanning laser microscope (Leica TCS SP8X, Germany; software LAS-AF, Austria). A set of 25-30 fields view for lumen and 15-20 for epithelium (X 63) were collected for each mouse for each set of probe. The microscope was equipped with an Ar-laser (495nm) for excitation of the Fluos-dyes and two He-Ne-lasers (550 nm and 635 nm) for excitation of Cy3 and Cy5. The pinhole size was set to 1µm and resolution used for all images ranged from 1024x1024 to 2396x2396 pixels and zoom factor of 1 were used for all pictures.

Alcian blue staining

Cryosection were submitted to alcian blue staining (alcian blue solution 1% w/v in 3% acetic acid, pH 2.5) in order to visualize goblet cells and mucins. Briefly, the samples were washed quickly in PBS 1X, then alcian blue were applied for 30 minutes at room temperature. The slides were washed with tap water and subsequently with MILLI-Q water. Lastly, slides were embedded with CitiFluor (Agar Scientific Ltd., Stansted, UK). Samples were visualized on optical microscope (Carl Zeiss GmbH, Germany, software Axio vision 4.8, Germany) and a set of 40 view (X100) of the ephitelial cells were collected. Moreover, 35-40 field (X100) of mucus or epithelium area were collected in order to measure the mucus layer thickness.

Laser capture microdissection (LCM)

The whole large intestine was cryopreserved in OCT (Thermoscientific, USA), 7 cm long, and subsampled in six parts corresponding to distal colon, middle colon and proximal colon. Proximal (lumen content) and distal (epithelium or mucus) areas were collected from each compartment (1 cm tissue block) (Figure 3.2 and 3.3). Unfixed cryosections were mounted onto UV-treated polyethylene terephthalate (PET) 1.4 µm thick LCM slides (Leica) and submitted to laser microdissection with a Laser Microdissection Systems Leica LCM700. The laser setting was the following: power 50, aperture 12, speed 100, specimen balance 25, head current 100%, pulse frequency 3500. Eight areas (10,000 μm^2) per section per mouse; four for epithelium or mucus and four for lumen content were dissected. 48 samples per mouse were collected for a total of 432 samplings. The mucus content was collected with a distance not more than 100 µm away from mucosa. One area outside the sample (10,000 μm^2) was collected as a negative control for each cryosection.

MUC2 and FISH staining combination

Part of distal colon was fixed in methacarn solution (60% absolute methanol, 30% chloroform, 10% glacial acetic acid) overnight. In order to enable immunofluorescence imaging of MUC2, we used methacarn fixation, which preserves the mucus layer structure compared to traditional formaldehyde-based fixatives in which the mucus collapses (Earle *et al*, 2015). The sections were washed in 70% ethanol 3 times for 10 min. Afterwards they were embedded in paraffin and then cut at the microtome (Leica, Germany) with a thickness of 10 µm. Sections were incubated at 46ºC for 1 hour, slides not used immediately were stored at 4ºC. Sections were deparaffinized in two changes xylene for 10 min each and then rehydrated in ethanol washes (95% and 90%) for 10 min each. A mixture of hybridization buffer and EUB 338 I-III probe was applied on the samples and incubated for 2 hours in humidified chambers at 46 ºC. After 2 hours, the slides were washed in the corresponding wash buffer as described by Daims, 2009.

Rabbit polyclonal MUC2 primary antibody (H-300 Santa Cruz technologies) was diluted 1:100 in 0.9M NaCl, 20mM Tris-H Cl (pH: 7.2) and 50 µl were added for each section, covered with plastic coverslip and incubated overnight at 4^0C in the dark. The day after the slides were washed 10 min in 0.9M NaCl, 20mM Tris-HCl (pH: 7.2) buffer at 4^0C and then incubated for 1 hour with 1:1000 Alexa 488 goat anti-rabbit secondary antibody Cy3 labelled at 4^0C in dark conditions. After the incubation 50 µl of 1:1000 DAPI solution (in PBS) were applied for 5 minutes at room temperature in the dark, and washed in cold MilliQ water. Slides were stored in the dark at -20 °C until visualization on the CLSM.

DNA extraction, preparation of 16S gene target amplicons libraries from fecal samples and laser microdissected samples

Extraction of nucleic acids from faecal samples was performed using a phenol-chloroform bead-beating procedure (Griffiths *et al*., 2000). Amplification was performed with a two-step barcoding approach according to Herbold et al, 2015. Briefly, DNA was subjected to a two-step PCR amplification targeting the 16S rRNA gene using a forward primes S-D-bact-0341-b-S-17 (5'-CCTACGGGNGGCWGCAG-3') and a reverse primer S-D-bact-0785-a-A-21 (5'-GACTACHVGGGTATCTAATCC-3'). The first PCR reaction was performed in triplicate with 25 cycles. In the second-step PCR, PCR products from the first step were amplified in 5 cycles with primers consisting of the 16 bp head sequence and a sample-specific 8 bp barcode from a previously published list at the 5′ end. Each PCR reaction (20 µL in first step, 50 µL in second step) consisted of 10× Taq buffer (Fermentas, USA), 2 mM dNTPmix (Fermentas), 25 mM $MgCl_2$ (Fermentas), 5 U/µl Taq DNA polymerase (Fermentas), 20 mg/ml bovine serum albumin (Fermentas), 50 µM of each of the forward and reverse primers and 5µl of sample. Thermal cycle conditions were: 95°C for 3 min, 95°C for 30 s, a primer-specific annealing temperature of 55°C for 30 s, 72°C for 1 min for 25 cycles and an elongation time of 72°C for 7 min (step1); 52°C for 30 s, 72°C for 1 min for 5 cycles (step 2) and an elongation step of 72°C for 7 min.

For laser microdissected samples, cryosections were captured in U/V treated tissue lysis buffer (ATL) (from the QiAmp mini DNA extraction kit, Qiagen) and DNA was extracted using the QiAmp mini DNA extraction kit according to the manufacturer's instructions. The same set of 16S primers and master mix components were used as described above. Laser microdissected samples underwent a 10 repeat PCR cycle as follows; 95^0C incubation for 3 mins, 95^0C for 30 secs, 55^0C for 30 secs, 72^0C for 1 min, with a final 72^0C phase for 7 mins. The second step was performed with 30 repeat cycle PCR programme as above, using 52^0C instead of 55^0C 30 sec step.

For both kind of samples the first PCR reaction was performed in triplicate, pooled for use as a template in the second step and evaluated qualitatively by gel electrophoresis. The barcoded amplicons from stool samples were purified after the second step with ZR-96 DNA Clean-up Kit (Zymo Research, USA) and the LCM samples were purified with Agencourt AMPure beads (Beckman Coulter Genomics, Danvers, MA). All samples were quantified using the Quant-iT PicoGreen dsDNA Assay (Invitrogen, USA). An equimolar library was constructed by pooling samples, and the resulting library was sent to be sequenced on the Illumina MiSeq platform at Microsynth AG (Balgach, Switzerland).

Sequence analysis

Sequence data were sorted into libraries using the 8 nt sample-specific barcode and primer using a custom-made in-house script, quality-filtered according to the Earth Microbiome Project guidelines, and paired end reads were concatenated (Bokulich *et al*., 2013). Reads were then clustered into species-level operational taxonomic units (OTUs) of 97% sequence identity, checked for chimeras using USEARCH, and taxonomically classified using the Ribosomal Database Project näive Bayesian classifier (Wang *et al*., 2007). Sequence data has been deposited in the NCBI Short Read Archive under BioProject: PRJNA338397.

To avoid biases related to uneven library depth, sequencing libraries were subsampled to a number of reads smaller than the smallest library (7500 reads for stool samples and 1000 reads for LCM samples) and the negative controls were excluded.

Images analysis

Images analysis were performed with the software digital image analysis in microbial ecology (Daime) and biovolume fraction and spatial arrangement of cells were calculated (Daims *et al*., 2006).

The biovolume fraction is the measure of the specifically labelled target population relative to the biovolume of the total biomass. The total biomass was stained by the general probe EUB 338 I-III. Automatic or semi-automatic 2D-segmentation were performed for each set of probes to detect the microbial cells and the goblet cells according to Daims et al, 2006.

In order to detect the real distribution of the cells (clusters formation, randomly distribution or mutual avoidance patterns), we performed the spatial arrangement analysis using the Linear Dipole algorithm for one population. The distance range was set from 0 to 120 µm every one cell and the analysis was performed with random dipoles adjusted to 200,000 per distance. The reference space for the analysis was specified by using the EUB338 images as reference space masks. The obtained pair correlation function (g(r)) indicates whether populations coaggregate, avoid each other, or are randomly distributed at distance r (in µm). Random distribution is indicated by g(r) =1, whereas g(r)>1 suggests co-aggregation and g(r) <1 mutual avoidance of the population (Daims *et al*., 2006). The spatial arrangement analysis was performed for each mouse for each location (lumen and epithelium areas) and single measurements were pooled by calculating the arithmetic mean curves with respective 95% confidence intervals.

In order to avoid overestimation of clusters and mutual avoidance patterns, the area of the cells were measured for the probes Dsp653 (*Desulfovibrio piger*) and Lab158 (*Lactobacillus* spp.

and *Enterococcus* spp.), in which the biomass detected was quite low (less then 2%). Once images have been segmented the area of the selected objects were measured.

The measurement of the thickness of the mucus layer was performed after Alcian blue staining. About 35-40 randomly selected fields were taken for each distal colon's mouse with a 100X magnification. A minimum of 10 different measurements were made perpendicular to the inner mucus layer per field. A total of about 3150-3600 measurements were performed and measured by using Fiji software (Schindelin *et al*, 2012).

Statistical analysis

Statistical analysis were performed using the statistical software R (https://www.r-project.org/) and Graph Pad Prism (Graph Pad Software, Inc., la Jolla, CA, USA).

The statistical significance of factors were evaluated using permutational multivariate analysis of variance (perMANOVA). Alpha diversity metrics and beta diversity were calculated using the vegan package (Oksanen *et al*.,2010) and indicator species analysis was carried out with the indicspecies package (De Caceres *et al*., 2009). The differences in the relative abundance between diets and compartments were performed using ANOVA for normal distribution or Kruskal-Wallis test for non-nomal distribution. Post-hoc tests were used for multiple comparisons between dietary groups (Tukey's and Dunn's tests after ANOVA and Kruskal-Wallis, respectively) and paired t test was used to compare the changes in relative abundance between day 1 and day 7 of weekly dietary treatment.

Variables were expressed as mean ± standard deviation (SD) and a p-value less or equal then 0.05 was considered statistically significant.

Table 3.2. Composition of mice's diet.

Proximate contents	**Diet without polysaccharides**	**Diet with polysaccharides without cellulose**	**Control diet**
Crude protein, %	18.5	18.5	19
Crude fat, %	7.1	7.1	3.3
Crude fiber,%	-	-	4.9
Crude ash, %	5.3	5.3	6.4
Starch, %	-	35.1	36.6
Sucrose, %	65.1	13	4.7
ME(atwater) MJ/kg	16.9	16.7	12.8
Protein, kcal %	18.3	18.6	33
Fat, kcal%	15.8	16.1	9
Carbohydrate, kcal %	65.8	65.3	58

Table 3.3. List of probes used for FISH analysis.

Probe name	**specificity**	**probe sequence (5'->3')**	**fluorophore**	**FA (%)**	**References**
Baci731A_87	*Bacteroides_acidifaciens* OTU_731	GCG CCG GTC GCC ATC AAA AGT TTG	Cy5 dope	35	Alm et al., 1996
Baci731B_87	*Bacteroides_acidifaciens* OTU_731	G CCG GTC GCC ATC GGA AGT TTG	Cy5 dope	35	Alm et al., 1996
Dsp653	*Desulfovibrio piger*	CCA CCC TCT CCC GGA TTC	Cy3	30	Reichert, 2012
Erec482	most of the *Clostridium coccoides-Eubacterium rectale* group *(Clostridium* cluster XIVa and XIVb*)*	GCT TCT TAG TCA RGT ACC G	Cy3 dope	0	Franks et al., 1998
Lab158	*Lactobacillus* and *Enterococcus* spp.	GGT ATT AGC AYC TGT TTC CA	Cy3	10	Harmsen et al, 1999
Bac303	most *Bacteroidaceae* and *Prevotellaceae*, some *Porphyromonadaceae*	CCA ATG TGG GGG ACC TT	Cy3 dope	10	Manz et al., 1996
ACA652	*Acinetobacter*	ATCCTCTCCCATACTCT A	Cy3	35	Wagner et al, 1994
Gam42a	Gammaproteobacteria	GCC TTC CCA CAT CGT TT	Cy5	35	Alm et al., 1996
Bet42a competitor	Betaproteobacteria	GCC TTC CCA CTT CGT TT	Cy3	35	Alm et al., 1996
EUB338-I	most Bacteria	GCTGCCTCCCGTAGGA GT	Flous	0-50	Amann et al. 1990
EUB338-II	*Planctomycetales*	GCAGCCACCCGTAGG TGT	Fluos	0-50	Daims et al. 1999
EUB338-III	*Verrucomicrobiales*	GCTGCCACCCGTAGGT GT	Fluos	0-50	Daims et al. 1999
Non-EUB	Complementary to EUB338 (Negative control)	ACTCCTACGGGAGGC AGC		0-50	Wallner et al. 1993

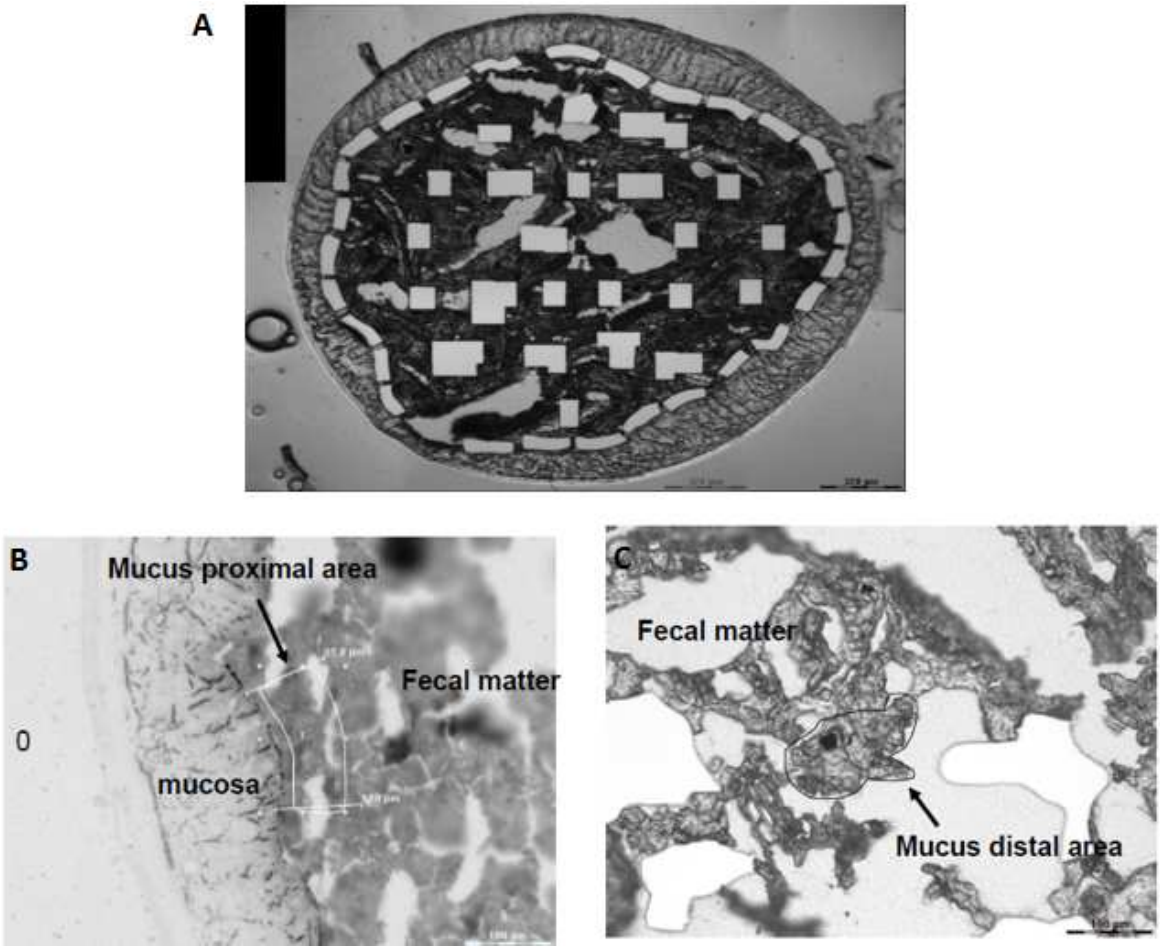

Figure 3.3. Pictures performed at the laser microdissection microscope **(A)** example of mucus and lumen samplings **(B):** mucus or epithelium, **(C):** lumen content.

3.4.3 RESULTS

Sample collections

To address how microbial population changes after a weekly dietary treatment and how mucus thickness is affected by diet shift, we fed three wild-type mice with a control diet (CON), three with diet deficient in fiber (FF) and three with diet deficient in polysaccharide (PF). Mice weights were assessed at day 1 and day 7 during the weekly dietary treatment. No statistical significant difference was present between day 1 and day 7 for each group [(FF (p=0.3845), PF (p=0.7546), CON (p=0.3388)] (Figure 3.4). Faecal pellet were collected at day 1, 4 and 7 and after the weekly dietary treatment, the mice were sacrificed and colon segments were harvested and fixed. 48 samples for each mouse were collected with laser microdissection microscope for a total of 432 samples.

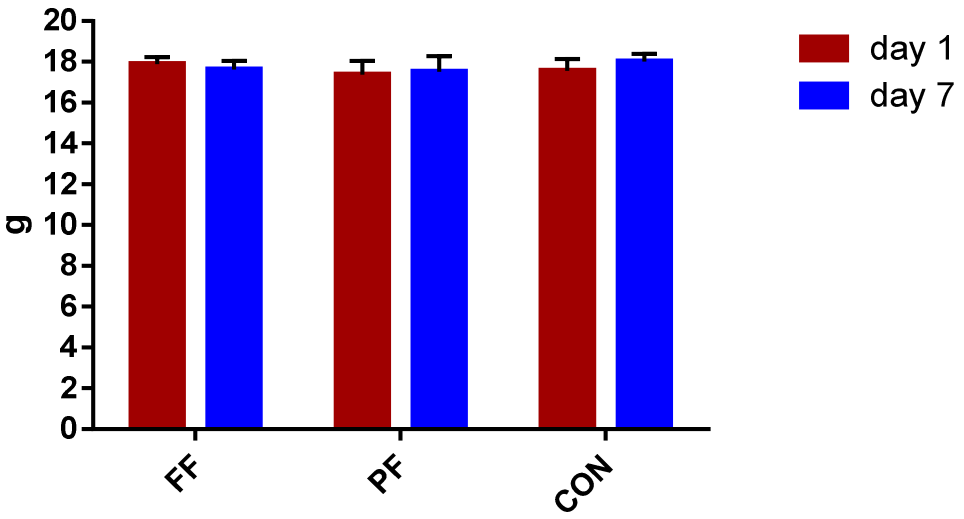

Figure 3.4. Weight of mice assessed at day 1 and day 7 during the weekly dietary treatment.

The intestinal microbiota is altered by diet composition

At the phylum level, the predominant bacterial taxa in the stool samples were *Bacteroidetes* and *Firmicutes,* followed by *Proteobacteria* and *Verrucomicrobia* (Figure 3.5A).

The most abundant families were S24-7, *Lachnospiraceae*, *Prevotellaceae*, *Desulfovibrionaceae, Ruminococcaceae*, *Rikenellaceae*, *Bacteroidaceae*, *Verrucomicrobiaceae*, *Lactobacillaceae*, *Porphyromonadaceae*, *Alcaligenaceae* and *Erysipelotrichaceae* (Figure 3.5B).

The most abundant genera were S24-7 members, *Blautia*, *Desulfovibrio, Prevotella*, *Alistipes, Bacteroides, Alloprevotella*, *Incertae_Sedis* (*Lachnospiraceae*), *Akkermansia*, *Incertae_Sedis* (*Ruminococcaceae*), *Lactobacillus*, *Parasutterella, Parabacteroides*, *Intestinimonas* and *Incertae_Sedis* (*Erysipelotrichaceae*) (Figure 3.5C).

A dramatic drop in all alpha diversity metrics in FF and PF diets at days 4 and 7 respect to CON was present (ANOVA: Observed species: $p<0.0001$; Chao1 estimated richness: $p<0.001$; Shannon:$p=0.0001$; Inverse Simpson: $p=0.0014$) (Figure 3.6A). Accordingly, a clear shift of communities at day 4 and 7 in FF and PF was present and it was further represented in the ordination analysis and in Beta diversity ($p<0.0001$) (Figure 3.6B and C).

In agreement with the previous observations, perMANOVA results considering diet and days and interaction diet and days, was significant at every taxonomic level (phylum to OTUs, $p<0.05$). Therefore, we compared the relative changes in abundance of the microbiota between days 1 and 7 for each group (Figure 3.7). An increased relative abundance of *Proteobacteria* from day 1 to 7 was significant for PF (Two tailed Paired t-test: $p=0.0012$). A similar trend was observed for FF but this trend was not statistical significant ($p= 0.1317$). A decrease of *Bacteroidetes* was present for both FF and PF but not significant ($p=0.1140$, $p=0.1223$). At family and genus level, an increase of *Ruminococcaceae* was significant only for FF while an increase of *Desulfovibrio* spp. at family and genus level was present only in PF, further confirmed by indicator species analysis. No statistical significant increase or decrease in relative abundance was found for CON at any taxonomic level (Table 3.4).

Indicator species analysis, which evaluated the impacts of environmental change on taxa, was used to identify the indicators OTUs changed from day 1 to 7. We identified 9 indicator OTUs for both FF and PF groups. The most of the bacterial species identified were implicated in fiber and polysaccharide degradation, meaning that the identifications of these species were diet dependent (Table 3.5).

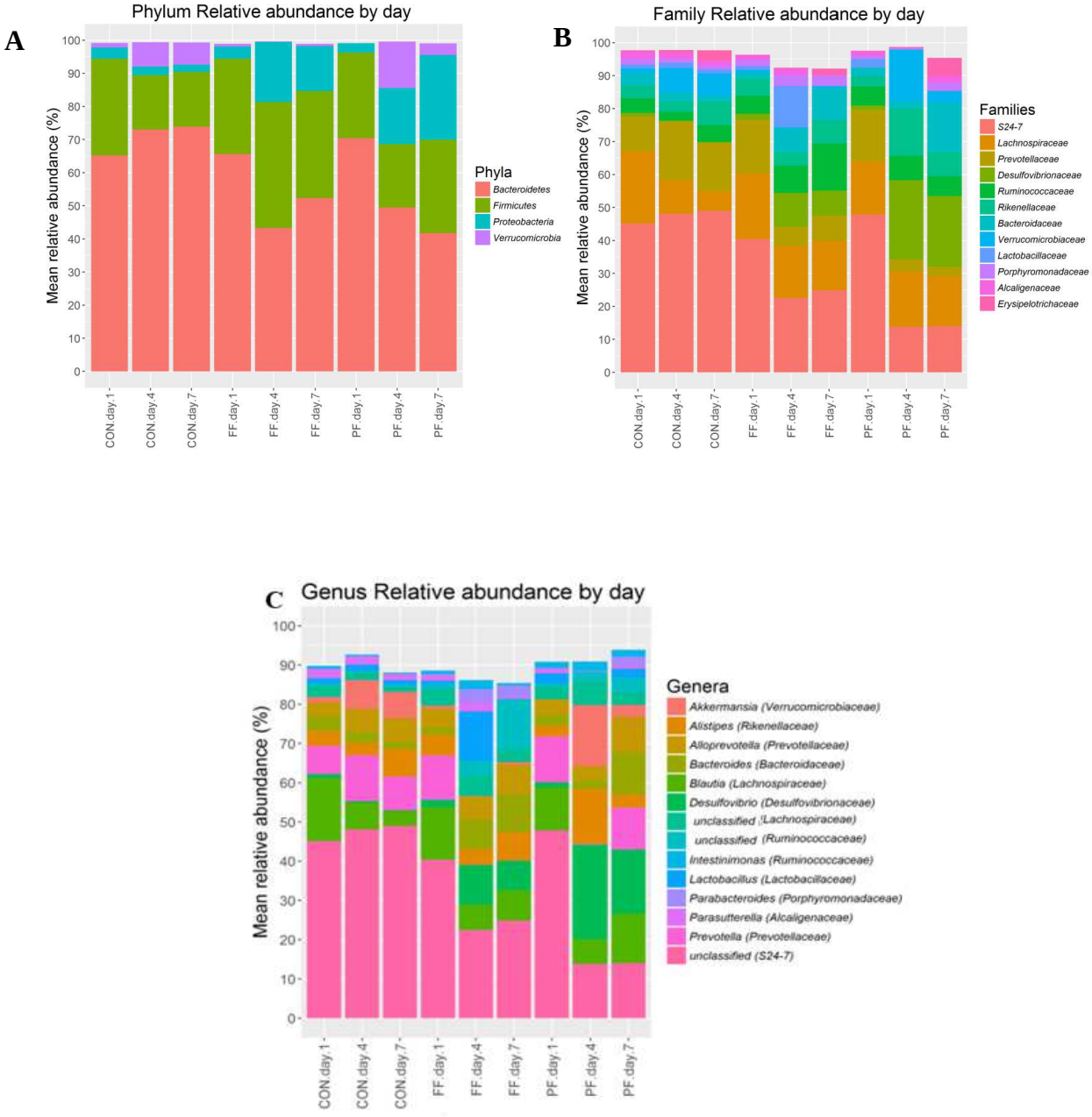

Figure 3.5. Abundant bacterial taxa in stool samples of fiber free (FF), polysaccharide free (PF) and control (CON) diet mice divided by diet intervention days. Phylum-level **(A)** and family-level **(B)** and genus-level **(C)** taxon profiles are shown. Abundant taxa, defined as having a mean relative abundance of >1%, are shown.

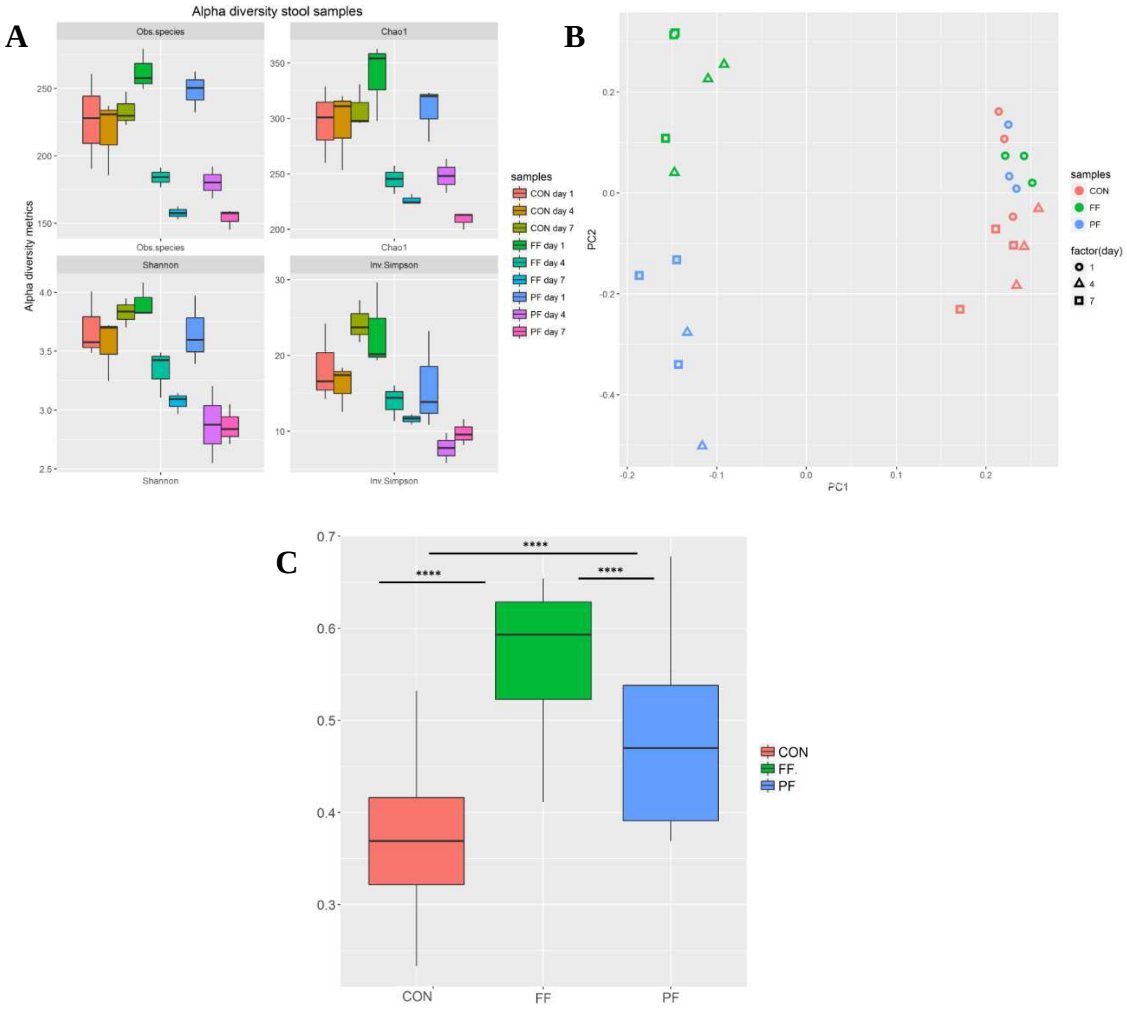

Figure 3.6. (A) Intestinal microbiota richness and diversity of fiber free (FF), polysaccharide free (PF) and control (CON) diet mice divided by dietary intervention days. (Tukey's test after ANOVA day 1 vs day 7: FF: Observed species: 0.0001; Chao1 estimated richness: 0.0008; Shannon: 0.0083; Inverse Simpson: p= 0.0471; **PF**: Observed species: 0.0003; Chao1 estimated richness: 0.0002; Shannon: 0.0154, Inverse Simpson: p= 0.05; **C ON**: Observed species: 0.9999; Chao1 estimated richness: 0.9920; Shannon: 0.9971; Inverse Simpson: p= 0.661) **(B) Principal component analysis** shows a grouping of samples at day 4 and 7 in PF and FF diet **(C) Beta diversity** shows a significant difference in the three groups (ANOVA:p<0.0001).

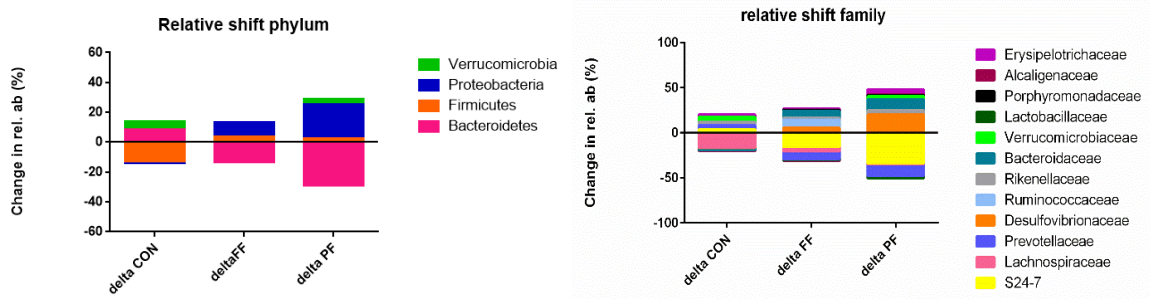

Figure 3.7. Shift of relative abundance at phylum and family level. The changes in relative abundance of taxa (day 1 relative abundance minus day 7 relative abundance) for each mouse is shown for the phylum-level (A) and family-level (B). Only taxa that displayed a mean change of at least 0.1% relative abundance are shown.

Table 3.4. Paired t test between day 1 and 7 from phylum to genus level. No significant taxa were different for CON. Significant shift respect to CON are shown. p-values <0.05 are represented.

Taxonomic level	Taxon	Significant shift	PF	FF
Phylum	*Proteobacteria*	+	0.0012	-
Family	S 24-7	-	0.0133	0.0024
	Ruminococcaceae	+	-	0.0162
	Desulfovibrionaceae	+	0.0103	-
	Lactobacillaceae	-	-	0.0422
Genus	S 24 7 unclassified	-	0.0133	0.0011
	Prevotella (Prevotellaceae)	-	0.05	0.0335
	Desulfovibrio (Desulfovibrionaceae)	+	0.0103	-
	Ruminococcaceae unclassified	+	-	0.0020
	Lactobacillus (Lactobacillaceae)	-	-	0.0422
	Parabacteroides (Porphyromonadaceae)	+	-	0.0356

Table 3.5. Indicator OTUs from day 1 to 7 for FF and PF groups. A p value <0.05 is shown.

OTU_ID associated with FF	**Closest related species**	**Similarity (%)**	**p value**
OTU_4006	*Bacteroides intestinalis*	91	0.010
OTU_20	*Clostridium thermocellum*	88	0.045
OTU_21	*Clostridium xylanolyticum*	91	0.005
OTU_314	*Clostridium thermocellum*	90	0.010
OTU_1942	*Clostridium saccharolyticum*	93	0.020
OTU_140	*Bacteroides xylanolyticus*	95	0.010
OTU_322	*Clostridium xylanolyticum*	95	0.015
OTU_2119	*Clostridium xylanovorans*	89	0.025
OTU associated with PF	**Closest related species**	**Similarity (%)**	**p value**
OTU_516	*Parabacteroides distasonis*	84	0.010
OTU_3061	*Clostridium saccharolyticum*	89	0.010
OTU_164	*Eubacterium cylindroides*	88	0.025
OTU_2569	*Bacteroides cellulosilyticus*	80	0.015
OTU_1617	*Ruminococcus obeum*	92	0.015
OTU_1895	*Bacteroides eggerthii*	99	0.010
OTU_3122	*Desulfovibrio desulfuricans*	88	0.050
OTU_1725	*Ruminococcus champanellensis*	87	0.030
OTU_2942	*Desulfovibrio intestinalis*	88	0.040

Microbial communities' composition in mice colon

At the phylum level, the predominant bacterial taxa in mice colon were *Firmicutes* and *Bacteroidetes* followed by *Actinobacteria* and *Proteobacteria* (Figure 3.8A). The most abundant families were *Lachnospiraceae*, *Ruminococcaceae*, S24-7 (*Bacteroidetes*), *Erysipelotrichaceae*, *Lactobacillaceae*, *Propionibacteriaceae*, *Streptococcaceae*, vadinBB60 (*Clostridiales*), *Veillonellaceae*, *Coriobacteriaceae*, *Rikenellaceae*, *Porphyromonadaceae* and *Clostridiaceae* (Figure 3.8B). The most abundant genera were *Lachnospiraceae* unclassified, S24-7 unclassified (*Bacteroidetes*), *Anaerotruncus* (*Ruminococcaceae*), *Lactobacillus* (*Lactobacillaceae*), *Ruminococcaceae* unclassified, *Blautia* (*Lachnospiraceae*), *Ruminococcus* (*Ruminococcaceae*), *Propionibacterium*, *Hespellia*, *Coprobacillus*(*Erysipelotrichaceae*), vadinBB60 unclassified (*Clostridiales*), *Streptococcus* (*Streptococcaceae*), *Coprococcus* (*Lachnospiraceae*), *Dialister* (*Veillonellaceae*), *Erysipelotrichaceae* unclassified, *Odoribacter* (*Porphyromonadaceae*), *Alistipes* (*Rikenellaceae*), *Roseburia* (*Lachnospiraceae*), *Enterorhabdusm* (*Coriobacteriaceae*), *Parasporobacterium*(*Lachnospiraceae*), *Allobaculum* (*Erysipelotrichaceae*), *Pseudoflavonifractor* (*Ruminococcaceae*) and *Intestinimonas* (*Ruminococcaceae*) (Figure 3.8C).

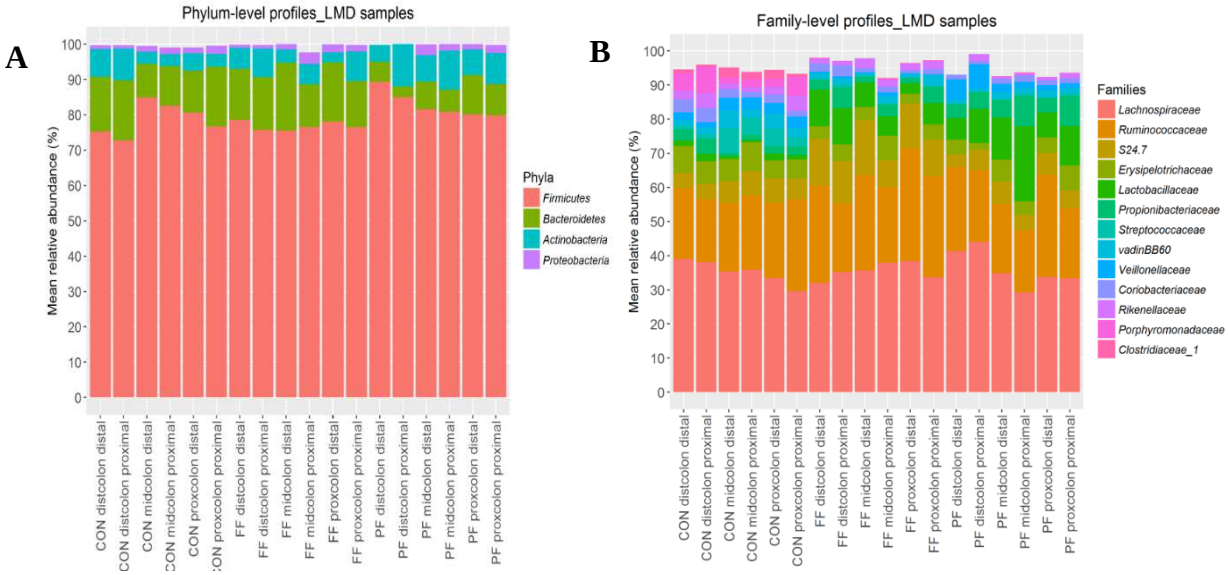

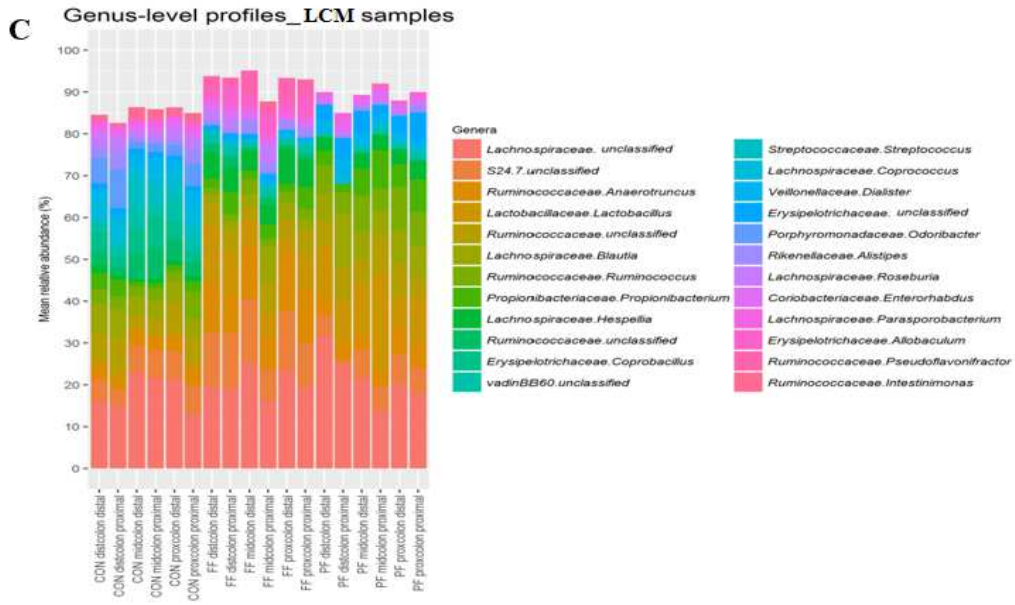

Figure 3.8. Abundant bacterial taxa in colon of fiber free diet (FF), polysaccharide free (PF) and control (CON) diet mice divided by compartment (distal colon, middle colon, proximal colon) and location [distal (lumen) and proximal (epithelium or mucus)]. Phylum-level **(A)** family-level **(B)** and genus-level **(C)** taxon profiles are shown. The mean of the relative abundance >1% for each group is shown.

Faecal and LCM samples have a different microbial profile

16S rRNA gene profiles showed that microbial populations associated with the intestinal mucosa were distinct from those found in fecal samples in CON group. At phylum level the most abundant in ascending order were *Bacteroidetes*, *Firmicutes*, *Proteobacteria* and *Verrucomicrobia*, while in LCM samples *Firmicutes*, *Bacteroidetes*, *Actinobacteria* and *Proteobacteria* predominated (T Student test: $p<0.0001$). At family level only S24-7, *Lachnospiraceae*, *Ruminoccoccae*, *Erysipelotricaceae* and *Porphyrimonodaceae* were shared with a significant difference between faecal and LCM samples for all families (T Student test: $p<0.0001$) (Figure 3.9).

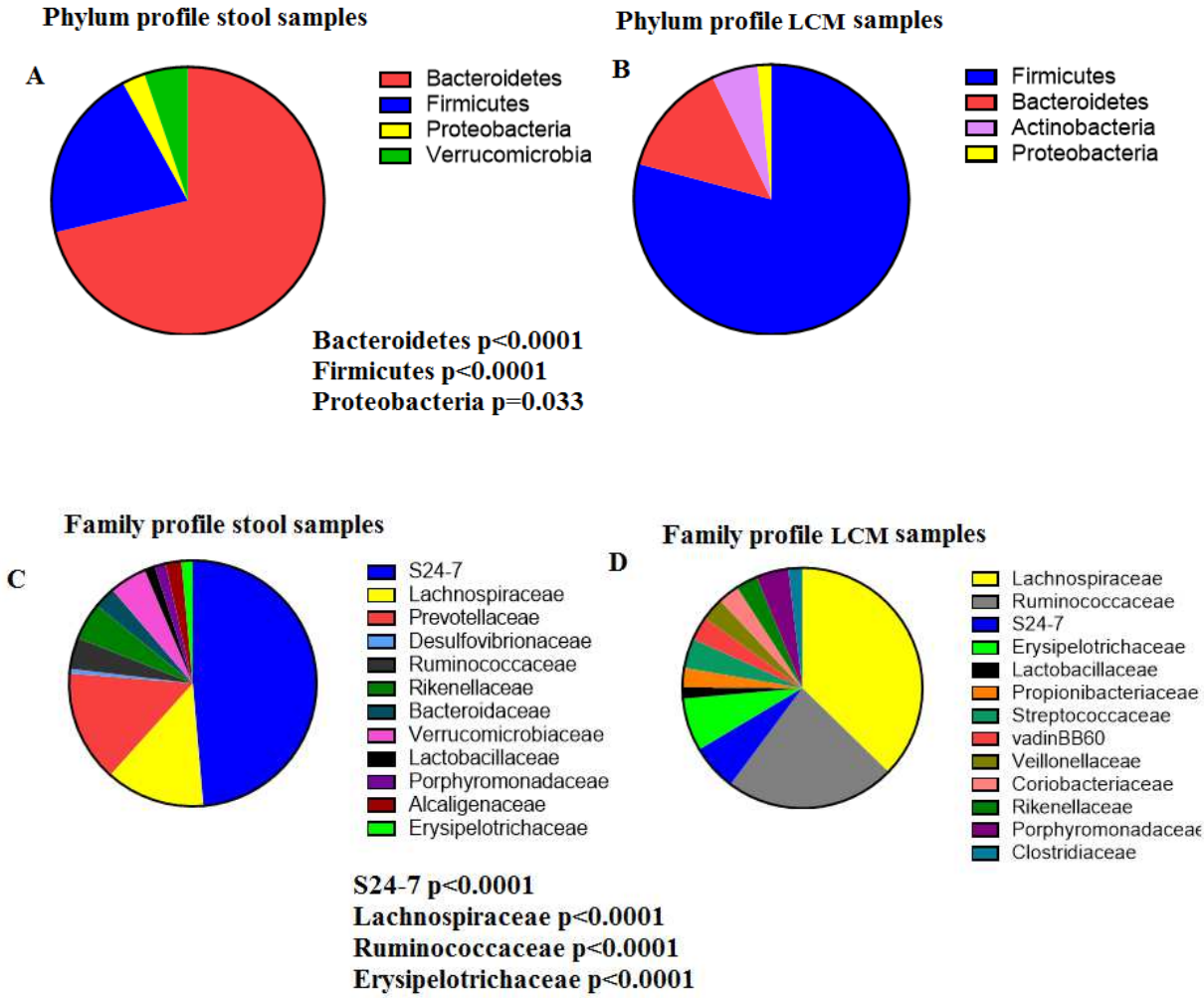

Figure 3.9. Comparison between stool and LCM samples in gut microbial communities. Pie chart performed at phylum (A, B) and family level (C,D) for CON group. A mean of relative abundance <1 % is shown.

The privation of fibers and polysaccharides affected the diversity and richness of colonic intestinal compartments

A similar reduction in alpha diversity is present in compartmentalized samples ($p<0.0001$ for all alpha diversity metrics) (Figure 3.10A). In agreement, a strong difference in CON diet vs. FF and PF was present as shown in the PCoA and in the Beta diversity ($p<0.0001$) (Figure 3.10B). perMANOVA analysis showed that diet, compartments (distal colon, middle colon, proximal colon) and location (distal, proximal) included their interactions, were significant at every taxonomic level ($p<0.05$). A clear separation within proximal, middle and distal colon is

present in CON, but the privation of fiber and above all the absence of polysaccharides compromised the beta diversity from proximal to distal colon (Figure 3.11A, B and C).

Beta diversity for epithelium and lumen area confirmed perMANOVA data ($p<0.0001$) (Figure 3.12A and B). Moreover, Bray Curtis mean distances for epithelium and lumen were significant for the three groups (proximal-distal: $p=0.0155$, proximal-proximal: 0.0196 and distal-distal: 0.0001) (Figure 3.13), showing a different bacterial distribution between lumen and epithelium.

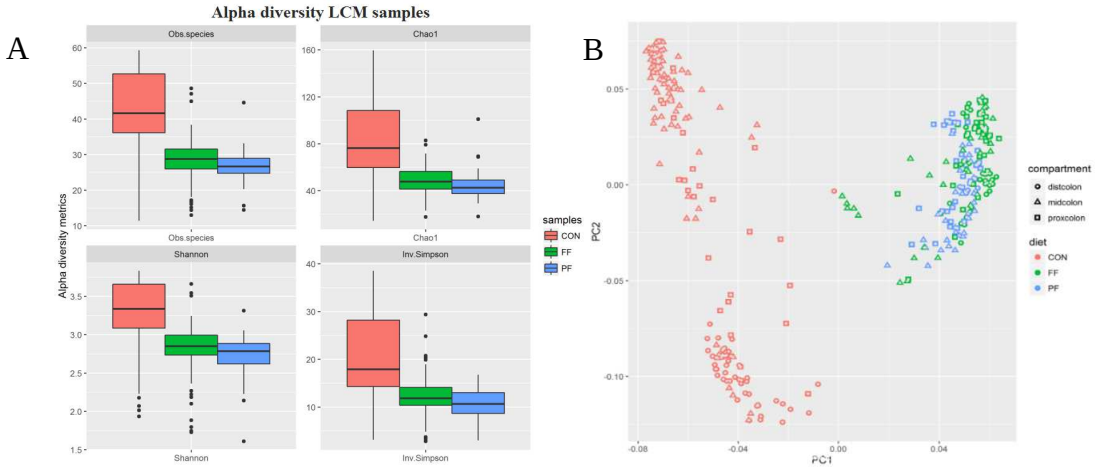

Figure 3.10. (A) Intestinal microbiota richness and diversity of fiber free (FF), polysaccharide free (PF) and control (CON) diet mice divided by compartment (distal colon, middle colon, proximal colon) and location (distal and proximal). Observed species, Chao1 estimated richness, Shannon diversity, and inverse Simpson diversity estimators show significant difference between the three groups [(ANOVA=$p<0.0001$, Tukey's test: **FF vs CON**: Observed species:$p<0.0001$; Chao1 estimated richness: $p<0.0001$; Shannon : $p<0.0001$; Inverse Simpson: $p<0.0001$; **PF vs CON**: Observed species:$p<0.0001$; Chao1 estimated richness: $p<0.0001$; Shannon : $p<0.0001$; Inverse Simpson: $p<0.0001$; **PF vs FF** Observed species:$p=0.5104$; Chao1 estimated richness:0.9818; Shannon :0.0785; Inverse Simpson:0.3152)]. (**B**) Principal component analysis shows a grouping of samples between CON vs PF and FF.

(A) CON

(B) FF

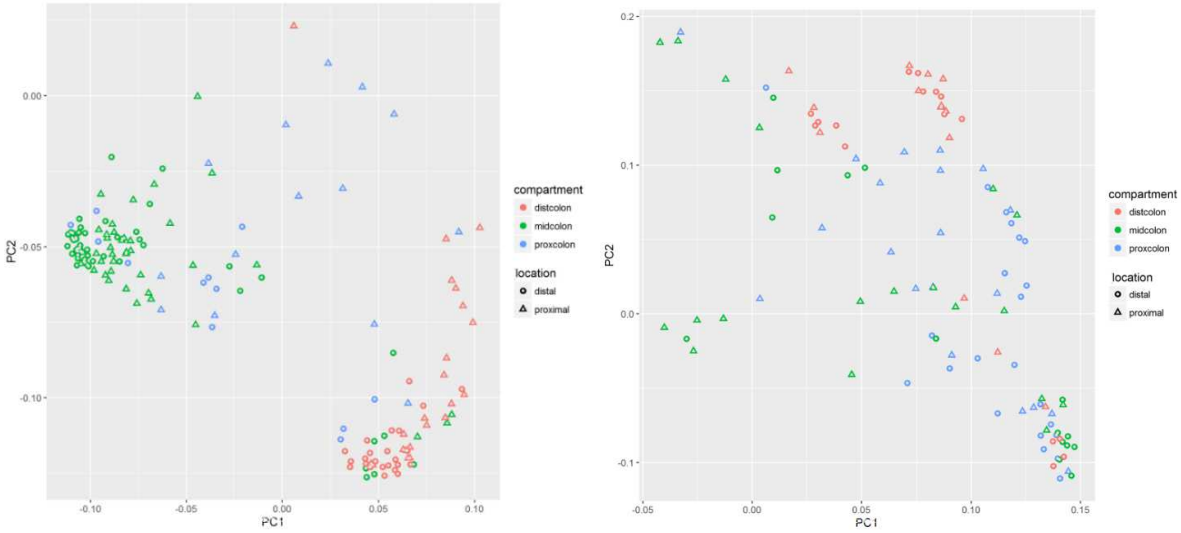

(C) PF

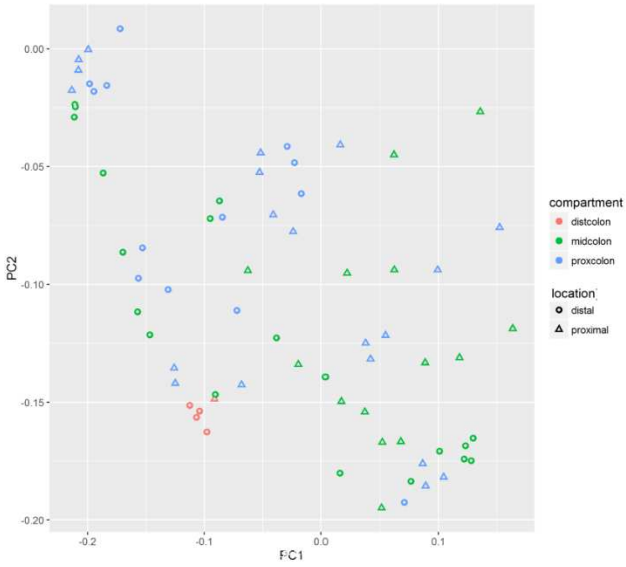

Figure 3.11. Beta diversity divided by diet. A clear separation is present for CON between proximal, middle and distal colon but the diet shift destroys the diversity of microbial communities from proximal to distal colon.

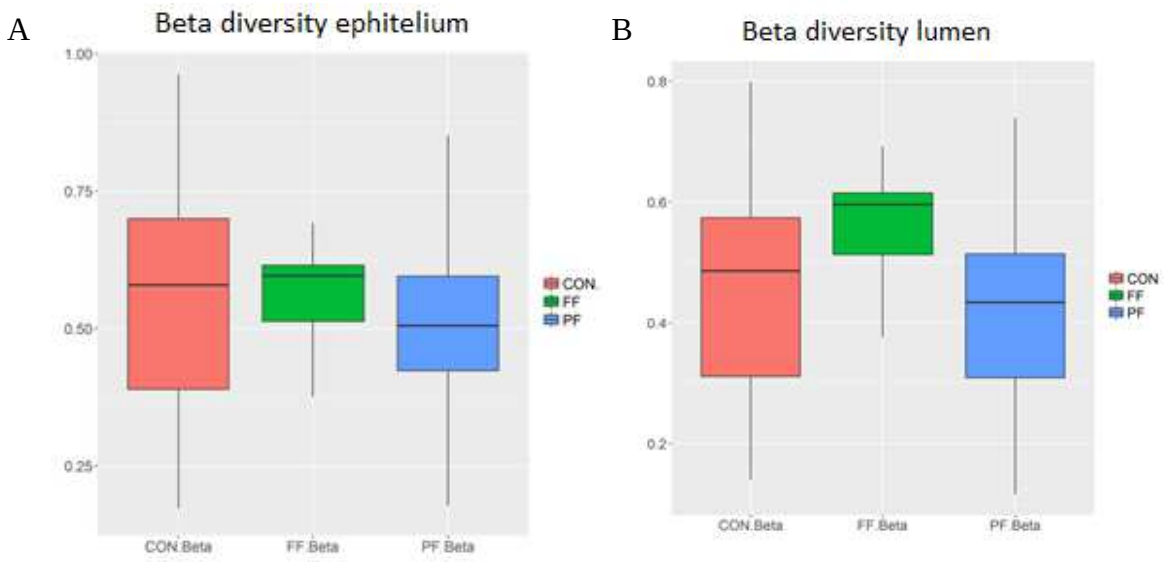

Figure 3.12. Beta diversity for epithelium (**A**) and lumen (**B**) show a significant difference ($p<0.0001$ for all comparison).

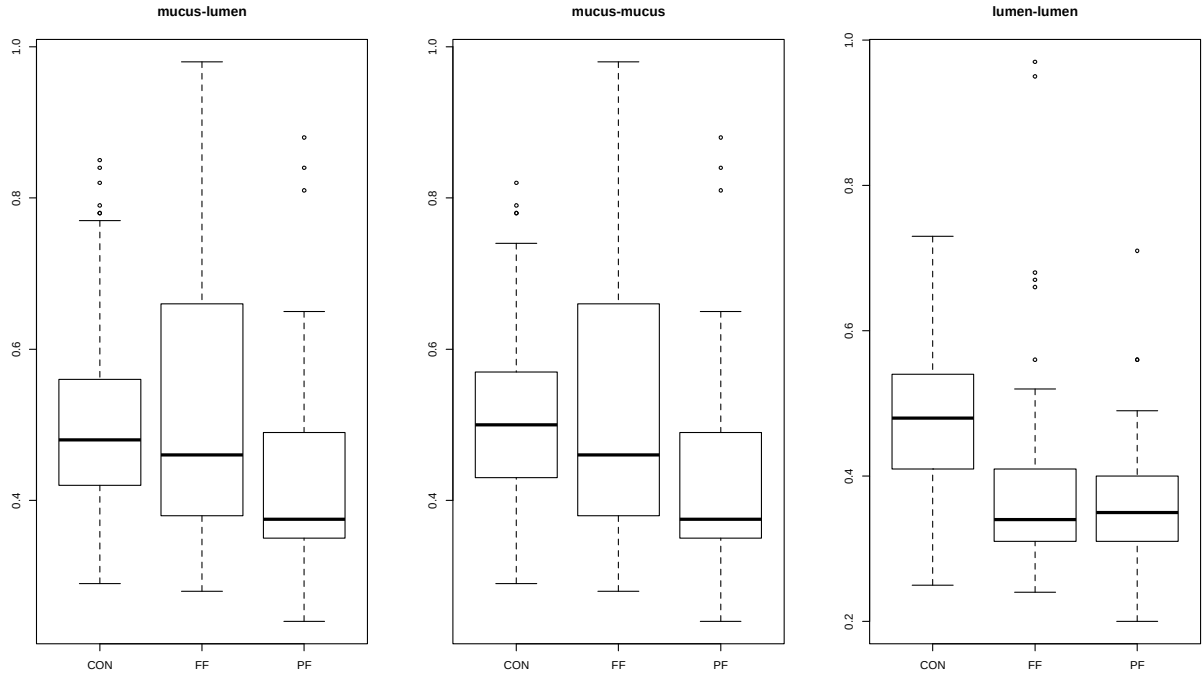

Figure 3.13. Mean of Bray Curtis distances for all groups (epithelium-lumen p=0.0155, epithelium-epithelium p=0.0196 , lumen-lumen p=0.0001).

Diet influences the gut microbiota composition from proximal to distal colon

Preferential colonization niches are normally present from proximal to distal colon. In the distal colon of CON, we observed an increase in: *Lachnospiraceae* (38% vs. 31%, p=0.0006); *Erysipelotrichaceae* (7.2% vs 5.2%,p=0.0076); *Coriobacteriaceae* (4% vs 2%, p=0.0001); *Propionibacteriaceae* (3.8% vs 2.3%, p=0.0033); and a decrease in: S24-7 (4.4% vs 6.8%, p=0.0007); *Ruminococcaceae* (19.6% vs 24.4%, p=0.0022); *Streptococcacaeae* (1.1% vs 3.7%, p<0.0001); vadinBB60 (1.8% vs 3.3%, p=0.0003); *Veillonellaceae* (1.9% vs 3.1%, p=0.0027) respect to proximal colon (Figure 3.14, Table 3.7).

Comparing the relative abundance in proximal, middle and distal colon, a more variability between compartments was present in CON; whereas in FF and PF groups this variability seemed to be partially lost at phylum and family level (Table 3.6, 3.7 and S3.1, S3.2) and they seemed to be diet dependent.

Several changes were present in PF and FF group respect to CON. In PF, an increase of *Bacteroidetes* is reported only in the proximal colon but a decrease of them is reported in the distal and middle colon. *Firmicutes* tended to increase in all compartments, *Actinobacteria* in middle and proximal colon and *Proteobacteria* increased only in the distal colon (Table 3.7).

In FF diet, *Firmicutes* decreased in the middle colon but increased in the proximal part. *Bacteroidetes* increased in the middle and proximal colon and *Actinobacteria* increased in the middle part (Table 3.7).

At family level, *Lachnospiraceae* decreased in FF but increased in PF in distal colon, *Ruminococcaceae* and S24-7 increased in FF in distal and proximal colon but decreased in PF in middle and proximal part. *Lactobacillaceae* and *Propionibacteriaceae* increased in FF and PF in all compartments. Several families decreased in PF and FF: *Streptococcaceae* *Erysipelotrichaceae*, VadinBB60, *Veillonellaceae*, *Coriobacteriaceae*, *Rikenellaceae*, *Porphyromonadaceae* and *Clostridiaceae* (Table S3.2). Details regarding shifts in the single compartments are presented in tables 3.7 and S3.2.

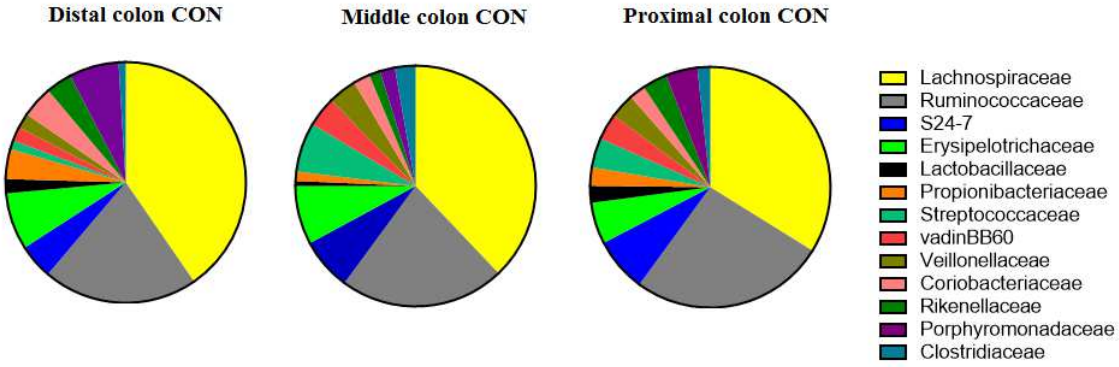

Figure 3.14. Microbial composition for distal, middle e proximal colon in CON diet at family level. Significant differences between compartments are represented also in Tables 3.6 ans S3.1.

Table 3.6. Comparison between compartments: distal, middle and proximal colon considering each group of diet. Multiple comparisons were performed with Dunn's test after Kruskal-Wallis test for each group of diet at phylum level.

Phylum level profiles	**CON**	**FF**	**PF**
	Sign.	**Sign.**	**Sign.**
Firmicutes m vs. *Firmicutes* d	****	ns	ns
Firmicutes m vs. *Firmicutes* p	***	ns	ns
Firmicutes d vs. *Firmicutes* p	****	ns	ns
Bacteroidetes d vs. *Bacteroidetes* m	****	ns	ns
Bacteroidetes m vs. *Bacteroidetes* p	****	ns	*
Bacteroidetes d vs. *Bacteroidetes* p	****	ns	ns
Actinobacteria d vs. *Actinobacteria* m	****	ns	ns
Actinobacteria d vs. *Actinobacteria* p	****	ns	ns
Actinobacteria m vs. *Actinobacteria* p	ns	ns	ns
Proteobacteria d vs. *Proteobacteria* m	**	ns	*
Proteobacteria d vs. *Proteobacteria* p	ns	ns	*
Proteobacteria m vs. *Proteobacteria* p	ns	ns	ns

Legend= d:distal colon, m:middle colon, p:proximal colon, ns:not significant, CON: control diet, FF: fiber free diet, PF: ploysaccharyde free diet.
**** $p \leq 0.0001$; *** $p \leq 0.001$; ** $p \leq 0.01$; * $p \leq 0.05$.

Table 3.7. Comparison between diets considering each compartment separately. Multiple comparison Dunn's test for each group of diet performed at phylum level.

Phylum level profile	Distal colon		Middle colon		Proximal colon	
	Sign.	**Shift**	**Sign.**	**Shift**	**Sign.**	**Shift**
Firmicutes con vs. *Firmicutes* ff	ns	-	****	ff-	****	ff+
Firmicutes con vs. *Firmicutes* pf	***	pf +	ns	-	****	pf+
Firmicutes ff vs. *Firmicutes* pf	*	pf +	**	pf+	ns	-
Bacteroidetes con vs. *Bacteroidete* ff	ns	-	**	ff+	****	ff+
Bacteroidetes con vs. *Bacteroidetes* pf	**	pf-	**	pf-	***	pf+
Bacteroidetes ff vs. *Bacteroidetes* pf	*	pf-	***	pf-	*	pf+
Actinobacteria con vs. *Actinobacteria* ff	ns	-	**	ff+	ns	-
Actinobacteria con vs. *Actinobacteria* pf	ns	-	****	pf+	*	pf+
Actinobacteria ff vs. *Actinobacteria* pf	ns	-	**	pf+	ns	-
Proteobacteria con vs. *Proteobacteria* ff	ns	-	ns	-	ns	-
Proteobacteria con vs. *Proteobacteria* pf	**	Pf+	ns	-	ns	-
Proteobacteria ff vs. *Proteobacteria* pf	ns	-	ns	-	ns	-

Legend= con: control diet, ff: fiber free diet, pf: ploysaccharyde free diet, ns: not significant, += increase, - = decrease in relative abundance (%) of pf and ff respect to con are shown.
**** $p \leq 0.0001$; *** $p \leq 0.001$; ** $p \leq 0.01$; * $p \leq 0.05$.

Longitudinal gradients along colon compartments

The differences between compartments are in agreement with distance decay analysis along all sections. Distance decay is a geographical term, which describes the effect of distance on spatial interactions. Distance decay analysis revealed a longitudinal gradient from proximal to distal colon [CON ($p<0.0001$), FF ($p<0.0001$), PF ($p=0.0002$)] (Figure 3.15) and a negative correlation between section's similarity and distance across sections. When the distance across sections increased the similarity between them decreased.

A distance-decay relationship with a negative correlation is also present for epithelium [CON ($p<0.0001$), FF ($p=0.0002$), PF ($p<0.0001$)] and lumen [CON ($p<0.0001$), FF ($p<0.0001$), PF ($p=0.0002$)].

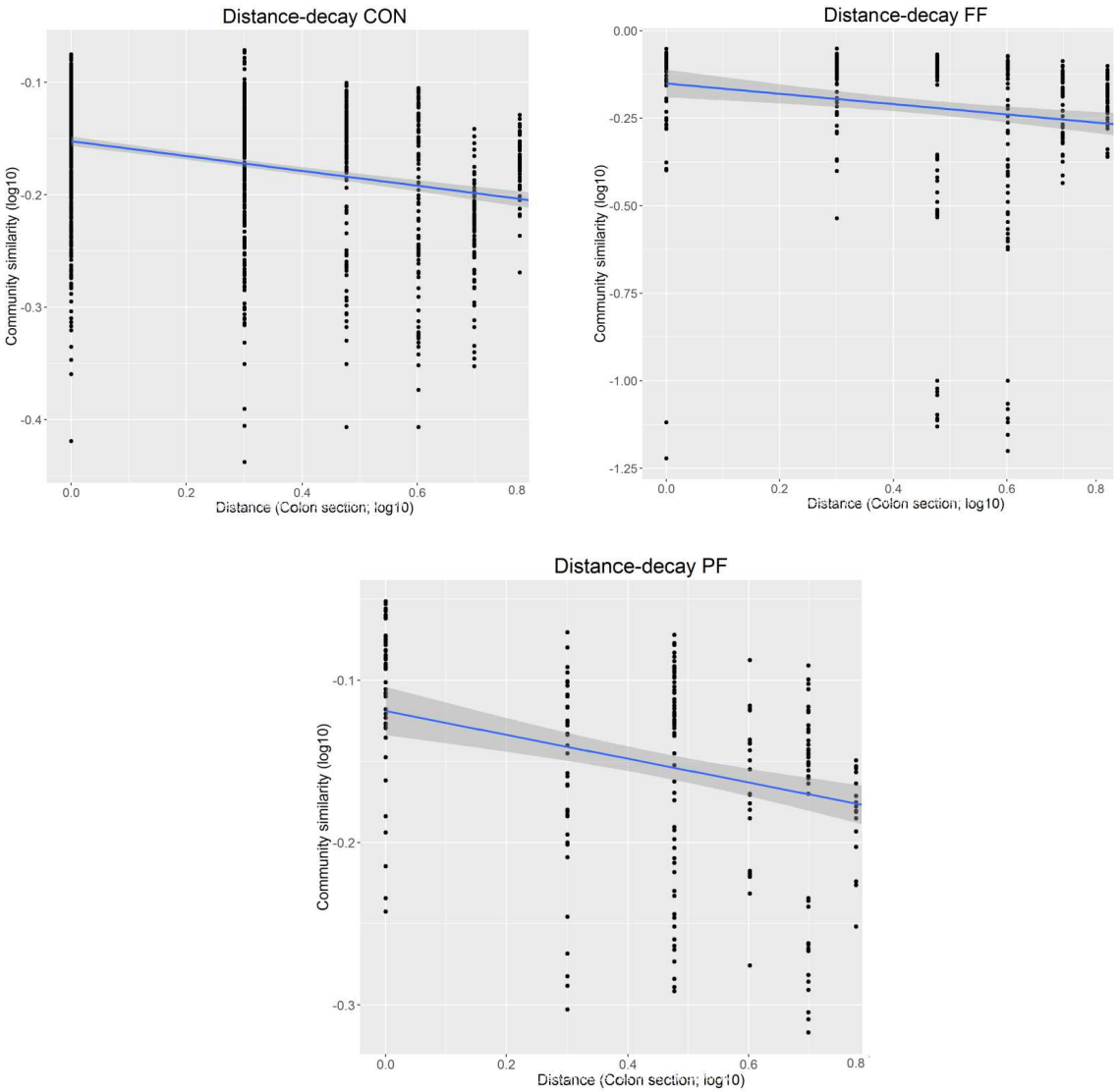

Figure 3.15. Distance-decay analysis for each group of diet shows the presence of a longitudinal gradient along all colon sections.

Supplementary results

Table S3.1. Comparison between compartments: distal, middle and proximal colon considering each group of diet separately. Multiple comparison were performed with Dunn's test after Kruskal-Wallis test for each group of diet at family level.

Family level profiles	CON	FF	PF
	Sign.	Sign.	Sign.
Lachnospiraceae d vs. *Lachnospiraceae* m	ns	ns	ns
Lachnospiraceae d vs. *Lachnospiraceae* p	***	ns	ns
Lachnospiraceae m vs. *Lachnospiraceae* p	*	ns	ns
Ruminococcaceae d vs. *Ruminococcaceae* m	ns	ns	ns
Ruminococcaceae d vs. *Ruminococcaceae* p	*	**	ns
Ruminococcaceae m vs. *Ruminococcaceae* p	ns	*	ns
S24-7 d vs. S24-7 m	***	ns	ns
S24-7 d vs. S24-7 p	**	ns	ns
S24-7 m vs. S24-7 p	ns	ns	ns
Erysipelotrichaceae d vs. *Erysipelotrichaceae* m	ns	ns	ns
Erysipelotrichaceae d vs. *Erysipelotrichaceae* p	*	ns	ns
Erysipelotrichaceae m vs. *Erysipelotrichaceae* p	*	ns	ns
Propionibacteriaceae d vs. *Propionibacteriaceae* m	***	ns	ns
Propionibacteriaceae d vs. *Propionibacteriaceae* p	**	ns	ns
Propionibacteriaceae m vs. *Propionibacteriaceae* p	*	ns	ns
Lactobacillaceae d vs. *Lactobacillaceae* m	****	**	ns
Lactobacillaceae d vs. *Lactobacillaceae* p	ns	***	ns
Lactobacillaceae m vs. *Lactobacillaceae* p	***	ns	*
Streptococcaceae d vs. *Streptococcaceae* m	***	ns	ns
Streptococcaceae d vs. *Streptococcaceae* p	**	ns	ns
Streptococcaceae m vs. *Streptococcaceae* p	*	ns	ns
vadinBB60 d vs. vadinBB60 m	**	ns	ns
vadinBB60 d vs. vadinBB60 p	*	ns	ns
vadinBB60 m vs. vadinBB60 p	ns	ns	ns
Veillonellaceae d vs. *Veillonellaceae* m	***	ns	*
Veillonellaceae d vs. *Veillonellaceae* p	ns	*	***
Veillonellaceae m vs. *Veillonellaceae* p	ns	ns	ns
Coriobacteriaceae d vs. *Coriobacteriaceae* m	****	*	ns
Coriobacteriaceae d vs. *Coriobacteriaceae* p	***	**	ns
Coriobacteriaceae m vs. *Coriobacteriaceae* p	ns	ns	ns
Rikenellaceae d vs. *Rikenellaceae* m	****	ns	ns
Rikenellaceae d vs. *Rikenellaceae* p	ns	ns	ns
Rikenellaceae m vs. *Rikenellaceae* p	****	ns	ns
Porphyromonadaceae d vs. *Porphyromonadaceae* m	****	ns	ns
Porphyromonadaceae d vs. *Porphyromonadaceae* p	**	ns	ns
Porphyromonadaceae m vs. *Porphyromonadaceae* p	*	ns	ns
Clostridiaceae d vs. *Clostridiaceae* m	****	ns	ns
Clostridiaceae d vs. *Clostridiaceae* p	ns	ns	ns
Clostridiaceae m vs. *Clostridiaceae* p	***	ns	ns

Legend= d: distal colon, m: middle colon, p:proximal colon, ns:not significant, CON: control diet, FF: fiber free diet, PF: ploysaccharyde free diet.
**** $p \leq 0.0001$; *** $p \leq 0.001$; ** $p \leq 0.01$; * $p \leq 0.05$.

Table S3.2. Comparison between diets considering each compartment separately. Multiple comparison Dunn's test for each group of diet performed at family level.

Family level profile	Distal colon		Middle colon		Proximal colon	
	Sign.	**shift**	**Sign.**	**shift**	**Sign.**	**shift**
Lachnospiraceae con vs. *Lachnospiraceae* ff	*	ff-	ns	-	ns	-
Lachnospiraceae con vs. *Lachnospiraceae* pf	ns	-	ns	-	ns	-
Lachnospiraceae ff vs. *Lachnospiraceae* pf	*	pf+	ns	-	ns	-
Ruminococcaceae con vs. *Ruminococcaceae* ff	*	ff+	ns	-	**	ff+
Ruminococcaceae con vs. *Ruminococcaceae* pf	ns	-	ns	-	ns	-
Ruminococcaceae ff vs. *Ruminococcaceae* pf	ns	-	*	pf-	**	pf-
S24-7 con vs. S24-7 ff	****	ff+	ns	-	**	ff+
S24-7 con vs. S24-7 pf	ns	-	ns	-	ns	-
S24-7 ff vs. S24-7 pf	*	pf-	**	pf-	****	pf-
Erysipelotrichaceae con vs. *Erysipelotrichaceae* ff	**	ff-	****	ff-	*	ff-
Erysipelotrichaceae con vs. *Erysipelotrichaceae* pf	ns	-	**	pf-	ns	-
Erysipelotrichaceae ff vs. *Erysipelotrichaceae* pf	ns	-	ns	-	ns	-
Lactobacillaceae con vs. *Lactobacillaceae* ff	****	ff+	****	ff+	*	ff+
Lactobacillaceae con vs. *Lactobacillaceae* pf	**	pf+	****	pf+	****	pf+
Lactobacillaceae ff vs. *Lactobacillaceae* pf	ns	-	**	pf+	**	pf+
Veillonellaceae con vs. *Veillonellaceae* ff	****	ff-	****	ff-	****	ff-
Veillonellaceae con vs. *Veillonellaceae* pf	*	pf+	**	pf-	**	pf-
Veillonellaceae ff vs. *Veillonellaceae* pf	****	pf+	***	pf+	***	pf+
Coriobacteriaceae con vs. *Coriobacteriaceae* ff	*	ff-	*	ff-	ns	ff-
Coriobacteriaceae con vs. *Coriobacteriaceae* pf	ns	-	ns	-	ns	pf-
Coriobacteriaceae ff vs. *Coriobacteriaceae* pf	ns	-	ns	-	ns	-
Rikenellaceae con vs. *Rikenellaceae* ff	***	ff-	ns	-	ns	-
Rikenellaceae con vs. *Rikenellaceae* pf	**	pf-	**	pf-	****	pf-
Rikenellaceae ff vs. *Rikenellaceae* pf	ns	-	***	pf-	*	pf-
Porphyromonadaceae con vs. *Porphyromonadaceae* ff	****	ff-	****	ff-	****	ff-
Porphyromonadaceae con vs. *Porphyromonadaceae* pf	***	pf-	****	pf-	****	pf-
Porphyromonadaceae ff vs. *Porphyromonadaceae* pf	ns	-	ns	-	ns	-
*Clostridiaceae*_con vs. *Clostridiaceae* ff	****	ff-	****	ff-	****	ff-
*Clostridiaceae*_con vs. *Clostridiaceae* pf	*	pf-	****	pf-	****	pf-
Clostridiaceae ff vs. *Clostridiaceae* pf	ns	-	ns	-	ns	
Propionibacteriaceae con vs. *Propionibacteriaceae* ff	ns	-	*	ff+	ns	-
Propionibacteriaceae con vs. *Propionibacteriaceae* pf	ns	-	****	pf+	*	pf+
Propionibacteriaceae ff vs. *Propionibacteriaceae* pf	ns	-	**	pf+	ns	-
Streptococcaceae con vs. *Streptococcaceae* ff	ns	-	****	ff-	****	ff-
Streptococcaceae con vs. *Streptococcaceae* pf	ns	-	****	pf-	****	pf-
Streptococcaceae ff vs. *Streptococcaceae* pf	ns	-	ns	-	ns	-
vadinBB60 con vs. vadinBB60 ff	ns	-	****	ff-	*	ff-
vadinBB60 con vs. vadinBB60 pf	ns	-	***	pf-	*	pf-
vadinBB60 ff vs. vadinBB60 pf	ns	-	ns	-	ns	-

Legend= con: control diet, ff: fiber free diet, pf: ploysaccharyde free diet, ns: not significant, += increase, - = decrease in relative abundance (%) of pf and ff respect to con are shown.

**** $p \leq 0.0001$; *** $p \leq 0.001$; ** $p \leq 0.01$; * $p \leq 0.05$.

Fluorescence *in situ* hybridization revealed a differential localization of specific bacteria cells in lumen and epithelium

Biovolume fraction and spatial arrangement of *Bacteroides acidifaciens*

The quantification of *B. acidifaciens* revealed an elevated abundance in PF (34.8±12.2; mean ± SD) respect to FF (17.3±10) and CON (14.7±10.7), (Kruskal Wallis test: $p<0.0001$) (Figure 3.17A). Comparing lumen vs epithelium we found a significant difference in the localization of cells in PF ($p=0.0077$) characterized by an elevated abundance in epithelium area. No statistical significant difference in the localization of cells were found for FF ($p=0.052$) and CON ($p=0.3649$) (Figures 3.16A and B, 3.17B). In order to see if an inter and intra-group variation in the three groups was present, the ratio epithelium/lumen was calculated and one-sample t test was performed. We did not find a significant difference inter and intra-group ($p=0.3511$ and $p=0.053$ respectively).

Spatial arrangement of cells revealed a similar trend for the three groups of diet in the lumen with co-aggregation patterns around 10 µm of distance and in a lesser extent at 25 µm; in particular another co-aggregation peak is described for FF at 45 µm of distance. A randomly distribution pattern is described for FF and PF but a trend of mutual avoidance is presented for CON from 35 to 80 µm (Figure 3.18A).

In the epithelium area a different trend is described. A co-aggregation pattern is presented for CON and FF at 10 µm then a randomly distribution pattern is described until 80 µm. Another co-aggreagtion pattern is detected for FF at 30 µm while in PF was observed a randomly distribution behavior and a mutual avoidance distribution from 60 to 80 µm (Figure 3.18B).

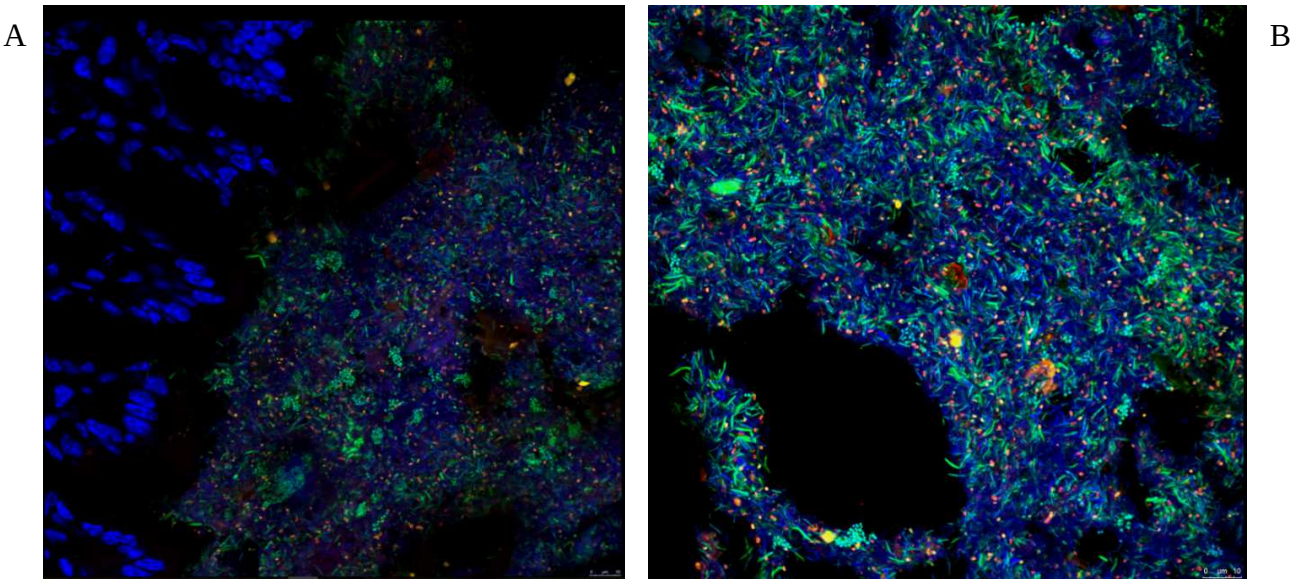

Figure 3.16. Representative picture of a distal colon stained with DAPI (blue) EUB I-II-III 338 DOPE in Fluos (green) for all Bacteria and the specific probe Baci731A_87, Baci731B_87 in Cy3 (red). Images were performed with confocal laser scanning microscope with: magnification 63X, resolution 2920x2920 for picture **A** (epithelium) and 1752x1752 for picture **B** (lumen), zoom factor 1.

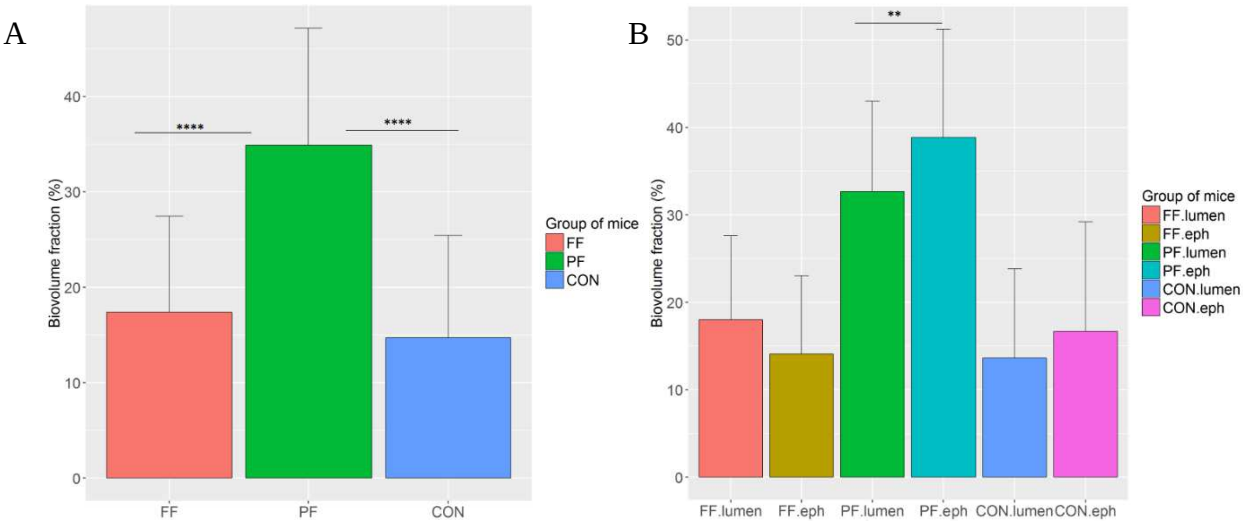

Figure 3.17. **(A)** Biovolume fraction (%) for each groups divided by lumen and epithelium. **(B)** Biovolume fraction of combined pictures of lumen and epithelium. Kruskal Wallis test was used to analyze the differences between the three groups and Dunn's test for multiple comparisons. **** $p \leq 0.001$, ** $p \leq 0.01$.

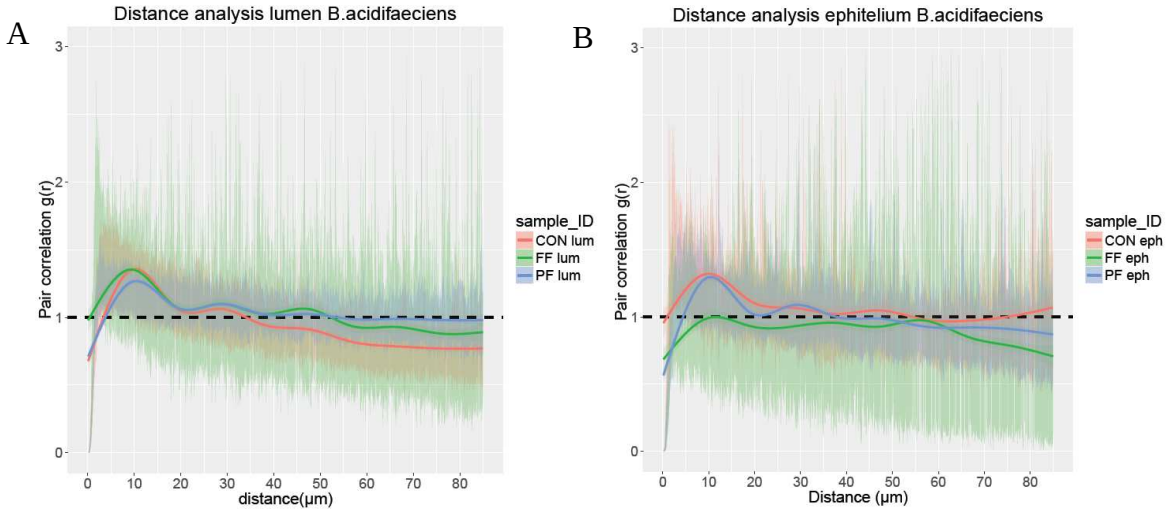

Figure 3.18. Pair-cross correlation (PCC) function curves of CON, FF and PF groups. To compare the results of bacterial cells localization, single measurements of each mouse for each location [lumen (A) and epithelium (B)] were pooled by calculating the arithmetic mean curves with respective 95% confidence interval (CI). The mean PCC curves for CON (pink line) versus FF (green line) and PF (blue line) was plotted with their respective 95% CI (same colour of the samples) against distances in a range from 0–85 µm.

Biovolume fraction of *Clostridium* cluster XIVa and XIVb and distance analysis

The quantification of *Clostridium* cluster XIVa and XIVb (most of *Clostridium coccoides* and *Eubacterium rectale*) group revealed a decreased abundance in CON (2.0±2.0; mean ± SD) respect to FF (10.7±9.1) and PF (11.5±7.6). There was a statistical significant difference in the three groups of diets driven by a low abundance in the CON group (Kruskal Wallis test: $p<0.0001$) and the difference between CON compared to FF and PF was highly significant (Dunn's test: $p<0.0001$) (Figure 3.20A). Comparing lumen vs epithelium we found a significant difference in the localization of cells in PF ($p= 0.0002$), in FF ($p= 0.0003$) and in CON ($p= 0.0099$) with an elevated abundance in the epithelium area respect to the lumen (Figure 3.20B). In order to see if a variation inter and intra-group were present, the ratio epithelium/lumen was calculated and one-sample t test was performed. We found a significant differences among the three groups ($p=0.003$) and also an intra-groups variation ($p=0.03$), indicating the presence of individuability between samples.

Spatial arrangements of bacterial cells are represented in figures 3.21 and 3.22. A different trend is presented for CON with clusterization from 0 to 10 µm in the lumen and a mutual avoidance

from 15 to 80 µm of distance. In the epithelium, a different pattern is described: a pronounced clusters formation seemed to be present from 0 to 25 µm and a random distribution pattern from 30 to 80 µm. In FF, clusters are presented from 0 to 30 µm in the lumen while in the epithelium a random distribution is described from 0 to 30 µm. From 30 to 80 µm of distance a mutual avoindance of cells is reported for both lumen and epithelium.

As shown in the CLSM images of epithelium and lumen area (Figure 3.19) co-aggregations of coccoid cells are presented but only in PF respect to CON and FF. In order to measure the behavior of these co-aggregates, a spatial arrangiament for rods and cocci separately was further performed. The mutual avoidance detected in figure 3.21 regarding PF group represented the pattern of rods and cocci considered together. Figure 3.22 shows the behavior of rods and cocci separately, revealing a different behaviour. Rods had a remarkable mutual avoidance distribution and cocci showed a random distribution pattern and a clusters presence from 15 to 30 µm in lumen. In the epithelium, clusters were detected from 0 to 15 µm and mutual avoidance from 20 to 80 µm in the epithelium. Cocci distributions is in accordance to Figures 3.19A and B, in which they seem to be very close to each other but very far away from the others cocci aggregates.

In summary, the spatial arrangements analysis showed different patterns in both lumen and epithelium, suggesting a diet-dependent distribution.

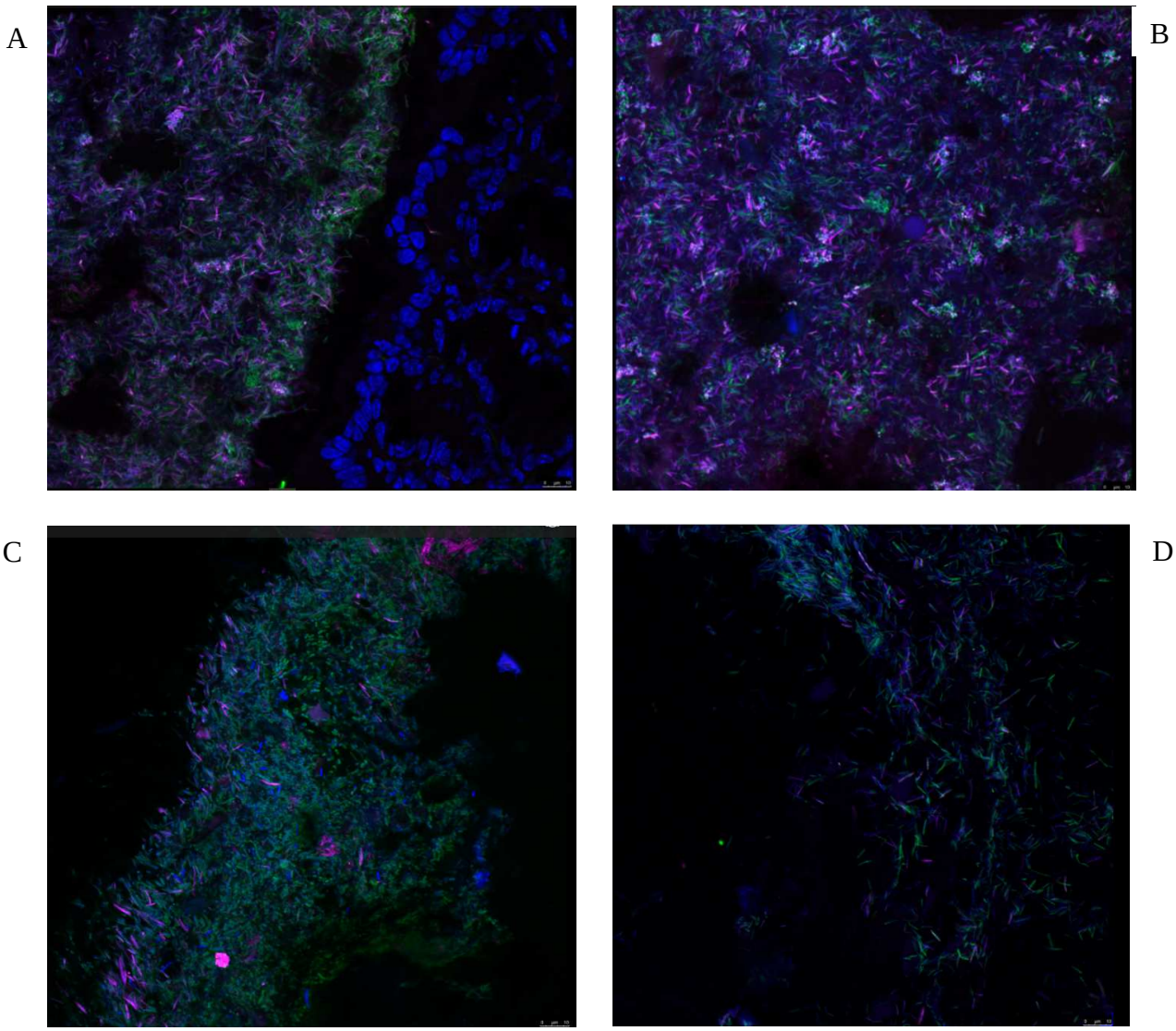

Figure 3.19. (A,B) Representative picture of the distal colon of a PF mouse stained with DAPI (blue) EUB I-II-III 338 DOPE in Fluos (green) for all Bacteria and and the specific probe Erec_482 in Cy5 (pink). Images were performed with confocal laser scanning microscope with: magnification 63X, resolution 1864x1864, zoom factor 1. **(C,D)** Representative picture of the distal colon of a CON (C) and FF (D) mouse respectively stained in the same conditions.

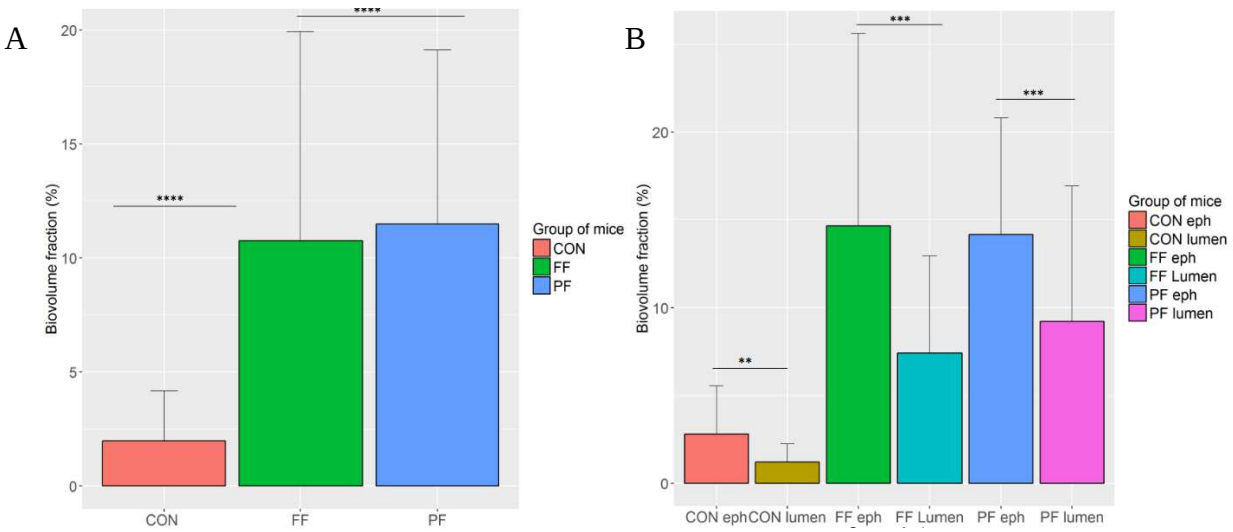

Figure 3.20. (A) Biovolume fraction (%) for each groups divided by lumen and epithelium. **(B)** Biovolume fraction of combined pictures of lumen and epithelium. Kruskal Wallis test was used to analyse the differences between the three groups and Dunn's test for multiple comparisons. **** p ≤0.001, *** p≤0.001, **p≤0.01.

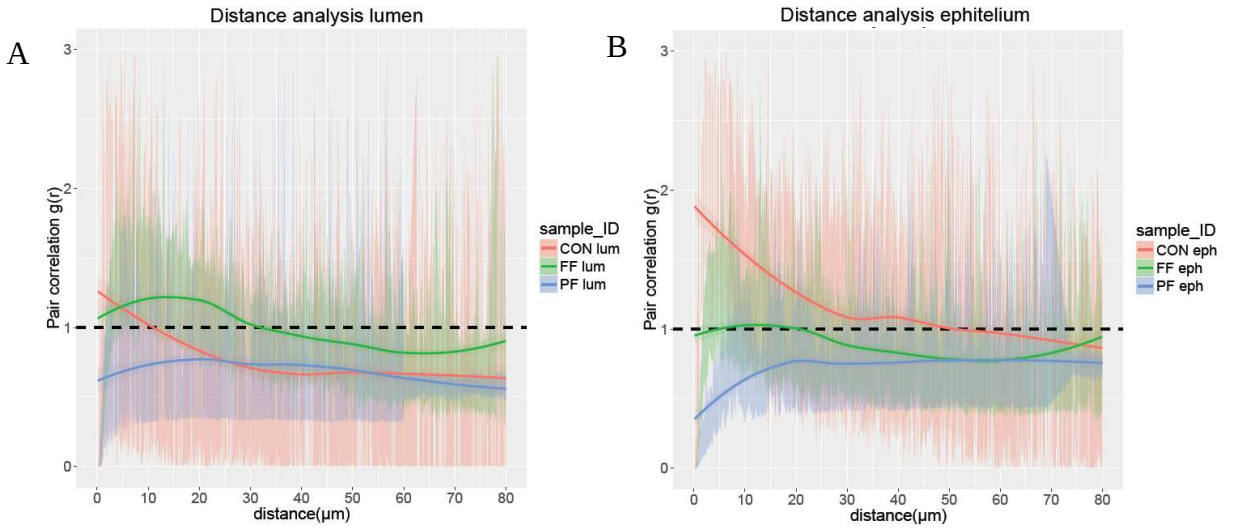

Figure 3.21. Pair-cross correlation (PCC) function curves of CON, FF and PF groups. To compare the results of bacterial cells localization, single measurements of each mouse for each location (lumen and epithelium) were pooled by calculating the arithmetic mean curves with respective 95% confidence interval (CI). The mean of PCC curves was plotted for CON (pink line) versus FF (green line) and PF (blue line) with their respective 95% CI (same colour of the samples) against distances in a range from 0–80 µm for lumen **(A)** and epithelium **(B)**.

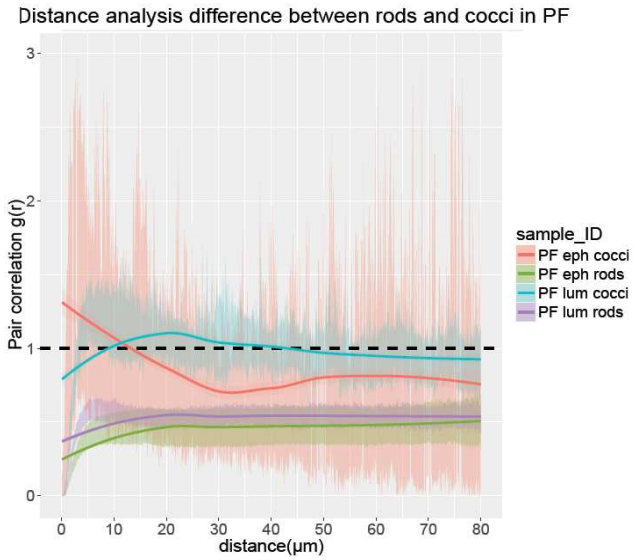

Figure 3.22. Spatial arrangement analysis of the positive hybridization signals of rods and cocci in PF mice. Pair cross correlation function curves (PCC) of PF mice: single measurements of each mouse for each location (lumen and epithelium) and for each bacterial shape (rods and cocci) were pooled by calculating the arithmetic mean curves with respective 95% CI of PF samples. The mean of PCC curves was plotted with their respective 95% CI (same colour of the samples) against distances in a range from 0–80 µm.

Biovolume fraction and cluster analysis of *Desulfovibrio* spp.

Desulfovibrio spp. was detected by FISH analysis only in one PF mouse (Figure 3.23A and B) The biovolume fractions of *Desulfovibrio* spp. were 3±2.5 (mean±SD) in the lumen and 2±1.8 (mean±SD) in the epithelium.

Spatial arrangement of cells was performed by calculating the areas of the cells, and the box-plots (Figure 3.24) show the presence of different out-groups, probably representing co-aggregation of cells in both lumen and epithelium.

A

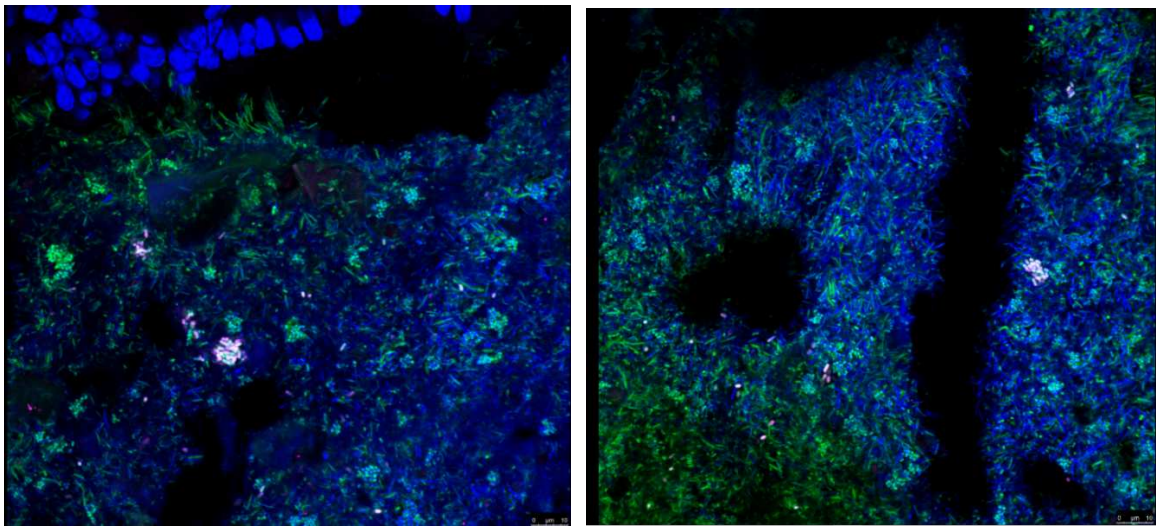

B

Figure 3.23. Representative picture of a distal colon stained with DAPI (blue) EUB I-II-III 338 DOPE in Fluos (green) for all Bacteria and the specific probe Dsp_653 in Cy5 (pink). Images were performed with confocal laser scanning microscope with: magnification 63X, resolution 1512x1512, zoom factor 1 for epithelium (A) and lumen (B).

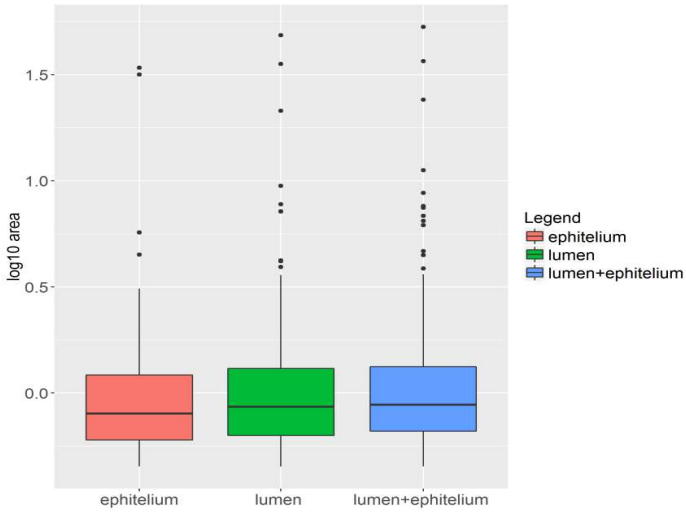

Figure 3.24. Cluster analysis of *Desulfovibrio* spp. The cluster analysis revealed the presence of co-aggregates of different sizes in both lumen and epithelium.

Biovolume fraction of *Bacteroidaceae, Prevotellaceae* and *Porphyromonadaceae*

The quantification of *Bacteroidaceae*, *Prevotellaceae* and *Porphyromonadaceae* revealed a different abundance in the three groups (FF: 25.7±16.6, PF: 34.1±21.0, CON: 39.9±13.7; mean ± SD). There is a statistical significant decrease in FF and in PF respect to CON (Kruskal Wallis test: $p<0.0001$) (Figure 3.26A). Comparing lumen vs epithelium we found a significant difference in the localization of cells in FF ($p= 0.0363$) characterized by an elevated abundance

in lumen area. No statistical significance in the localization of cells were found for PF (p= 0.2654) and CON (p=0.990) (Figures 3.26B, 3.25A and B). The ratio epithelium/lumen revealed no difference inter and intra-group (p=0.1532 and p=0.7073 respectively).

Spatial arrangement analysis showed a similar trend for the three groups of mice in both lumen and ephiltelium, with cell aggregations from 0 to 25 µm in the epithelium and a more randomly distribution pattern in the lumen for shorter distances. A mutual avoidance of cells is presented from 40 to 80 µm (Figure 3.27A and B).

A 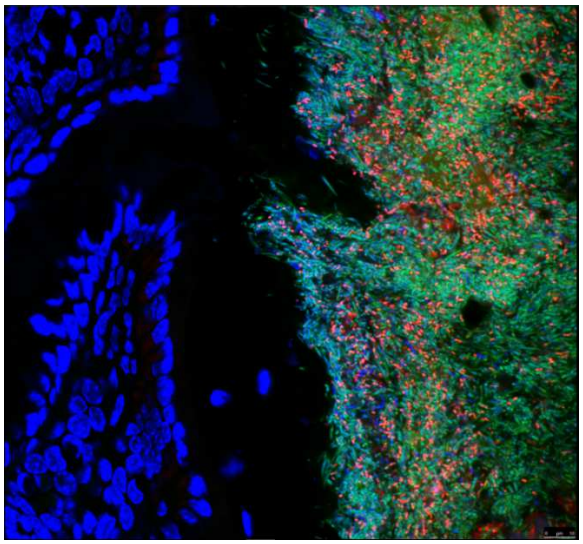 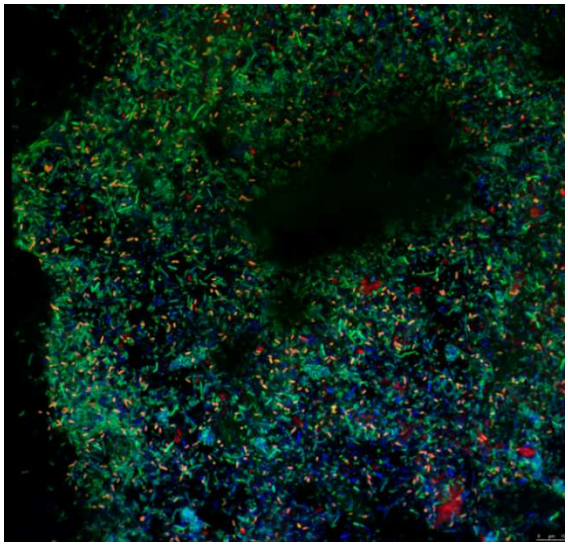 B

Figure 3.25. Representative picture of a distal colon stained with DAPI (blue) EUB I-II-III 338 DOPE in Fluos (green) for all Bacteria and the specific probe Bac_303 in Cy3 (red). Images were performed with confocal laser scanning microscope with: magnification 63X, resolution1944x1944, zoom factor 1 for epithelium **(A)** and lumen **(B)**.

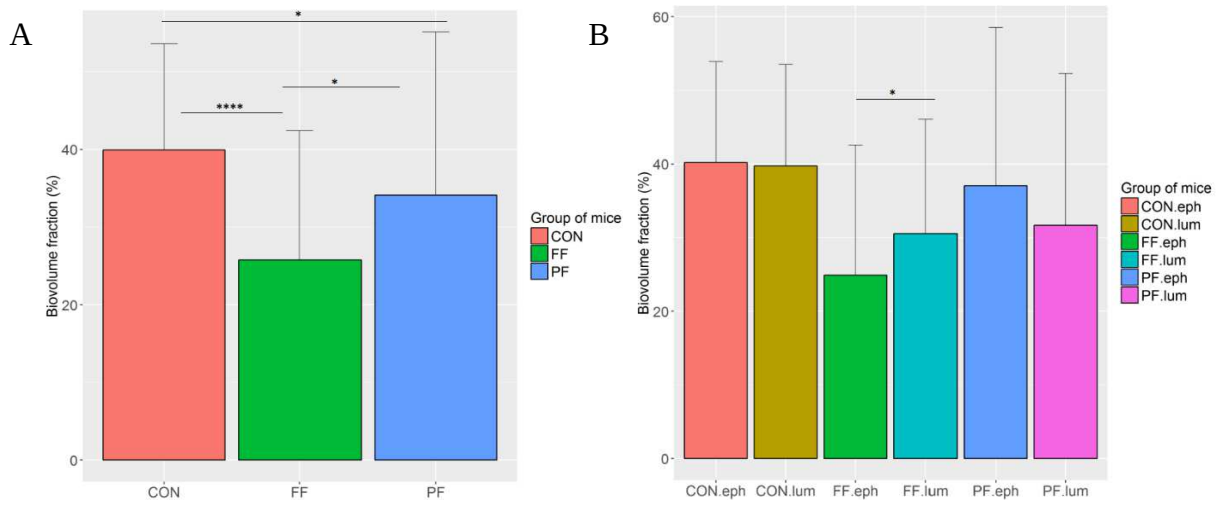

Figure 3.26. (A) Biovolume fraction (%) for each groups of mice divided by lumen and epithelium. **(B)** Biovolume fraction of combined pictures of lumen and epithelium. Kruskal Wallis test was used to analysed the differences between the 3 groups and Dunn's test for multiple comparisons. **** p ≤0.001, *p≤0.05.

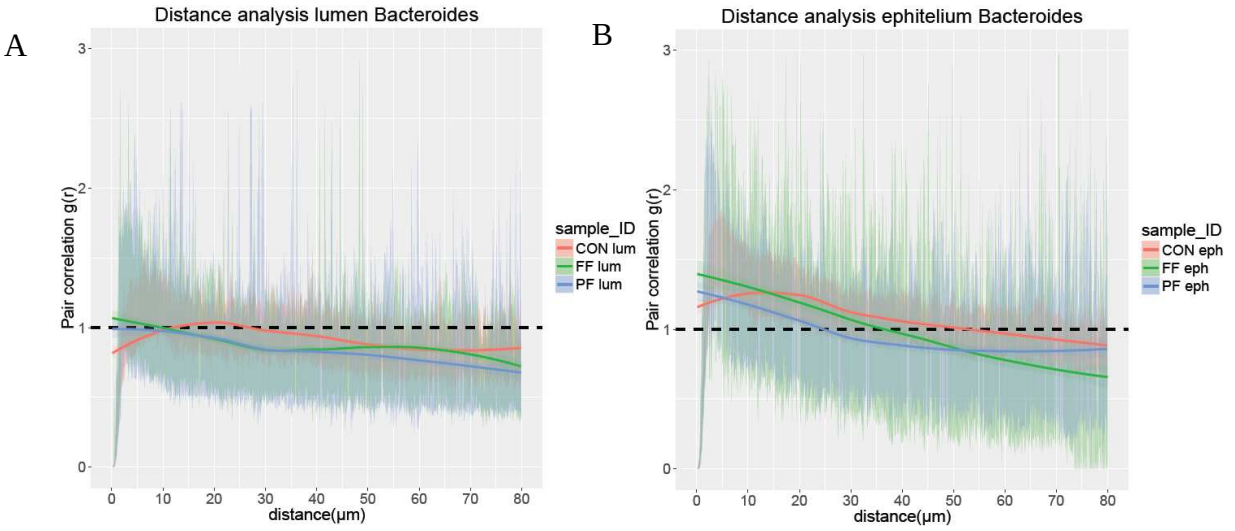

Figure 3.27. Pair-cross correlation (PCC) function curves of CON, FF and PF groups. To compare the results of localization of bacterial cells, single measurements of each mouse for each location (lumen and epithelium) were pooled by calculating the arithmetic mean curves with respective 95% confidence interval (CI). The mean PCC curves for CON (pink line) versus FF (green line) and PF (blue line) was plotted with their respective 95% CI (same colour of the samples) against distances in a range from 0–80 µm for lumen **(A)** and epithelium **(B)**.

Lactobacillus spp. and *Enterococcus* spp. detection in mouse's distal colon

Lactobacillus spp. were detected in the distal colon in two FF, two PF and in the three CON mice (Figure 3.28) with a low abundance [(FF:0.70±0.9 mean±SD; PF: 0.43±0.32; CON: 0.72±0.70, (Kruskal Wallis test: p=0.00806)] and divided by location [FF lumen: 0.88±1.0 mean±SD; FF epithelium:0.33±0.26 (p=0.9967); PF lumen:0.45±0.33; PF epithelium: 0.40±0.30 (p=0.4088); CON lumen:1.0±0.77;CON epithelium:0.34±0.31(p<0.0001)].

Cluster analysis revealed co-aggregation of cells above all in the lumen area, in particular CON showed a clear clusterization of cells (Figure 3.29).

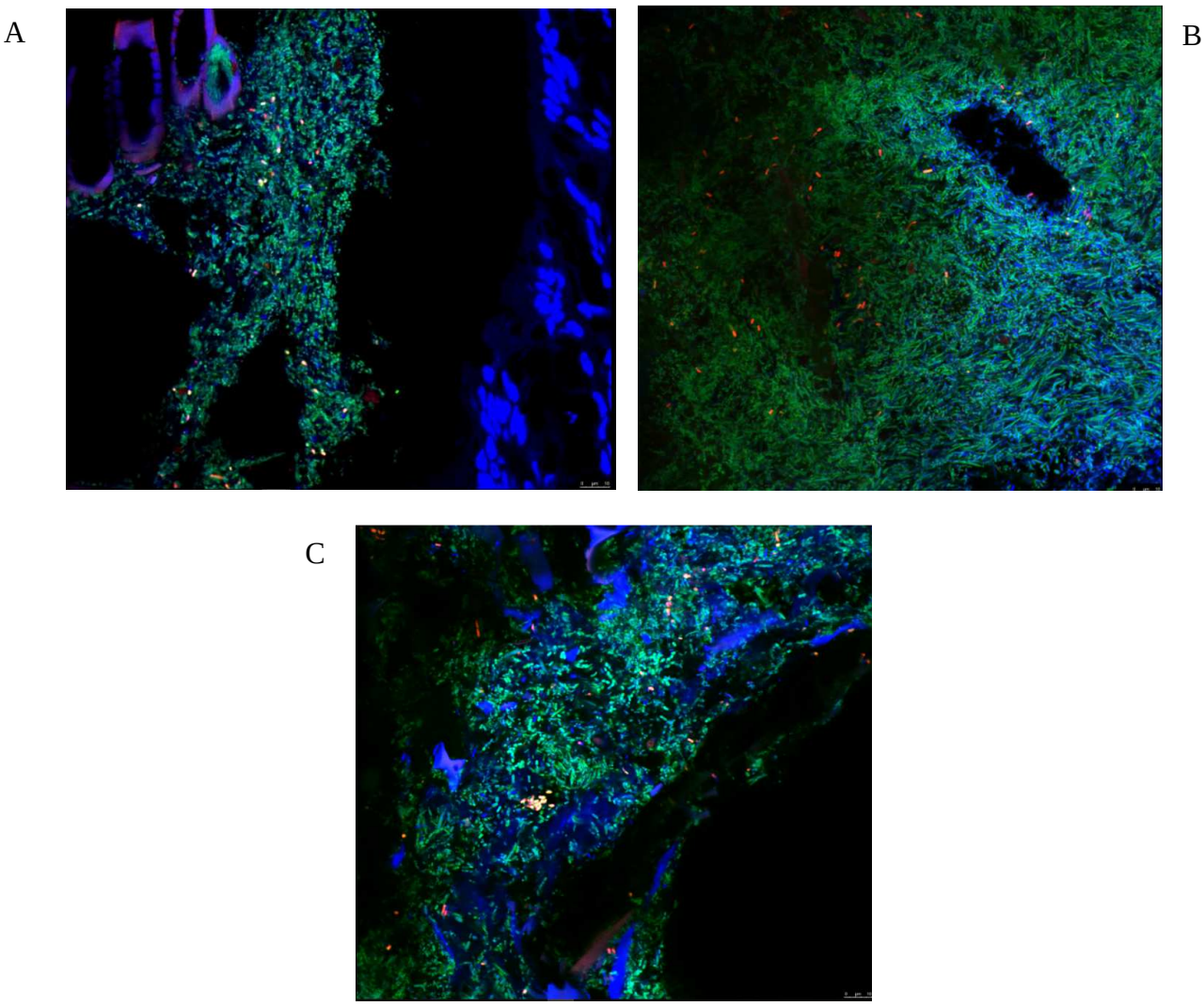

Figure 3.28. Representative picture of a distal colon stained with DAPI (blue) EUB I-II-III 338 DOPE in Fluos (green) for all Bacteria and the specific probe LAB_158 in Cy3 (red). Images were performed with confocal laser scanning microscope with: magnification 63X, resolution1944x1944, zoom factor 1 for epithelium **(A)** and lumen **(B)**. **(C)** shows co-aggregate presence in CON.

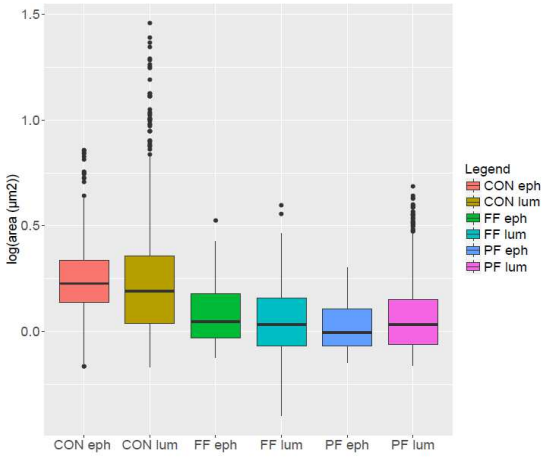

Figure 3.29. Cluster analysis of *Lactobacillus* spp. and *Enterococcus* spp. The cluster analysis revealed the presence of co-aggregates of different sizes above all in CON and more localized in the lumen.

No bacteria presence was found in the inner mucus layer

It has been reported that the inner mucus layer can be dominated by *Acynetobacter* spp. (Donaldson *et al*, 2015). *Acynetobacter* spp. was detected in the sequencing data at low abundance. Therefore, *Acynetobacter* specific probe and *Acynetobacter baumanni* positive control were tested to find a possible presence of these bacteria in the inner mucus layer. FISH analysis revealed the absence of these bacteria close to the mucus layer. We can conclude that it has been probably a contamination or FISH analysis could not detect *Acynetobacter* spp. (Figure 3.30A and B).

A

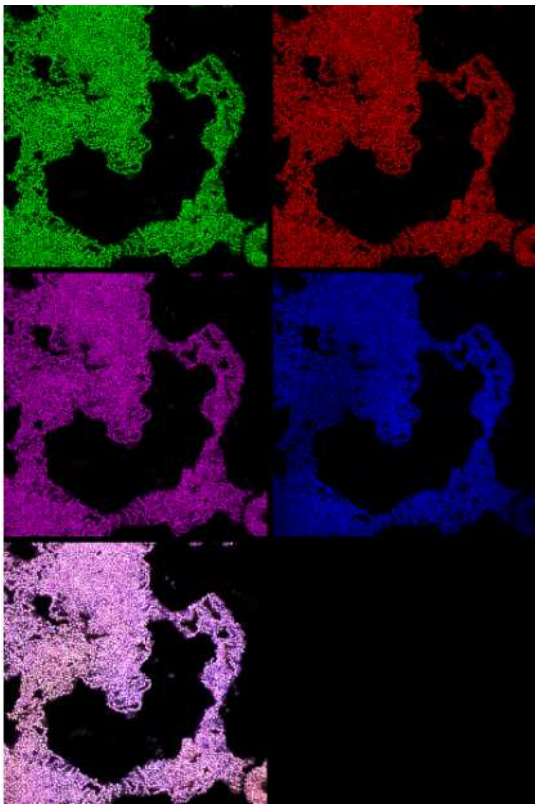

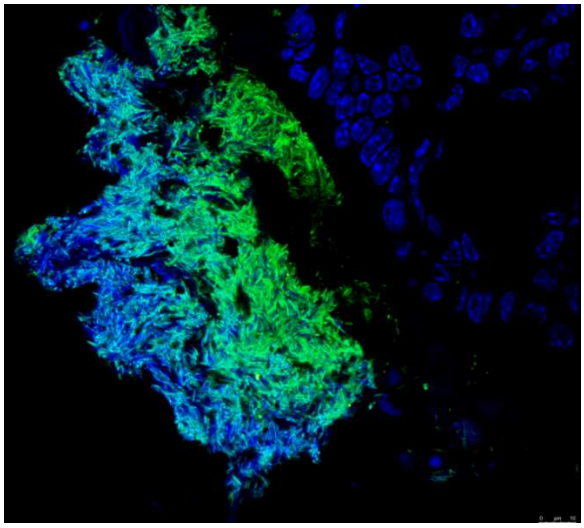

B

Figure 3.30. *Acynetobacter baumanni* positive control stained with Eubmix 338 I, II, III DOPE in fluos (green), the specific probe Aca 652 Cy3 (red), Gam42a Cy5+ Bet42a competitor (pink), dapi (blue), resolution:2376px x 2376px, size: 150,00 um x 150,00 um, zoom factor: 1.23. **(A)** positive control, **(B)** representative picture of a distal colon stained with the same set of probes. Resolution:1944px x 1944px, zoom factor: 1. No positive signal was present for Aca 652 Cy3 and Gam42a Cy5+ Bet42acompetitor.

Goblet cells quantification and thickness of the mucus layer

Goblet cells were stained with alcian blue, the biovolume fraction and the thickness of the mucus layer were calculated. The biovolume fraction was more elevated in CON (49.4±12.5; mean ± SD) and FF (41.2±5.5) respect to PF (29.6±8.4) (Figure 3.30) (Kruskal Wallis test: $p<0.0001$). The thinnest mucus layer was measured in PF (27.4 µm±6.1; mean ± SD), followed by FF (40.3 µm ±9.0) respect to CON (58.5 µm ±9.0) (Kruskal Wallis test: $p<0.0001$) (Figure 3.31). A representative picture of the intestinal mucus layer using methacarn fixation and a combination of FISH and MUC2 staining is shown in figure 3.32.

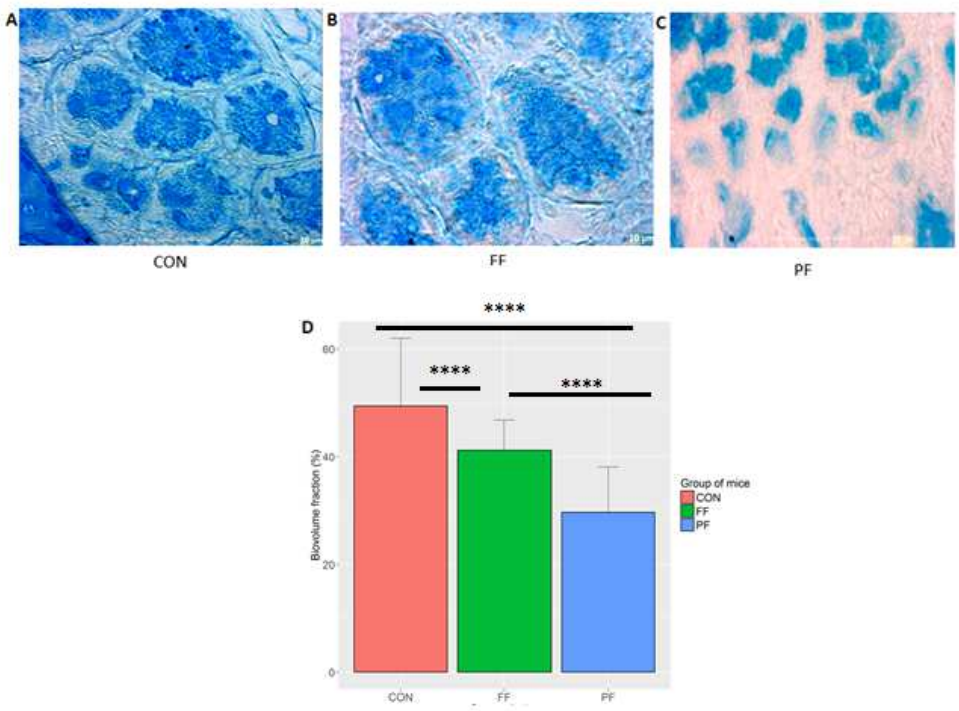

Figure 3.30. Biovolume fraction of goblet cells: **(A)** CON, **(B)** FF and **(C)** PF, **(D).** Kruskal Wallis test was used to analyzed the differences of the biovolume fraction in the three groups ($p<0.0001$) and Dunn's test for multiple comparisons. **** $p \leq 0.001$.

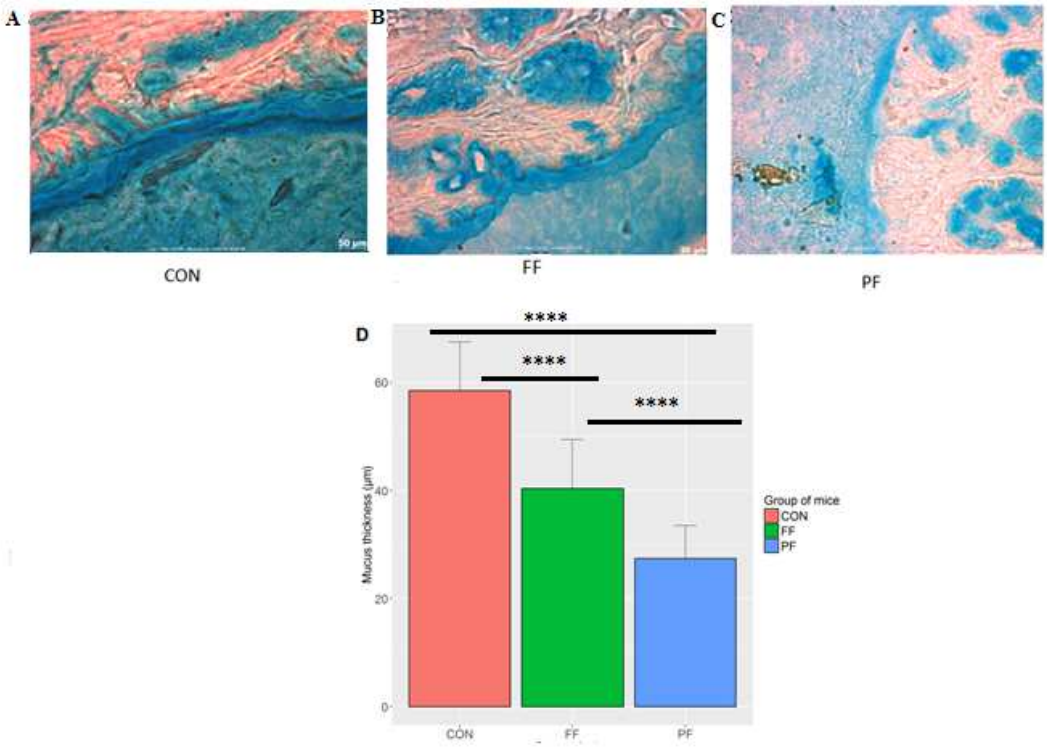

Figure 3.31. Mucus layer thickness: **(A)** CON, **(B)** FF and **(C)** PF, **(D).** Kruskal Wallis test was used to analysed the differences of the mucus layer thickness in the three groups ($p<0.0001$) and Dunn's test for multiple comparisons. **** $p \leq 0.001$.

A 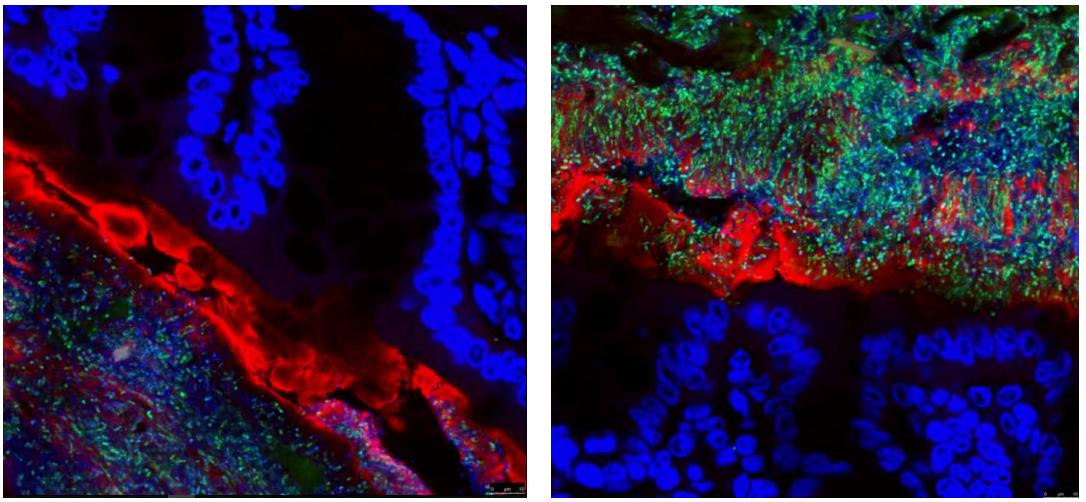 B

Figure 3.32. Representative pictures of the mucus layer in the distal colon of a CON mouse stained with DAPI (blue), EUB I-II-III 338 DOPE in Fluos (green) for all Bacteria and Alexa 488 goat anti-rabbit secondary antibody Cy3 (red) for the mucus layer. Images were performed with confocal laser scanning microscope with: magnification 63X, resolution1944x1944, zoom factor 1.

3.4.4 DISCUSSION

Complex microbial populations are organized in relation to their environment. The complex host-microbe organization exemplify the power and necessity of high-throughput imaging and analysis of microbial communities for revealing changes in spatial patterning across multiple scales (Earle *et al,* 2015). Gut mucosa-associated microbes are defined as the microbial community that reside in the colonic epithelial cell surface and constitute a biofilm with a polysaccharide-rich mucus gel layer. Mucosa-associated microbes are in intimate contact with the host, affecting pivotal functions such as immune activation, epithelial growth and development and mucus production (Wang *et al*., 2010). Changes in the diet can disturb the gut microbiota composition, for example the elimination of microbiota-accessible carbohydrates can have an impact on gut microbiota and mucus layer (Earle *et al,* 2015).

In our study the privation of fiber and above all polysaccharides affected the diversity and richness in the gut. A significant drop in alpha diversity was present for FF and PF diet. The same trend was found for both LCM and stool samples and seemed to be diet and day

dependent. A clear separation within proximal, middle and distal colon was present in CON, but the privation of fiber and above all the absence of polysaccharides compromised the beta diversity from proximal to distal colon.

After the weekly dietary treatment in privation of fiber or polysaccharides, we found significant shifts in species implicated in the breakdown of cellulose and polysaccharides. *Prevotella* spp. and members of S24-7 (*Bacteroidaceae*) decreased in FF and PF; in fact members of *Bacteroides* spp. and *Prevotella* spp. are capable of degrade complex plant polysaccharides such as starch, cellulose, xylans, and pectins (Rajilic´-Stojanovi *et a*l.,2014; Despres *et al*., 2016). Members of *Proteobacteria* increased in PF diet in particular *Desulfovibrionaceae* and *Desulfovibrio* spp. In accordance with this data, *Desulfovibrio intestinalis* and *desulfuricans* were identified as indicator OTUs only in PF.

The indicators species (OTUs) describe the OTUs whose abundance indicates evidence for the community changes within a speficic area or condition. Most of the bacterial species detected were implicated in fiber and polysaccharide degradation, meaning that the detection of these OTUs is diet dependent.

Indicators OTUs for FF and PF revealed changes in species implicated in cellulose (*Ruminococcus obeum, Ruminococcus champanellensis, Bacteroides eggerthii*) (Chassard *et al*., 2012) and xylan (*Bacteroides xylanisolvens, Clostridium xylanisolvens*) degradation. Plant cell wall polysaccharides and especially xylans constitute an important part of human diet. Xylans are not degraded by human digestive enzymes in the upper digestive tract, therefore reach the colon where they are degraded by the symbiotic microbiota. Xylanolytic bacteria are the first degraders of these complex polysaccharides and they release breakdown products that can have beneficial effects on human health (Despres *et al*., 2016).

16S rRNA gene profiles showed that microbial populations associated with the intestinal compartments are distinct from those found in fecal samples, as observed in other studies (Nava *et al*., 2011; Eckburg *et al*., 2005). The analysis of stool and LCM samples revealed a distinct

microbial population. In stool samples, the most abundant phyla were *Bacteroidetes*, *Firmicutes*, *Proteobacteria* and *Verrucomicrobia*, while in LCM sample *Firmicutes*, *Bacteroidetes*, *Actinobacteria* and *Proteobacteria* predominated.

Comparing the relative abundance in proximal, middle and distal colon, more differences between compartments seemed to be present in CON, whereas in FF and PF diets this variability seemed to be partially lost in agreement with Beta diversity results. The relative abundance changes between the compartments may be diet dependent and the privation of fiber and polysaccharides may destroy the normal niche-specific colonization, decreasing richness and diversity.

In the microbial world, spatial patterns of microbial diversity are driven by environmental heterogeneity. Microbial ecology studies have shown that microbes exhibit spatially predictable and aggregated patterns. Thus, one might expect to find similar microbial communities in similar habitats and differentiated microbial communities along an environmental gradient (Green and Bohannan, 2006). With the distance-decay analysis, a negative correlation between sections similarity and distance across sections was present, meaning that when the distance across sections increases the similarity decreases. A similar negative trend was present in the three groups but the same behavior already described in beta diversity is reported. The privation of fiber and above all the absence of polysaccharides compromises the biogeography structure from proximal to distal colon.

A pipeline for analyzing large imaging datasets is critical for building an understanding of microbiota localization in an unbiased way. To gain more insight of the spatial organization of gut bacteria, the relative abundance between lumen and epithelium was compared and the distance between cells was measured using the spatial arrangements measurement every one cell. Therefore, we performed FISH analysis in order to explore the different localization *in situ* of specific bacteria (lumen vs epithelium) and their spatial organization.

To explore the role of polysaccharide privation on mucus-degrading bacteria, we investigated target bacteria capable of consuming mucin glycans near the mucus like *Bacteroides acidifaciens*, mucus-associated bacteria like *Clostridium* cluster XIVa group and bacteria implicated in polysaccharide degradation like *Bacteroidaceae, Prevotellaceae*. We quantified and measured the cells localization of *Desulfovibrio* spp. found enriched in PF diet after sequencing data analysis. We further quantified bacteria commonly present in the colon like *Lactobacillus* spp. and *Enterococcus* spp.

In this study, PF mice had a higher abundance of *Bacteroides acidifaciens* compared to the control, and in particular, the highest abundance was present in the epithelium. *B.acidifaciens* is a mucin-degrading bacterium that use the mucus layer as source of polysaccharides (Donaldson *et al*, 2015) and in a diet free of polysaccharides the mucosal glycans are the only carbohydrate source.

Moreover, in a PF mouse we detected *Desulfovibrio* spp. in accordance with the increased relative abundance previously described in stool samples. Consistent with these observations, Rey et al described that liberation of sulfate from sulfated mucins promotes *Desulfovibrio* spp growth. They found that the increased sulfatase gene expression in *Bacteroides* species observed in mice consuming low polysaccharide diet, was accompanied by significantly higher levels of *Desulfovibrio piger* and significantly elevated concentrations of H_2S in cecal contents. *Bacteroides* spp. expresses sulfatases that are required for its adaptive foraging on mucosal glycans when the diet lacks complex polysaccharides. Consequently, *D. piger* can benefit from diets that provide low levels of complex carbohydrates because *Bacteroidets* increases the utilization of host sulfated glycans thereby providing free sulfate for *D.piger* (Rey *et al*, 2013). Moreover, the sulfide, produced by certain bacteria, reduces disulfide bonds in the mucus network. The resulting breaks in the mucus barrier allow exposure of the epithelium to bacteria and toxins, causing inflammation (Ijssennagger *et al*, 2016). *Desulfovibrio* spp. may be a

potential candidate that can influence mucus structure and may be considered disease-liable commensals, mainly due to their tight association with the colonic epithelium (Li *et al*, 2015). In accordance with this observation, we can hypothesize that the increased hydrogen sulfide production by the *Desulfovibrio* spp. under the PF diet may be, at least partly, responsible for the reduced mucus layer. We can hypothesize that in a diet without polysaccharides the mucin-degrading bacteria increase the usage of the mucins as carbon source, consequently the goblet cells are not able to produce the same amount of mucus required from these bacteria. This may provide a stressful condition for the goblet cells and may be an explaination of the decrease biovolume fraction. This effect is much more present in PF diet but in a secondary extent in FF diet. Therefore, the privation of polysaccharides as well as cellulose may decrease the biovolume fraction of goblet cells and the mucus layer thickness. Interestingly, goblet cells are reported to be affected in different pathological conditions. During acute intestinal infections, goblet cells are induced to proliferate and consequently mucin synthesis and secretion increase. On the contrary, chronic infections result in the depletion of goblet cells and quantitative and qualitative alteration in mucus layers due both to altered synthesis and secretion of mucins. Goblet cells are also reduced in number and size in ulcerative colitis (Kim and Ho, 2010). Whereas the mucus layers play key roles in the establishment of the commensal intestinal microbiota and the protection from colonization and invasion by the pathogenic bacteria; the defective mucosal barrier, abnormal commensal bacteria and defective host innate and adaptive immune response, result in intestinal inflammation and injury (Kim and Ho, 2010).

The dietary fiber are reported to be able to modulate the balance between secretion/synthesis of mucin, the recovery of mucin in the lumen and the composition of mucins. For example, studies in rats provide evidence that an increase in luminal mucus erosion observed with some dietary fiber is counterbalanced by the synthesis and secretion of mucus by goblet cells (Montagne *et al*., 2003).

Some of the gut bacteria able to degrade fiber are *Bacteroidaceae* and *Prevotellaceae*. In condition of fiber and polysaccharide privation, a decreased abundance of *Bacteroideaceae, Prevotellaceae* and *Porphyromonodaceae* is detected for FF and PF as shown in gut microbiota communities from stool and LCM samples.

The spatial arrangement of cells seemed to be not affected by diet shift revealing a similar trend for the three groups of diet in both lumen and ephiltelium. The lack of changes in FF and PF in the spatial arrangement may be explained by the high adaptability of *Bacteroides* spp. in the intestine. Compared with other gut bacteria, *Bacteroides* spp. have the largest number and greatest diversity of genes involved in polysaccharide degradation. *Bacteroides* spp., are sometimes referred to as 'generalists', as they are capable of occupying a variety of metabolic niches depending on the availability of diverse polysaccharide nutrients. Many studies of *Bacteroides* spp. glycan metabolism in mice have shown that restricting the polysaccharide content of the mouse diet allows selection for species (or strains) that are capable of metabolizing the complex glycans present, such as fructans, fucosylated mucin glycans and mannan. Presumably, the variety of starch utilization systems (Sus) present in the genomes of *Bacteroides* spp. provides the metabolic plasticity required to persist in the gut despite short- and long-term changes in nutrient availability (Ouwerkerk *et al*., 2013).

In our study an increased abundance in the epithelium is observed for *Clostridium* cluster XIVa and b members in accordance with Ouwerkerk et al. (Ouwerkerk *et al*, 2013). Bacteria belonging to *Clostridium* cluster XIVa have been associated in vitro with the colonization of a mucin rich environment, and include butyrate producers like *Retortamonas intestinalis* and *Eubacterium rectale* (Ouwerkerk *et al*, 2013; Nava *et al*., 2011). In our study, a significant elevated relative abundance in the ephitelium was present for all groups. Interestingly, in PF diet a different bacteria shapes were present: coccoid and long rods. In the spatial arrangement analysis, these two bacteria morphologies avoided each other. The spatial distribution of bacteria in the murine colon is also shape- and not only taxonomy-dependent, indicating the

existence of vertical (surface to lumen) and longitudinal (proximal to distal colon) viscosity gradients within the mucus layer. Mobility is shape-dependent: long rods with a spiral and curly form prefer a higher viscosity, whereas short coccoid bacteria favour a low viscosity and are trapped and immobilized by moderate viscosity (Swidsinski *et al*, 2007). The difference between rods and cocci could therefore result from bacterial preference to a specific viscous environment.

Members of the *Lactobacillus* genus are a minor part of the intestinal microbiota in the colon but a much greater component higher up in the gut (Ahrne *et al*, 2011). In our study, we could detect with FISH a low amount of *Lactobacillus* spp. and *Enterococcus* spp. and we observed an elevated abundance and clusters in the lumen. In particular, the controls have more elevated abundance and clusters, while they seemed to decrease in condition of fiber and polysaccharides privation.

The spatial arrangement of cells revealed different patterns that are diet and/or location dependent. A different localization of cells is present comparing lumen with mucosa, even if in some cases a high inter-individual variation is present. Taken togheter, our data capture dramatic changes in the spatial arrangement of the gut microbiota.

In summary, this study has established new insights into the spatial organization and diversity of microbes across the murine intestine. Using a high-resolution microbial capture system in conjunction with current nucleic acid analytic techniques, we showed that the microbial communities of distal, middle, proximal colon and stool samples were different in three diverse dietary treatments. Furthermore, this high-resolution system suggests a model in which the privation of dietary polysaccharides results in an increased bacterial consumption of mucin glycans, in a thinner mucus layer and in the alterations of goblet cells improving our understanding of host-microbial interactions.

CHAPTER 4:

THE ORAL MICROBIOTA

Introduction

4.1 The oral microbiota

The human mouth is heavily colonised by microorganisms, including viruses, protozoa, fungi, archaea and bacteria. In contrast to the commensal microbiota found at other body sites, which typically live in harmony with the host, the normal microbiota of the mouth is also responsible for the two commonest diseases of man: dental caries and the periodontal diseases. The bacterial communities found in the mouth are highly complex with around 1000 species present and has been shown to be the second most complex in the body, after the colon (Wade, 2013).

The use of culture-independent methods of determining the composition of the oral microbiota, allied with next generation DNA sequencing methods is providing a far deeper analysis than hitherto possible. The human oral microbiota is defined as all the microorganisms that are found on or in the human oral cavity and its contiguous extensions (stopping at the distal esophagus), though most of the studies and samples have been obtained from within the oral cavity (Wade, 2013). Studies have shown that different oral structures and tissues are colonized by distinct microbial communities (Dewhirst *et al*., 2010). The oral cavity harbors at least five communities: the teeth, which are non-shedding surfaces, the saliva, the dorsal and lateral surfaces of the tongue, the gingival sulcus, the periodontal pocket and the remaining epithelial surfaces of the oral mucosae (Costalonga and Herzberg, 2014).

4.1.1 Composition of the oral microbiota

In general, the mouth harbours at least six billion bacteria which are represented by more than 1000 species as well as other types of microorganisms, including fungi, protozoa and possibly even viruses (How *et al*., 2016) :

- **Protozoa**

Two protozoan species are found as part of the normal microbiota: *Entamoeba gingivalis* and *Trichomonas tenax*. The numbers of these organisms is raised in subjects with poor oral hygiene. They are currently regarded as harmless saprophytes and the apparent link with disease is nutritional, in that poor oral hygiene leads to increased amounts of food debris and bacteria, both food sources for protozoa (Wade, 2013).

- **Fungi**

Candida species are carried symptomlessly by around half of individuals with the prevalence increasing with age, and even cause a wide range of acute and chronic infections. A culture independent survey of the oral mycobiome in healthy individuals found 85 fungal genera in the mouths of 20 healthy individuals. The predominant genera were *Candida*, *Cladosporium*, *Aureobasidium*, *Saccharomycetales*, *Aspergillus*, *Fusarium*, and *Cryptococcus* (Wade, 2013).

- **Archaea**

The Archaea make up only a minor component of the oral microbiota and the archaeal community is restricted to a small number of species/phylotypes, all of which are methanogens. They can be detected in health but their prevalence and numbers are raised in subjects with periodontitis. The species found are *Methanobrevibacter oralis* and two un-named *Methanobrevibacter* phylotypes, *Methanobacterium curvum*/*congolense* and *Methanosarcina mazeii* (Wade, 2013).

- **Bacteria**

Generally, oral bacteria are composed of Gram-positive and Gram-negative bacteria, and secondarily as either anaerobic or facultatively anaerobic according to their oxygen requirements. Despite the diverse community of oral microbiota, the oral cavity is, nonetheless, characterized by a stable community known as the “core” community. Therefore, if imbalance in the oral resident microbiota occurs, oral diseases such as caries and periodontal diseases seem to appear, leading to multiplication of potentially pathogenic microorganisms. Several studies

have illustrated that a change in microbial species in the gingival sulcus from Gram-positive, facultative, fermentative microorganisms to predominantly Gram-negative, anaerobic, chemoorganotrophic, and proteolytic organisms has been highly associated with destruction of periodontal tissue (How *et al*., 2016).

Complex bacterial communities such as the oral microbiota have been characterised by culture-independent methods based on the analysis of the sequences of conserved housekeeping genes directly isolated from samples of saliva or oral biofilms. The gene most commonly used for this purpose has been that encoding the 16S rRNA. The use of this method has allowed the comprehensive description of the oral bacterial biota (Wade, 2013).

Today, one of the most important databases of taxa present in the oral cavity is the Human Oral Microbiome Database (HOMD) (http://www.homd.org/). HOMD stores 34,753 filtered cloned sequences representing a wide variety of healthy and diseased sites throughout the oral cavity such as the dorsum of the tongue, lateral sides of the tongue, buccal fold where the gingiva folds into the cheek, surface of the cheeks (buccal mucosa), hard palate, softpalate, labial gingiva, tonsils, and supragingival and subgingival plaques from tooth surfaces (Costalonga and Herzberg, 2014) (Figure 4.1). As an open system, can potentially include all of the microorganisms in the environment.

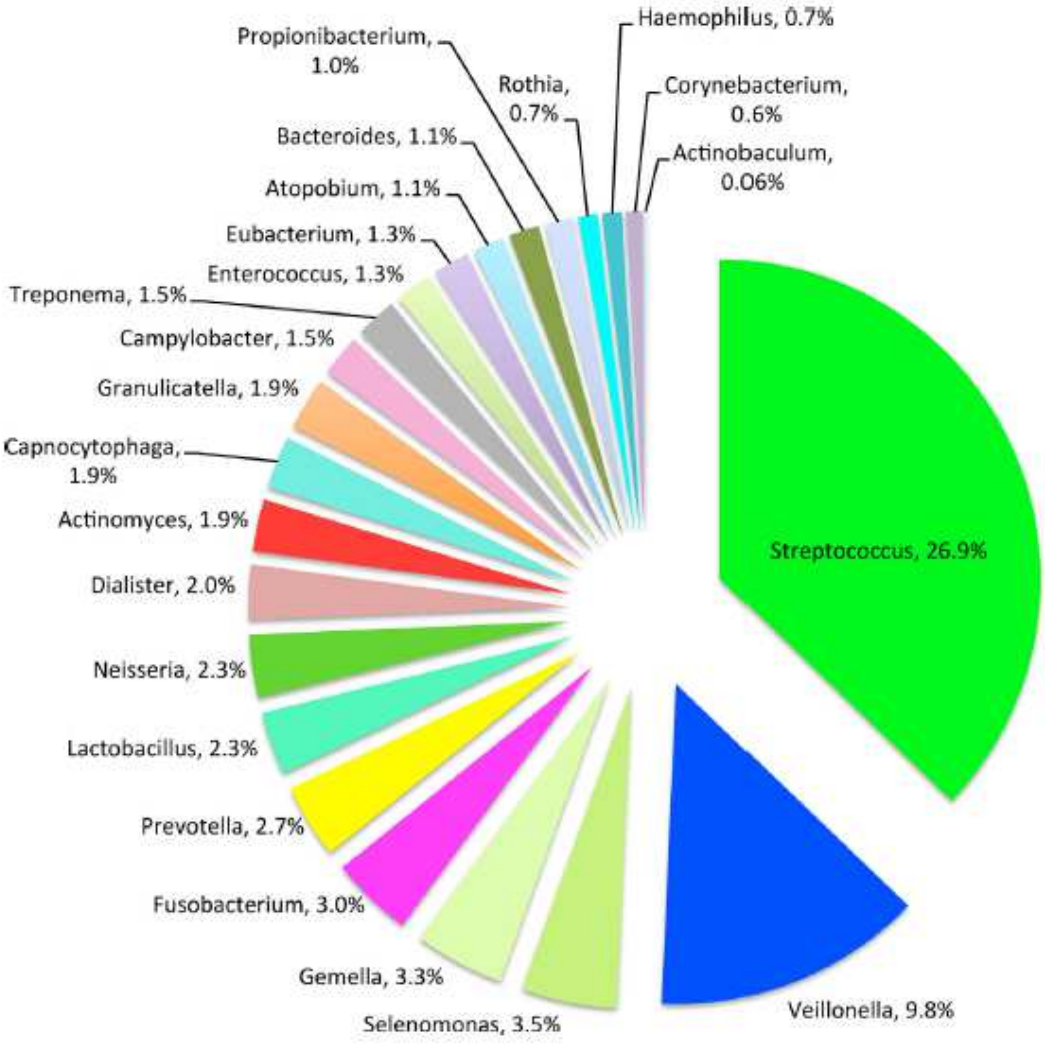

Figure 4.1. Proportions of oral microorganisms in the Human Oral Microbiome Database (HOMD) (Costalonga and Herzberg, 2014).

The oral microbiota was well explored by different studies (Zaura *et al*., 2009; Lazarevic *et al*.,2010). Zaura and co-authors sampled and sequenced microbiota from several intraoral niches (dental surfaces, cheek, hard palate, tongue and saliva) in three healthy participants with 454 pyrosequencing. Interestingly, principal component analysis discriminated the profiles of the samples originating from shedding surfaces (mucosa of tongue, cheek and palate) from the samples that were obtained from solid surfaces (teeth). Moreover, there was a large overlap in the higher taxonomic level (genus level or above), "species-level" phylotypes and unique sequences among the three microbiota: 84% of the higher taxonomic level, 75% of the OTUs and 65% of the unique sequences were present in at least two of the three microbiota. The three

individuals shared 1660 of 6315 unique sequences. These 1660 sequences (the "core microbiota") contributed 66% of the reads. The overlapping OTUs contributed to 94% of the reads, while nearly all reads (99.8%) belonged to the shared higher taxa showing that the major proportion of bacterial sequences of unrelated healthy individuals is identical, supporting the concept of a core microbiota at health (Zaura *et al*., 2009) (Figure 4.2).

In another study, the salivary microbiota from five adults was analyzed at three time-points ranging within a 29-day period and showed subject-specific taxa profiles. The salivary bacterial community comparisons revealed that samples from the same individual were clustered and the salivary microbial community appeared to be stable over at least 5 days including samples from more distant time points (15-29 days). These results point to the persistence of subject-specific taxa whose frequency fluctuates between the time points showing the presence of a relative stability (Lazarevic *et al*.,2010).

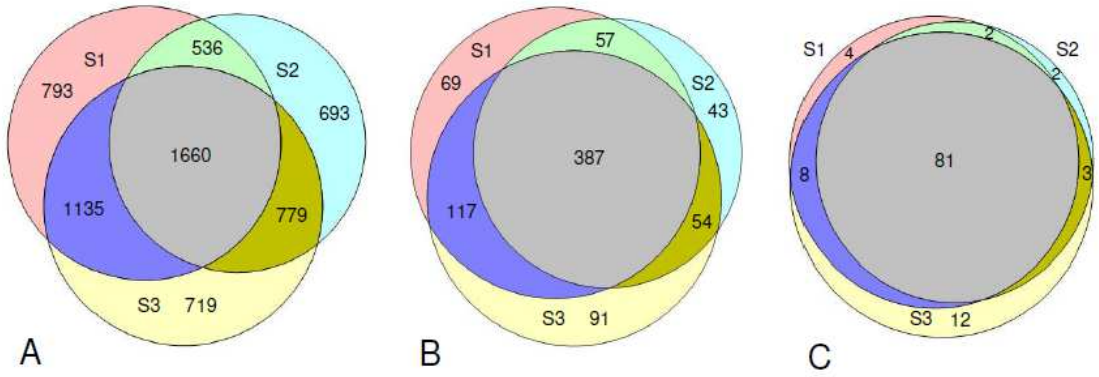

Figure 4.2. The extent of overlap of oral microbiota between three individuals. The extent of overlap between subjects S1 (pink circle), S2 (light blue circle) and S3 (yellow circle) at the level of **(A)** unique sequences, **(B)** OTUs clustered at 3% difference and **(C)** higher taxa (genus or more inclusive taxon). The data were obtained by combining all samples of the respective individual microbiota. The Venn Diagrams show that 26% of the unique sequences, 47% of the OTUs and 72% of the higher taxa were common (area in grey) to the three individuals (Zaura *et al*., 2009).

4.1.2 Metabolic pathways of oral bacteria

- **Carbohydrates and sugar alcohols**

Polysaccharides can be hydrolyzed into oligosaccharides, disaccharides, and monosaccharides by host and bacterial glycosidases. For example, host α-amylase hydrolyzes cooked starch into carbohydrates, which can then be incorporated and metabolized by oral bacteria.

Oral bacteria are capable of utilizing most dietary carbohydrates and some sugar alcohols. Incorporated carbohydrates and sugar alcohols are subjected to glycolysis via metabolic reactions catalyzed by constitutive and inducible enzymes. The bacterial sugar metabolism is known to be regulated by environmental factors, such as the availability of sugar and oxygen that change dynamically in the oral cavity. Saccharolytic bacteria including *Streptococcus, Actinomyces*, and *Lactobacillus* species degrade carbohydrates into organic acids via the Embden-Meyerhof-Parnas pathway resulting in dental caries (Takahashi, 2015).

- **Proteins, peptides, and amino acids**

Proteins can be degraded into peptides and amino acids by bacterial and host proteases and peptidases. In general, bacteria utilize amino acids for biosynthesis, but periodontal disease–and oral malodor–associated bacteria also ferment amino acids to produce energy. In the latter process, amino acids are deaminated and then converted into short-chain fatty acids with the production of adenosine triphosphate (ATP). Proteolytic amino acid–degrading bacteria, including *Prevotella* and *Porphyromonas* species, break down proteins and peptides into amino acids and degrade them further via specific pathways to produce short-chain fatty acids, ammonia, sulfur compounds, and indole/skatole, which act as virulent and modifying factors in periodontitis and oral malodour (Takahashi, 2015).

4.1.3 The oral microbiota is modulted by dietary habits and environmental factors

The organisms of the oral cavity differ among individuals reflecting diet, sampling times of day, geographical locations (Costalonga and Herzberg, 2014), age, gender, smoke, oral hygiene, use of antibiotics and genetic factors (Lazarevic *et al*.,2010). The members of the oral microbiota in health or disease appear to be selected depending on the dietary habits. Diet of the human host appears to shape the symbiosis of the microbiota residing on the mucosae and on the non-shedding surfaces of teeth. A simple example is the use of refined carbohydrates in the diet of modern humans. Sucrose contributes to increased risk of caries. Shifts in the diet of early human ancestors to modern foods have contributed to subtle changes in the oral microbial community (Costalonga and Herzberg, 2014).

Clearly, the environment and perhaps host genetics modify the oral microbiota. In South American Amerindians living in a remote village of the Amazon forest, who are less exposed to selective pressures of modern diet and are genetically less diverse than multiracial and multiethnic urban societies, show a more restricted oral mucosal microbiota than urban people. Despite the lower number of genera identified, the Amerindians harbor an increased frequency of previously unclassified *Proteobacteria* (Contreras et al., 2010). Remote Eskimo tribes were characterized by a low prevalence of periodontal diseases and caries (Russell *et al*., 1961) until modern diets were introduced (Kristoffersen *et al*., 1973), whereas Sri Lankans with diets essentially identical to early ancestors and in the absence of conventional oral hygiene measures had little caries but showed a range of incidence and severity of periodontitis as people aged in a landmark longitudinal study (Loe *et al*.,1986). Since the Sri Lankans employed no oral hygiene measures and enjoyed similar diets, host genetic polymorphisms within racially and ethnically similar populations may account for differences in acquisition or outgrowth of pathogens and the occurrence of disease. During the past few hundred years, the human mouth appears to have become a substantially less biodiverse ecosystem. Since higher phylogenetic diversity is associated with greater ecosystem resilience, the decreased diversity of the modern

oral environment may be associated with less resistance to perturbations and greater susceptibility to insertion of pathobionts or even true pathogens in the microbial community. Whereas this hypothesis has yet to be tested, the microbiota of different ecological niches within the oral cavity may reflect greater or less stability over time (Costalonga and Herzberg, 2014).

4.1.4 Cross-talk between oral microbiota and immunity

The gingival sulcus is lined by a non-keratinized, stratified squamous epithelium that is in constant contact with bacteria and their products. As such, this epithelial barrier is integral to the maintenance of oral health and immune homeostasis (Ramage *et al*., 2016).

Gingival epithelium works in many ways for the protection of underlying connective tissue. First, it provides a physical barrier which does not allow microbes to invade while permitting selective transaction with oral environment. Second, upon interaction with microbes, it secretes cytokines as well as chemokines to activate the influx of neutrophils and other immune cells into the sulcular area. Third, the gingival epithelium has been found to be source of epithelial antimicrobial peptides (EAP). These EAPs are considered to be important for the innate immunity of the host. These peptides are known to possess a wide spectrum of antimicrobial activity acting against Gram-positive and Gram-negative bacterial species as well as yeast and some viruses. Thereby, EAPs have the potential to prevent various oral diseases of microbial origin such as periodontitis, dental caries, candidiasis, and herpetic gingivo stomatitis (Hans and Hans, 2014).

Several families of antimicrobial peptides have been identified in oral cavity, which includes α-defensins, β-defensins, calprotectin, adrenomedullin, histatins, and cathelicidin. Of these, α-defensins are of non epithelial origin, with their major source being the neutrophils migrating into the gingival sulcus as primary host response, whereas histatins are secreted in saliva, produced by parotid and submandibular salivary gland duct cells. The EAPs work in tandem with the salivary antimicrobial agents such as histatins, immunoglobulins, and lysozyme to

strengthen first line of host defence. These antimicrobial peptides are expressed in oral epithelium constitutively and are inducible; thus, they have both functions, of surveillance and of host defence (Hans and Hans, 2014).

The outer membrane of Gram-negative bacteria consists of lipopolysaccharide (LPS). This is an amphipathic molecule that can be divided structurally in three parts: (a) the O-polysaccharide (or O-antigen), (b) the core polysaccharide, and (c) the lipid A. The O-antigen is the outmost part of LPS expressed on bacteria and therefore is the major antigen targeted by host antibody responses. LPS from Gram-negative bacteria is well known for its ability to induce a wide range of proinflammatory responses. Specifically, LPS can stimulate macrophages/ monocytes to produce pro-inflammatory cytokines, such as interleukin-1β (IL-1β), tumour necrosis factor-α (TNF-α), interleukin-6 (IL-6), interferon- γ (IFN-γ), IL-12, IFN inducible protein-10 (IP-10), chemotactic cytokines, like monocyte chemotactic protein-5 (MCP-5), IL-8, macrophage inflammatory protein (MIP-1α) and MIP-2, prostaglandin E2 (PGE2), and nitric oxide (NO) (Madianos *et al*., 2005).

Interleukin (IL)-8 mRNA expression was investigated in human dental pulp fibroblast cultures after stimulation with LPS prepared from *Prevotella intermedia* (Nagaoka *et al.*,1996), *Porphyromonas gingivalis* (Tamura *et al.*, 1992) and inflammatory cytokines. The expression of IL-8 mRNA and the release of IL-8 induced by *P. intermedia and P. gingivalis* LPS were detected in pulpal fibroblast cultures, suggesting that pulpal fibroblasts are immunoresponsive cells and can elaborate IL-8 upon stimulation with *P. intermedia and P. gingivalis* LPS (Nagaoka *et al.*,1996; Tamura *et al*., 1992).

Perturbations in the microbial community can be caused by growth of microorganisms such as *P. gingivalis*, which can alter the nutrient foundation of the niche and disrupt the equilibrium between symbionts and pathobionts (Costalonga and Herzberg, 2014).

Despite considerable recent attention to the composition of the human microbiota and microbiome, the mechanisms underlying complex host bacterial and interbacterial interactions that lead to polymicrobial inflammatory diseases remain poorly defined. An attractive model to address this issue is periodontitis, an oral inflammatory disease induced by a multispecies biofilm that is readily accessible for investigation (Hajishengallis *et al*., 2011).

4.1.5 Future research into the functions of the oral microbiota

It is difficult to measure bacterial metabolic activity, particularly in the oral microbiota, due to the small sample sizes involved; however, recent advances in metabolomic technology have made it possible to analyze the levels of various types of metabolites in small samples. Comprehensive analyses of metabolites (metabolome analysis or metabolomics) can provide insights into the metabolic functions of the oral microbiota. Together with comprehensive analyses of the mRNA molecules present within the oral microbiome (metatranscriptome analysis), the metabolomic approach might make it possible to obtain an overview of the metabolic activity of the oral microbiota and its relationship with oral microbiota-associated oral diseases (Takahashi, 2015).

4.2 Aim of the project

"An altered oral microbiota is associated with IL-8 production status of gingival epithelial cells in healthy individuals"

Understanding changes in the oral microbiota at the early stages of periodontitis and dental caries, the most prevalent chronic oral diseases, would allow diagnosis and treatment before the appearance of periodontal pockets or dental hard tissue loss (Zaura *et al*., 2009).

This study aimed at establishing associations of nutrition, oral hygiene habits and basal release of IL-8 from gum ephitelial cells with the oral bacterial community to identify indicator OTUs that might predict onset of oral inflammation related to diseases. For this purpose, we investigated IL-8 release from the gum epithelial cells (GECs) and the oral microbiota profiles from 21 healthy participants. We measured the basal and endotoxin-induced IL-8 release from the GECs over 6 h. Whereas the oral microbiota is influenced by diet and environmental factors (Costalonga and Herzberg, 2014), we further evaluated the correlations between nutritional and oral hygiene habits in regard to the bacterial community. Finally, in order to identify bio-markers in the oral microbiota community, we performed an indicator species analysis associated with the release of IL-8 in the GECs. These indicators may open the possibility to identify bio-markers for the early onset of oral inflammation.

4.3 PRELIMINARY DATA

4.3.1 EXPERIMENTAL DESIGN

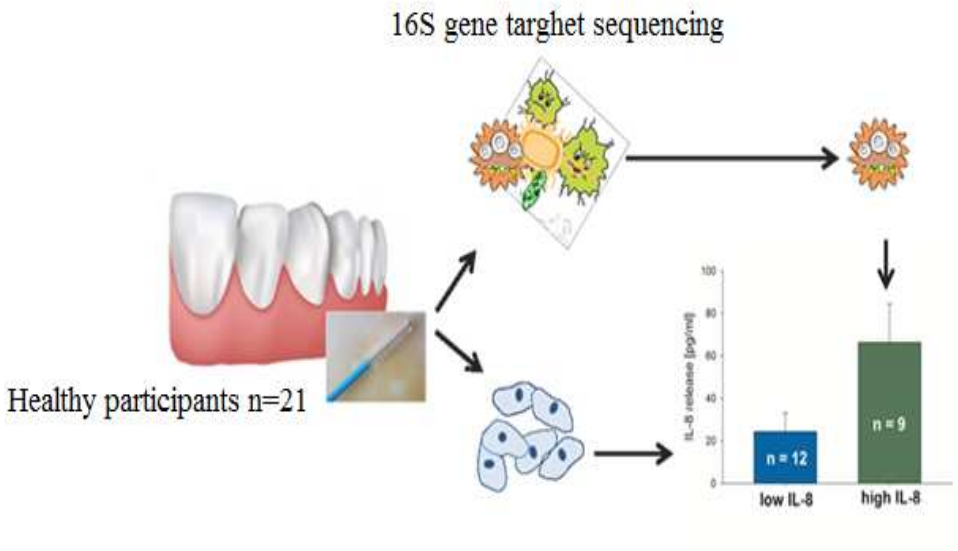

Figure 4.3. Gum epithelial cells (GECs) were sampled from 21 healthy participants. Bacterial DNA was extracted and sequenced. IL-8 release from GECs over 6 h was measured, as well as IL-8 release after 6 h incubation with bacterial endotoxins. Basal and endotoxin-induced IL-8 release over 6 h, as well as nutritional and oral hygiene habits were analyzed in regard to the bacterial community.

4.3.2 MATERIALS AND METHODS

Study population and questionnaire

21 healthy participants (13 female, 8 male) between the ages of 22 and 55 were recruited for the study. Exclusion criteria were pregnancy, smoking and antibiotic therapy in the last three months. Participants signed an informed consent and were asked to complete a questionnaire including general information, eating and drinking habits, as well as personal oral hygiene and medication prior to enrolling in the study (Table 4.1). All participants self-reported to be free of oral diseases.

Table 4.1. Factors considered in the questionnaire

general	nutrition	oral hygiene	medication
age	tea[a,b]	toothpaste	hormones[g,*]
height	coffee[a]	mouthwash[f,*]	pain killers[h,*]
weight	meat[c]	flossing[f,*]	
gender	beer[c]	chewing gum[f,*]	
allergies*	red wine[d]		
	white wine[d]		
	fruits[e]		
	sweets[c]		

Legend: a) per day [L], b) black, green and herbal tea, c) per week [g] or [L], d) per month [L] ,e) portions per week, f) >1 per week, g) oral contraceptives, hormone replacement therapy, h) oral intake in the last 30 days; *categories yes/no

Collection of GECs and bacteria

Participants were asked to abstain from brushing their teeth and eating breakfast in the morning of GEC collection. Material (cells and bacteria) were collected by the participants themselves by thoroughly brushing the upper and lower outer gums using three sterile brushes (Praxisdienst, Longuich, Germany). Brushes were then rinsed in 7.2 ml of DMEM containing 10% fetal bovine serum (FBS, Thermo Scientific, Waltham, MA USA) and 8 mM Glutamine. After thoroughly resuspending the collected material, 1 ml of suspension was centrifuged at 16,000xg for 7 minutes at 4 °C and the supernatant was removed. The pellet was then flash-frozen in liquid nitrogen and kept at -80 °C until DNA extraction.

***Ex vivo* incubation of GECs**

Epithelial cells were counted, the cell suspension aliquoted into three 15 ml tubes, centrifuged for 5 min at 400xg at room temperature and re-suspended in fresh medium to a final concentration of 150,000 living cells/ml, as determined by trypan blue exclusion test. Two different LPS (EC-stock 1 mg/ml ddH_2O from Sigma-Aldrich and PG-stock 1 mg/ml ddH_2O, euBio, Vienna, Austria) were added to the respective aliquots for final concentrations of 10 µg/ml LPS. The third aliquot was left without any addition for determination of basal levels of IL-8. Cells were incubated for 6 h in triplicate in 24-well plates in an incubator at 37°C and 5% CO_2. After incubation, pH measurements of all three incubations were done with pH strips, and the mean pH of three measurements was used for analysis (interval 0.5 units).

Measurement of IL-8

After 6 h incubation, supernatants of the 24-well plates were collected, centrifuged at 16,000 x g for 10 min at 4°C and two aliquots per well were stored at -80 °C further analysis. Basal IL-8 levels after 6 h incubation, IL-8 levels after incubation with 10 µg/ml EC-LPS for 6 h (ecLPS) and IL-8 levels after incubation with 10 µg/ml PG-LPS for 6 h (pgLPS) were determined in the

supernatant by ELISA (Merck Millipore, Darmstadt, Germany), following the manufacturer's instructions.

DNA extraction, preparation of 16s gene target amplicons libraries and sequence analysis

DNA was extracted from samples using a phenol–chloroform protocol with bead-beating and precipitated with 0.1 volume of 3M Na-Acetate and 0.6 volumes of ice-cold isopropanol (Griffiths *et al*., 2000). DNA was subjected to a two-step PCR amplification targeting the 16S rRNA gene using a forward primer S-D-bact-0341-b-S-17 (5'-CCTACGGGNGGCWGCAG-3') and a reverse primer S-D-bact-0785-a-A-21 (5'-GACTACHVGGGTATCTAATCC-3'). The first PCR reaction was performed in triplicate with 25 cycles. The PCR products were then pooled and submitted to a second step PCR of 10 cycles with the addition of 8 nt sample-specific barcode sequence (Herbold *et al*., 2015). The barcoded amplicons were purified after the second step with ZR-96 DNA Clean-up Kit (Zymo Research, USA) and quantified using the Quant-iT PicoGreen dsDNA Assay (Invitrogen, USA). An equimolar library was constructed by pooling samples, and the resulting library was sequenced on the Illumina MiSeq platform at Microsynth AG (Balgach, Switzerland). Sequence data were sorted into libraries using the 8 nt sample-specific barcode and primer using a custom-made in-house script, quality-filtered according to the Earth Microbiome Project guidelines, and paired-end reads were concatenated (Bokulich *et al*., 2013). Reads were then clustered into species-level operational taxonomic units (OTUs) of 97% sequence identity, checked for chimeras using USEARCH, and taxonomically classified using the Ribosomal Database Project näive Bayesian classifier (Wang *et al*., 2007). Sequence data has been deposited in the NCBI Sequence Read Archive under SRP075956.

Data Analysis

IL-8 data analysis

Data were analyzed using SigmaPlot 11.0 (SystatSoftware, USA). Correlations of basal IL-8 values and metric questionnaire variables were done with Spearman Rank correlations, comparisons of two groups were done using Student's t-test. In case of not normally distributed data, comparisons between two groups were done using Mann-Whitney Rank Sum test. A p-value ≤0.05 was considered significant. For analysis of the response to stimulation with LPS, participants with relative IL-8 values lower than 100% (as determined by LPS-treated over basal IL-8 levels) after stimulation were designated as "non-responders", while participants with relative IL-8 values over 100% after stimulation with LPS were designated as "responders".

Microbiota Analysis

Statistical analysis was performed using the statistical software R (https://www.r-project.org/). To avoid biases related to uneven library depth, sequencing libraries were subsampled to a number of reads smaller than the smallest library (4,500 reads). Significant factors were evaluated using permutational multivariate analysis of variance (perMANOVA) and ordination was performed using redundancy analysis (RDA) in the vegan package in R version 1.17-4 (Oksanen *et al*., 2010). Alpha diversity metrics were calculated using the vegan package and statistical differences in alpha diversity was performed using the Student's t-test. Variables were expressed as mean ± SD and a *p*-value ≤0.05 was considered significant. Indicator species analysis was carried out using the indicspecies package (De Caceres *et al*., 2009).

4.3.3 RESULTS

Basal IL-8 levels

Ex vivo incubated GECs showed a release of IL-8 into the supernatant of 9.9 to 98.2 pg/ml after 6 h, with a mean value of 42.4 pg/ml for all participants (n = 21, tr = 3). In order to gain further insight into the differences in basal IL-8 release, while maintaining sufficient group sizes for indicator OTUs analysis, participants were divided into two groups with n = 12 (designated 'low IL-8') and n = 9 (designated 'high IL-8'), based on the residuals analysis, as determined by positive and negative residual values (Figure 4.4A). Both groups were normally distributed as determined by Shapiro-Wilk normality testing ($P_{low\ IL\text{-}8} = 0.974$, $P_{high\ IL\text{-}8} = 0.525$) and QQ-plots (Figure 4.4B).

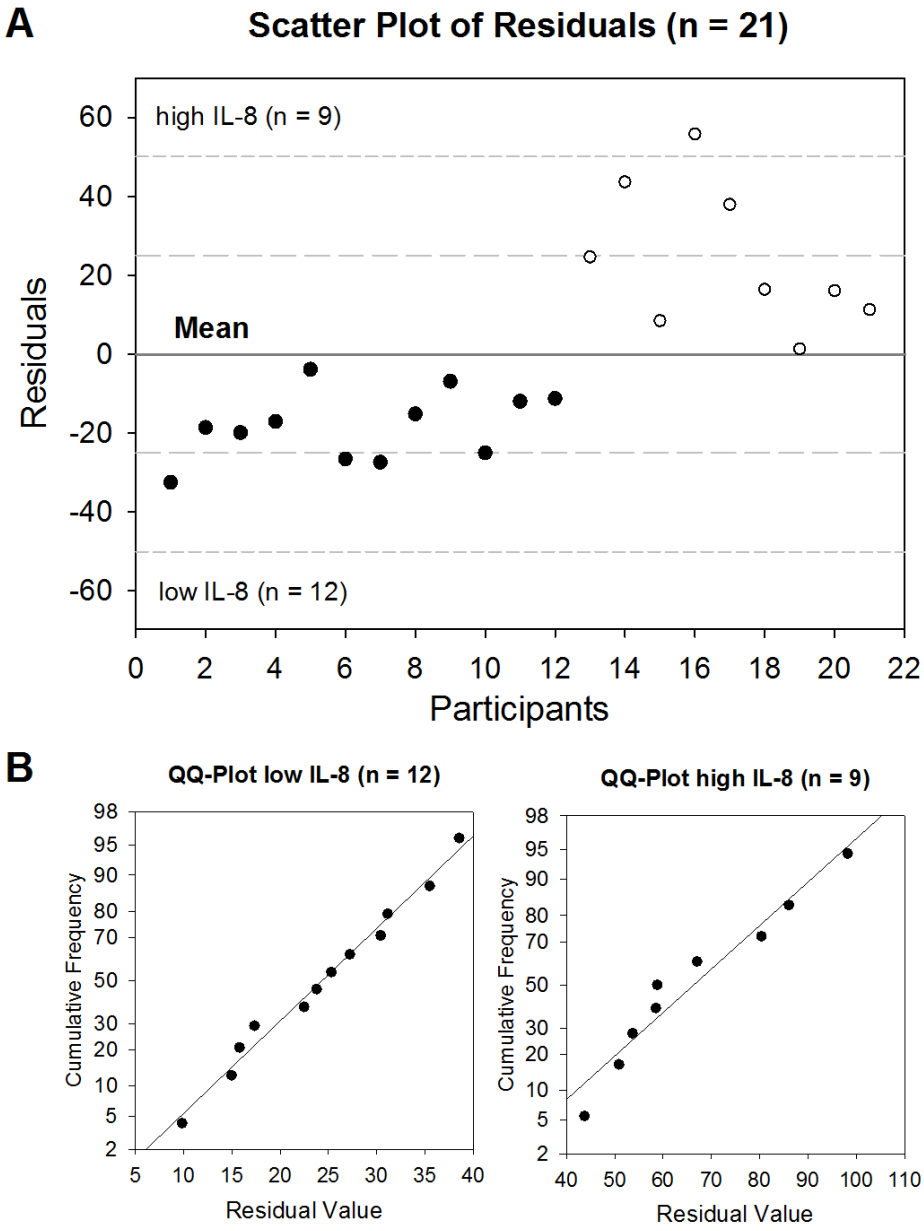

Figure 4.4. (A) Scatter plot of residuals of all participants (n = 21). The solid line represents the mean value, the medium dashed line the specification level of mean ± 1 SD, the short dashed line the specification level of mean ± 2 SD. **(B)** QQ-Plots for low IL-8 group (n = 12) and high IL-8 group (n = 9).

Correlations of basal IL-8 and metric questionnaire data (n = 21)

Statistical analysis for the questionnaire data was done with all participants (n = 21). The correlation of basal IL-8 levels with all metric parameters of the questionnaire (Table 4.2) showed a positive correlation (R = 0.477) with the pH of the supernatant (p = 0.029), as well as the consumption of red wine (R = 0.457, p = 0.037) and white wine (R = 0.485, p = 0.026).

Table 4.2. Spearman rank correlation between basal IL-8 levels and questionnaire parameters. a p-value ≤ 0.05 was considered significant.

IL-8 vs	Corr Coeff n=21	p-value n=21
age	0.104	0.649
BMI	-0.0286	0.899
pH	0.477	**0.029***
tea	0.275	0.223
coffee	-0.109	0.633
meat	-0.0939	0.682
beer	0.0305	0.895
red wine	0.457	**0.037***
white wine	0.485	**0.026***
fruits	0.107	0.637
sweets	-0.150	0.509

Pairwise comparison of basal IL-8 and nominal questionnaire data

For pairwise comparison, toothpaste ingredients were differentiated (no/yes) by the addition of zinc, film formers (methyl vinyl ether/maleic anhydride copolymer) and plant extracts (*chamomilla*, *mentha*, *salvia*, *myrrha*, *krameria triandra*). Pairwise comparison of basal IL-8 levels with nominal data for all participants (n = 21) showed no differences in basal IL-8 levels concerning gender, allergies, the use of floss, mouthwash, the consumption of chewing gum, the intake of hormones (only women) and pain killers (Table 4.3).

Table 4.3. Analysis of basal IL-8 levels regarding nominal questionnaire data. Additionally, the factors tea, white wine, red wine and beer were also categorized with yes/no, and sample sizes of compared groups (Student's t-test, Mann-Whitney Rank Sum test) are stated in parentheses next to calculated p-values; a p-value ≤0.05 was considered significant.

Factor (no/yes)	**group sizes (p-value)**
gender (f/m)	13 vs 8 (0.447)
allergies	13 vs 8 (0.980)
toothpaste ingredients	
zinc	12 vs. 9 (0.382)
plant extracts	17 vs 4 (**0.046***)
filmformer	15 vs 6 (0.791)
mouthwash	13 vs 8 (0.262)
flossing	8 vs 13 (0.753)
chewing gum	9 vs 12 (0.386)
tea	13 vs 8 (0.139)
white wine	10 vs 11 (**0.032***)
red wine	12 vs 9 (0.082)
beer	9 vs 12 (0.370)
hormones	5 vs 8 (0.195)
pain killers	8 vs 13 (0.525)

The presence of zinc and film formers in the toothpaste reported by participants did not have an influence on basal IL-8 levels, but for plant extracts, pairwise comparison resulted in $p = 0.046$, with mean values of 47.6 ± 24.5 pg/ml ($n = 17$) in the absence, and 20.2 ± 12.6 pg/ml ($n = 4$) in the presence of plant extracts in the toothpaste, respectively. Using a nominal dataset for the consumption of tea, beer, white and red wine (no or yes), a difference was found between white wine drinkers, and non-white wine drinkers ($p = 0.032$), with mean values of basal IL-8 for non-white wine drinkers ($n = 10$) and white wine drinkers ($n = 11$) were 29.5 ± 13.7 pg/ml and 54.1 ± 27.8 pg/ml, respectively. The observed significant correlation in basal IL-8 levels for red wine consumption (Table 4.2) did not occur after nominal categorization of data ($p = 0.082$).

The oral microbiota composition

The predominant bacterial phyla (in % abundance) in gum brushes were *Firmicutes* (70.5 ± 17.2; mean ± SD), followed by *Proteobacteria* (12.2 ± 10.7; mean ± SD), *Actinobacteria* (6.6 ± 4.5; mean ± SD), *Bacteroidetes* (6.1 ± 6.5; mean ± SD), *Fusobacteria* (2.5 ± 3.1; mean ± SD) and Candidate division TM7 (1.1 ± 1.9; mean ± SD) (Figure 4.5A). The most dominant family detected was *Streptococcaceae* (59.3 ± 21.3; mean ± SD) (Figure 4.5B), which was represented at the genus level by *Streptococcus* (59.3 ± 21.3; mean ± SD) (Figure 4.5C).

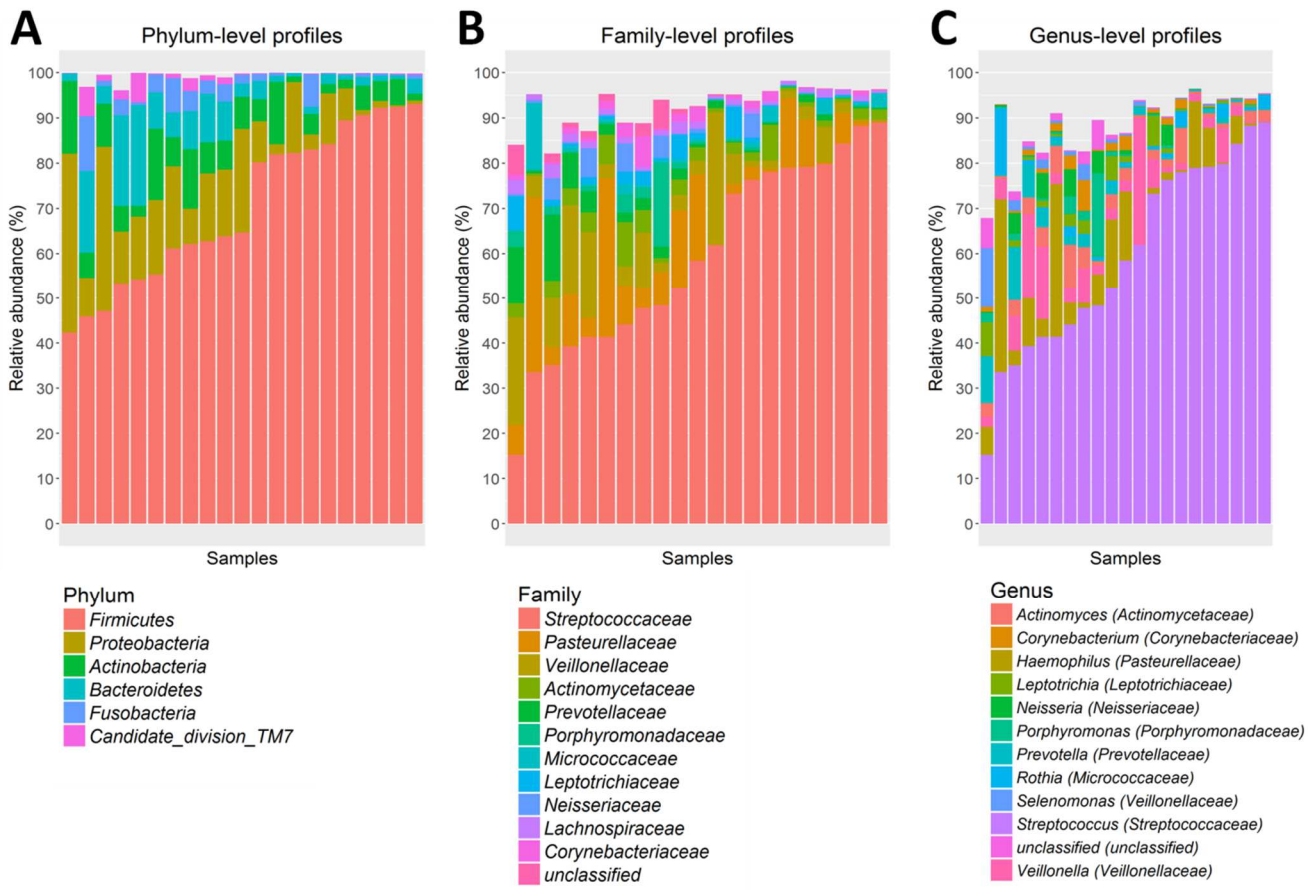

Figure 4.5. Abundant bacterial taxa from gum brushes. **(A)** Phylum, **(B)** family and **(C)** genus-level taxon profiles are shown. Abundant taxa, defined as having a mean relative abundance of >1%, are shown.

Alpha diversity

Oral microbiota richness was not significantly different between low and high basal IL-8 levels (observed species: p=0.534; Chao1 estimated richness: p=0.163). Likewise, alpha diversity metrics, which take into account both community richness and evenness, were not significantly different (Shannon: p=0.449; inverse Simpson p=0.895).

Associations of oral microbiota with nutrition and oral hygiene habits

The composition of the oral microbiota was associated with nutrition and oral hygiene habits at the OTU level as well as taxonomic levels from genus to phylum, with significant associations with basal IL-8 levels, gender, BMI, allergies, flossing habits, chewing gum use, and consumption of tea, meat, beer, white wine, and sweets (perMANOVA; $p<0.05$, Table 4.4). We performed redundancy analysis (RDA) considering these significant parameters to visualize these associations. RDA ordination revealed a strong correlation between basal IL-8 levels and meat consumption, but not for tea, floss habits and allergies (Figure 4.6).

Table 4.4. perMANOVA analysis performed at every taxonomical level. Significant nutritional and oral hygiene habits are shown.

Parameters	Taxonomical level	p-value
IL-8	OTU	0.016
tea	OTU	0.007
	Phylum	0.001
	Family	0.041
meat	OTU	0.005
	Phylum	0.018
allergies	OTU	0.033
flossing	OTU	0.010
	Phylum	0.015
gender	OTU	0.058
	Phylum	0.014
BMI	Phylum	0.005
	Family	0.050
beer	Phylum	0.007
white wine	Phylum	0.001
	Family	0.009
	Genus	0.022
sweets	Phylum	0.041
chewing gum	Phylum	0.007

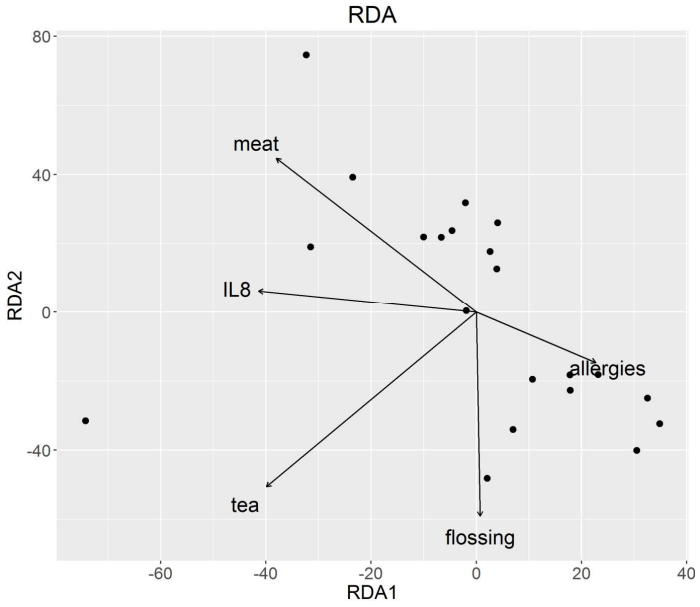

Figure 4.6. Redundancy analysis of oral microbiota at OTU level. Parameters significant at OTU level in the perMANOVA analysis were plotted and are represented by arrows. The direction of the arrows shows the association between variables, in this case with meat and IL-8.

Stimulation of oral GECs with 10 µg/ml LPS from EC and PG

*Ex vivo c*hallenge of brushed cells with EC- and PG-LPS did not significantly affect basal IL-8 levels, with means for IL-8, ecLPS and pgLPS of 42.4 ± 25.0 pg/ml, 39.2 ± 22.3 pg/ml and 40.7 ± 24.1 pg/ml, respectively (Table 4.5). Also, for the earlier designated low IL-8 (n = 12) and high IL-8 (n = 9) groups, no differences in absolute basal IL-8 levels compared to levels after treatment with EC- and PG-LPS were found. In the low IL-8 group, the absolute mean values for IL-8, ecLPS and pgLPS were 24.4 ± 8.8 pg/ml, 24.1 ± 8.5 pg/ml and 24.2 ± 9.6 pg/ml, respectively. Absolute means for high IL-8 group were 66.4 ± 18.1 pg/ml, 59.3 ± 18.5 pg/ml and 62.8 ± 19.2 pg/ml for IL-8, ecLPS and pgLPS, respectively. On relative levels (ecLPS/pgLPS over basal IL-8 in percent), differences to control (100%) were found in the high level ecLPS group with an unexpected decrease in IL-8 levels of -10.6 ± 16.1 % (p = 0.038) whereas no other group showed significant alterations in IL-8 release levels.

In order to prevent overinterpretation of data, release data after challenge with EC-LPS were excluded from indicator species analysis.

Table 4.5. p-values for pairwise comparisons of IL-8 on absolute [pg/ml] and relative [LPS/basal IL-8 %] levels for all participants (n = 21), low IL-8 (n = 12) and high IL-8 (n = 9) groups after *ex vivo* stimulation of oral GECs with EC LPS (10 µg/ml) or PG LPS (10 µg/ml) for 6 hours. a p-value ≤0.05 was considered significant.

	IL-8 absolute [pg/ml]		**IL-8 relative [LPS/basal IL-8 %]**	
	ecLPS p-value	**pgLPS p-value**	**ecLPS p-value**	**pgLPS p-value**
All participants (n = 21)	0.763	0.860	0.405	0.788
Low (<40 pg/ml, n = 12)	0.938	0.981	0.478	0.478
High(>40 pg/ml, n = 9)	0.425	0.659	**0.038***	0.178

To analyze whether the response to the *ex vivo* stimulation of GECs with EC-LPS and PG-LPS was dependent on basal IL-8 levels, data within the low and high IL-8 groups were divided into two categories (non-responders and responders) and a Fisher's exact test was done with the resulting counts for non-responders and responders (contingency table). This analysis resulted in a p-value of 0.065.

Indicator species based on IL-8 levels and PG LPS-induced IL-8 response in GECs

We used an indicator species analysis to determine the strength of the association between OTU abundances and the levels of basal IL-8 release (low IL-8, high IL-8) combined with responder/non-responder status from LPS challenge (expressed as LPS-induced IL-8/basal IL-8 in percent). We considered the abundances of individual OTUs and determined indicator species for the following groups: low IL-8, high IL-8 (irrespective of response to LPS challenge), as well as low IL-8 non-responders to PG-LPS, low IL-8 responders to PG-LPS, high IL-8 non-responders to PG-LPS, high IL-8 responders to PG-LPS. Statistically significant indicators for either single groups or combinations of groups were then identified.

We identified 11 indicator OTUs in total: one for "low IL-8", two for "high IL-8" and eight for "high IL-8" responders. Figure 4.7 shows an elevated abundance of indicator OTUs in the high IL-8 group, in particular for high IL-8 responders. OTU_216 (*Veillonellaceae*) and OTU_60 (*Neisseriaceae*) were the most abundant indicators for high IL-8 status.

Indicator for:	OTU_ID	Classification	Closest related species	Similarity
Low IL8	OTU_393	*Erysipelotrichaceae*	*Turicibacter sanguinis*	100% (427bp)
High IL8	OTU_216	*Veillonellaceae*	*Selenomonas* sp. oral taxon 478	100% (427bp)
	OTU_133	*Flavobacteriaceae*	*Capnocytophaga ochracea*	97% (422bp)
High IL8 responders	OTU_60	*Neisseriaceae*	*Neisseria bacilliformis*	100% (427bp)
	OTU_204	*Actinomycetaceae*	*Actinomyces dentalis*	97% (423bp)
	OTU_399	*Veillonellaceae*	*Selenomonas artemidis*	98% (427bp)
	OTU_202	*Erysipelotrichaceae*	*Eggerthia catenaformis*	76% (432bp)
	OTU_229	*Lachnospiraceae*	*Lachnospiraceae bacterium* oral taxon F15	90% (405bp)
	OTU_162	*Propionibacteriaceae*	*Propionibacterium propionicum*	99% (409bp)
	OTU_238	*Comamonadaceae*	*Ottowia* sp. oral taxon 894	96% (428bp)
	OTU_247	*Propionibacteriaceae*	*Propionibacterium propionicum*	97% (410bp)

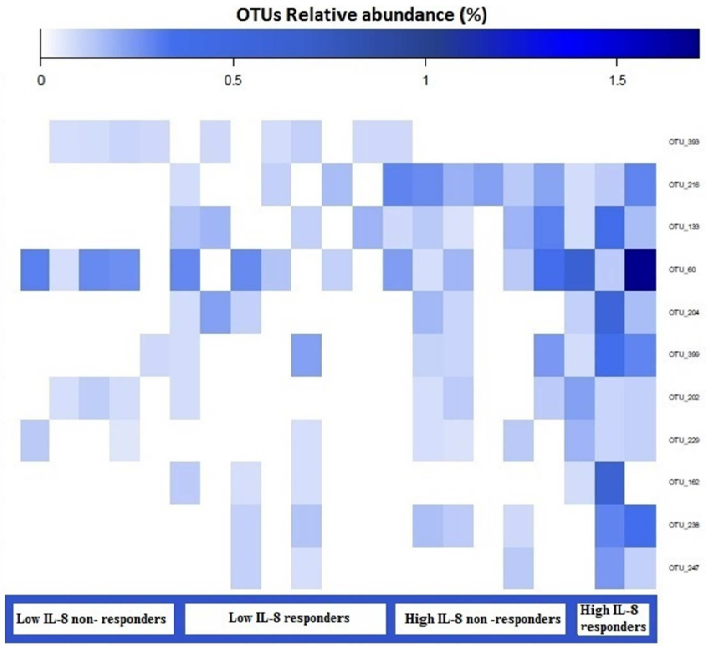

Figure 4.7. Dominant indicator OTUs are presented for pgLPS response with their relative abundance (as percent) for each sample. Each OTU is annotated with the closest reference sequence and sequence similarity performed with BLAST. The indicator species are grouped according to the condition for which they are an indicator for each combination. Each column of the heatmap represents a single sample.

4.3.4 DISCUSSION

This study aimed at establishing associations of nutrition, oral hygiene habits and basal release of IL-8 from GECs with the oral bacterial community to identify indicator OTUs that might predict onset of oral pathologies. Basal IL-8 levels obtained in this study were neither comparable to levels found in crevicular fluid of patients with periodontitis (over 90,000-fold higher), nor to levels obtained by stimulated salivary measurement (250 pg/ml) in healthy individuals, which is to be expected due to impaired oral health and different sampling method as compared to our study (Goutoudi *et al*., 2012; Navazesh *et al*., 1982). Comparable to our study, release levels of about 30-50 pg/ml IL-8 were found in primary sterile cultures of fibroblasts and periodontal ligament cells from tooth resections in healthy patients (Scheres *et al*., 2010). The basal levels of IL-8 in this study were found to positively correlate with pH (Table 4.2) but no significant association between pH and the bacterial community composition were found. Nevertheless, the positive correlation of the pH (values between 5.2 and 8.5) could be related to acidic or basic bacterial and cellular products released into the medium. It has to be considered that although the incubations were done without addition of antibiotics, the culture medium contains buffering salts, thus possibly biasing pH measurements. In our study, the bacterial community of the mouth was dominated by the phyla *Firmicutes,* followed by *Proteobacteria, Actinobacteria*, *Bacteroidetes*, *Fusobacteria* and Candidate division TM7, which is consistent with the oral "core" microbiota reported in previous studies (Lazarevic *et al*., 2010; Zaura *et al*., 2009). Nutrition and oral hygiene habits can influence the oral microbiota composition. Considering the latter, the presence of plant extracts in toothpaste showed an effect on basal IL-8 release (Table 4.3). This is in accordance with literature, as many medicinal plants that are used in toothpastes are anti-inflammatory, anti-bacterial, anti-fungal or astringent (Hotwani *et al*., 2014). The present analysis found a positive correlation of white and red wine consumption with basal IL-8 levels, and a significant difference between non-white wine

drinkers and white wine drinkers (Tables 4.2 and 4.3). Studies on alcohol consumption and the risk of periodontitis have reported variable findings. Susin et al. (Susin *et al*., 2015) reported that a higher alcohol intake related to the incidence of periodontitis in women, whereas no such correlations could be shown in men (n = 1115). On the other hand, Kongstad et al. (Kongstad *et al*., 2008) found a negative association of alcohol consumption and clinical signs of oral disease in men but not in women (n = 1521). In the present study, the separate analysis of gender subdivided by alcohol consumption would results in very small number of participants, which do not allow for such an analysis (n = 1-3 for some groups). It is surprising that red wine consumption was also positively correlated with IL-8 levels, as red wine is especially rich in polyphenols, molecules able to attenuate inflammatory markers in gastric inflammation as well as colonic epithelial cells (Mayo *et al*., 2000; Nunes *et al*., 2012). Considering our results of healthy participants, it is possible that moderate consumption of alcohol activates immune pathways indirectly exposed oral cells, leading to higher basal release levels of IL-8.

In our study, associations could be found between the composition of the oral microbiota and the use of chewing gum as well as oral hygiene habits like flossing. It is demonstrated that the use of xylitol gum decreased *Streptococcus mutans*, but did not change the salivary microbial composition (Söderling *et al*., 2015) and flossing habits reduce gingival inflammation removing some interproximal plaque (Berchier *et al*., 2008).

Moreover, we found associations between the composition of the oral microbiota and consumption of different foods and drinks such as meat, sweets, white wine, beer and tea.

Tea polyphenolic catechins, in particular epigallocatechin gallate and epicatechin gallate, can inhibit the growth of a wide range of gram positive and gram negative bacterial species with moderate potency. These molecules may be useful in the control of common oral infections, such as dental caries and periodontal disease (Taylor *et al*., 2005). In particular, catechin gallates inhibit growth and adherence to oral epithelial cells of *Porphyromonas gingivalis* (Sakanaka *et al*., 1996) and *Prevotella* spp. (Hirasawa *et al*., 2002).

As oral bacteria possess constitutive glucose transport systems, they are capable of utilizing most dietary carbohydrates and some sugar alcohols. Incorporated carbohydrates and sugar alcohols are subjected to glycolysis via metabolic reactions catalysed by constitutive and inducible enzymes. Polysaccharides can be hydrolysed into oligosaccharides, disaccharides, and monosaccharides by host and bacterial glycosidases. For example, host α-amylase hydrolyses cooked starch into carbohydrates, which can then be incorporated and metabolized by oral bacteria (Takahashi, 2015).

Interestingly, there was a strong association between oral microbiota, meat consumption and basal IL-8 levels (Figure 4.6). The association between oral microbiota and meat can be explained by the degradation activity of proteins into peptides and amino acids by bacterial proteases and peptidases in the oral cavity (Takahashi, 2015). Moreover, L-carnitine is an abundant compound in red meat and contains a trimethylamine structure. Intestinal microbiota metabolize choline and phosphatidylcholine to trimethylamine (TMA), which is further metabolized to trimethylamine-*N*-oxide (TMAO). TMAO directly activates inflammatory pathways, including nuclear factor-kB (NF-kB) signaling (Seldin *et al*., 2016) but which specific microbial species contribute to TMAO formation, have not been fully clarified (Koeth *et al*., 2013).

A connection between gut and oral microbiota was shown by Ding and Schloss (Ding *et al*., 2014), who demonstrated that stool samples showed a significant association with samples from within the oral cavity. The strongest association was with the community observed in saliva. Saliva was dominated by members belonging to the genera *Prevotella*, *Streptococcus*, *Pasteurellaceae*, *Veillonella*, and *Fusobacterium*; among these taxa, only *Prevotella* spp. were abundant in the stool communities. Ding and Schloss (Ding and Schloss, 2014) stated that although the oral and stool communities seemingly share little taxonomic resemblance, oral bacterial populations could possibly seed the gut. Those populations experience the ecological milieu of the gut to give rise to consistent community types by the time they reach the stool

(Ding and Schloss, 2014). If a connection between gut and oral bacterial communities is present, it might be possible that some similar metabolic activities are shared.

In established *in vitro* oral and immune cell lines, levels of inflammatory markers are up-regulated after stimulation with LPS from various bacterial strains (Ehrnhöfer-Ressler *et al*., 2013; Walker *et al*., 2013; Schueller *et al*., 2015). This is also true for primary sterile cultures of oral fibroblasts (Nagaoka *et al*., 1996). In our study, however, using freshly sampled epithelial cells and not using antibiotics, this kind of up-regulation was not established for IL-8 after 6 h of stimulation with PG-LPS. Muthukuru et al. (Muthukuru *et al*., 2005) found that in healthy tissues, the expression of TLRs is much lower than in periodontal disease, which would account for the absence of stimulation by their agonist LPS. Additionally, Scheres and Crielaard (2012) demonstrated that primary sterile gingival fibroblast cultures were desensitized to live *Prophyromonas gingivalis* after repeated contact with the pathogen. In this study, cells were cultured directly after sampling from the mouth, with live plaque bacteria still present. It is therefore very likely that GECs exhibited tolerance to EC- and PG-LPS, as observed in the experiments by Scheres and Crielaard (Scheres and Crielaard, 2012). The significant down-regulation of IL-8 release after stimulation of GECs with a non-oral-derived bacterium (*Escherichia coli*) only occurred in the high IL-8 group on relative levels. Muthukuru et al. (Muthukuru *et al*., 2005) demonstrated that a repeated challenge with LPS from *Escherichia coli* results in a significant down-regulation of TLRs on the cell-surface, thus impeding or reducing activation of IL-8 transcription and subsequent protein release. No association could be found between basal IL-8 levels and response to LPS challenge ($p=0.065$). However, the indicator species analysis yielded very interesting results (Figure 4.7). The indicator species that we identified are typical members of the oral cavity according to the Human Oral Microbiome Database (HOMD) (http://www.homd.org/) and some have also been associated with periodontal disease or other inflammatory pathologies. For example,

Capnocytophaga ochracea is present in the dental plaque biofilm of patients with periodontitis and it has been reported in several cases of periodontal disease (Hosohama-Saito *et al*., 2016). *Propionibacterium propionicum* was found in root canal-treated teeth with apical periodontitis (Siqueira *et al*., 2009), *Eggherthia catenaformis* was recently isolated in a patient with a dental abscess (Kordjian *et al*., 2015) and *Actinomyces dentalis* was isolated from pus of a human dental abscess (Hall *et al*., 2005). In particular, the genus *Actinomyces* houses several long-established human pathogens. Some species cause the inflammatory disease actinomycosis, whereas others are associated with various nonspecific inflammatory processes, or may play a role in the development of dental plaque and subsequent caries or periodontal diseases (Hall *et al*., 2005). Likewise, *Selenomonas* species dominated the diseased sites of subjects with generalized aggressive periodontitis. *Selenomonas sputigena* was the most frequently detected bacterial species whereas other species of *Selenomonas* were often present in high levels, including *Selenomonas noxia, Selenomonas* oral clone EW076, *Selenomonas* oral clone EW084 and *Selenomonas* oral clone CS002. Gonçalves et al. (Goncalves *et al*., 2012) revealed that *Selenomonas* phylotypes were frequently part of the subgingival microbiota of generalized aggressive periodontitis patients. Also Drescher et al. (Drescher *et al*., 2010) analyzed the topography of the subgingival biofilm by fluorescence *in situ* hybridization (FISH) and electron microscopy in subjects with generalized aggressive periodontitis, chronic periodontitis and periodontitis-resistant subject, revealing that *Selenomonas* spp. appeared in large numbers in all parts of the collected biofilms and seemed to make a relevant contribution to their structural organization.

In our study we found an association between basal IL8 levels and microbiota, suggesting a link between oral bacteria and inflammatory state. Moreover, a link was also observed between nutrition, personal oral hygiene with oral microbiota and IL8 levels.

The elevated abundance of some bacterial OTUs in high IL-8 responders indicating a higher inflammatory activity GEC, may be causally linked to stimulation by LPS. The indicator OTUs

that we identified in healthy subjects may hold promise as biomarkers for inflammatory status of the oral cavity as well as for risk of onset of oral pathologies. The validation of these biomarkers will require further studies with larger cohorts and designs where cohorts are followed until some develop disease so that we can evaluate their prognostic values.

CHAPTER 5:

CONCLUSIONS AND PERSPECTIVES

Conclusions and perspectives

It is becoming clear that an altered gut microbiota is associated with human pathologies like obesity, type 2 diabetes, cardiovascular disease, etc. as well as an altered oral microbiota is implicated in the onset of the periodontal disease and in the oral cavity inflammations. In the first study, we investigated the human gut microbiota composition in obese and normal-weight children revealing a clear alteration in the gut microbiota of obese children. In the third study, we verified an association with the oral microbiota communities, diet, hygiene habits and the release of the inflammatory marker IL-8 from gingival epithelial cells (GEC).

To move forwards, it will be essential to understand whether the gut microbiota is causally linked to host metabolism in humans. Prospective studies should be performed to determine whether the gut microbiota is altered before or after the onset of disease. To improve the understanding of how the microbiota affects the metabolism in humans, metagenomics, transcriptomics, proteomics and metabolomics data from key target tissues and the microbiota during various disease states and interventions should be combined to provide a map of co-occurrences. These data enable the formation of testable hypotheses that can be pursued in validated animal models, and they will form the foundation for specific interventions.

In the second project, we studied the role of polysaccharide and fiber privation in wild type mice to gain more insight into the role of diet on gut microbiota and we found an alteration in gut microbial communities and in the large intestine compartments and even in mucus layer and goblet cells structure.

Therefore, it will also be important to gain a more precise understanding of the foundational principles of the microbiota, such as the cross-sectional or longitudinal spatial organization of interactions between the host and its microbes in the intestine. The majority of studies in humans and mice rely on faecal samples, which provide some representation of what is occurring throughout the digestive

tract; however, aspects of microbial communities and host responses that are specific to the large intestine might be obscured by faecal sampling (Sonnenburg and Bäckhed, 2016).

Microbial metabolites probably act as mediators for the host metabolism and can be either beneficial (for example, butyrate) or detrimental like the Trimethylamine *N*-oxide (TMAO). Such molecules might therefore provide therapeutic approaches in which beneficial metabolites could be supplemented pharmacologically or the bacteria that produce them are developed into probiotics and receptor antagonists could be developed from detrimental metabolites (Sonnenburg and Bäckhed, 2016).

Controlled dietary interventions that document the utility of various supplements, probiotics, nutrients and foods in modulating aspects of the gut microbiota and human health are required. Prebiotics and probiotics have physiologic functions that contribute to gut microbiota's homeostasis, maintenance of a healthy body weight and control of factors associated with metabolic disorders through their effects on mechanisms controlling food intake, body weight and gut microbiota (Sanchez *et al*.,2015). Future treatments for human pathologies may be possible through the modulation of the gut microbiota using probiotics, prebiotics, and microbiota transplants. A better understanding of dietary effects on the microbiota may allow individualized nutritional recommendations and guide food production and distribution. The microbiota may change the future of health care, providing new diagnostic biomarkers of health and new pharmacologic agents derived from members of the human microbiota or their chemical products. The ability to accurately profile each individual's microbiota may open the possibility of personalized medical treatments and prevention strategies.

Clearly, there are still more questions than answers. However, the potential implications of this exciting and rapidly advancing field are staggering. The measurement of multiple aspects of individuality, including the microbiota, will provide insight into the characteristics of people who

respond beneficially to a given intervention and will pave the way for microbiota-focused precision nutrition.

BIBLIOGRAPHY

References

Aguilera, C.M., Olza, J., and Gil, Á. Genetic susceptibility to obesity and metabolic syndrome in childhood. *Nutr Hosp*, 2013, *28*:44-55.

Ahrne, S., and Johansson Hagslatt, M.L. Effect of Lactobacilli on paracellular permeability in the gut. *Nutrients* 2011, *3*:104-117.

Alm, E. W., Oerther, D. B., Larsen, N., Stahl, D. A., Raskin, L. The oligonucleotide probe database. *Appl Environ Microbiol* 1996, *62*: 3557-9.

Amann, R. I., Binder, B. J., Olson, R. J., Chisholm, S. W., Devereux, R. and Stahl, D. A. Combination of 16S rRNA-targeted oligonucleotide probes with flow cytometry for analyzing mixed microbial populations. *Appl Environ Microbiol* 1990 *56*: 1919-1925.

Armougom, F., Henry, M., Vialettes, B., Raccah, D., and Raoult, D. Monitoring bacterial community of human gut microbiota reveals an increase in *Lactobacillus* in obese patients and methanogens in anorexic patients. *PLoS ONE* 2009, *4*:1-8.

Bäckhed, F., Ding, H., Wang, T., Hooper, L. V, Koh, G. Y., Nagy, A., and Gordon, J. I. The gut microbiota as an environmental factor that regulates fat storage. *Proc Natl Acad Sci USA* 2004, *101*: 15718–23.

Bäckhed, F., Manchester, J. K., Semenkovich, C. F., and Gordon, J. I. Mechanisms underlying the resistance to diet-induced obesity in germ-free mice, *Proc Natl Acad Sci USA* 2007, *104*:979-84.

Balamurugan, R., George, G., Kabeerdoss, J., Hepsiba, J., Chandragunasekaran, A.M., and Ramakrishna, B.S. Quantitative differences in intestinal *Faecalibacterium prausnitzii* in obese Indian children. *Br J Nutr* 2010, *103*: 335–8.

Berchier, C.E., Slot, D.E., Haps, S., and Van der Weijden, G.A. The efficacy of dental floss in addition to a toothbrush on plaque and parameters of gingival inflammation: a systematic review. *Int J Dent Hyg* 2008, *6*:265-79.

Bervoets, L., Van Hoorenbeeck, K., Kortleven, I., Van Noten, C., Hens, N., Vael, C., Goossens, H., Desager, K.N., and Vankerckhoven, V. Differences in gut microbiota composition between obese and lean children: a cross-sectional study. *Gut Pathog*, 2013, *5*:1-10.

Biasucci, G., Rubini, M., Riboni, S., Morelli, L., Bessi, E., & Retetangos, C. Mode of delivery affects the bacterial community in the newborn gut. *Early Hum Dev*, 2010, *1*:13–15.

Bibiloni, R. Rodent models to study the relationships between mammals and their bacterial inhabitants. *Gut Microbes*, 2012, *3*: 536–543.

Bokulich, N.A., Subramanian, S., Faith, J.J, Gevers, D., Gordon, J.I., Knight, R., *et al*. Quality-filtering vastly improves diversity estimates from Illumina amplicon sequencing. *Nat Methods* 2013, *10*:57-59.

Bowcutt, R., Forman, R., Glymenaki, M., Carding, S. R., Else, K. J., Bowcutt, R., and Sci, F. L. Heterogeneity across the murine small and large intestine. *World J Gastroenterol* 2014, *20*:15216–15232.

Cani, P.D., Dewever, C., Delzenne, N.M. Inulin-type fructans modulate gastrointestinal peptides involved in appetite regulation (glucagon-like peptide-1 and ghrelin) in rats. *Brit J Nutr* 2004, *92*: 521–526.

Cani, P. D., Lecourt, E., Dewulf, E. M., Sohet, F. M., Pachikian, B. D., Naslain, D., and Delzenne, N. M. Gut microbiota fermentation of prebiotics increases satietogenic and incretin gut peptide production with consequences for appetite sensation and glucose response after a meal. *Am J Clin Nutr* 2009, *90*:1236–1243.

Chassard, C., Delmas, E., Robert, C., Lawson, P.A. and Bernalier-Donadille, A. *Ruminococcus champanellensis* sp. nov., a cellulose-degrading bacterium from human gut microbiota. *Int J Syst Evol Microbiol* 2012, *62*: 138–143.

Choquet, H. and Meyre, D. Genomic insights into early-onset obesity. *Genome Med* 2010, *36*: 2-12.

Contreras, M., Costello, E. K., Hidalgo, G., Magris, M., Knight, R., and Dominguez-bello, M. G. The bacterial microbiota in the oral mucosa of rural Amerindians. *Microbiology* 2010, *156*:3282–3287.

Costalonga, M., and Herzberg, M. C. The oral microbiome and the immunobiology of periodontal disease and caries. *Immunol Lett* 2014, *162*:22–38.

Daims, H., Brühl, A., Amann, R., Schleifer, K.H., and Wagner M. The domain specific probe EUB338 is insufficient for the detection of all Bacteria: Development and evaluation of a more comprehensive probe set. *System Appl Microbiol* 1999, *22*: 434-444.

Daims, H., Lucker, S., and Wagner, M. Daime, a novel image analysis program for microbial ecology and biofilm research. *Environ Microbiol*, 2006, *8*: 200–213.

Daims, H. Use of fluorescence in situ hybridization and the *daime* image analysis program for the cultivation-independent quantification of microorganisms in environmental and medical samples. *Cold Spring Harb Protoc* 2009, *4*:1-8.

David, L. A., Maurice, C. F., Carmody, R. N., Gootenberg, D. B., Button, J. E., Wolfe, B. E., Ling, A.V. *et al*. Diet rapidly and reproducibly alters the human gut microbiome. *Nature* 2014, *505*:559-562.

De Caceres, M., and Legendre, P. Associations between species and groups of sites: indices and statistical inference. *Ecology* 2009, *90*:3566-3574.

De Filippo, C., Cavalieri, D., Di Paola, M., Ramazzotti, M., Poullet, J. B., Massart, S., and Lionetti, P. Impact of diet in shaping gut microbiota revealed by a comparative study in children from Europe and rural Africa. *Proc Natl Acad Sci USA*, 2010, *107*:14691–6.

Derrien, M., Vaughan, E. E., Plugge, C. M., and Vos, W. M. De. *Akkermansia muciniphila* gen. nov., sp. nov., a human intestinal mucin degrading bacterium. *Int J Syst Evol Microbiol* 2004, *54*:1469

Despres, J., Forano, E., Lepercq, P., Comtet-marre, S., Jubelin, G., Chambon, C., *et al*. Xylan degradation by the human gut *Bacteroides xylanisolvens* XB1A T involves two distinct gene clusters that are linked at the transcriptional level. *BMC Genomics* 2016, *17*:1–14.

Dewhirst, F. E., Chen, T., Izard, J., Paster, B. J., Tanner, A. C. R., Yu, W., and Wade, W. G. The human oral microbiome. *J Bacteriol* 2010, *192*:5002–5017.

Drescher, J., Schlafer, S., Schaudinn, C., Riep, B., Neumann, K., Friedmann, A., Petrich, A., *et al.* Molecular epidemiology and spatial distribution of *Selenomonas* spp. in subgingival biofilms. *Eur J Oral Sci* 2010, *118*:466-474.

Dibaise, J.K., Zhang, H., Crowell, M.D., Krajmalnik-Brown, R., Decker, G. A. and Rittmann, B. E. Gut microbiota and its possible relationship with obesity. *Mayo Clin Proc*, 2008, *83*:460-469.

Ding, T., and Schloss, P., D. Dynamics and associations of microbial community types across the human body. *Nature* 2014, *509*, 357-360.

Donaldson, G.P., Lee, M.S. and Mazmanian, S.K. Gut biogeography of the bacterial microbiota. *Nat Rev Microbiol* 2015, *14*:20-32.

Eckburg, P. B., Bik, E. M., Bernstein, C. N., Purdom, E., Dethlefsen, L., Sargent, M., and Relman, D. A. Diversity of the human intestinal microbial flora. *Science* 2005, *308*: 1635–1639.

Earle, K.A., Billings, G., Sigal, M. R. Amieva, M.R., Huang, K.C., and Sonnenburg, J.L. Quantitative Imaging of Gut Microbiota Spatial Organization. *Cell Host and Microbe* 2015, *18*:1–11.

Ehrnhöfer-Ressler, M. M., Fricke, K., Pignitter, M., Walker, J. M., Walker, J., Rychlik, M., and Somoza, V. Identification of 1,8-Cineole, Borneol, Camphor, and Thujone as Anti-inflammatory Compounds in a Salvia officinalis L. Infusion Using Human Gingival Fibroblasts. *J Agric Food Chem* 2013, *61*: 3451-3459.

Ericsson, A. C., and Franklin, C. L. Manipulating the gut microbiota: Methods and challenges. *ILAR Journal*, 2015, *56*:205–217.

Franks, A.H., Harmsen, H.J., Raangs, G.C., Jansen, G.J., Schut, F., and Welling, G.W. Variations of bacterial populations in human feces measured by fluorescent in situ hybridization with group-specific 16S rRNA-targeted oligonucleotide probes. *Appl Environ Microbiol* 1998, *64*:3336–3345.

Fernandez, L. M. B., Lasa, J. S., and Man, F. Intestinal microbiota: its role in digestive diseases. *J Clin Gastroenterol*, 2014, *48*:657–666.

Green, J., and Bohannan, B. J. M. Spatial scaling of microbial biodiversity. *Trend Ecol Evol* 2006, *21*: 501-7.

Griffiths, R.I., Whiteley, A.S., O'Donnell, A.G., Bailey, M.J. Rapid method for coextraction of DNA and RNA from natural environments for analysis of ribosomal DNA- and rRNA-based microbial community composition. *Appl Environ Microbiol* 2000, *66*: 5488–5491.

Goldani, H. A.S., Bettiol, H., Barbieri, M. A., Silva, A. A.M., Agranonik, M., Morais, M.B., and Goldani, M.Z. Cesarean delivery is associated with an increased risk of obesity in adulthood in a Brazilian birth cohort study. *Am J Clin Nutr* 2011, *93*:1344–1347.

Goncalves, L. F. H., Fermiano, D., Feres, M., Figueiredo, L. C., Teles, F.R.P., Mayer, M.P.A., and Faveri, M. Levels of *Selenomonas* species in generalized aggressive periodontitis. *J Periodont Res* 2012, *47*:711-718.

Goutoudi, P., Diza, E., and Arvanitidou, M., Effect of Periodontal Therapy on Crevicular Fluid Interleukin-6 and Interleukin-8 Levels in Chronic Periodontitis. *Int J Dent* 2012, *2012*:1-8.

Gu, S., Chen, D., Zhang, J.N., Lv, X., Wang, K., Duan, L.P. *et al.* Bacterial community mapping of the mouse gastrointestinal tract. *PLoS ONE* 2013, *8*: 1-9.

Hajishengallis, G., Liang, S., Payne, M. A., Hashim, A., Jotwani, R., Eskan, M. A., and Curtis, M. A. Low-abundance biofilm species orchestrates inflammatory periodontal disease through the commensal microbiota and complement. *Cell Host and Microbe*, 2011, *10*:497–506.

Hall, V., Collins, M. D., Lawson, P. A., Falsen, E., and Duerden, B. I. *Actinomyces dentalis* sp nov., from a human dental abscess. *Int J Syst Evol Microbiol* 2005, *55*:427-431.

Hans, M., and Hans, V. M. Epithelial antimicrobial peptides : guardian of the oral cavity, *Int J Pept* 2014, 1-13.

Harmsen, H.J. M., Elfferich, P., Schut, F., and Welling G.W. A 16S rRNA-targeted Probe for Detection of Lactobacilli and Enterococci in faecal samples by fluorescent *in situ* hybridization. *Microb Ecol Health Dis* 1999, 11: 3–12.

Herbold, C.W., Pelikan, C., Kuzyk, O., Hausmann, B., Angel, R., Berry, D., and Loy, A. A flexible and economical barcoding approach for highly multiplexed amplicon sequencing of diverse target genes. *Front Microbiol* 2015, *6*:1-8.

Hirasawa, M., Takada, K., Makimura, M., and Otake, S. Improvement of periodontal status by green tea catechins using a local delivery system: a clinical pilot study. *J Periodontal Res* 2002, *37*:433–438.

Hollister, E.B., Riehle, K., Luna, R.A., Weidler, E.M., Rubio-Gonzales, M., Mistretta, T.A., *et al*. Structure and function of the healthy pre-adolescent pediatric gut microbiome. *Microbiome* 2015, *3*: 1-13.

Hosohama-Saito, K., Kokubu, E., Okamoto-Shibayama, K., Kita, D., Katakura, A., Ishihara, K. Involvement of luxS in biofilm formation by *Capnocytophaga ochracea*. *PLoS ONE* 2016, *11*, e0147114.

Hotwani, K., Baliga, S., and Sharma, K., Phytodentistry: use of medicinal plants. *J Complement Integr Med* 2014, *11*: 233-251.

How, K. Y., Song, K. P., Chan, K. G., and Caldwell, C. C. *Porphyromonas gingivalis* : An overview of periodontopathic pathogen below the gum line. *Front Microbiol* 2016, *7*:1–14.

Ijssennagger, N., Van der Meer, R., and Van Mil, S.W. Sulfide as a mucus barrier-breaker in inflammatory bowel disease? *Trends Mol Med* 2016, 22:190-9.

Ismail, N. A., Ragab, S.H., ElBaky, A.A., Shoeib, A.R.S., Alhosary, Y., and Fekry, D.. Frequency of *Firmicutes* and *Bacteroidetes* in gut microbiota in obese and normal weight Egyptian children and adults. *Arch Med Sci* 2011, *3*:501-507.

Johansson, M.E.V., Larsson, J.M.H., and Hansson, G.C. The two mucus layers of colon are organized by the MUC2 mucin, whereas the outer layer is a legislator of host–microbial interactions. *PNAS*, 2011, *108*: 4659–4665

Jakobsson, H.E., Rodríguez-Piñeiro, A.M., Schütte, A., Ermund, A., Boysen, P., Bemark, Mats., et al. The composition of the gut microbiota shapes the colon mucus barrier. *EMBO Rep* 2015. *16*: 164–177.

Jiménez, E., Marín, M.L., Martín, R., Odriozola, J.M., Olivares, M., Xaus, J., Fernández , L., and Rodríguez, J.M. Is meconium from healthy newborns actually sterile? *Res Microbiol* 2008, *159*:187-193.

John, G. K., and Mullin, G. E. The gut microbiome and obesity. *Curr Oncol Rep* 2016, *18*: 1-7.

Kalliomaki, M., Collado, M.C., Salminen, S. and Isolauri, E.. Early differences in fecal microbiota composition in children may predict overweight. *Am J Clin Nutr* 2008, *87*:534-538.

Karlsson, C.L.J., Önnerfält, J., Xu, J., Molin, G., Ahrné, S. and Thorngren-Jerneck, K. The Microbiota of the gut in preschool children with normal and excessive body weight. *Obesity*, 2012, *20*: 2257-2261.

Kim, Y. S., and Ho, S. B. Intestinal goblet cells and mucins in health and disease: Recent insights and progress. *Curr Gastroenterol Rep* 2010, *12*:319–330.

Kobyliak, N., Virchenko, O., and Falalyeyeva, T. Pathophysiological role of host microbiota in the development of obesity. *Nutr J* 2015, *15*:1-12.

Koenig, J. E., Spor, A., Scalfone, N., Fricker, A. D., Stombaugh, J., Knight, R., and Ley, R. E. Succession of microbial consortia in the developing infant gut microbiome. *Proc Natl Acad Sci USA* 2011, *108*: 4578–4585.

Koeth, R., A. , Wang, Z., Levison, B., S. , Buffa, J., A. , Org, E., Sheehy, B.T., *et al.*, Intestinal microbiota metabolism of l-carnitine, a nutrient in red meat, promotes atherosclerosis. *Nat Med* 2013, *19*:576-85.

Kongstad, J., Hvidtfeldt, U. A., Gronbaek, M., Jontell, M., Stoltze, K., and Holmstrup, P. Amount and type of alcohol and periodontitis in the Copenhagen City Heart Study. *J Clin Periodontol* 2008, *35*:1032-1039.

Kordjian, H. H., Schultz, J. D. J. H., Rosenvinge, F. S., Moller, J., and Pedersen, R. M. First clinical description of *Eggerthia catenaformis* bacteremia in a patient with dental abscess. *Anaerobe* 2015, *35*:38-40.

Koropatkin, N. M., Cameron, E. A., and Martens, E. C. How glycan metabolism shapes the human gut microbiota. *Nat Rev Microbiol* 2012, *10*: 323–335.

Kristoffersen, T., and Bang, G. Periodontal disease and oral hygiene in an Alaskan Eskimo population. *J Dent Res* 1973, *52*:791–6.

Lazarevic, V., Whiteson, K., Hernandez, D., François, P., and Schrenzel, J. Study of inter- and intra-individual variations in the salivary microbiot. *BMC Genomics* 2010, 11:1-11.

Li, H., Limenitakis, J. P., Ganal, S. C., and Macpherson, A. J. Penetrability of the inner mucus layer : who is out there ? *EMBO Rep* 2015, *16*:127–129.

Loe H, Anerud A, Boysen H, Morrison E. Natural history of periodontal disease in man. Rapid, moderate and no loss of attachment in Sri Lankan labourers 14 to 46 years of age. *J Clin Periodontol* 1986, *13*:431–45.

Louis, P., Hold, G. L., and Flint, H. J. The gut microbiota , bacterial metabolites and colorectal cancer. *Nat Rev Microbiol* 2014, *12*:661-72.

Macfarlane, S., and Macfarlane, G. T. Regulation of short-chain fatty acid production, *Proc Nutr Soc* 2003, *62*:67-72.

Madianos, P.N.,Bobetsis, Y.A., and Kinane, D.F. Generation of inflammatory stimuli : how bacteria set up inflammatory responses in the gingiva. *J Clin Periodontol* 2005,*6*:57-71.

Magrone, T., and Jirillo, E. Childhood obesity : immune response and nutritional approaches. *Front Immunol* 2015, *6*:1–13.

Manz, W., Amann, R., Ludwig, W., Vancanneyt, M., Schleifer, K. H. Application of a suite of 16S rRNA-specific oligonucleotide probes designed to investigate bacteria of the phylum *Cytophaga-Flavobacter-Bacteroides* in the natural environment. *Microbiology* 1996, *142*:1097–1106.

Martin, R., Natua, A.J, Amor, K.B., Knippels, L.M.J., Knol, J. and Garssen, J.. Early life: gut microbiota and immune development in infancy. *Benef Microbes* 2010, *1*: 367-382.

Martins dos Santos, V., Müller, M., and de Vos, W. M. (2010). Systems biology of the gut: The interplay of food, microbiota and host at the mucosal interface. *Curr Opin Biotechnol* 2010, *21*:539–550.

Mayo, K., Castagnino, C., Cheze, C., Vercauteren, J., De Mascarel, A., and Megraud, F. Amelioration of gastric inflammation by polyphenols from red wine: A mouse model using Helicobacter felis. *Gut* 2000, *47*, A61.

McCarville, J. L., Caminero, A., and Verdu, E. F. Novel perspectives on therapeutic modulation of the gut microbiota. *Therap Adv Gastroenterol* 2016, *9*:580–593.

Milani, C., Ferrario, C., Turroni, F., Duranti, S., Mangifesta, M., van Sinderen, D., and Ventura, M. The human gut microbiota and its interactive connections to diet. *J Hum Nutr Diet* 2016, *29*:539-46.

Montagne, L., Pluske, J. R., and Hampson, D. J. A review of interactions between dietary fiber and the intestinal mucosa , and their consequences on digestive health in young non-ruminant animals. *Anim Feed Sci Technol* 2003, *108*:95–117.

Mueller, N.T., Whyatt, R., Hoepner, L., Oberfield, S., Dominguez-Bello, M.G., Widen, E.M., *et al*. Prenatal exposure to antibiotics, cesarean section and risk of childhood obesity. *Int J Obes (Lond)* 2015, *39*: 665–670.

Muegge, B. D. Kuczynski, J., Knights, D., Clemente, J.C., González, A., Fontana, L., *et al.* Diet drives convergence in gut microbiome functions across mammalian phylogeny and within humans. *Science* 2011, *332*:970–974.

Muthukuru, M., Jotwani, R., and Cutler, C. W. Oral mucosal endotoxin tolerance induction in chronic periodontitis. *Infect Immun* 2005, *73*:687-694.

Nagaoka, S., Tokuda, M., Sakuta, T., and Taketoshi, Y. Interleukin-8 gene expression by human dental pulp fibroblast in cultures stimulated with prevotella intermedia lipopolysaccharide. *J Endod* 1996, *22*:9-12.

Nakamura, K., Sakuragi, N., Takakuwa, A., and Ayab T. Paneth cell α-defensins and enteric microbiota in health and disease. *Biosci Microbiota Food Health* 2016, *35*:57–67.

Nava, G. M., Friedrichsen, H. J. and Stappenbeck, T. S. Spatial organization of intestinal microbiota in the mouse ascending colon. *ISME J* 2011 5: 627–638.

Nava, G.M., Carbonero, F., Croix, J.A., Greenberg, E., and Gaskins, H.R. Abundance and diversity of mucosa-associated hydrogenotrophic microbes in the healthy human colon. *ISME J* 2012, *6*:57–70.

Navazesh, M., and Christensen, C. M., A comparison of whole mouth resting and stimulated salivary measurement procedures. *J Dent Res* 1982, *61*:1158-1162.

Ng, M., Fleming, T., Robinson, M., Thomson, B., Graetz, N., Margono, C., *et al*. Global, regional, and national prevalence of overweight and obesity in children and adults during 1980–2013: a systematic analysis for the global burden of disease study 2013. *Lancet* 2014, *384*: 766–81.

Nguyen,T.L.A., Vieira-Silva, S., Liston, A., and Raes, J. How informative is the mouse for human gut microbiota research ? *Dis Model Mech* 2015, *8*:1–16.

Nguyen, N., Warnow, T., Pop, M., and White, B. A perspective on 16S rRNA operational taxonomic unit clustering using sequence similarity. *npj Biofilms and Microbiomes* 2016, *2*: 1-8.

Nicholson, J.K., Holmes, E., Kinross, J., Burcelin, R., Gibson, G., Jia, W., and Pettersson, S. Host-gut microbiota metabolic interactions. *Science* 2012, *336*:1262-1267.

Nunes, C., Freitas, V., Barbosa, R. M., Almeida, L., and Laranjinha, J., Red wine protects intestinal epithelial cells from inflammation by activating the Nrf2 pathway and reinforcing tight junctions. *Free Radic Biol Med* 2012, *53*: S195.

Oksanen, J., Blanchet, F.G., Kindt, R., Legendre, P., O'Hara, R.B., Simpson GL *et al*. Vegan: community ecology package, 2010, R package version 1.17-4 (http:// cran.r-project.org/).

Ouwerkerk, J.P., de Vos, W.M., and Belzer, C. Glycobiome: Bacteria and mucus at the epithelial Interface. *Best Pract Res Cl Ga* 2013, *27*:25–38.

Pédron, T., Mulet, C., Dauga, C., Frangeul, L., Chervaux, C., Grompone, G., and Sansonetti, P.J. A crypt-specific core microbiota resides in the mouse colon. *mBio* 2012, *3*: 1-7.

Portela, D.S., Vieira, T.O., Matos, S.M.., de Oliveira, N.F., and Vieira, G.O. Maternal obesity, environmental factors, cesarean delivery and breastfeeding as determinants of overweight and obesity in children: results from a cohort. *BMC Pregnancy Childbirth* 2015, *15*:1-10.

Putignani, L., Del Chierico, F., Petrucca, A., Vernocchi, P., Dalla piccola, B. The human gut microbiota: a dynamic interplay with the host from birth to senescence settled during childhood. *Pediatr Res* 2014, *76*: 1-10.

Rajilic´-Stojanovic,´M., and. de Vos, W. M. The first 1000 cultured species of the human gastrointestinal microbiota. *FEMS Microbiol Rev* 2014, *38*:996–1047.

Ramakrishna, B. S. Role of the gut microbiota in human nutrition and metabolism. *J Gastroenterol Hepatol*, 2013 *28*:9–17.

Ramage, G., Df, L., Millhouse, E., Malcolm, J., Jose, A., Yang, J., and Dj, B. The epithelial cell response to health and disease associated oral biofilm models. *J Periodontal Res* 2016,1-9.

Reichert J. Illuminating the mammalian gut microbiota using metagenomic and single cell techniques. Master thesis (2012).

Rey, F.E., Gonzalez, M.D., Cheng, J., Wu, M., Ahern, P.P., and Gordon, J.I. Metabolic niche of a prominent sulfate-reducing human gut bacterium. *Proc Natl Acad Sci USA.* 2013, *110*:13582-7.

Riva, A., Borgo, F., Lassandro, C., Verduci, E., Morace, G., Borghi, E., Berry, D. Pediatric obesity is associated with an altered gut microbiota and discordant shifts in *Firmicutes* populations**.** *Environ Microbiol* 2016 [Epub ahead of print]

Russell, A.L., Consolazio, C.F., and White, C.L. Periodontal disease and nutrition in Eskimo Scouts of the Alaska National Guard. *J Dent Res* 1961, *40*:604–13.

Russell, W.R., Gratz, S.W., Duncan, S.H., Holtrop, G., Ince, J., Scobbie, L., Duncan, G., *et al*. High protein, reduced-carbohydrate weight-loss diets promote metabolite profiles likely to be detrimental to colonic health. *Am J Clin Nutr* 2011, *93*:1062–1072.

Sakanaka, S., Aizawa, M., Kim, M., and Yamamoto, T. Inhibitory effects of green tea polyphenols on growth and cellular adherence of an oral bacterium, *Porphyromonas gingivalis*. *Biosci Biotechnol Biochem* 1996, *60*:745–749.

Samuel, B. S., Shaito, A., Motoike, T., Rey, F. E., Backhed, F., Manchester, J. K., and Gordon, J. I. Effects of the gut microbiota on host adiposity are modulated by the short-chain fatty-acid binding G protein-coupled receptor. *Proc Natl Acad Sci USA* 2008, *105*:16767–16772.

Sanchez, M., Panahi, S., and Tremblay, A. Childhood Obesity : A role for gut microbiota ? *Int J Environ Res Public Health* 2015, *12*:162–175.

Scheres, N., Laine, M. L., de Vries, T. J., Everts, V., and van Winkelhoff, A. J., Gingival and periodontal ligament fibroblasts differ in their inflammatory response to viable Porphyromonas gingivalis. *J Periodontal Res* 2010, *45*: 262-270.

Scheres, N., and Crielaard, W., Gingival fibroblast responsiveness is differentially affected by *Porphyromonas gingivalis*: implications for the pathogenesis of periodontitis. *Mol Oral Microbiol* 2012, *28*:204-218.

Schindelin, J., Arganda-Carreras, I., and Frise, E. *et al*. Fiji: an open-source platform for biological-image analysis. *Nat Methods* 2012, *9*: 676-682,

Schwiertz, A., Taras, D., Schäfe, K., Beijer, S., Bos, AN., Donus, C. and Hardt, D.F. (2009) Microbiota and SCFA in lean and overweight healthy subjects. *Obesity* 2009,*18*:190–195.

Schueller, K., Pignitter, M., and Somoza, V. Sulfated and glucuronated trans-resveratrol metabolites regulate chemokines and sirtuin-1 expression in U-937 macrophages. *J Agric Food Chem* 2015, *63*:6535-6545.

Sekirov, I., Russell, S.L., Antunes, L.C.M., and Finlay, B.B. Gut microbiota in health and disease. *Physiol Rev* 2010, *90*: 859–904.

Seldin, MM., Meng, Y., Qi, H., Zhu, W.,Wang, Z., Hazen, S.L., Lusis,A.J., and Shih, D.M. Trimethylamine N-Oxide Promotes Vascular Inflammation Through Signaling of Mitogen-Activated Protein Kinase and Nuclear Factor-κBJ. *Am Heart Assoc* 2016, *5*:1-12.

Siqueira, J. F., and Rocas, I. N. Distinctive features of the microbiota associated with different forms of apical periodontitis. *J Oral Microbiol* 2009, *1*:1-12.

Söderling, E., ElSalhy, M., Honkala, E., Fontana, M., Flannagan, S., Eckert, G., Kokaras, A., *et al*. Effects of short-term xylitol gum chewing on the oral microbiome. *Clin Oral Investig* 2015, *19*:237-44.

Sonnenburg, J. L., and Bäckhed, F. Diet–microbiota interactions as moderators of human metabolism. *Nature* 2016, *535*:56–64.

Stappenbeck, T.S., Hooper, L.V., and Gordon, J.I. Developmental regulation of intestinal angiogenesis by indigenous microbes via Paneth cells. *Proc Natl Acad Sci USA* 2002, *99*:15451–5.

Susin, C., Wagner, M. C., Haas, A. N., Oppermann, R. V., and Albandar, J. M., The association between alcohol consumption and periodontitis in southern Brazilian adults. *J Periodont Res* 2015, *50*:622-628.

Swidsinski, A., Sydora, B. C., Doerffel, Y., Loening-Baucke, V., Vaneechoutte, M., Lupicki, M., and Dieleman, L. A. Viscosity gradient within the mucus layer determines the mucosal barrier function and the spatial organization of the intestinal microbiota. *Inflamm Bowel Dis* 2007,*13*:963- 970.

Swidsinski, A., Loening-Baucke, V., Verstraelen, H., Osowska, S., and Doerffel, Y. Biostructure of fecal microbiota in healthy subjects and patients with chronic idiopathic diarrhea. *Gastroenterology* 2008, *135*:568-579.

Takahashi, N., Oral Microbiome Metabolism: From "Who Are They?" to "What Are They Doing?". *J Dent Res* 2015, *94*:1628–1637.

Tamura, M., Tokuda, M., Nagaoka, S., Takada, H., Lipopolysaccharides of *Bacteroides intermedius* (*Prevotella intermedia*) and *Bacteroides* (*Porphyromonas*) *gingivalis* induce interleukin-8 gene expression in human gingival fibroblast cultures. *Infect Immun* 1992, *60*:4032-4937.

Taylor, PW., Hamilton-Miller, J.M., and Stapleton, P.D. Antimicrobial properties of green tea catechins. *Food Sci Technol Bull* 2005, *2*:71-81.

The Human Microbiome Project Consortium. Structure , function and diversity of the healthy human microbiome. *Nature* 2012,*486*: 207–214.

Tsai, F. and Coyle, W.J. The Microbiome and Obesity: is obesity linked to our gut flora?. *Current Gastroenterol Rep* 2009, *11*:307–313.

Van den Abbeele, P., Gerard, P., Rabot, S., Bruneau, A., El, Aidy, S., Derrien, M., *et al*. Arabino xylans and inulin differentially modulate the mucosal and luminal gut microbiota and mucin-degradation in humanized rats. *Environ Microbiol* 2011, *13*:2667–80.

Van den Abbeele, P., Belzer, C., Goossens, M., Kleerebezem, M., De Vos, W.M., Thas, O., *et al*. Butyrate-producing Clostridium cluster XIVa species specifically colonize mucins in an in vitro gut model. *ISME J* 2012, *7*:949-61.

Vinolo, M.A.R., Rodrigues, H.G., Nachbar, R.T., and Curi, R. Regulation of Inflammation by Short Chain Fatty Acids. *Nutrients* 2011, *3*:858-876.

Wade, W. G. The oral microbiome in health and disease. *Pharmacol Res* 2013, *69*:137–143.

Wagner M., Erhart, R., Manz, W., Amann, R., Lemmer, H., Wedi, D. and Schleifer, K.H. Development of an rRNA-targeted oligonucleotide probe specific for the genus Acinetobacter and its application

for in situ monitoring in activated sludge. *Appl Environ Microbiol* 1994, *60*: 792-800.

Wang, Q., Garrity, G.M., Tiedje, J.M., and Cole, J.R. Naïve Bayesian Classifier for rapid assignment of rRNA sequences into the new bacterial taxonomy. *Appl Environ Microb* 2007, *73*: 5261–5267.

Wang, Y., Antonopoulos, D.A, Zhu, X., Harrell, L., Hanan, I., Alverdy J.C., Meyer, F., et al. Laser capture microdissection and metagenomic analysis of intact mucosa-associated microbial communities of human colon. *Appl Microbiol Biotechnol* 2010, *88*:1-16.

Wang, W. L., Xu, S. Y., Ren, Z. G., Tao, L., Jiang, J. W., and Zheng, S. Sen. Application of metagenomics in the human gut microbiome. *World J Gastroentero* 2015, *21*: 803-814.

Wallner, G., Amann, R. and Beisker, W. Optimizing fluorescent in situ hybridization with rRNA-targeted oligonucleotide probes for flow cytometric identification of microorganisms. *Cytometry* 1993, *14*:136-143.

Walker, A. W. Ince, J., Duncan, S.H., Webster, L.M., Holtrop, G., Ze, X., *et al.* Dominant and diet-responsive groups of bacteria within the human colonic microbiota. *ISME J* 2011, *5*:220–230.

Walker, J., Schueller, K., Schaefer, L.-M., Pignitter, M., Esefelder, L., Somoza, V. Resveratrol and its metabolites inhibit pro-inflammatory effects of lipopolysaccharides in U-937 macrophages in plasma-representative concentrations. *Food Funct* 2013, *5*:74-84.

Wu, G. D. Chen, J., Hoffmann, C., Bittinger, K., Chen, YY., Keilbaugh, S.A.,*et al.* Linking long term dietary patterns with gut microbial enterotypes. *Science* 2011, *334*:105-108.

Zaura, E., Keijser, B. J. F., Huse, S. M., and Crielaard, W. Defining the healthy "core microbiome" of oral microbial communities. *BMC Microbiol* 2009, *9*:1–12.

Zhang, H., Dibaise, J. K., Zuccolo, A., Kudrna, D., Braidotti, M., Yu, Y., and Krajmalnik-brown, R. Human gut microbiota in obesity and after gastric bypass, *Proc Natl Acad Sci USA* 2008, *106*:2365-70.

Zoetendal, E. G., Collier, C. T., Koike, S., Mackie, R. I., Rex Gaskins, H., and Gaskins, H. R. Molecular ecological analysis of the gastrointestinal microbiota: A review. *J Nutr* 2004, *134*:465-472

Acknowledgements

This PhD program started at University of Milan, Department of Health Science and continued at the University of Vienna, Division of microbial ecology.
Firstly, I would like to thank my supervisor Prof. Giulia Morace for the good supervision of my work and my thesis and to give me the possibility to start the PhD program on gut microbiota field. I would like to thank Dott.ssa Elisa Borgi and Francesca Borgo for the supervision of my work and my colleagues Gaia Ortalli, Federica Perdoni, Daniela Cirasola.
A special thank is for Prof. David Berry for the excellent supervision of my job and to give me the possibly to improve my skills, learn new techniques and to motivate me to do always better.
I would like to thank all the division of microbial ecology (DoMe) at University of Vienna for all the help, support and great time during my stay in Vienna.
I would like to thank also the Erasmus placement program to give me the chance to continue my research abroad.
Special thanks are for the gut group (Barbara, Fatima, Buck, Owen, Jesse, Nika, Christos) and special thank is for Orest. Thanks Orest to help me and give me the motivation to continue the projects. I will carry your memory in my heart.
Thanks to my parents, my boyfriend and my friends to support me during all my PhD.

Ringraziamenti

Questo programma di dottorato è iniziato presso l'Università di Milano, Dipartimento di Scienze della Salute ed e'continuato presso l'Università di Vienna, Divisione di Ecologia Microbica.
In primo luogo, vorrei ringraziare i miei supervisori Prof. Giulia Morace per l'ottima supervisione del mio lavoro e della mia tesi e per avermi dato la possibilità di iniziare il programma di dottorato nel settore del microbiota intestinale. Vorrei ringraziare le dottoresse Elisa Borghi e Francesca Borgo per la supervisione del mio lavoro e le mie colleghe Gaia Ortalli, Federica Perdoni, Daniela Cirasola.
Un ringraziamento speciale è per il Prof. David Berry per l'eccellente supervisione del mio lavoro e per avermi dato la possibilità di migliorare le mie capacità, di imparare nuove tecniche e per avermi motivata a fare sempre meglio.
Vorrei ringraziare tutta la divisione di ecologia microbica (DoMe) presso l'Università di Vienna per tutto l'aiuto, il sostegno e il buon tempo trascorso durante il mio soggiorno a Vienna.
Vorrei ringraziare anche il programma di stage Erasmus per avermi dato la possibilità di continuare la mia ricerca all'estero.
Un ringraziamento speciale è per il "gut group" (Barbara, Fatima, Buck, Owen, Jesse, Nika, Christos) e un ringraziamento speciale è per Orest. Grazie Orest per avermi aiutata e di avermi dato la motivazione di continuare i progetti iniziati insieme. Porterò il tuo ricordo nel mio cuore.
Grazie ai miei genitori al mio fidanzato e ai miei amici per avermi sostenuta durante tutto il mio dottorato di ricerca.